Viral and non-viral generation and characterization of induced pluripotent stem cells from human amniotic fluid cells.

Dissertation
zur Erlangung des akademischen Grades
"doctor rerum naturalium"
(Dr. rer. nat.)

eingereicht am
Fachbereich für Biologie, Chemie und Pharmazie
der Freien Universität Berlin

von
Katharina Drews

May 24, 2012

1. Gutachter:	Prof. Dr. Hans Lehrach (Max Planck Institut für Molekulare Genetik)
2. Gutachter:	Prof. Dr. Petra Knaus (Freie Universität Berlin)
Disputation am:	October 01, 2012

Erfolg ist ein Gesetz der Serie, und Misserfolge sind Zwischenergebnisse.
Wer weitermacht, kann gar nicht verhindern, dass er irgendwann auch Erfolg hat.
Thomas Alva Edison

Acknowledgements

I would like to thank Prof. Dr. Hans Lehrach for the opportunity to conduct this work at the Max Planck Institute for Molecular Genetics. Additionally, I would especially like to thank Dr. James Adjaye for dedicating this interesting PhD project to me, for his guidance and constant support throughout the last years.

I would also like to gratefully acknowledge Prof. Dr. Petra Knaus of the Freie Universität Berlin for the time she has taken to discuss and support my project, despite great demands on supervising her own and other external PhD students.

I appreciate the financial support I received from the Berlin-Brandenburg School of Regenerative Therapies (BSRT). Furthermore, I am thankful for the numerous opportunities to attend various courses and programs which have promoted me as a young scientist in many ways.

I would like to thank ALL former and current members of the 'Molecular Embryology and Aging Group' for their scientific assistance and for creating such a pleasant atmosphere in the lab. I have had a lot of fun with you!

Thanks to all other colleagues at the MPI who supported me in different ways, who helped out with knowledge and/or reagents from time to time or who simply made my time at the MPI so enjoyable.

Moreover, I would particularly like to thank my co-worker Geertrui Tavernier and her supervisors from the University of Ghent, without whom the final phase of my project would not have been so efficient and successful.

I am also thankful to all other external collaborators for fruitful team work.

Thanks to Drs. Justyna and Szymon Jozefczuk, Rainer Rahmfeld and Martin Dieringer for their LaTeX support.

I would like to thank my parents for their continuous support and their faith in me. Thanks also to my sister and close friends.

Through the love and understanding of my husband Christian I have found the strength to accomplish this project. Together we have gone through the ups and downs of the last three and a half years. Thanks for always listening to my problems—I am very grateful for your patience.

Contents

List of Figures

List of Tables

Abbreviations

6-well	one well of a 6-well cell culture plate, ~9 cm^2 growth area
AFC(s)	amniotic fluid cell(s)
AFiPSC(s)	amniotic fluid-derived induced pluripotent stem cell(s)
ALK	anaplastic lymphoma kinase
AP	alkaline phosphatase
BAPN	β-amino-proprionitrile
BMP	bone morphogenetic protein
BP	biological process
BSA	bovine serum albumin
CC	cellular compartment
cDNA	complementary deoxyribonucleic acid
CM	conditioned medium
cRNA	complementary ribonucleic acid
C_T	threshold cycle
DAPI	4',6-diamidino-2-phenylindole
DMSO	dimethyl sulfoxide
DNA	deoxyribonucleic acid
dNTP	deoxyribonucleotide triphosphate
EB	embryoid body
EDTA	ethylenediaminetetraacetic acid
EGFP	enhanced green fluorescent protein
EMT	epithelial-to-mesenchymal transition
ERK	extracellular signal-regulated protein kinases
ESC(s)	embryonic stem cell(s)
FACS	fluorescence-activated cell sorting
FBS	fetal bovine serum
FDA	Food and Drug Administration
FDR	false discovery rate
FGF2	fibroblast growth factor 2 (basic fibroblast growth factor)
GFP	green fluorescent protein
GO	gene ontology

GSK	glycogen synthase kinase
hLIF	human leukemia inhibitory factor
iPSC(s)	induced pluripotent stem cell(s)
IRES2	internal ribosome entry site 2
IRG(s)	interferon-regulated gene(s)
IVF	*in vitro* fertilization
IVT	*in vitro* transcription
MACS	magnetic activated cell sorting
MAPK	mitogen-activated protein kinase
MEF(s)	mouse embryonic fibroblast(s)
MEF-CM	mouse embryonic fibroblast-conditioned medium
MEK	mitogen-activated protein kinase kinase
MET	mesenchymal-to-epithelial transition
mRNA	messenger ribonucleic acid
miRNA	microRNA
NaB	sodium butyrate
NIH	National Institute of Health
OCT4-EGFP	*OCT4* promoter-driven enhanced green fluorescent protein
ON	overnight
OSKM	OCT4, SOX2, KLF4 and c-MYC
OSKML	OCT4, SOX2, KLF4, c-MYC and LIN28
PA cells	Phoenix amphotropic 293 cells
padj	false discovery rate-adjusted 'diff' p-value
PBS	phosphate buffered saline
PBST	0.05 % Tween 20 in phosphate buffered saline
PCR	polymerase chain reaction
pdet	'detection' p-value
PDK	phosphoinositide-dependent protein kinase
PFA	paraformaldehyde
PS	penicillin/streptomycin
PSC(s)	pluripotent stem cell(s)
Px	passage x of an *in vitro* cell culture
qRT-PCR	quantitative real-time polymerase chain reaction
RNA	ribonucleic acid
ROS	reactive oxygen species
RT	room temperature
SCNT	somatic cell nuclear transfer
SD	standard deviation
SDS	sodium dodecyl sulfate
shRNA	short hairpin ribonucleic acid
siRNA	small interfering ribonucleic acid

SSEA	stage-specific embryonic antigen
TGFβ	transforming growth factor β
TGFP	turbo green fluorescent protein
TRN	transcriptional regulatory network
TRA	tumor rejection antigen
UM	unconditioned medium
VPA	valproic acid

Semantics

bp	base pairs
°C	degrees Celsius
× g	times gravity
rpm	revolutions per minute
g	gram
mg	milligram
µg	microgram
ng	nanogram
l	liter
ml	milliliter
µl	microliter
mol	mole
pmol	picomole
M	molar concentration, 1 mol per liter
mM	millimolar
µM	micromolar
nM	nanomolar
s	second
min	minute
h	hour
d	day
mm	millimeter
nm	nanometer
µm	micrometer
U	enzyme unit

Abstract

The ability to induce pluripotency in somatic cells offers unprecedented opportunities in basic and applied research. The implementation of induced pluripotent stem cells (iPSCs) into clinical settings, however, is hampered by genetic modifications associated with retro- or lentivirus-mediated reprogramming. The quest for efficient alternative reprogramming approaches has been closely connected with the identification of cell sources, which readily acquire the pluripotent stem cell (PSC) state. Human amniotic fluid cells (AFCs) represent routinely available cells with stem cell-like features, which could presumably facilitate efficient reprogramming even by non-integrating techniques. The goal of this project was to generate and comparatively characterize iPSCs derived from human AFCs by viral and non-viral techniques with respect to human embryonic stem cells (ESCs), the golden standard of PSCs, and iPSCs generated from cells of other tissues of origin. Retrovirus-mediated overexpression of the reprogramming factors in primary human AFCs resulted in fast and efficient generation of iPSCs (AFiPSCs), which resembled human ESCs with regards to morphology, proliferation and marker expression. Their ability to differentiate into derivatives of the three embryonic germ layers was demonstrated *in vitro* and *in vivo* and upon BMP2 and BMP4-treatment expression of trophoblast markers, including *CDX2*, *KRT7* and *HAND1*, was confirmed. Detailed microarray-based transcriptome analysis of ESCs, AFiPSCs, fibroblast-derived iPSCs (FiPSCs) and the respective parental cell lines revealed the activation of a transcriptional regulatory network common to all PSCs but also highlighted, for example, residual gene expression signatures in iPSCs from different tissues of origin. These findings were summarized in a concept coined the LARGE Principle of Cellular Reprogramming. Genetic manipulation of AFiPSCs was not accomplished. Attempts to reprogram human AFCs by non-viral, non-integrating methods included nucleofection of episomal plasmids and lipofection of mRNAs encoding the reprogramming factors. Despite multiple trials fully reprogrammed iPSCs could not be established. In depth analysis of the cellular response to the transfected mRNAs uncovered an extensive induction of interferon-regulated immune-related genes to be the key roadblock in mRNA-mediated reprogramming. Subsequent efforts to identify chemicals which could suppress this innate immune reaction did not yield potent candidates. The data presented herein, however, provide the basis for further investigations into this effect. In summary, this work highlights the value of human AFCs for the derivation of iPSCs and emphasizes the obstacles that need to be overcome before AFiPSCs can potentially be employed into clinical settings.

1 Introduction

1.1 Regenerative medicine

"Regenerative medicine," as originally described by Kaiser (1992) (given in Lysaght and Crager (2009)), "[...] attempts to change the course of chronic disease and in many instances will regenerate tired and failing organ systems." Since then, the term 'regenerative medicine' has been re-defined by Mason and Dunnill to address all essential aspects of the broad, cross-disciplinary modern field, while keeping it simple and concise: "Regenerative medicine replaces or regenerates human cells, tissue or organs to restore or establish normal function" (Mason and Dunnill, 2008). To meet these requirements regenerative medicine combines cell-based regenerative therapies, including gene-based methods, molecular medicines, new technologies such as nanomedicines, biomaterials and tissue engineering (Mason and Dunnill, 2008). In a pioneering practical example of regenerative medicine, symptoms caused by severe bladder dysfunction were markedly improved by the implantation of tissue-engineered bladder constructs which had been generated from autologous, *in vitro* expanded urothelial and muscle cells seeded onto three-dimensional scaffolds (Atala et al., 2006). Due to technical advances, regenerative therapies based on human cells have a great significance in regenerative medicine these days (Mason and Dunnill, 2008). However, the access to specialized human cell types which can be obtained from biopsies, expanded and re-implanted is limited. This therapeutic strategy is, hence, ineligible for the treatment of a large number of diseases such as, for example, neuronal diseases. Consequently, the field strives to find sources of stem cells which, due to their inherent differentiation potential and their ability to self-renew, qualify for broad application in regenerative medicine. Accordingly, several kinds of so-called adult stem cells, which reside in their particular tissue or organ of origin to contribute to homeostasis and repair, are thought to be applicable in the treatment of various disorders as reviewed by Mimeault et al. (2007). Their differentiation potential, however, is generally restricted to certain lineages and numerous groups have reported decreased differentiation potential and limited proliferation capacities of adult stem cells maintained *in vitro* (Digirolamo et al., 1999; Banfi et al., 2000; Glimm et al., 2000; Baxter et al., 2004; Bonab et al., 2006; Wagner et al., 2008; Schellenberg et al., 2011). Consequently, "the limitations in availability of most specialist somatic cells and the restriction in the expansion of adult stem cells" drives a great interest in pluripotent stem cells (PSCs) (Mason and Dunnill, 2008). The term pluripotent refers to the ability to develop into derivates of all three primary germ layers and, thus, any cell type of the embryo, fetus

and adult (Evans, 2011). Such PSCs naturally occur during early embryonic development of mammals (Pera et al., 2000; Evans, 2011).

1.2 Human pluripotent stem cells

1.2.1 The first week of human embryonic development

To provide the basis for comprehending the origin and nature of human PSCs, the following paragraph briefly describes the first week of human embryonic development post-fertilization (Adjaye et al., 2005; Schoenwolf et al., 2008). The fertilized human egg, the totipotent zygote, eventually develops into all cell types of the human organism, including extraembryonic tissues such as the placenta. It travels from the ampulla of the oviduct to the uterus, where it implants by the end of the first week post-fertilization. During this pre-implantation development, the oocyte undergoes several symmetric and asymmetric mitotic cell divisions, the so-called cleavage, giving rise to the two-cell stage embryo, the four- and eight-cell stage embryo prior to formation of the morula, a compact sphere of blastomeres (Figure 1.1). During cleavage, these roundish daughter cells polarize and segregate into a thin outer layer of epithelium, the trophoblast, and the inner cell mass to form the blastocyst, a fluid filled sphere, by day five post-fertilization. This represents the first specification of cell fate during embryogenesis. The surrounding trophectoderm cells, which express trophoblast markers such as BMP4, will later on give rise to the embryonic part of the placenta and other supporting tissues, whereas the embryo proper will arise from the OCT4, SOX2, NANOG-expressing pluripotent inner cell mass or embryoblast.

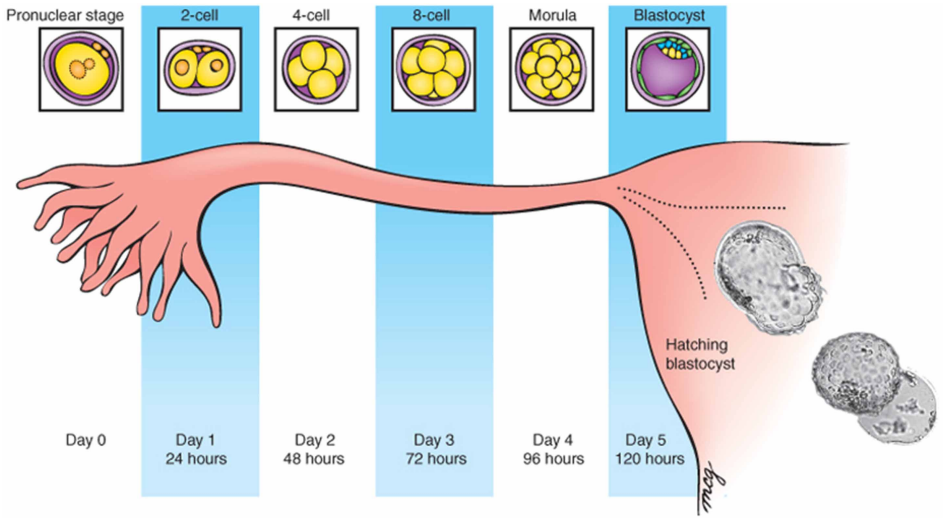

Figure 1.1: Cleavage and transport down the oviduct. Fertilization occurs in the ampulla of the oviduct. During the first five days, the zygote undergoes cleavage as it travels down the oviduct and enters the uterus. On day five, the blastocyst hatches from the zona pellucida and is then able to implant in the uterine endometrium Taken from Schoenwolf et al. (2008).

1.2.2 Human embryonic stem cells

Thomson et al. (1998) derived the first pluripotent human embryonic stem cells (ESCs) from the inner cell mass of surplus blastocyst stage embryos generated by *in vitro* fertilization (IVF). These cells maintain the potential to form derivatives of all three embryonic germ layers throughout pro-longed undifferentiated proliferation *in vitro*, as characterized by staining for the non-human primate ESCs and human embryonal carcinoma cell surface markers stage-specific embryonic antigen (SSEA)-3 and SSEA-4, tumor rejection antigen (TRA)-1-60 and TRA-1-81 and alkaline phosphatase (AP) as well as the formation of teratomas upon injection into immune-compromised mice *in vivo* (Thomson et al., 1998). Human ESCs grow as flat, sharp-edged colonies, have a high nucleus to cytoplasmic ratio and express high levels of telomerase activity enabling them to escape senescence and to continuously self-renew (Thomson et al., 1998). At the molecular level, human ESCs are of epithelial nature. This is highlighted by the apico-basal polarity, the presence of epithelial cell-cell adhesion complexes such as cadherin-1(CDH1)-mediated adherens junctions, tight junctions, desmosomes and gap junctions, correlating with the poor clonal survival of human ESCs (Thomson et al., 1998) and the lack of, for example, mesenchymal markers such as the intermediate filament vimentin (Wong et al., 2004; Eastham et al., 2007; Van Hoof et al., 2008).

"The gene-expression program" and, hence, the phenotype of pluripotent human ESCs "is a product of regulation by specific transcription factors, chromatin-modifying enzymes, regulatory RNA molecules (miRNAs), and signal-transduction pathways" as illustrated in Figure 1.2 (Jaenisch and Young, 2008).

Key functions of OCT4, SOX2 and NANOG, the master transcription factors of pluripotent mammalian stem cells (Nichols et al., 1998; Avilion et al., 2003; Chambers et al., 2003; Hart et al., 2004; Hay et al., 2004; Matin et al., 2004; Babaie et al., 2007; Jung et al., 2010) in maintaining complex self-renewal- and pluripotency-associated transcriptional regulatory networks (TRNs) in human ESCs were first identified by Boyer et al. (2005). According to their findings, these three proteins co-operate to establish auto-regulatory and feed-forward loops, thereby activating or repressing genes encoding components of distinct signaling pathways and developmental processes, chromatin regulators and regulatory miRNAs to shape ESC identity. Furthermore, various extracellular stimuli contribute to the maintenance of the undifferentiated human ESC phenotype. As such, basic fibroblast growth factor (bFGF, also known as FGF2) is a key component of human ESC culture medium designed to maintain self-renewal and pluripotency of human ESCs *in vitro* (Thomson et al., 1998; Amit et al., 2000). Via the activation of the corresponding receptors, FGF2 is believed to be an up-stream regulator of other key signaling pathways operative in undifferentiated human ESCs (Greber et al., 2007a). Regarding these, the Smad2/3-mediated branch of the transforming growth factor β (TGFβ)/Activin A/Nodal signaling pathway is of particular importance to note (James et al., 2005; Vallier et al., 2005; Greber et al., 2007a; Vallier et al., 2009a). Likewise, canonical WNT signaling has long been believed to promote self-renewal of human ESCs, however, the actual relevance of this pathway in this respect remains controversial (Sato et al., 2004;

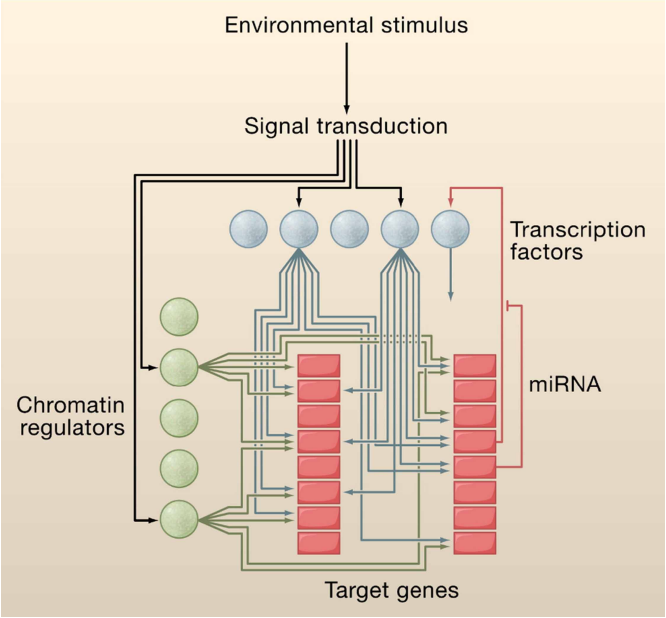

Figure 1.2: Pluripotency and the transcriptional regulatory circuitry. Cartoon showing hypothetic connections between signal transduction pathways, transcription factors (blue balls), chromatin regulators (green balls), and their target genes (orange squares) to form an image of transcriptional regulatory circuitry. Some target genes produce miRNAs, which function at posttranscriptional levels. Taken from Jaenisch and Young (2008).

Davidson et al., 2012). Figure 1.3 depicts a simplified scheme of selected pathways to illustrate how signals are transduced from the cellular membrane to the nucleus and integrated to sustain undifferentiated proliferation of human ESCs. Essential steps in this network are the FGF2-mediated up-regulation of signaling molecule-encoding genes including *TGFB1* and *INHBA* (encoding subunits of ACTIVIN A) which feedback in autocrine and paracrine fashion upon translation to promote self-renewal and pluripotency (Greber et al., 2007a). Simultaneously, differentiation-inducing factors such as *BMP4* are either directly or indirectly repressed by up-regulation of corresponding antagonists such as *GREM1* and *CER1* (Xu et al., 2005; Greber et al., 2007a). As a result major self-renewal and pluripotency-associated genes such as *OCT4*, *SOX2* and *NANOG* are up-regulated, feeding into the complex human ESC-specific transcriptional regulatory networks described above. Importantly, mouse embryonic fibroblasts (MEFs) of certain strains, e.g., CF1, NMRI, support the undifferentiated proliferation of human ESCs due to similar expression patterns and release of homologous signaling molecules upon FGF2-stimulation. For this reason, MEFs are routinely used in co-culture systems with human ESCs (Greber et al., 2007a).

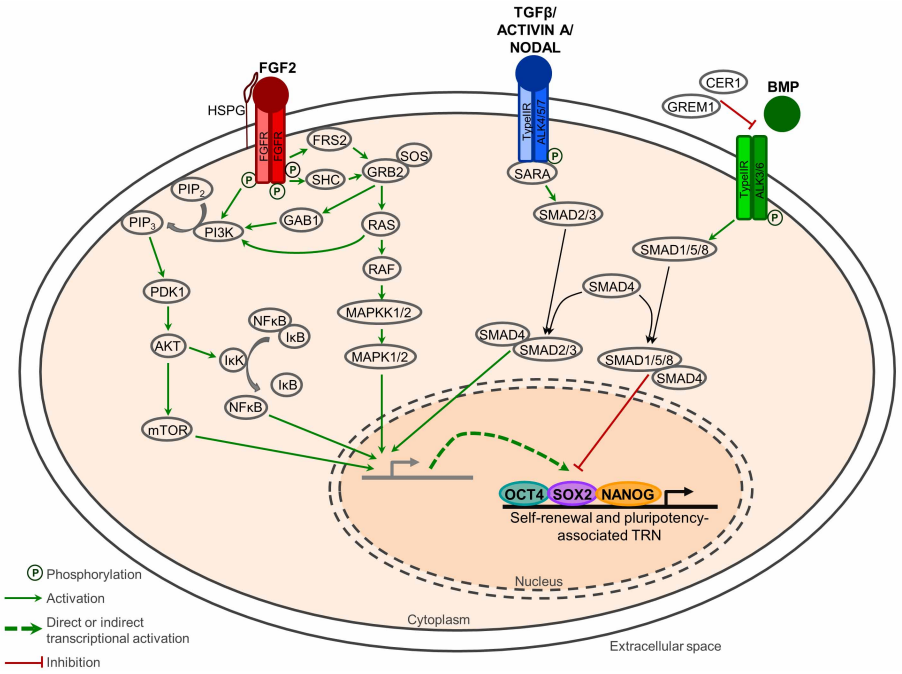

Figure 1.3: Core signaling pathways that maintain self-renewal and pluripotency in undifferentiated human ESCs. Binding of FGF2 to its receptor is regulated by heparan sulfate proteoglycans. Once initiated FGF2 signaling follows different routes within the cell—only PI3K/AKT and MAPKK1/2/MAPK1/2 branches, known for their key contribution towards self-renewal and pluripotency via regulated transcription of distinct target genes, are depicted. Likewise, active TGFβ/ACTIVIN A/NODAL signaling plays an essential role in undifferentiated human ESCs via SMAD2/3-mediated expression/repression of target genes. Both FGF2 and TGFβ/ACTIVIN A/NODAL signaling interact, e.g. by up-regulation of components of the respective other pathway, and synergistically suppress BMP-induced differentiation, e.g. via down-regulation of BMPs and up-regulation of BMP antagonists such as *GREM1* and *CER1*. As a result, regulated transcripts are indirectly or directly conducive to the establishment and maintenance of the OCT4, SOX2, NANOG-driven self-renewal and pluripotency-associated TRN in human ESCs. Various other pathways, branches of pathways and mediators have been excluded for the sake of clarity.
AKT, AKT kinase; ALK4/5/7 and ALK3/6, anaplastic lymphoma kinase 4/5/7 and anaplastic lymphoma kinase 3/6; BMP, bone morphogenetic protein; CER1, cerberus protein; GREM1, gremlin 1 protein; FGF2, fibroblast growth factor 2; FGFR, fibroblast growth factor receptor; FRS2, FGF receptor substrate 2; GRB2, growth factor receptor-bound protein 2 GAB1, GRB2-associated binding protein 1; HSPG, heparan sulfate proteoglycans; IκB, inhibitor of κB; IκK, IκB kinase; MAPK1/2, mitogen-activated protein kinase 1/2; MAPKK1/2, mitogen-activated protein kinase kinase 1/2; mTOR, mammalian target of rapamycin; NFκB, nuclear factor κ-light-chain-enhancer of activated B cells; PDK1, 3'-phosphoinositide-dependent protein kinase 1; PI3K, phosphoinositide 3-kinase; PIP_2, phosphatidylinositol (3,4)-bisphosphate; PIP_3, phosphatidylinositol (3,4,5)-trisphosphate; RAS, rat sarcoma viral oncogene homolog; RAF, rat fibrosarcoma proto-oncogene serine/threonine-protein kinase; SARA, SMAD anchor for receptor activation protein; SHC, SH2 domain containing transforming protein 1; SOS, son of sevenless; TGFβ, transforming growth factor β; TRN, transcriptional regulatory network; TypeIIR, type II receptor. Adapted from http://www.cellsignal.com/reference/pathway/pdfs/esc_pluripotency.pdf, Nugent and Iozzo (2000); Vallier et al. (2005); Armstrong et al. (2006); Okita and Yamanaka (2006); Xu et al. (2008); Greber et al. (2007a); Zhou et al. (2009).

1.2.2.1 Applications of human ESCs in basic research and regenerative medicine

The establishment of *in vitro* cultures of human ESCs was a major breakthrough in regenerative medicine. Thomson and colleagues emphasized the value of human ESCs for studies of early developmental processes, especially post-implantation processes, and the importance of unveiling mechanisms underlying their differentiation to distinct cells types. Healthy, diseased and genetically modified human ESCs provide basic knowledge required for practical applications of these cells as well as the opportunity to model diseases in a dish (Thomson et al., 1998; Tropel et al., 2010). To this end, several disease-specific human ESC lines have been established so far (Table 1.1) (Maury et al., 2011).

Table 1.1: Disease modeling using human ESCs. Modified from Maury et al. (2011).

Disease (responsible gene)	**Molecular defect**	**Reference**
Huntington (Huntingtin)	Not determined	Mateizel et al. (2010); Tropel et al. (2010)
Cystic Fibrosis (*CFTR*)	Not determined	Mateizel et al. (2006, 2010); Tropel et al. (2010)
X-linked myotubular myopathy (*MTM1*)	Not determined	Tropel et al. (2010)
Turner syndrome (Monosomy X)	Not determined	Urbach and Benvenisty (2009)
Fabry syndrome (*GLA*)	Not determined	Tropel et al. (2010)
Multiple endocrine neoplasia Type 2 (*RET*)	Not determined	Tropel et al. (2010)
Marfan syndrome (*FBN1*)	Not determined	Mateizel et al. (2010)
Charcot-Marie Tooth Type 1A (*PMP22*)	Not determined	Mateizel et al. (2010)
Facioscapulohumeral muscular dystrophy	Not determined	Mateizel et al. (2010)
Spino-cerebellar Ataxia type 2 (*ATXN2*)	Not determined	Tropel et al. (2010)
Spino-cerebellar Ataxia type 7 (*ATXN2*)	Not determined	Mateizel et al. (2010)
Fragile-X Syndrome (*FRM1*)	Extension of FRM1 expression during early differentiation	Eiges et al. (2007); Mateizel et al. (2010)
Myotonic dystrophy type 1 (*DMPK*)	Detection of the ribonuclear inclusions, *NMDAR1* alternate splicing defect, defect in neuritogenesis and synaptogenesis in human ESCs-derived motoneurons	Mateizel et al. (2006, 2010); Marteyn et al. (2011)
Lesch-Nyhan Syndrome (*HRPT1*), introduction of the mutation by homologous recombination	Absence of HRPT1 activity, increased production of uric acid	Urbach et al. (2004)

ATXN2, ataxin 2; *CFTR*, cystic fibrosis transmembrane conductance regulator; *DMPK*, dystrophia myotonica-protein kinase; *FBN1*, fibrillin 1; *FRM1*, fragile X mental retardation 1; *GLA*, galactosidase α; *HRPT1*, hypoxanthine phosphoribosyltransferase 1; *MTM1*, myotubularin 1; *NMDAR1*, N-methyl D-aspartate receptor1; *PMP22*, peripheral myelin protein 22; *RET*, ret proto-oncogene.

Combining the theoretically indefinite proliferation capacities of human ESCs with their pluripotent differentiation potential, it can be anticipated that human ESCs represent an unlimited supply of any desired specialized human cell types which are otherwise difficult to obtain. This offers new perspectives with respect to drug discovery, pre-clinical drug testing, toxicity tests as well as repair and replacement of impaired tissues (Thomson et al., 1998; Davila et al., 2004; McNeish, 2004; Jensen et al., 2009).

Concerning the latter aspect, the first clinical trials involving human ESC-derived, specialized cell types have started. In 2009, approximately ten years after the first human ESC derivation, Geron, a US-based biopharmaceutical company, was first to be granted approval by the Food and Drug Administration (FDA) to initiate clinical studies to evaluate human ESC-based therapies. Geron intended to test oligodendrocyte progenitor cells generated from human ESCs, which were shown to have "remyelinating and nerve growth-stimulating properties", for the treatment of severe spinal injuries in ten patients (Alper, 2009). Following a series of intermissions by the regulatory authorities (Strauss, 2010), Geron started the treatment of four patients with their stem cell-based product in 2010 but ended the trial precociously due to financial concerns in November 2011 (Frantz, 2012). There has yet been no publication of the clinical results. The second on-going FDA-approved clinical trial of this kind is conducted by Advanced Cell Technology and is meant to examine the safety and effectiveness of human ESC-derived retinal pigmented cells, transplanted into the sub-retinal space, in rescuing photoreceptor loss and improving vision in patients suffering from macular degeneration, a leading cause of blindness. Preliminary results of this study in two patients highlighted the absence of abnormal growth and immune rejection of the grafted cells in the eye, which is an immune-privileged organ, while visual acuity was slightly improved (Schwartz et al., 2012b). Furthermore, ViaCyte (formerly Novocell) plans to test human ESCs-derived pancreatic progenitor cells for treating type 1 diabetes (Wu and Hochedlinger, 2011). Likewise, Life Technologies pursue trials to improve symptoms of amyotrophic lateral sclerosis with astrocyte precursor cells generated from human ESCs (Fox, 2011).

Despite these promises human ESCs have inherent problems. The two most critical issues when considering the use of human ESCs for any of the above mentioned applications are (i) the ethical dispute that is associated with the destruction of human pre-implantation embryos for the purpose of generating human ESCs and (ii) the immune rejection that can be caused if non-autologous human ESCs are transplanted. There is no apparent way to completely solve the first issue despite juridically prohibiting human ESC-based research, thereby, abandoning its tremendous biological value. The latter problem, however, could be resolved by banking human ESCs in order to provide matching major histocompatibility complex backgrounds or by genetic modification of human ESCs with the aim of suppressing immune rejection (Jensen et al., 2009). Yet, human ESC generation and banking, which appear to be technically less challenging than genetic modification of human ESCs (Strulovici et al., 2007; Maury et al., 2011), enforce the ethical concerns and are, hence, self-contradictory.

1.2.3 Human induced pluripotent stem cells

The search for approaches capable of circumventing the two major concerns associated with human ESCs entailed attempts to de-differentiate somatic cells including somatic cell nuclear transfer (SCNT) and cell fusion experiments. The term SCNT refers to the transplantation of a differentiated somatic cell nucleus into an enucleated, unfertilized egg to produce an offspring that is genetically identical to the donor of the somatic cell—Dolly the sheep was cloned using this technique (Wilmut et al., 1997). Instead of using an oocyte, Cowan and colleagues fused terminally differentiated human fibroblast cells with human ESCs, generating tetraploid hybrids with human ESC characteristics, to show that human ESCs have the potential to re-set a somatic cell nucleus to an embryonic-like state (Cowan et al., 2005). These experiments were of great value for developmental biology as they demonstrated that differentiation processes are reversible and that certain oocyte- and ESC-specific factors can convey their differentiation potential to terminally differentiated cells. With this in mind, Takahashi and Yamanaka screened a library of 24 putatively essential pluripotency-associated genes for their potential to induce pluripotency in somatic cells, leading to the next groundbreaking achievement in stem cell biology: They found that ectopic expression of a combination of four transcription factor genes, namely *Pou5f1* (encoding the Oct4 protein), *Sox2*, *Klf4* and *c-Myc*, was sufficient to reprogram mouse somatic cells back to an ESC-like developmental stage (Takahashi and Yamanaka, 2006). Without comprising oocytes or human ESCs they managed to turn the developmental clock of terminally differentiated cells back. One year later, the same research group could generate such so-called induced pluripotent stem cells (iPSCs) by retroviral overexpression of the same set of genes in human somatic cells, including neonatal fibroblasts and cells obtained from skin and synovial tissue biopsies (Takahashi et al., 2007). In parallel, the group of Thomson reported that human fibroblast cells can also acquire an ESC-like state by transduction of constitutive lentiviruses encoding a slightly different set of reprogramming factor genes—*POU5F1* (OCT4), *SOX2*, *NANOG* and *LIN28* (Yu et al., 2007). Hence, in both protocols OCT4 and SOX2 are obligatory factors to induce pluripotency in somatic cells.

1.2.3.1 Molecular events underlying direct reprogramming

Despite a basic understanding of the OCT4, SOX2, NANOG-regulated TRN that underlies the undifferentiated human PSC identity (Boyer et al., 2005; Babaie et al., 2007; Jung et al., 2010), we have a confined knowledge of mechanisms and distinct pathways involved in the de-differentiation of somatic cells into PSCs. The following paragraphs and Figure 1.4 briefly summarize what has been known to date.

The most obvious feature of the cellular reprogramming process is the major change of the transcriptional profile which needs to take place to facilitate the switch of cellular phenotypes. Thus, epigenetic remodeling through distinct alteration of histone modifications and CpG methylation patterns is required (Takahashi et al., 2007) in order to repress characteristic somatic cell-specific genes and to enable transcription of pluripotency-associated genes. Recently, several genome-wide studies have been conducted to profile the epigenetic landscape

of parental cells, iPSCs and ESCs and to analyze the kinetics of distinct chromatin remodeling steps employing both murine and human iPSCs (Kim et al., 2010, 2011; Mattout et al., 2011).

To obtain a better understanding of other molecular events underlying of the reprogramming process we analyzed early events induced in human fibroblasts by retroviral transduction of the reprogramming factors OCT4, SOX2, KLF4 and c-MYC. This revealed that in response to viral infection levels of reactive oxygen species (ROS) increased significantly, leading to DNA damage and ultimately to the activation of p53 (Mah et al., 2011). As this tumor suppressor protein is responsible for arresting the cell cycle and inducing apoptosis and senescence, p53 activation resulted in an over-representation of transcripts involved in apoptosis, cell cycle regulation and aging (Mah et al., 2011). Hence, overcoming the p53-mediated cell cycle arrest is a crucial step in acquiring the pluripotent state.

Another critical step in the process of cellular reprogramming is the suppression of the epithelial-to-mesenchymal transition (EMT) and promotion of the reverse process, the mesenchymal-to-epithelial transition (MET), as shown for mouse cells of mesenchyme origin (Li et al., 2010; Samavarchi-Tehrani et al., 2010; Liao et al., 2011). Accordingly, we identified the initiation of MET as an early reprogramming event in human fibroblasts (Mah et al., 2011), which eventually resulted in the establishment of the epithelial ESC-like phenotype as characterized by multiple cell-cell adhesion complexes (Wong et al., 2004; Eastham et al., 2007; Van Hoof et al., 2008).

Recent findings from our group (Prigione et al., 2010, 2011b) and from others (Armstrong et al., 2010; Suhr et al., 2010; Zhu et al., 2010; Folmes et al., 2011; Kelly et al., 2011; Varum et al., 2011; Zhang et al., 2011a) further suggest that the derivation of iPSCs is associated with a re-configuration of mitochondria and bioenergetic metabolism. Developing cancer cells are known to undergo reprogramming of the energy metabolism (Hsu and Sabatini, 2008). As they proliferate, their metabolism switches from mitochondrial oxidative phosphorylation to cytoplasmic glycolysis even in the presence of oxygen, a phenomenon known as the Warburg effect (Warburg, 1956). This is believed to be caused by the change of energy requirements and anabolic demands of tumor cells as cancer cells need to produce macromolecules to proliferate while evading the generation of high levels of ROS, a common by-product of mitochondrial respiration (Vander Heiden et al., 2009). Thus, cancer cells opt for re-routing the energy flux outside the mitochondria (Drews et al., b). These findings may be transferable to somatic cells undergoing cellular reprogramming. Accordingly, the quantity of mitochondria within iPSCs is reduced and they are transformed into an immature state with less well defined cristae (Armstrong et al., 2010; Prigione et al., 2010; Suhr et al., 2010; Kelly et al., 2011). Simultaneously, oxidative phosphorylation is decreased in iPSCs, which translates into increased glycolysis (Prigione et al., 2010; Folmes et al., 2011; Prigione et al., 2011b; Varum et al., 2011; Zhang et al., 2011a) and lower production of ROS (Armstrong et al., 2010; Prigione et al., 2010, 2011a). As these metabolic changes occur before the establishment of the human ESC-like properties they are likely to be essential for the process of cellular reprogramming (Folmes et al., 2011).

1.2.3.2 The promise and potential of human iPSCs in basic research and regenerative medicine

Human iPSCs closely resemble ESCs with respect to morphology, expression of ESC-specific markers, proliferation, the ability to indefinitely self-renew and differentiation potential (Takahashi et al., 2007; Yu et al., 2007). Thus, human iPSCs are considered as equally potent for studies of differentiation processes, drug discovery, pre-clinical drug testing, toxicity studies and repair and replacement of impaired tissues. The fact that iPSCs could potentially be derived from ethically safe biopsies is one of the main advantages of human iPSCs over ESCs. At the same time, derivation of iPSCs from virtually any individual is feasible, thus, solving immune rejection concerns. Moreover, iPSCs allow for the reflection of a healthy or diseased individual's genetic background *in vitro*, without the necessity for banking genetically modified human ESCs, taking regenerative medicine to a new level of personalized medicine. Altogether, with the development of human iPSCs, there will be a potentially limitless source of donor-specific differentiated cell types available for disease modeling, drug and toxicity screens and cellular replacement therapies (Figure 1.4) (Drews et al., b). The full potential of the iPSC technology can be valued when considering recent achievements using murine iPSCs. Impressively, Jaenisch and colleagues reported amelioration of sickle cell anemia-associated symptoms in mice following bone marrow transplantation of genetically-corrected hematopoietic progenitors derived from autologous iPSCs (Hanna et al., 2007). Similarly, they could show that murine iPSC-derived neural precursors efficiently differentiate into various functional neuronal cell types which migrate and integrate into the developing brain upon injection into the embryonic cerebral ventricles (Wernig et al., 2008). Furthermore, *in vitro* generated neurons from these iPSCs have the potential to improve behavioral deficits in a rat model of Parkinson's disease (Wernig et al., 2008). Accordingly, ViaCyte, for example, also considers generating pancreatic beta cell progenitors derived from human iPSCs instead of human ESCs, to pursue treatment of type 1 diabetes (Fox, 2011). Meanwhile, a number of human iPSC lines have been generated from patients suffering from a variety of diseases. Table 1.2 lists selected disease models for which iPSC-derived somatic cells have been shown to possess the disease phenotype or which have been used for drug screens or other functional studies (Drews et al., b).

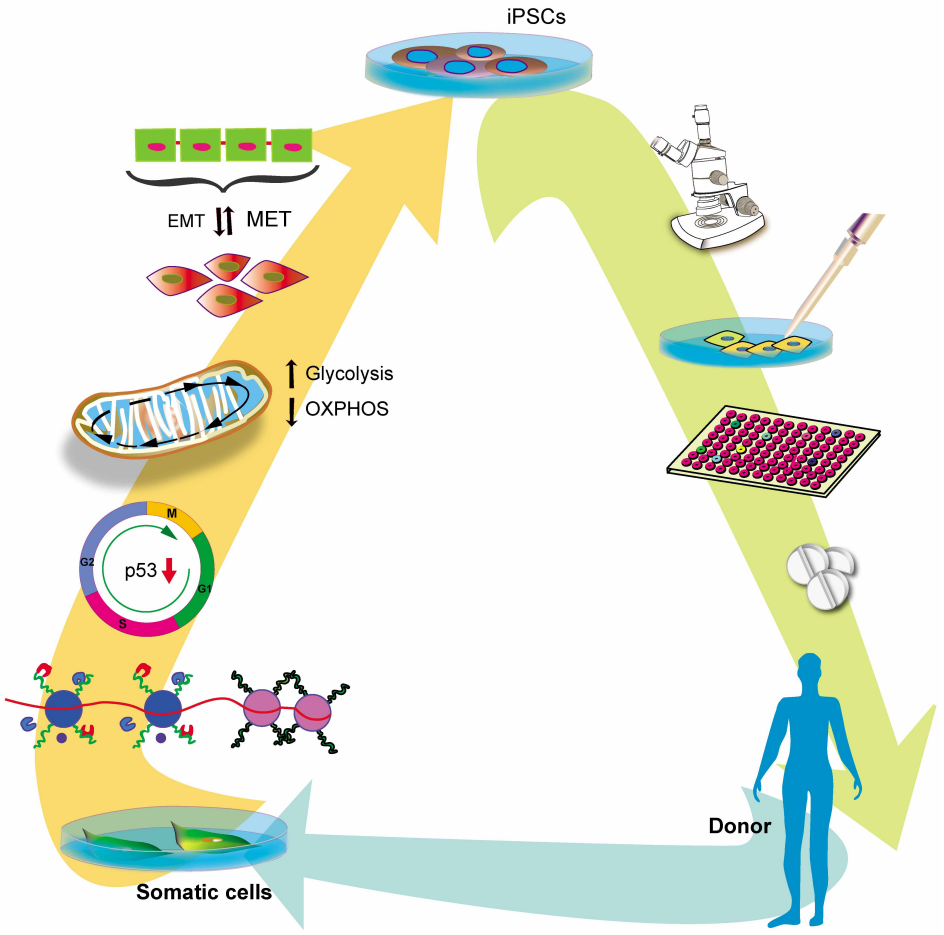

Figure 1.4: Hallmarks of cellular reprogramming and applications of human iPSCs. Somatic cells obtained from any given donor can be reprogrammed to induced pluripotent stem cells (iPSCs) using a number of different techniques. Key molecular events that mark this de-differentiation process include global chromatin remodeling, circumvention of p53-induced cell cycle arrest, reprogramming of mitochondria and, in close context the energy metabolism toward increased glycolysis and decreased mitochondrial oxidative phosphorylation (OXPHOS), and the process of mesenchymal-to-epithelial transition (MET). Once human iPSC lines from healthy or diseased individuals have been established and fully characterized, they offer unprecedented opportunities in personalized regenerative medicine. Human iPSCs are valuable tools for studying early developmental processes, to model human diseases in a dish, thereby enabling the identification of new diagnostic markers and tools and potential new drug targets, and to perform large scale toxicity and drug screens upon differentiation into appropriate other cell types. Eventually, human iPSCs are envisaged to directly treat a particular condition of the donor through cellular replacement therapy, if needed by transplantation of genetically corrected autologous cells. Taken from Drews et al. (b).

Table 1.2: Examples of successful iPSC-based modeling of complex disorders in a dish. Modified from Drews et al. (b).

Disease	Molecular defect	Cells derived from iPSCs	Recapitulated phenotype in iPSCs-derived cells	Drug or functional tests	Reference
Ectoderm					
Spinal muscular atrophy (SMA)	Mutations in *SMN1*	Astrocytes, neurons, mature motor neurons	Yes	Tobramycin and VPA	Ebert et al. (2009)
Parkinson's disease	Mutation in LRRK2 and/or *SNCA*	Dopaminergic neurons	No	Transplanted into rats with Parkinson's disease	Hargus et al. (2010); Park et al. (2008); Soldner et al. (2009); Swistowski et al. (2010)
Parkinson's disease (idiopathic and familial)	Mutation in *LRRK2*	Ventral midbrain dopaminergic neurons	Yes (impaired autophagy)	No	Sanchez-Danes et al. (2012)
Rett's syndrome	Mutation in *MECP2*	Neural progenitor cells	Yes	High dose gentamicin and IGF1	Hotta et al. (2009); Marchetto et al. (2010)
Mucopolysaccharidosis type IIIB	Mutation in *NAGLU*	Differentiated neurons and neural stem cells	Partially	Exogenous NAGLU	Lemonnier et al. (2011)
Schizophrenia	Complex trait	Neurons	Yes	Loxapine	Brennand et al. (2011)

Continued on next page

Table 1.2 – *Continued from previous page*

Disease	Molecular defect	Cells derived from iPSCs	Recapitulated phenotype in iPSCs-derived cells	Drug or functional tests	Reference
X-linked adrenoleukodystrophy (X-ALD), childhood cerebral ALD (CCALD) and adrenomyeloneuropathy (AMN)	Mutation in *ABCD1*	Neurons, oligodendrocytes	Partially	4-phenylbutyrate and lovastatin	Jang et al. (2011)
Retinitis pigmentosa	Mutations in *RP9*, *RP1*, *PRPH2* or *RHO*	Photoreceptor precursors, retinal-pigment epithelial cells, rod photoreceptor cells, retinal progenitors	Yes	Ascorbic acid, α-tocopherol, β-carotene	Jin et al. (2011)
Alzheimer's disease (familial and sporadic)	*APP duplication*	Neurons	Yes	β-secretase inhibitors	Israel et al. (2012)
Mesoderm					
Fanconi's anaemia	*FAA* and *FAD2*	Hematopoietic cells	No (rescued)	No	Raya et al. (2009)
LEOPARD syndrome	Mutation in *PTPN11*	Cardiomyocytes	Yes	No	Carvajal-Vergara et al. (2010)
Type 1 long QT syndrome	Mutation in *KCNQ1*	Cardiomyocytes	Yes	No	Moretti et al. (2010)

Continued on next page

Table 1.2 – *Continued from previous page*

Disease	Molecular defect	Cells derived from iPSCs	Recapitulated phenotype in iPSCs-derived cells	Drug or functional tests	Reference
Type 2 long QT syndrome	Mutation in *KCNH2*	Cardiomyocytes	Yes	Nifedipine, E-4031, pinacidil, ranolazine, cisapride	Itzhaki et al. (2011)
Recessive dystrophic epidermolysis bullosa (RDEB)	Mutation in *COL7A1*	Hematopoietic and non-hematopietic cells	Partially	Gene correction with *Col7a1*	Tolar et al. (2011)
Familial dilated cardiomyopathy	Mutation in *TNNT2*	Cardiomyocytes	Partially	Metoprolol, overexpression of *Serca2a*	Sun et al. (2012)
Huntington disease	Expansion of a CAG trinucleotide repeat in *HTT*	Neurons	Partially (increased lysosomal activity)	No	Camnasio et al. (2012)
Endoderm					
Glycogen storage disease Ia (GSD1a)	Defect in *SLC37A* or absent hepatic glucose-6-phosphatase enzyme	Hepatocyte-like cells (fetal)	Yes	No	Ghodsizadeh et al. (2010); Rashid et al. (2010)
Familial hypercholesterolaemia	Mutation in *LDLR*	Hepatocyte-like cells (fetal)	Yes	No	Rashid et al. (2010)
Wilson's disease	Mutation in *ATP7B*	Hepatocyte-like cells	Yes	Gene correction with *ATP7B*, curcumin	Zhang et al. (2011b)

Continued on next page

Table 1.2 – *Continued from previous page*

Disease	Molecular defect	Cells derived from iPSCs	Recapitulated phenotype in iPSCs-derived cells	Drug or functional tests	Reference
Hepatitis C	Hepatitis C virus (HCV) infection	Hepatocyte-like cells infected with genotype 2a HCV	Yes	Cells supported the HCV life cycle, appropriate aniviral inflammatory response	Schwartz et al. (2012a)
A1AT deficiency	Mutation in *A1AT*	Hepatocyte-like cells	Yes (corrected)	Transplanted into mice with liver injury	Yusa et al. (2011)
Several germ layers					
Down's syndrome	Trisomy 21	Teratoma	Yes	No	Park et al. (2008)
Familial dysautonomia	Mutation in *IKBKAP*	Hematopoietic cells, endothelial cells, central nervous-system and peripheral neurons, endodermal cells	Yes	Kinetin	Lee and Studer (2011)
Friedreich's ataxia (FRDA)	GAA repeat in *FXN*	Cardiomyocytes, peripheral neurons	Partially	No	Liu et al. (2011)

A1AT, α–1–antitrypsin; *ABCD1*, ATP–binding cassette, sub–family D, member 1; *APP*, amyloid–β precursor protein; *ATP7B*, copper–transporting ATPase 2; *CFTR*, cystic fibrosis transmembrane conductance regulator; *COL7A1*, α1–chain of type VII collagen; *FAA*, Fanconi's anaemia, complementation group A; *FAD2*, Fanconi's anaemia, complementation group D2; *FXN*, frataxin; HCV, hepatitis C virus; *HTT*, huntingtin; IGF1, insulin–like growth factor 1; *IKBKAP*, I–κ–B kinase complex–associated protein; *KCNH2*, potassium voltage-gated channel, subfamily H (eag-related), member 2; *KCNQ1*, potassium voltage-gated channel; *LDLR*, low–density lipoprotein receptor; *LRRK2*, leucine–rich repeat kinase 2; *MECP2*, methyl CpG binding protein 2; *NAGLU*, α–N-acetylglucosaminidase; *PRPH2*, peripherin 2; *PTPN11*, protein tyrosine phosphatase, non–receptor type 11; *RHO*, rhodopsin; *RP*, retinitis pigmentosa; *Serca2a*, sarcoplasmic/endoplasmic reticulum calcium ATPase 2; *SLC37A*, solute carrier family 37 (glucose–6–phosphate transporter); *SMN1*, survival of motor neuron 1; *SNCA*, α-synuclein; *TNNT2*, troponin T type 2; VPA, valproic acid. Modified from Drews et al. (b).

A contemporary overview of existing human iPSC lines world-wide, with a focus on disease-specific lines, can be viewed at the International Stem Cell Registry (http://www.umassmed.edu/iscr/index.aspx). As of today there are 232 records of human iPSC lines that could be used in basic research and, eventually, for pre-clinical and clinical application. However, before human iPSCs can be applied in the clinics, it will be essential to obtain a more detailed understanding of the molecular processes involved in cellular reprogramming, to establish efficient, non-integrating reprogramming techniques and to clarify the biological and clinical relevance of mutations that can be induced in the genome of the parental cells. Furthermore, efficient differentiation protocols into mature cell types and high quality purification of defined, terminally differentiated cells need to be developed in order to generate powerful therapeutics and to eliminate the risk of tumor formation upon transplantation. Although hurdles remain before the human iPSCs technology can be utilized as an *in vitro* model system and in the clinics, progress has already been made and the field will benefit from the efforts which are currently being made with respect to on-going and proposed clinical trials of human ESC-derived therapeutic products (Drews et al., b).

1.2.3.3 Recent technical progress in the generation of human iPSCs towards clinical application

One major drawback hampering the utilization of human iPSCs in the clinic is owing to the use of integrating retro- or lentiviruses to generate them. These viruses induce random, unpredictable genetic modifications in the donor cells that could have an impact on the tumorigenicity and differentiation potential of the cells (Takahashi et al., 2007; Yu et al., 2007; Barrilleaux and Knoepfler, 2011). Aiming at the production of putative clinical grade human iPSCs, numerous research groups have tried to modify the iPSC generation protocol with the intention to reduce the number of reprogramming factors and /or vectors required, hence, minimizing or possibly avoiding insertional mutagenesis in the target cells. There has been a stunning wave of articles, that have been published since mouse and human iPSC lines were first established. Due to this abundance of scientific reports, I will particularly focus on publications related to human iPSCs.

One of the early improvements included the development of single polycistronic lentiviral vectors which encode all necessary reprogramming factors in a single piece of integrating DNA (Carey et al., 2009; Somers et al., 2010). Additionally, several groups investigated if such single reprogramming factor cassettes were excisable to offer promising reprogramming tools. These would be efficient with respect to the levels of ectopic transgene expression due to the genomic integration but could be excised out of the target cells' genomes once the reprogramming process is accomplished. Following this strategy, Somers and colleagues reported successful generation of human iPSCs free of reprogramming factor sequences using loxP-flanked lentiviruses that could be removed from the iPSCs' genomes by subsequent expression of the Cre recombinase (Somers et al., 2010). Yet, despite the targeted excision of the transgene sequences, one of the inherent disadvantages of the Cre/*lox*P recombination

system is that it leaves one of the two *lox*P sites flanking the transgene behind, thereby, still modifying the genome (Nagy, 2000; Somers et al., 2010). Another approach to remove transgene sequences upon induction of pluripotency in somatic cells involves the use of class II transposable elements, namely *piggyback* transposons. Transfection of doxycycline-inducible reprogramming factor-encoding transposons successfully enabled the generation of human iPSCs, however, the excision of the transgenes from iPSCs to produce footprint-free iPSCs has only been demonstrated in murine cells to date (Kaji et al., 2009; Woltjen et al., 2009).

In contrast, the use of non-integrating expression systems such as transduction of reprogramming factor-encoding adenoviruses (Zhou and Freed, 2009) or repeated transfection of expression plasmids (those lentiviral vectors used to generate the first iPSCs by overexpression of OCT4, SOX2, NANOG and LIN28 (Yu et al., 2007)) (Si-Tayeb et al., 2010) yielded human iPSCs without DNA integration. Furthermore, Yu et al. (2009) succeeded in generating human iPSCs by electroporation of combinations of large episomal plasmids. These did not integrate into the genome, instead, remained in the cells as self-replicating episomes and were successively diluted with pro-longed culture periods and progressive cell divisions. Hence, these plasmids facilitated efficient transgene expression during the reprogramming process while being absent in the established iPSC lines (Yu et al., 2009). Similar results were obtained by Chou et al. (2011) later on, who constructed an improved episomal plasmid. Recently, deep whole-genome sequencing was used to demonstrate that episomal-derived iPSCs do not harbor integration events (Cheng et al., 2012). One of the latest published methods to induce pluripotency in human somatic cells on the basis of putatively non-integrating DNA vectors included repeated nucleofections of minicircle DNAs encoding the reprogramming factors (Jia et al., 2010). One of the major drawbacks of these methods, however, is the necessity of the DNA to translocate to the nucleus of the target cells to be transcribed. This still poses a certain risk of random integration into the genome.

To avoid this, Fusaki and co-workers transduced human fibroblast cells with Sendai viruses, an RNA-based virus, which does not require access to the nucleus of the host cell to produce the encoded transgenes (Fusaki et al., 2009). While the field has advanced, novel reprogramming techniques have been developed including repeated treatment of human newborn fibroblasts with recombinant reprogramming factor proteins fused with a sequence of nine arginines, which served as cell-penetrating peptide, thereby, demolishing the risk of genomic insertions (Kim et al., 2009a). Moreover, delivery of messenger RNAs (mRNAs) of the reprogramming factors induced up-regulation of pluripotency-associated genes in human somatic cells (Plews et al., 2010; Yakubov et al., 2010) and ultimately lead to the generation of fully reprogrammed human cells (Warren et al., 2010). The most recent published progress was reported by Anokye-Danso et al. (2011) and Anokye-Danso et al. (2011), who expressed human ESC-specific miRNAs instead of the well established set of reprogramming factors to induce pluripotency in somatic cells. While Anokye-Danso et al. (2011) made use of constitutive lentiviruses to express the miR-302/367 cluster, Anokye-Danso et al. (2011) repeatedly transfected the miRNAs mimics miR-200c together with the miR-302 and miR-369 clusters. Interestingly, since these non-integrating reprogramming approaches have first been published the stream of follow-up

reports has markedly diminished indicating that their reproduction and the development of improved methods are coupled with difficulties.

Along the search for novel techniques to induce pluripotency in somatic cells, research groups have also been focusing on finding ways to increase the yield of fully reprogrammed cells in less time, while potentially reducing the number of required reprogramming factors. The two main routes to accomplish this goal resemble (i) the identification of small molecules that modify distinct signaling pathways involved in the acquisition of the pluripotent state, e.g. epigenetic remodeling, MET or metabolic pathways, as mentioned above, and (ii) the choice of cell type to reprogram which defines the developmental starting point. With regards to the latter aspect, it can be assumed that cells at different developmental stages require more or less powerful strategies to enter the pluripotent state. Accordingly, it has been shown, for example, that human and mouse neural stem cells, which express *SOX2*, *KLF4* and *c-MYC* in abundance, can be reprogrammed with only OCT4 instead of the original set of four reprogramming factors (Kim et al., 2009b,c; Medvedev et al., 2011). It is further conceivable, that the combination of both aspects, i.e. the use of cells amenable for reprogramming plus supporting chemical conditions, would tremendously alleviate cellular reprogramming processes. Along these lines, Huangfu et al. (2008) demonstrated that the addition of valproic acid (VPA), a substance involved in epigenetic remodeling processes, increased the number of ESC-like colonies generated by transduction of only three reprogramming factors (OCT4, SOX2 and KLF4) in human fibroblasts by 10- to 20-fold. Furthermore, VPA treatment facilitated the induction of pluripotency even if only OCT4 and SOX2 were ectopically expressed (Huangfu et al., 2008). Similarly, we were able to show that the combination of VPA together with 8-bromoadenosine 3', 5'-cyclic monophosphate (8-Br-cAMP), an analog of cyclic AMP (cAMP), synergistically increased the yield of iPSCs by 6.5-fold (Wang and Adjaye, 2011). Esteban et al. (2010) reported enhanced efficiency of human adipose stem cell reprogramming by treatment with VPA and vitamin C. Transient inhibition of TGFβ and MAPK/ERK pathways by combination of the ALK4/5/7 inhibitor SB431542 with the MEK inhibitor PD0325901 together with thiazovivin, a compound that increases survival of clonal human ESCs, was shown to increase reprogramming efficiency in human fibroblasts by approximately 200-fold (Lin et al., 2009). Similarly, the GSK-3 inhibitor CHIR99021 together with Parnate (also known as tranylcypromine), an inhibitor of lysine-specific demethylase 1, enabled the induction of pluripotency in human neonatal keratinocytes transduced with only OCT4 and KLF4 (Li et al., 2009c). In a follow-up study, Sheng Ding and colleagues found PS48, an allosteric activator of 3'-phosphoinositide-dependent kinase-1 (PDK1), combined with sodium butyrate (NaB, a histone deacetylase inhibitor) to enhance the efficiency of iPSC generation from two factor-transduced (OCT4 and KLF4) neonatal human keratinocytes (Zhu et al., 2010). In addition to that, they were able to establish a protocol based on chemical treatments including NaB, PS48, A-83-01 (another TGFβ/Activin A/Nodal receptor inhibitor) and PD0325901 as well as CHIR99021 and Parnate over defined periods of time to reprogram neonatal human keratinocytes, adult human keratinocytes and other human somatic cells by transduction of only one reprogramming factor—OCT4 (Zhu et al., 2010). Likewise, Yu et al. (2011) enhanced episo-

mal reprogramming efficiency using a cocktail containing A-83-01, PD0325901, CHIR99021, ROCK inhibitor HA-100 and human leukemia inhibitory factor (hLIF). Zhao et al. (2008) reported 100-fold increased reprogramming efficiency by adding two additional factors, *UTF1* and an siRNA against the gene *TP53*, which encodes the tumor suppressor protein p53, to the OSKM mix of reprogramming factors. Subsequently, a series of five reports was published in *Nature*, volume 460, highlighting that direct or indirect down-regulation of p53 enhanced cellular reprogramming events in mouse and human somatic cells (Hong et al., 2009; Kawamura et al., 2009; Li et al., 2009b; Marion et al., 2009; Utikal et al., 2009b). Accordingly, we could also show that the transient down-regulation of p53 is likely to be one of the mechanisms leading to an increased efficiency of inducing pluripotency in fibroblast cells following the above mentioned, combined treatment with VPA and 8-Br-cAMP (Wang and Adjaye, 2011).

As the identification of other molecules supporting cellular reprogramming requires insight into the mechanisms underlying cellular reprogramming, the quest for eligible small molecule cocktails continues as the field advances. In this respect, the development of drug-inducible lentiviral vectors which allow reproducible generation of homogeneous, so-called 'secondary' human iPSCs (reprogramming of somatic cells to iPSCs, differentiation of these iPSCs to somatic cells, 2nd round of reprogramming of the iPSC-derived somatic cells) with 100-fold higher efficiency when compared to first round iPSC generation should prove useful for studies of kinetics and mechanisms underlying cellular reprogramming as well as for screening the potential of small molecules in increasing reprogramming efficiency (Maherali et al., 2008; Hockemeyer et al., 2008).

As a result of all the efforts that have been made in the iPSC field, a variety of more or less terminally differentiated human cell types have been reprogrammed to an embryonic-like state besides the original publications based on fetal, neonatal and adult human fibroblasts as well as fibroblast-like synoviocytes from synovial tissue (Takahashi et al., 2007; Yu et al., 2007). As partly mentioned above, these include, for instance, lung fibroblasts (Haase et al., 2009), neonatal and adult keratinocytes (Aasen et al., 2008; Li et al., 2009c; Zhu et al., 2010), melanocytes (Utikal et al., 2009a), human umbilical vein endothelial cells (Zhu et al., 2010), cord blood-derived cells (Haase et al., 2009; Chou et al., 2011; Yu et al., 2011) and adult peripheral blood cells (Loh et al., 2009; Chou et al., 2011; Kunisato et al., 2011), cells derived from adipose tissue (Sun et al., 2009; Esteban et al., 2010; Miyoshi et al., 2011; Yu et al., 2011), pancreatic islet β cells (Bar-Nur et al., 2011), hepatocytes (Ohi et al., 2011), retinal-pigmented cells (Hu et al., 2010b) and fetal neural stem cells (Medvedev et al., 2011). Besides the advances in refining reprogramming techniques, the development of feeder-free and xeno-free iPSC derivation strategies further drive potential clinical applications of human iPSCs forward (Rodríguez-Pizà et al., 2010; Ross et al., 2010; Sugii et al., 2010; Yu et al., 2011).

In view of the rapid recent progress that has been made within the last four years it can be assumed that, from a technical point of view, genetically unimpaired human iPSCs could soon be generated with high efficiency. However, as mentioned above, an in-depth biological understanding of the reprogramming process itself and the properties of human iPSCs are required before human iPSCs could actually find their way into the clinics. Consequently, basic

research with respect to human iPSCs and ESCs, as an essential reference, the gold standard of human PSCs, will need to be perpetuated.

1.3 Human amniotic fluid cells

Human amniotic fluid cells (AFCs) are obtained from the amniotic cavity of a developing fetus in a procedure called amniocentesis. During folding of the embryo, the amniotic cavity successively encloses the entire embryo. It fills with fluid and fills out and fuses with the chorion by 4 to 8 weeks of gestation (Figure 1.5 (A)). Initially, fluid is transported across the amniotic membrane. At later stages of gestation fetal urine contributes to the composition of amniotic fluid as well. As blood plasma, human amniotic fluid comprises metabolic byproducts, yet, additionally it contains cells of fetal origin, putatively shed from different tissues such as skin, the urogenital, respiratory and digestive systems as well as cells from the amnion depending on the gestational age and potential fetal pathologies (Hoehn and Salk, 1982; Prusa and Hengstschlager, 2002; Schoenwolf et al., 2008). Amniocentesis is one of four main techniques used in prenatal pediatrics (Schoenwolf et al., 2008). It is normally performed during 14 to 16 weeks of gestation (Figure 1.5 (B)) to detect, for instance, chromosomal aberrations or infections and to evaluate lung maturity amongst others by examining the cells, metabolites or other constituents of the fluid withdrawn (Schoenwolf et al., 2008).

1.3.1 Biological characteristics of human AFCs

Although the isolation of human AFCs for prenatal diagnostic purposes can be traced back to the year 1956 (Sachs et al., 1956), considerably little has initially been published on the biological features of these cells. Only within the last two decades molecular biology-based studies have revealed remarkable features of human AFCs. In 1999, for instance, activity of the telomere-elongating enzyme telomerase, an essential prerequisite for human ESC self-renewal, was detected in young AFCs, yet, with decreasing activity in aged AFCs (Mosquera et al., 1999). Likewise, the presence of cells exhibiting certain human ESC features, including expression of the key pluripotency-associated transcription factor OCT4, among bulk primary AFCs has been reported (Prusa et al., 2003; Karlmark et al., 2005). Due to the heterogeneity of AFCs and varying selection procedures during *in vitro* cell culture, some of the more recently published data are different from previous findings. In 't Anker et al. (2003), for example, demonstrated the existence of mesenchymal stem cells (MSCs), a certain adult stem cell type, within the amniotic fluid. De Coppi et al. (2007) confirmed several earlier findings to some extent by highlighting that clonal amniotic fluid cell lines are capable of self-renewal for about 250 passages *in vitro*, express some embryonic but also adult stem cell markers and have the potential to differentiate into functional derivatives of all three embryonic germ layers *in vitro*. For this reason, they describe human AFCs as broadly multipotent. Likewise, Kim et al. (2007) stated that some of the AFCs have stem cell-like immunophenotypes and expression profiles. They also suggest these cells also to have multi-lineage differentiation potential, however, they refer to these cells as 'pluripotent stem cells'. The same group reported senescence of their

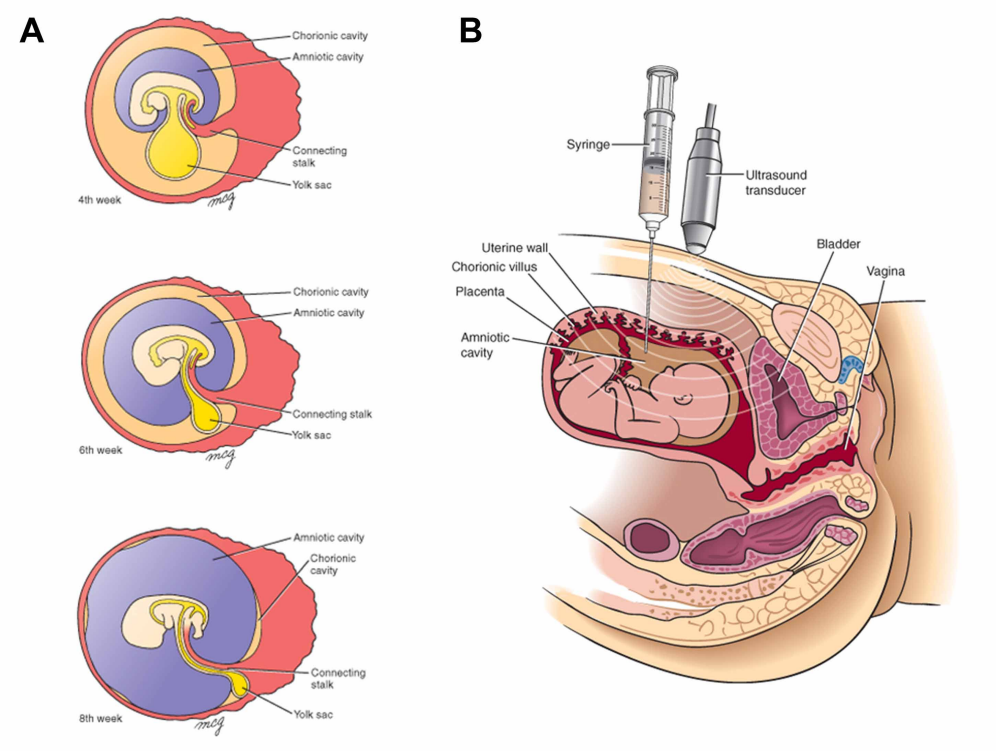

Figure 1.5: Expansion of the amniotic cavity and amniocentesis. (A) The rapidly expanding amniotic cavity fills with fluid and obliterates the chorionic cavity between weeks four to eight (B) Schematic illustration of amniocentesis. Guided by ultrasound the amniotic cavity is punctured and a volume of approximately fifteen to twenty milliliters of amniotic fluid is withdrawn for down-stream analysis. Modified from Schoenwolf et al. (2008).

human amniotic fluid-derived stem cells after about 27 passages *in vitro* which proves against true self-renewal capacities and, hence, pluripotency of these cells. Aside from that, Iacovitti et al. (2008). could not generate functional dopamine neurons from AFCs *in vitro* or after transplantation *in vivo*. Furthermore, AFCs have not been shown to induce teratomas to date (De Coppi et al., 2007; Li et al., 2009a; You et al., 2009) suggesting that these cells are not truly pluripotent.

As the composition of the amniotic fluid samples varies between different individuals and depending on the gestational age at the time of isolation (Prusa and Hengstschlager, 2002), a thorough biological characterization of human AFCs is rather impossible. However, further studies are required to integrate the existing data and to decipher the existence of distinct subpopulations of stem cell-like cells within human amniotic fluid.

1.3.2 The potential of human AFCs in regenerative medicine

With respect to potential application of human AFCs, multipotent properties (Chiavegato et al., 2007; De Coppi et al., 2007; Wang et al., 2008; Ditadi et al., 2009) and potential immune-privileged characteristics of particular subpopulations of AFCs (Fauza, 2004; Walther et al., 2009) support the notion that amniotic fluid is a suitable source of fetal stem cells with po-

tential use in regenerative medicine, especially in fetal tissue engineering approaches (Fauza, 2004). However, the relatively early onset of senescence in bulk primary cultures of human AFCs (Wolfrum et al., 2010; Kim et al., 2007) impedes their application in clinical settings. Moreover, as the capacity of AFCs to form specialized cell types and to contribute to the formation of certain tissues or organs *in vitro* and in xenotransplantation experiments *in vivo* is a subject of debate (Chiavegato et al., 2007; Cipriani et al., 2007; De Coppi et al., 2007; Perin et al., 2007; Carraro et al., 2008; Iacovitti et al., 2008; Trovato et al., 2009; Gekas et al., 2010; Yeh et al., 2010), the differentiation potential of human AFCs generally seems to be restricted when compared with human PSCs, thus, further limiting feasible applications.

1.4 Aim of this work

Driven by the intention to provide a more detailed understanding of the molecular-biological characteristics of putatively clinically relevant human iPSCs, we sought to exploit the stem cell-like characteristics of distinct human AFC subpopulations in order to mediate efficient cellular reprogramming even without genetic modification of the target cells. As a result of re-setting the developmental clock in human AFCs, their limited proliferation and differentiation potential should be enhanced to the levels of PSCs. Furthermore, the establishment of viral and non-viral-derived human iPSCs from the same donor cells would allow for comparative studies of human iPSCs with identical genetic background with respect to the effects of viral integrations on self-renewal and pluripotent differentiation potential.

- Hence, this PhD thesis first aimed at inducing pluripotency in human AFCs using the robust protocol of retroviral overexpression of the reprogramming factors OCT4, SOX2, KLF4 and c-MYC.
  - To putatively enhance the efficiency of this process, stem cell-like subpopulations should be sorted from bulk primary AFCs and used as target cells for cellular reprogramming.
  - The generation of amniotic fluid-derived iPSCs should be followed by an in-depth characterization.
  - Furthermore, the resulting human iPSCs should be used to study the role of a recently identified pluripotency-associated gene, *USP44*, including human ESCs as a reference.
- Subsequently, this project was designed to reprogram the original stem cell-like subpopulations of human AFCs using alternative, non-integrating techniques, followed, in turn, by a detailed characterization of the amniotic fluid-derived iPSCs.

2

Materials and Methods

2.1 Ethics statement

Auxiliary samples of human AFCs obtained during routine amniocentesis after written informed consent were kindly donated by Prof. Dr. Wegner and PD Dr. Stumm (Zentrum für Pränataldiagnostik, Kudamm-199, Berlin, Germany) and passed on by the laboratory of Prof. Dr. Sperling, Institute of Human Genetics, Charité - Universitätsmedizin Berlin. Utilization of these cells was approved by the ethics commission of the Charité Universitätsmedizin Berlin.

2.2 *In vitro* cell culture conditions

All procedures involving mammalian cell culture were carried out under aseptic conditions on laminar flow clean benches (HERAsafe HSP12, Heraeus, Thermo Fischer Scientific, Waltham, MA, USA). Cells were incubated in a humidified 5 % CO_2 / 95 % air atmosphere at 37 °C (Innova CO-170 Incubator, New Brunswick Scientific, Edison, NJ, USA).

2.2.1 Maintenance of non-pluripotent human cell lines

Human AFCs were obtained as aliquots of frozen cells at approximately passage 2 (P2). For the initial culture period (up to P5) AFCs were grown in AmnioMAX-C100 (Invitrogen/Life Technologies, Grand Island, NY, USA). Subsequently, AFCs were cultured in what is henceforth referred to as 'DeCoppi medium' (De Coppi et al., 2007) (Section A.1). Human foreskin fibroblasts (HFF1 and BJ, SCRC-1041 and CRL-2522 from ATCC, respectively) as well as HEK293 (CRL-1573, ATCC) and Phoenix amphotropic 293 cells (PA cells, SD-3443, ATCC) were maintained in DMEM (Gibco/Life Technologies) containing 10 % fetal bovine serum (FBS, Biochrom, Berlin, Germany). Growth media were replaced every 2 to 3 d. All cell lines were routinely passaged when 80-90 % confluent. To this end, cells were washed twice with PBS devoid of Ca^{2+} and Mg^{2+} and treated with 2 ml 0.05 % Trypsin/EDTA (Gibco) per T75 culture flask (TPP, Trasadingen, Switzerland) for 5 min at 37 °C. Tryptic activity was terminated by the addition of at least one volume fresh medium containing FBS. Cells were further detached from the flask by pipetting and collected, followed by 5 min centrifugation at 300 × g.

The supernatant was completely aspirated, the cell pellet was resuspended in complete optimal medium and re-plated at ratios of 1:3 to 1:6.

2.2.1.1 Cryopreservation and thawing of non-pluripotent human cell lines

To cryopreserve non-pluripotent human cell lines, cell monolayers were harvested by 0.05 % Trypsin/EDTA-treatment as during routine passaging. Cell pellets were then resuspended in cold freezing medium (Section A.1), dispensed into a suitable number of freezing vials (TPP) and kept in a pre-cooled (at 4 °C) freezing container ('Mr. Frosty', Nalgene/Thermo Fischer Scientific) at −80 °C ON to ensure a cooling rate of −1 °C/min. The following day, vials of frozen cells were transferred into liquid nitrogen for long-term storage.

To recover frozen cells, the desired number of vials were thawed quickly in a 37 °C water bath until only a few ice crystals remained. The cell suspension was then immediately transferred into 10 ml of the respective warm growth medium drop-wise. After mixing, cells were pelleted by centrifugation at 300 × g for 5 min, resuspended in fresh complete optimal medium and seeded with respect to suitable splitting ratios.

2.2.2 Human PSC culture conditions

To exploit the full potential of human ESCs or iPSCs it is crucial to maintain their undifferentiated state even during long-term culture *in vitro*. Ever since human ESCs were first established (Thomson et al., 1998), mouse embryonic fibroblasts (MEFs) have been widely used due to their highly efficient support of the undifferentiated growth of human pluripotent stem cells (PSCs). Thus, human PSCs cultured in the course of this PhD project were usually maintained and expanded on a layer of mitotically-inactivated MEFs, especially after thawing. However, human PSCs were switched to feeder-free conditions prior to performing experiments to assess human PSC characteristics. The protocol of human PSCs culture described herein combines methods adapted from several published protocols (Thomson et al., 1998; Xu et al., 2001; Du and Zhang, 2010) and applies to the culture of H1 and H9 (WiCell Research Institute, Madison, WI, USA) human ESCs on one hand and AFiPSCs, which were derived in the course of this PhD project, on the other hand.

2.2.2.1 Isolation and maintenance of MEFs

MEF isolation from pregnant CF-1 mice (Harlan Laboratories, Indianapolis, IN, USA) was performed following the detailed protocol, which is currently being published by our laboratory (Jozefczuk et al.). Freshly isolated MEFs were grown in MEF medium (Section A.1), which was replaced 1 d post-isolation and every other day henceforth. At 80-90 % confluency, P0 cells were either frozen or expanded for a maximum of four to five passages. Before the onset of senescence MEFs were mitotically inactivated and utilized as feeder cells to support the undifferentiated growth of human PSCs either as a basal cell layer in a co-culture system or in the form of MEF-conditioned medium (CM).

2.2.2.2 Passaging, cryopreservation and thawing of MEFs

To split MEF cultures, MEFs were trypsinized as described above for non-pluripotent human cell lines. During the early passages MEFs were re-plated at ratios of up to 1:6. However, the splitting ratio was reduced to 1:2 or 1:3 after P3. To cryopreserve MEFs, the cell pellet obtained by the passaging procedure was resuspended with cold freezing medium (Section A.1) and divided into a suitable number of freezing vials (TPP, e.g. half of the cells of a T150 flask per vial). As described before, these aliquots were kept at −80 °C ON before being transferred to liquid nitrogen.
Thawing of MEFs was carried out as described for non-pluripotent human cell lines.

2.2.2.3 Mitotic inactivation of MEFs and plating for downstream applications

Mitotic inactivation of MEFs by mitomycin C-treatment was carried out following the detailed protocol, which is currently being published by our laboratory (Jozefczuk et al.).
If used as a feeder cell layer, freshly inactivated MEFs or frozen feeder cells were plated onto Matrigel-coated 6-well plates (TPP, for Matrigel preparations and coating of labware refer to Section A.1) at a density of 0.2×10^6 or 0.23×10^6 cells per well, respectively, in MEF medium the day before needed for human PSC culture.

If to be used for preparing CM, freshly inactivated MEFs are seeded into T150 cell culture flasks coated with 0.2 % gelatine (from bovine skin, Sigma, autoclaved, 0.2 µm filter-sterilized) for a minimum of 1 h at a density of 56,000 cells / cm^2 and incubated for 24 h at 37 °C before the production of MEF-CM was initiated.

2.2.2.4 Preparation of MEF-CM

Preparation of MEF-CM was carried out following the detailed protocol, which is currently being published by our laboratory (Jozefczuk et al.). FGF2 (4 ng/ml, Peprotech, Rocky Hill, NJ, USA) was added directly before its utilization for culturing human PSCs.
During the second half of this PhD project, MEF isolation, culture, inactivation and preparation of CM were done by Elisabeth Socha, the technical assistant of the laboratory.

2.2.2.5 Feeder-dependent maintenance of human PSCs

One day after plating feeder cells onto Matrigel-coated 6-well cell culture plates they were washed three times with Ca^{2+}/Mg^{2+}-free PBS. Next, unconditioned human ESC medium (UM) supplemented with FGF2 was added to the wells and human ESCs or AFiPSCs were seeded onto these feeder cells. Nutrient-depleted medium was replaced daily.

Once the human PSC colonies took up 80-90 % of the well and contacted each other (normally within 7 to 10 d), human PSCs were passaged by a combination of enzymatic and mechanical splitting techniques and re-seeded at a ratio of up to 1:4. To this end, the culture plates were taken to a semi-open clean bench (HERAguard HPH9, Heraeus, Thermo Fischer

Scientific Inc.) with a stereomicroscope (MZ9.5, LEICA, Vashaw Scientific Inc.) placed in it. There, the majority of spontaneously differentiated cells (readily identifiable due to the formation of less compact colonies with irregular shapes and stronger light scattering properties when compared to human PSCs) were manually removed from the cultures using sterile 10 to 20 µl pipet tips (SafeSeal-Tips, Biozym, Hessisch Oldendorf, Germany). Back at the laminar flow cabinet, floating cell aggregates were aspirated, 1 ml Collagenase IV (Roche, 1 mg/ml in UM, 0.2 µm filter-sterilized) added per well of a 6-well cell culture plate (6-well) and the cells were incubated at 37 °C for 20 to 30 min. During this time the feeder cells detached from the plate and the edges of human PSC colonies curled up. Following this incubation the colonies were completely dislodged from the plate using a sterile cell lifter (TPP) and carefully collected in a 15 ml tube (Corning). The human PSC colonies settled down within a few minutes. At this point the supernatant was aspirated and the cells were washed with 3 to 4 ml of fresh UM. Washing was repeated two more times. Meanwhile human PSC colonies were dissociated by pipetting the clumps up and down approximately three times. Following the last washing step, the supernatant was aspirated once more, fresh UM was added to the cells and the cell suspension was transferred into an appropriate number of Matrigel-coated wells prepared with feeder cells as described above. During the entire period of manipulation and splitting the human PSCs were kept at 37 °C from time to time to ensure sufficient warming of the cells.

2.2.2.6 Feeder-free maintenance of human PSCs

Under feeder-free conditions human PSCs were maintained on 6-well cell culture dishes precoated with Matrigel (Growth factor reduced, BD, Section A.1) in MEF-CM or commercially available chemically defined human ESC media, e.g. N2B27 (Invitrogen) or mTeSR1 (STEMCELL Technologies, Vancouver, BC, Canada) as indicated. Medium was changed daily until the colonies become 80-90 % confluent.

Splitting of human PSCs in feeder-free conditions was done as follows: First, spontaneously differentiated human PSC colonies were manually removed as described above. The remaining human PSC colonies were cut into equally large squares using a BD Microlance 3 injection needle (ca. 19 G, BD). Next, the medium including floating cell clusters was aspirated and the cells were washed with Ca^{2+}/Mg^{2+}-free PBS once before 1 ml of Dispase solution (Gibco, 5 mg/ml in Knockout DMEM, 0.2 µm sterile-filtered) was added to each well. The plate was incubated at 37 °C for 3 to 4 min until the edges of the colony pieces lifted up while the centers of the cell clusters remained attached to the plate. At this point the cells were gently washed three times with UM to remove any residual Dispase. Subsequently, the human PSC aggregates were completely detached from the bottom of the cell culture dish using a cell lifter, collected in 15 ml tubes and pelleted by centrifugation at 200 × g for 15 s. The resulting pellet was gently resuspended in pre-warmed, fresh CM (or defined medium) and dispensed into Matrigel-coated plates at a ratio of up to 1:4. During the entire period of manipulation and splitting human PSCs were kept at 37 °C from time to time to ensure sufficient warming of the cells.

2.2.2.7 Cryopreservation and thawing of human PSCs

To cryopreserve human PSCs, they were split according to the appropriate one of the two above described methods. Fragments of human PSC colonies were slightly larger than those obtained during routine passaging procedures to warrant high cell viability after thawing. Human PSC colony pieces were resuspended in human PSC freezing medium (Section A.1), aliquoted into freezing vials and immediately kept at −80 °C in a pre-cooled freezing container before being transferred to liquid nitrogen the next day.

Human PSCs were quickly thawed in a 37 °C water bath. Immediately afterwards, the colonies were transferred drop-wise into 10 ml of warm UM, followed by centrifugation for 15 s at 200 × g. The medium, containing DMSO, was completely aspirated and fresh UM added to dispense the colonies into the appropriate amount of Matrigel-coated wells prepared with a layer of mouse feeder cells washed and covered with UM. It could take up to two weeks for colonies to emerge and grow. Until colonies were ready to be passaged, UM was exchanged daily and, if necessary, switched to CM after 10 days (once the mitotically-inactivated feeder cells were exhausted).

2.3 Basic molecular biology methods

2.3.1 RNA isolation

For comparative gene expression analysis ESCs and AFiPSCs were adapted to feeder-free culture conditions in mTeSR1 (Stemcell Technologies, Vancouver, BC, Canada). All other cell lines were maintained in their respective growth medium.

Total RNA was isolated from cell lysates using the RNeasy Mini Kit (Qiagen, Germantown, MD, USA) according to the manufacturer's instructions. Cells were either directly lysed on the cell culture plate or trypsinized, pelleted by centrifugation and subsequently lysed using the lysis buffer RLT provided by the manufacturer including β-mercaptoethanol (Sigmal, 10 µl per 1 ml buffer); all samples of one experiment were treated as equal. The optional on column DNase I-treatment was included in the isolation procedure.

2.3.2 Measuring RNA concentration and assessing RNA integrity

Concentrations of the resulting RNA eluates were determined by UV spectrophotometric measurements using the NanoDrop (NanoDrop Technologies, Wilmington, DE, USA) at 260 nm. RNA quality was assessed by measurements at 280 nm/260 nm and 260 nm/230 nm (both ratios must be > 1.8). 1 % agarose (Roth, Karlsruhe, Germany) gel electrophoresis of total RNA had to reveal a 2:1 ratio of sharp 28 S vs. 18 S ribosomal RNA bands without apparent smears especially at low molecular weights. In a few cases, the Agilent RNA 6000 Nano Kit (Agilent, Santa Clara, CA, USA) was employed to assess RNA quality.

2.3.3 cDNA synthesis

For M-MLV (Affymetrix/USB Corporation, Cleveland, OH, USA)-driven reverse transcription 1 to 1.5 µg RNA, but equal amounts for all samples to be compared, were diluted to 9.5 µl with RNase/DNase-free distilled water (Gibco). cDNA synthesis was primed by oligo-dT annealing to the poly A-tail of the mRNAs. To this end, 0.5 µl oligo-dT (1 µg/µl, 15mer) were added, the mixture was incubated at 72 °C for 5 min and cooled down on ice. Meanwhile, a reverse transcription master mix was prepared as follows (per reaction):

RNase/DNase-free dH2O (Gibco)	9.4 µl
5 X M-MLV reaction buffer (USB)	5.0 µl
dATP, dCTP, dGTP, dTTP mix (25 mM each, USB)	0.5 µl
M-MLV (USB)	0.1 µl

15 µl of this master mix were added to each RNA/oligo-dT sample, followed by incubation at 42 °C for 1 h and inactivation of the enzyme at 65 °C for 10 min. The resulting cDNA was kept at 4 °C for direct use or stored at −20 °C.

2.3.4 Quantitative real-time polymerase chain reaction (qRT-PCR) and data analyses

Small scale gene expression studies were based on qRT-PCR. All primer sequences are provided in Table A.3. For each target gene (and a house keeping gene (*ACTB*, *GAPDH*) as endogenous control for normalization) technical triplicates of all samples were amplified; an additional triplicate served as negative control (no template control, NTC). Target gene-specific reaction master mixes were prepared as follows (per reaction):

ddH2O	2 µl
fwd/rev primer mix (5 µM each)	1 µl
SYBR Green PCR Master Mix (Applied Biosystems)	3 µl

For each reaction, 6 µl of this mix were pipetted into one well of an ABI PRISM 384-Well Optical Reaction Plate (Applied Biosystems) and 2 µl of 1:8 to 1:12-diluted M-MLV-synthesized cDNA template were added. The PCR was performed on the ABI 7900HT Fast Real-Time PCR System (Applied Biosystems, Foster City, CA, USA) using the default PCR cycle protocol (Section A.3). Dissociation curve analysis was included at the end of each PCR cycle.

Data analysis was carried out using the ABI PRISM SDS 2.2.1 software (Applied Biosystems) and Microsoft Excel (Microsoft Corporation, Redmond, WA, USA). Housekeeping gene-normalized, relative mRNA levels of each gene were calculated based on the $2^{-\Delta\Delta C_T}$ Method (Livak and Schmittgen, 2001). Data are presented as mean LOG2 ratios with respect to biological controls and standard deviation.

2.3.5 Illumina bead chip hybridization and data analyses

Global gene expression analysis was carried out on the Illumina microarray platform. For each sample, 500 ng quality-checked total RNA were used as input for the amplification and biotin labeling reactions (Illumina TotalPrep RNA Amplification Kit, Ambion, Austin, TX, USA), which precede bead chip hybridizations. Briefly, the mRNA present in the samples was used as template to generate first and second strand cDNA. After degradation of all RNAs, this cDNA, in turn, served as template to synthesize biotinylated antisense RNA copies (cRNA) of the original mRNA. Purified cRNA was hybridized to Illumina HumanRef-8 v3 Expression BeadChips (Illumina, San Diego, CA, USA) on the Illumina Beadstation 500 platform followed by washing and blocking of the samples, staining with streptavidin-Cy3 and quantitative detection of the resulting fluorescent array image. RNA preparations and hybridizations were carried out by Aydah Sabah and Claudia Vogelgesang of the Illumina Microarray Core Facility of the Max Planck Institute for Molecular Genetics.

The resulting gene expression data were background subtracted and normalized on the basis of the 'rank invariant' algorithm of the Gene Expression Module version 1.8.0 provided with the GenomeStudio software (formerly BeadStudio, Illumina). An arbitrary cut-off value was set to eliminate negative gene expression signals, which may have resulted from background subtraction. GenomeStudio calculates a 'Detection p-value' for every gene by comparing its signal intensity with that of negative control beads to determine the probability that this gene is expressed. For the generation of Venn Diagrams and to carry out correlation coefficient analyses, the normalized data sets were filtered for genes present in either sample or in at least one of the samples under investigation ('Detection p-value'/$p_{det} < 0.01$). Differential gene expression was computed using the 'Illumina Custom Model' (Kuhn et al., 2004). Resulting 'Diff p-values' (p-value, describing the probability that a gene's signal intensity has changed between two samples or groups of samples) were adjusted by the Benjamini and Hochberg false discovery rate (FDR) correction algorithm (Benjamini and Hochberg, 1995). To be considered differentially expressed, genes had to be at least 1.5 fold up- or down-regulated between the samples of interest and the corresponding FDR-adjusted 'Diff p-value' had to be $p_{adj} < 0.05$.

Functional annotation and enrichment analyses were performed using the DAVID platform version 6.7 (http://david.abcc.ncifcrf.gov/home.jsp) (Dennis et al., 2003; Huang da et al., 2009). Illumina ProbeIDs or official gene symbols were used as input against the background of Homo sapiens; analyses were executed based on DAVID default parameter settings. Graphical representation of the transcriptome data with respect to distinct cellular processes was achieved through the KEGG database (Kanehisa and Goto, 2000). The AmiGO Browser version 1.7 of the Gene Ontology database (http://www.geneontology.org) (Ashburner et al., 2000) was utilized in addition to the publication by Vaziri et al. (Vaziri et al., 2010) to derive the list of human senescence-associated genes. Interferon-regulated genes were identified with the help of the Interferome database (Samarajiwa et al., 2009). Heatmaps were either created using the MultiExperiment Viewer software (MeV v4.4.1, http://www.tm4.org/mev/) (Saeed et al., 2003, 2006) or the gplots package (Warnes et al., 2010) in R (http://www.r-project.org/)

(R Development Core Team, 2010).

2.3.6 DNA isolation

Cells were harvested by trypsinization and genomic DNA was isolated from the cell pellets using the PureLinkTM Genomic DNA Mini Kit (Invitrogen) according to the manufacturer's guidelines. Subsequently, DNA concentration and quality was assessed by NanoDrop measurements as described for RNA samples before.

2.3.7 Immunofluorescent protein labeling

To assess the expression of proteins, cells were fixed in 4 % PBS (Calbiochem/Merck, Darmstadt, Germany)-buffered paraformaldehyde (PFA, Electron Microscopy Sciences, Hatfield, PA, USA) for 12 min at RT, while shaking, followed by two washes with 0.05 % Tween 20 (Sigma) in PBS (PBST) and permeabilization with 1 % Triton X-100 (Sigma) diluted in PBS. Cells were washed again twice and blocked in a solution containing 5 % FBS and 1 % bovine serum albumin (BSA, Sigma) in PBST for 1 h at RT. Incubation with the primary antibody was carried out for 1 h at RT. The list of primary and secondary antibodies and the respective dilutions used are provided in Table A.1. Prior to and following the 1 h incubation period with the secondary antibody, cells were washed five times with PBST, 5 min each. Counterstaining of cell nuclei was achieved by incubation with 100 ng/ml 4',6-diamidino-2-phenylindole (DAPI, Vector Laboratories, Burlingame, CA, USA) in PBST for 12 min at RT. Finally, cells were washed thoroughly with PBST.

All stainings were visualized and images were acquired using the confocal microscope LSM 510 Meta (Carl Zeiss, Oberkochen, Germany) in combination with the AxioVision V4.6.3.0 software (Zeiss). Processing of images was done with the help of AxioVision and Adobe Photoshop CS version 8.0 (Adobe, Munich, Germany).

2.3.8 Plasmid DNA amplification

All plasmids used in the course of this PhD project are listed in Table A.2. If purchased as purified plasmids, DNA constructs were first transformed into competent Escherichia coli (E.coli) JM109 by means of heat shock and glycerol stocks were established as described in Section A.2. Plasmid-carrying bacteria were selectively expanded in growth medium, including adequate antibiotics (Table A.2), and amplified plasmids were purified by application of the NucleoBond Xtra Maxi EF Kit (MACHEREY-NAGEL, Düren, Germany). Plasmid yield was determined by NanoDrop measurements; plasmid integrity was assessed by 1.5 % agarose gel electrophoresis. The identity of most plasmids was confirmed by a diagnostic restriction digest. To this end, 10 to 20 U restriction enzyme (Table A.2) were incubated with 5 µg purified plasmid DNA in a total volume of 25 µl at 37 °C ON, followed by resolution on a 1.5 % agarose gel.

2.4 Experimental set-ups

2.4.1 Quantification and sorting of stem cell like sub-populations from amniotic fluid by fluorescence-activated cell sorting (FACS)

To quantify and sort the stem cell-like cell population present in samples of bulk AFCs by FACS, cells were harvested by Accutase-treatment (Millipore, Bilerica, MA, USA), washed with Ca^{2+}/Mg^{2+}-free PBS and resuspended in 0.5 % FBS in Ca^{2+}/Mg^{2+}-free PBS at a density of 1×10^6 cells per 100 µl. 5 µl APC-conjugated anti-CD117 antibody solution (Invitrogen, CD11705) was added per 100 µl of cell suspension and incubated for 1 h at 4 °C. Next, cells were washed with approximately 2 ml 0.5 % FBS in Ca^{2+}/Mg^{2+}-free PBS, pelleted by centrifugation at 200 × g for 4 min, followed by two additional washes. Finally, stained AFCs were resuspended in 100 to 200 µl FACSFlow (BD Biosciences), filtered using a 70 µm cell strainer (BD Falcon), analyzed and sorted at the BD FACSAria II flow cytometry cell sorter (BD Biosciences).

2.4.2 Sorting of stem cell like sub-populations from amniotic fluid by magnetic activated cell sorting (MACS)

To sort the stem cell-like cell population present in samples of bulk AFCs by MACS, cells were harvested by Accutase-treatment (and additional Trypsin-treatment if necessary). For the actual sorting procedure, the human CD117 MicroBead Kit (Miltenyi Biotec, Bergisch Gladbach, Germany) was used with the following modifications: Any centrifugation steps were carried out at 200 × g for 4 min. AFCs were passed through a 70 µm cell strainer prior to the incubation with blocking reagent and before the cell suspension was applied onto the column. Incubation with the MicroBeads was done in the refrigerator and the cells were shaken every 10 min during this incubation period.

2.4.3 Cellular reprogramming by means of retroviral transduction

2.4.3.1 Production of reprogramming factor-encoding retroviruses

PA cells, which are stably transfected HEK cells encoding the viral *gag*, *pol* and *env* genes required for retroviral particle formation, were seeded onto 0.2 % gelatin-coated T75 cell culture flasks ($7.5 \times ^6$ cells/flask) and grown for 16 h. The cells in each flask were then transfected with one of the retroviral pMX vectors encoding either *POU5F1* (OCT4), *SOX2*, *KLF4* or *c-MYC* or the pLIB-GFP vector using the FuGENE HD transfection reagent (Roche, Basel, Switzerland) as follows: 12 µg transfer vector were gently mixed with 1 ml OptiMEM (Gibco) and 30 µl FuGENE HD transfection reagent and incubated for 15 min at RT in the dark. Meanwhile, medium of PA cells was replaced by 9 ml of fresh medium. Next, the complex of DNA/transfection reagent was added to the PA cells drop-wise while the flask was gently swirled to mix. The PA cells were incubated for 14 to 16 h at 37 °C before the medium was replaced by

fresh medium. The virus-containing supernatant was harvested 48 and 72 h post-transfection, passed through a 0.45 µm syringe driven filter unit (Millipore) and kept at 4 °C.

2.4.3.2 Determination of the retroviral titer

30,000 HFF1 cells were seeded into one well of a 24-well plate. The following day triplicates of 1, 10 and 100 µl of GFP retrovirus containing supernatant were added to 0.5 ml medium supplemented with 4 µg/ml polybrene (hexadimethrine bromide, Sigma-Aldrich, Munich, Germany). The plate was centrifuged at 800 × g for 99 min (Centrifuge 5810R, Eppendorf, Hamburg, Germany). Afterwards, the infectious medium was replaced by fresh medium. 48 h post-transduction medium was aspirated, the cells were washed with PBS and fixed in 4 % PFA in PBS for 12 min at RT. Cell nuclei were counterstained using 100 ng/ml DAPI in PBS. Fluorescence was observed using the confocal microscope LSM 510 Meta. The average number of transducing units per milliliter viral supernatant (TU/ml) was calculated from GFP-positive versus total cell counts in several images according to the following equation:

$$\frac{\text{TU}}{\text{ml}} = \frac{(\text{GFP}^+\text{cells per image})}{(\text{Total number of cells per image})} \times (\text{Cells seeded per well}) \times F$$

where $F = 1000\,\mu\text{l} \div$ (Volume of viral supernatant added to the corresponding well in µl).

2.4.3.3 Retrovirus-mediated iPSC generation

For the generation of AFiPSCs, 180,000 AFCs (line 101, P5) in one well of a 6-well culture plate were transduced with a 1:1:1:1 cocktail of the OCT4, SOX2, KLF4 and c-MYC retrovirus-containing media supplemented with 4 µg/ml polybrene on days 1 and 2 after plating. Based on the retroviral titer calculations each viral supernatant was calculated to contain a number of transducing viral units equivalent to 1.25 or 2.5 times the number of plated cells (multiplicity of infection, MOI = 1.25 or 2.5). Each time, directly after the addition of retroviruses, the entire plates were centrifuged at 800 × g for 99 min before replacement of the infectious medium by fresh medium. On d3, the infected cells were plated onto mitotically inactivated MEFs on Matrigel-coated dishes in DMEM/10 % FBS. Another 24 h later, the medium was switched to UM for a total period of 10 d, with replacement on alternate days. Afterwards, the infected cells were grown in CM, which was also changed at an interval of 2 d. AFiPSC colonies were manually picked at a stereomicroscope using sterile pipette tips 24 d post-transduction and expanded under the previously described human PSC conditions.

The generation of FiPSCs from HFF1 and BJ human foreskin fibroblasts used for the comparative transcriptome analysis has been described (Prigione et al., 2010, 2011b).

2.4.4 AFiPSC characterization

2.4.4.1 Cellular senescence and alkaline phosphatase staining

The Senescence β-Galactosidase Staining Kit (Cell Signaling, Danvers, MA, USA,) was employed according to the manufacturer's instructions to stain senescent cells.

To detect activation of the early pluripotency marker, alkaline phosphatase (AP), the Alkaline Phosphatase Detection Kit (Millipore, Billerica, MA, USA) was applied to all manually picked AFiPSC lines following the manufacturer's guidelines.

Brightfield and phase contrast images were acquired and analyzed using the LSM510 Meta microscope.

2.4.4.2 DNA fingerprinting

To amplify genomic regions containing highly variable numbers of tandem tetranucleotide repeats by polymerase chain reaction the primer pairs D7S796, D10S1214 and D21S2055 (Table A.3) (Park et al., 2008) were used. The exact PCR reaction protocol can be found in Section A.3. The resulting DNA fragments were resolved on a 3 % agarose gel in SB buffer (Section A.3) at 150 V to portray the cell line-specific band patterns.

2.4.4.3 Karyotyping

To detect potential karyotypic abnormalities in AFiPSC lines 4, 5, 6, and 41, which may have resulted from the retroviral interference during the process of direct reprogramming, chromosomal analysis was performed after GTG-banding at the Human Genetic Center of Berlin. For each line, 25 metaphases were counted and 10 karyograms analyzed.

2.4.4.4 *In vitro* and *in vivo* differentiation of AFiPSCs

For *in vitro* differentiation, embryoid body (EB) formation of AFiPSC lines 4, 5 and 41 was induced in ESC medium lacking FGF2 supplementation by the hanging-drop method (Cerdan et al., 2007). After 2 to 3 d, EBs were placed into Ultra Low Attachment Culture Dishes (Corning). One week later, EBs were plated onto gelatin-coated dishes, allowed to differentiate for 10 to 14 additional days and then fixed and stained according to the immunofluorescent protein labeling procedure.

The *in vivo* differentiation experiments (teratoma formation) were performed by EPO-Berlin GmbH (Germany, http://www.epo-berlin.de). Briefly, two aliquots of approximately 2×10^6 cells of the AFiPSC lines 4 and 41 was collected by combined type IV collagenase-treatment and 0.05 % Trypsin/EDTA-treatment and washed. Cells were resuspended in Matrigel and immediately injected subcutaneously into NOD.Cg-Prkdcscid Il2rgtm1Wjl/SzJ mice, commonly known as NOD scid gamma (NSG). Mice bearing teratomas were carefully monitored and sacrificed 63 d after injection. The teratomas were collected and processed by means of standard procedures for paraffin embedding and hematoxylin and eosin staining. Histological analysis was performed by a pathologist.

2.4.4.5 Trophoblast differentiation of AFiPSCs

To induce differentiation into the trophoblast lineage, AFiPSC lines 5 and 41 were transferred onto Matrigel-coated cell culture dishes after splitting and grown in CM until they

attained 30 to 50 % confluency. At this point, medium was changed to defined N2B27 medium lacking FGF2 but supplemented with either 100 ng/ml BMP2 (PeproTech) or BMP4 (R&D Systems, Minneapolis, MN, USA) for 5 d or a combination of 10 ng/ml BMP4 and 10 µM SB431542 (Sigma-Aldrich) for 7 d. Undifferentiated controls were maintained in N2B27 including 20 ng/ml bFGF instead. After 5 d or 7 d, including daily replacement of media, cells were harvested for RNA isolation or fixed for immunofluorescence microscopy analysis. For qRT-PCR analysis of BMP2- or BMP4-induced trophoblast differentiation of AFiPSCs, placental RNA (Clontech, Mountain View, CA, USA) was used as a positive control.

2.4.5 shRNA-mediated *USP44* knock down in human PSCs

2.4.5.1 Production of lentiviral particles

To produce lentiviruses encoding shRNAs against USP44, HEK293 cells were co-transfected with a combination of the desired transfer vector and compatible, commercially purchased packaging plasmids (MISSION Lentiviral Packaging Mix, Sigma) as follows: 0.8×10^6 HEK293 cells were seeded per T25 cell culture flask (TPP) approximately 24 h prior to transfection. On the day of transfection 110 µl OptiMEM were mixed with 10 µl MISSION Lentiviral Packaging Mix, 4 µg of the shRNA-encoding transfer vector or a turboGFP(TGFP)-encoding control vector (SHC003, Sigma, Table A.2) and 10 µl of FuGENE HD, followed by 15 min incubation at RT. This transfection cocktail was added drop-wise to the cell culture dish containing 3.3 ml of DMEM/10 % FBS, while the flask was gently swirled to mix. 18 h later, medium was aspirated, the cells were washed with PBS and 3.3 ml of UM added to the flask. 48 h post-transfection the lentivirus-containing supernatant was harvested and replaced by 3.3 ml of fresh UM. The second harvest was done 72 h post-transfection. Both samples of viral medium were pooled and filtered using a 0.45 µm syringe-driven filter unit. Half of the virus containing medium was kept at 4 °C for direct use, whereas the volume of other half was filled up to 30 ml with PBS and centrifuged at 72,000 × g and 4 °C for 2 h (Beckman L7-65 Ultracentrifuge L7, Beckman Coulter, Brea, CA, USA). The viral pellet was re-suspended in 120 µl sterile Ca^{2+}/Mg^{2+}-free PBS containing 1 % BSA, aliquoted and stored at −80 °C.

2.4.5.2 Lentiviral test transductions

The efficiency of lentivirus was determined by transducing HFF1 and HEK293T cells with series of 10, 50 and 100 µl of fresh as well as 2, 4 and 10 µl of frozen TGFP-encoding lentiviral supernatants in 0.5 ml DMEM/10 %FBS supplemented with 4 µg/ml polybrene per 24-well. The infected cells were centrifuged on cell culture plates at 800 × g for 99 min and the virus incubated ON before the infectious medium was replaced by fresh growth medium. Cells were analyzed by microscopy analysis 72 h post-transduction.

2.4.5.3 Lentiviral transduction of human PSCs

Lentiviral transductions of the human ESC line H1 and AFiPSCs maintained in feeder-free conditions were based on the protocol of Du and Zhang (2010) including parts of the MISSION RNAi 'hESC Transduction Protocol' from Sigma (originally from Dr. J Moore, A. Toro-Ramos and Dr. R. Cohen, Stem Cell Research Center, Rutgers University, Piscataway, NJ, USA) and modifications as follows: Briefly, human PSCs were incubated with 10 μM ROCK inhibitor (Y-27632, Cayman Europe, Tallinn, Estonia) in CM at 37 °C 1 h prior to dissociation of the colonies to single cells with TrypLE Select (Gibco), and pelleting of the cells by centrifugation at 200 × g for 4 min. Single cells equivalent to one 12-well were re-suspended in 500 μl CM including polybrene (4 μg/ml) and incubated with 200 μl freshly prepared shRNA- or TGFP-encoding lentiviral supernatant for 2 h at 37 °C (an exact MOI cannot be stated in this case, as the exact number of human PSCs cannot accurately be determined). The volume of virus-containing medium was then increased to plate the cells onto Matrigel-coated cell culture plates. Incubation continued ON, including 10 μM ROCK inhibitor and 2 μM thiazovivin (Stemgent), followed by replacement of the viral medium with fresh complete medium. In subsequent lentiviral transduction experiments this protocol was modified step-wise:

- The amount of fresh viral supernatant varied from100 to 250 μl per 12-well of human PSCs to transduce;
- Incubation was pro-longed to 3 h;
- Dissociation of human PSCs into small colony fragments using the Dispase-splitting procedure prior to lentiviral transduction;
- Direct lentiviral transduction of non-dissociated human PSCs;
- Centrifugation of non-dissociated human PSCs at 811 × g for 99 min during the lentiviral incubation period.

2.4.5.4 Transfection of lentiviral plasmids

In addition to the lentiviral transduction approach, human PSCs were subjected to transfections of the same TGFP and shRNA lentiviral plasmids or two additional reporter constructs encoding *OCT4* promoter-driven enhanced GFP (*OCT4*-EGFP, kindly provided by Dr. Wei Cui, Department of Gene Expression and Development, Roslin Institute, Roslin, Midlothian, UK, described in Gerrard et al. (2005), Table A.2) or a CMV promoter-driven GFP (maxGFP encoded by the pmaxGFP vector, provided with the VPE-1001 Human MSC Nucleofector Kit (Amaxa/Lonza, Basel, Switzerland). Referring to the transduction experiments, human PSCs were also either transfected as non-dissociated colonies (regular transfection) or as single cells in suspension (reverse transfection after TrypLE Select or Accutase-treatment, including 10 μM ROCK inhibitor and/or 2 μM thiazovivin incubation as indicated). Transfections were carried out using the FuGENE HD and the Lipofectamine 2000 (Invitrogen) transfection reagents according to the manufacturers' instructions. The exact amounts of plasmid DNA

and transfection reagent in OptiMEM used per 12-well will be stated in the results section. Incubation of the DNA/transfection reagent complex was either carried out in defined N2B27 medium devoid of antibiotics ON or in OptiMEM followed by replacement with N2B27 medium following two hours incubation as indicated.

2.4.6 Cellular reprogramming by means of episomal plasmid nucleofection

Direct reprogramming of different lines of AFCs (P5-P10) by episomal plasmid nucleofection was conducted on the basis of the protocol published by Yu et al. (2009) which was adapted to meet the conditions of the VPE-1001 Human MSC Nucleofector Kit (Lonza, Basel, Switzerland). For each nucleofection sample, the most potential combinations of episomal plasmids (Yu et al., 2009) were mixed in 1.5 ml reaction tubes (Sarstedt, Nümbrecht, Germany) as follows:

Combination 3.19	'ET2K'	'EN2K'	'M2L'
µg per 1.0×10^6 cells per nucleofection	3.00	3.00	2.00
µg per 0.5×10^6 cells per nucleofection	1.50	1.50	1.00
µg per 0.4×10^6 cells per nucleofection	1.20	1.20	0.80
Combination 4.4	**'6F EN2L'**	**'ET2K'**	
µg per 1.0×10^6 cells per nucleofection	7.30	3.20	
µg per 0.5×10^6 cells per nucleofection	3.65	1.60	
µg per 0.4×10^6 cells per nucleofection	2.92	1.28	
Combination 4.6	**'4F EN2L'**	**'ET2K'**	**'EM2K'**
µg per 1.0×10^6 cells per nucleofection	4.20	3.20	4.60
µg per 0.5×10^6 cells per nucleofection	2.10	1.60	2.30
µg per 0.4×10^6 cells per nucleofection	1.68	1.28	1.84

100 µl cell suspension, prepared to contain 0.4 or 0.5×10^6 cells in Human MSC Nucleofector Solution, was added to the mixture of plasmid DNA, thoroughly mixed and electroporated using the nucleofector programs C-17 and U-23. The cells of one nucleofection sample were seeded into 2 to 5 wells of a 6-well plate, which had been pre-coated with Matrigel and contained a layer of MEF feeder cells, and maintained in DeCoppi medium for the following 3 to 4 d. At this point medium was switched to UM either free of further supplements or containing 0.25 mM β-aminopropionitrile (BAPN, Sigma) or 2 µM thiazovivin for an unlimited period of time or a combination of 2 µM thiazovivin, 2 µM SB431542 and 0.5 µM PD0325901 (Stemgent) for five days. 10 d later, AFCs were maintained in CM with or without treatment until human ESC-like colonies emerged, which could be picked. 2 µg per 0.5×10^6 nucleofected cells of the pmaxGFP vector provided with the nucleofection kit was used as positive control (equivalent to the amount of 'M2L' in combination 3.19).

2.4.7 Cellular reprogramming by means of mRNA transfection

2.4.7.1 *In vitro* mRNA synthesis

The five plasmids each encoding one of the reprogramming factor genes (*POU5F1*, *SOX2*, *KLF4*, *c-MYC* or *Lin28A*, Addgene, Table A.2) and a GFP-encoding plasmid (pGEM4Z-EGFP-A64, kindly provided by Prof. Dr. E. Gilboa, Duke University Medical Center, Durham, NC, USA, previously described by Nair et al. (1998), Table A.2) were purified using columns and buffers provided with the QIAquick PCR Purification Kit (Qiagen, Hilden, Germany) to serve as template for a T7-driven *in vitro* transcription (IVT) producing the respective mRNAs. To this end, approximately 12 µg plasmid were first linearized using 40 U of the restriction enzyme *Xba* I (all of the OSKM-encoding plasmids) or 20 U *Spe* I (GFP-encoding plasmid) in 40 µl total reaction volume at 37 °C ON and then column-purified again. The linearized DNA was *in vitro* transcribed using the mMessage mMachine T7 Kit (Ambion) according to the manufacturer's instructions to synthesize capped mRNA. The template DNA was then degraded by TURBO DNase. Next, poly(A) tails were added to the mRNAs using the poly(A) tailing kit provided by Ambion. Because the GFP-encoding plasmid contained a poly(T) sequence at the end of the coding sequence the produced GFP mRNA already contained a poly(A) tail after the IVT and, thus, was not included in the tailing reaction. All mRNAs were precipitated by incubation with LiCl at −20 °C for 2 h, pelleted by centrifugation at 18000 × g and 4 °C for 15 min and then washed with 70 % ethanol before repeated centrifugation. Finally, the mRNA pellets were resuspended in 20 µl nuclease-free water (Ambion) and quantified by NanoDrop measurement. RNasin Plus RNase Inhibitor (1 U/mg, Promega, Madison, WI, USA) was added to each of the mRNA stock solution prior to aliquoting and storage at −80 °C.
The *in vitro* synthesis of mRNA was carried out by our collaboration partner Geertrui Tavernier from the Research Group on Nanomedicines at Ghent University, Ghent, Belgium.

Predictions of the minimum free energy secondary structures of the reprogramming factor-encoding mRNAs were obtained from the RNAfold WebServer at http://rna.tbi.univie.ac.at/cgi-bin/RNAfold.cgi (Gruber et al., 2008). The FASTA format files for each of the mRNA sequences of *POU5F1* (NM_002701.4), *SOX2* (NM_003106.3), *KLF4* (NM_004235.4), *c-MYC* (NM_002467.4) and *LIN28A* (NM_024674.4) provided by the National Center for Biotechnology Information (NCBI, http://www.ncbi.nlm.nih.gov/) were used as input. The queries were run based on default parameter settings.

2.4.7.2 General mRNA transfection procedure

HFF1, BJ or AFCs were seeded into 6-well plates at a density of approximately 180,000 cells/well the day before transfection. Cells were transfected with a total of 4 µg mRNA per 6-well. For distinct applications, such as FACS and microscopic analysis, cells were seeded into 12 and 24-well plates instead. In these cases, the number of cells and amount of mRNAs to be transfected was scaled down accordingly. The mRNAs were either synthesized as herein described or commercially purchased as modified mRNAs from Stemgent (San Diego, CA, USA). GFP-encoding mRNA was used as positive control. mRNA concentrations were adjusted to

1 µg/µl with water and the required cocktails were mixed. Next, those 4 µg to be transfected were pre-diluted with 46 µl OptiMEM and complexed with 4µl Lipofectamine RNAiMAX (Invitrogen), which had been pre-diluted in 46 µl OptiMEM simultaneously. The transfection mixture was incubated for 10 min at RT. Ad interim, medium was aspirated from the relevant wells. Following the incubation the RNA/Lipofectamine complex was further diluted with 900 µl OptiMEM and incubated with the cells at 37 °C. After 2 h, the transfection solution was replaced by fresh growth medium. Cells were harvested for RNA isolation, subjected to FACS analysis or fixed for immunofluorescence staining at indicated time points.
All HFF1 and BJ mRNA transfection experiments were conducted in close cooperation with Geertrui Tavernier.

2.4.7.3 Quantification of GFP expression following mRNA transfection

HFF1 cells were plated in 12-well plates (90,000 cells / well) and transfected with 2 µg of GFP-encoding mRNA per well as described above. To assess the number of GFP-positive cells, culture medium was removed from the wells and the cells were washed with PBS. Images were taken 24 post-transfection with a confocal microscope LSM 510 (Zeiss, Oberkochen, Germany). Alternatively, the cells were detached with trypsin (0.05%, Life Technologies), centrifuged (340 × g for 4 min) and re-suspended in 100-200 µl FACSFlow (BD Biosciences). The samples were kept on ice until GFP expression was evaluated by a Beckman Coulter Flow Cytometer FC500 (BD Biosciences), equipped with a 488 nm laser.
These assays were performed with the aid of Geertrui Tavernier.

2.4.7.4 Detection of OSKML protein expression following mRNA transfection

HFF1 cells were plated in 24-well plates (45,000 cells / well) and transfected with 1 µg of mRNAs encoding one of the reprogramming factors (OSKML) or with a 1:1:1:1:1 cocktail of the same mRNAs per well as described above. Following transfection, cells were fixed and reprogramming factor protein expression assessed by the above described immunofluorescent protein labeling procedure at indicated time points.
These stainings were performed with the aid of Geertrui Tavernier.

2.4.7.5 mRNA-mediated iPSC generation

To attempt direct reprogramming by delivery of reprogramming factor-encoding mRNAs, AFCs, and for optimization of the protocol also HFF1 or BJ cells, were transfected up to nine times daily or on alternate days with a total of 4 µg per 6-well of an mRNA cocktail composed of

Mix 1:	1:1:1:1	*POU5F1*, *SOX2*, *KLF4* and *c-MYC*-mRNA,
Mix 2:	1:1:1:1:1	*POU5F1*, *SOX2*, *KLF4*, *c-MYC* and *LIN28A*-mRNA or
Mix 3:	3:2:1:1:1	*POU5F1*, *SOX2*, *KLF4*, *c-MYC* and *LIN28A*-mRNA

on a layer of MEF feeder cells or, alternatively, without a layer of feeder MEF feeder cells. Following the last transfection, cells were passaged onto layers of MEF feeder cells in Matrigel-coated 6-well plates. Medium was then switched from DC medium or DMEM/10 %FBS to UM for a period of 10 d before the cells were maintained in CM. Alternatively, transfections were carried out on Matrigel-coated plates in NutriStem XF/FF Culture Medium (Stemgent). Cells were monitored for morphological changes towards human ESC-like colonies. Medium was replaced every other day. If indicated, treatments of the cells with one or combinations of chemical substances were included in the post-transfection culture period as follows:

- 2 μM SB431542
- 0.5 μM PD0325901
- 500 μM ethyl 3,4-dihydroxybenzoate (EDHB) (Sigma)
- 2 μM thiazovivin

As a control, HFF1 cells mRNA-mediated reprogramming was conducted according to the Stemgent protocol using the modified mRNAs (Stemgent mRNA Reprogramming Factors Set: hOSKML, Cat. No. 00-0067) and medium (Stemgent Pluriton mRNA Reprogramming Medium, Cat. No. 00-0070) provided, yet including the following modifications: HFF1 foreskin fibroblasts were employed as target cells for reprogramming. HFF1 cells were also mitotically inactivated to serve as feeder cells. Per transfection and 6-well of cells at suggested densities, 25 μl of the mRNA cocktail containing OSKML mRNAs at the recommended ratio were diluted in 25 μl OptiMEM and mixed with 2 μl LF RNAiMAX pre-diluted with 48 μl OptiMEM. The resulting 100 μl transfection solution were incubated for 10 min, subsequently further diluted with 900 μl OptiMEM and added to the cells after removal of the growth medium. After 2 h of incubation the transfection mix was substituted by the appropriate equilibrated growth medium. B18R treatments were not performed.

2.4.7.6 Determination of cell viability following mRNA transfections

HFF1 cells were plated in 12-well plates (90,000 cells / well) and transfected daily with 2 μg of a 1:1:1:1 cocktail of *in vitro* synthesized mRNAs encoding the reprogramming factors OSKM as described above. Cell viability was evaluated 24 h after each transfection by an MTT assay (Roche, Vilvoorde, Belgium) performed according to the manufacturer's instructions.
This cytotoxicity assay was carried out by our collaboration partner Geertrui Tavernier.

2.4.7.7 Analysis of the immune response to different cellular reprogramming approaches

Approximately 180,000 HFF1 cells were plated per 6-well and maintained in DMEM/10 % FBS for 24 h. As described for AFCs in the context of cellular reprogramming above, HFF1 cells were

- transfected once or twice with 'Mix 1' of the mRNA reprogramming factor cocktails or the equivalent total amount of GFP-encoding mRNA;
- infected once with a 1:1:1:1 cocktail of retroviruses encoding four reprogramming factors (OSKM) or a GFP-encoding retrovirus equivalent to the amount of a single reprogramming factor (no change of infectious medium until cell harvest);
- transfected once with a 1:1:1:1:1 cocktail of hsa-miR-302a, hsa-miR-302b, hsa-miR-302c, hsa-miR-302d and hsa-miR-367 mimics (100 pmol total, Ambion) or the equivalent total amount of a non-target (scrambled) miRNA (Ambion).

All cells were harvested 24 h post-transduction/transfection for RNA isolation and the regulation of immune response-associated genes was assessed by qRT-PCR.

To determine the immunemodulatory effect of different substances following OSKM mRNA transfection, cells were pre-incubated with these substances 1 h prior to transfection, during the incubation of the complexed mRNA with the cells and 24 h post-transfection at the following concentrations:

- 200 ng/ml B18R (eBioscience/biocompare)
- 5, 50 and 100 μM chloroquine (Sigma)
- 50, 100 and 500 nM trichostatin A (Sigma)
- 20 μM pepinh-TRIF (InvivoGen, San Diego, CA, USA)
- 20 μM pepinh-MYD (InvivoGen)

2.4.8 Cellular reprogramming by means of miRNA transfection

For reprogramming attempts by miRNA transfection, two recently published protocols (Anokye-Danso et al., 2011; Miyoshi et al., 2011) were combined as follows: Per 6-well to be transfected, 7.5 μl LF RNAiMAX were diluted in 250 μl OptiMEM. At the same time a 1:1:1:1:1 cocktail of hsa-miR-302a, hsa-miR-302b, hsa-miR-302c, hsa-miR-302d and hsa-miR-367 mimics (100 pmol total, Ambion) was diluted in 250 μl OptiMEM. The miRNA mix was added to the transfection reagent solution, gently mixed and incubated at RT for 30 min. Thereafter, the complexed miRNAs were transferred into the 6-wells containing approximately 200,000 AFCs each in 1.5 ml fresh DC medium lacking antibiotics. Four subsequent transfections were carried out (d1, d4, d6, d8 after plating at d0) before AFCs were passaged onto layers of MEF feeder cells in Matrigel-coated 6-well plates and maintained in UM, supplemented with 2 μM thiazovivin. To monitor the morphology of cells further, medium was switched to MEF-CM containing 2 μM thiazovivin after 10 d.

3

Virus-mediated generation of amniotic fluid-derived iPSCs

3.1 Introduction

In the first part of this project, distinct subpopulations of human amniotic fluid cells (AFCs) will be sorted and used as starting material to render efficient cellular reprogramming possible. Implementation of the originally published retrovirus-mediated reprogramming protocol by Yamanaka et al. (Takahashi et al., 2007) should further enable reliable induction of pluripotency in human AFCs. Once amniotic fluid-derived induced pluripotent stem cells (AFiPSCs) are established these will be characterized in depth using the parental cells and human embryonic stem cells (ESCs) as references to monitor the de-differentiation and verify their potential to self-renew and the complete induction of pluripotency. The newly generated AFiPSCs will subsequently be utilized together with human ESCs to investigate the role of the pluripotency-associated gene USP44 in maintaining self-renewal.

3.2 Results

3.2.1 Expansion and senescence of primary human AFCs

One of the major limitations of primary cell lines is their relatively early arrest of proliferation when compared to ESCs, cancer or transformed cell lines. This phenomenon is commonly known as replicative or cellular senescence (Hayflick and Moorhead, 1961; Hayflick, 1965) and was associated with the lacking ability of somatic cells to maintain full telomere length throughout the life cycle when compared to immortal cells (Mishiev et al., 1979; Allsopp et al., 1992; Counter et al., 1994). Primary human AFCs, maintained and expanded for the purpose of this PhD project, senesced at a maximum of 17 passages (P17) (Wolfrum et al., 2010). At this stage, AFCs stopped dividing and senescence was further indicated by their enlarged, flattened morphology and verified by positive staining for the senescence-associated beta-galactosidase (Figure 3.1) (Wolfrum et al., 2010).

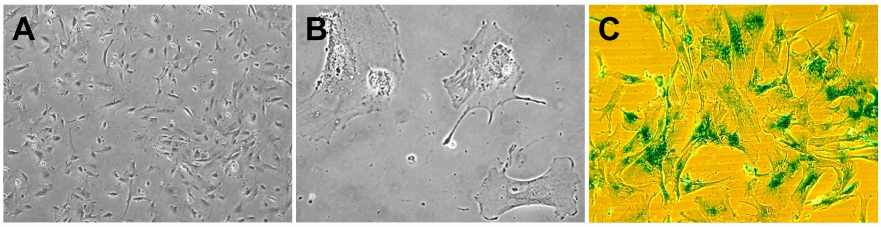

Figure 3.1: Morphology of early passage and senescent bulk primary AFCs. (A) Early passage, proliferative human AFCs (line 101, P5). (B, C) The same line of AFCs after proliferation arrested at P17; the morphology of senescent AFCs is depicted without and with staining for the senescence-associated beta-galactosidase, respectively. Taken from Wolfrum et al. (2010).

3.2.2 Quantification and sorting stem cell-like subpopulations from bulk primary human AFCs by FACS

Bulk AFCs contain subpopulations of cells that possess stem cell-like properties, such as CD117-positive cells (De Coppi et al., 2007). We hypothesized that the use of these stem cell-like cells as target cells for cellular reprogramming experiments would be inherently more efficient compared to routinely employed fibroblast cells. To test this hypothesis we sought to enrich stem cell-like sub-populations from bulk AFC samples for subsequent reprogramming experiments. Accordingly, CD117-expressing AFCs were detected by immunofluorescent labeling for flow cytometric quantification and sorting of bulk AFCs. This revealed about 3 % CD117-positive cells within bulk primary AFCs, which is comparable to the previously reported 1 % (De Coppi et al., 2007) Figure 3.2. However, sorting of this subpopulation from bulk AFC samples was not successful as the staining and sorting procedure severely affected the cellular integrity of generally very large and seemingly fragile AFCs. This resulted in an extremely low yield of intact, sorted cells, which could not be sufficiently re-expanded for cellular reprogramming attempts before the onset of cellular senescence.

3.2.3 Sorting stem cell-like subpopulations from bulk primary human AFCs by MACS

Magnetic activated cell sorting (MACS), which entails labeling of cell surface markers by specific antibodies coupled with magnetic beads and sorting of the cells in a magnetic field, was employed as potentially less harmful, alternative technique to sort stem cell-like cells of bulk AFCs. The outcome of this sorting approach, however, was comparable to that obtained by FACS. Sorting, for example, of as many as 18.3×10^6 cells at P9 resulted in approximately 1.6 % CD117-posititve cells (2.9×10^5 cells). However, only 1.3×10^5 of these were intact as determined by the trypan blue exclusion method. Of these, in turn, only a limited number of cells were able to attach. Based on their morphology, these cells appeared to be stressed Figure 3.3 and after protracted re-expansion, no CD117-expression was detectable by immunofluorescence microscopy in this subpopulation when applying the same anti human CD117 antibody as used for FACS quantification and sorting. In this instance, the CD117-positive fraction was

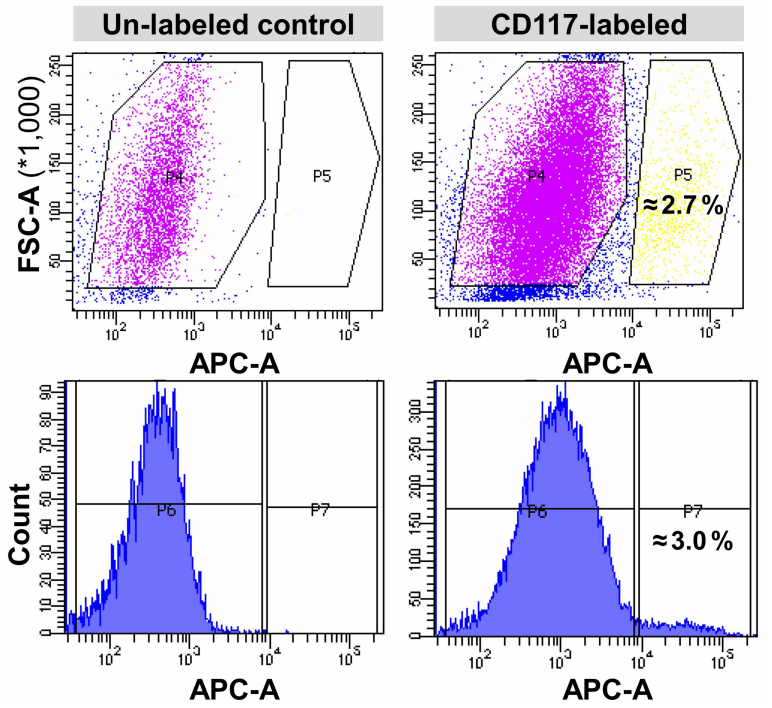

Figure 3.2: FACS-based quantification of the CD117-positive subpopulation in bulk primary AFCs. CD117-positive cells in bulk primary AFCs (line 101, P15) were labeled by an APC-conjugated antibody prior to FACS analysis. Results are given as average, n = 2.

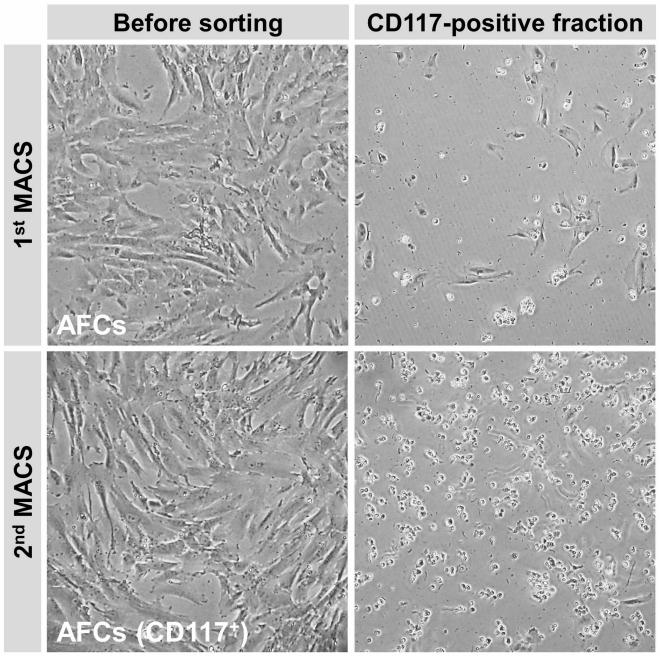

Figure 3.3: Morphology of human AFCs prior to and following MACS of CD117-postive cells. Upper panel: Unsorted human AFCs (line 101, P9) prior to CD117 MACS (left) and the resulting CD117-positive fraction one day after plating (P10, right). Lower panel: The same CD117-positive subpopulation after steady re-expansion, prior to repeated sorting at P13 (left) and the resulting CD117-positive fraction one day after plating (P14, right).

repeatedly sorted (3.5×10^6 AFCs at P13), which yielded approximately 2.7 % CD117-positive cells, 1.1×10^4 of which were intact. Plating of these cells revealed extensive cell debris and an even smaller fraction of cells attached Figure 3.3. In conclusion, none of the singularly nor re-sorted CD117-positive subpopulations fully recovered before the onset of senescence. As a result of this, a subpopulation of AFCs with confirmed stem cell-like characteristics eligible for reprogramming could not be established by MACS.

3.2.4 Cellular reprogramming of human AFCs by means of retroviral transduction

As sorting of stem cell-like sub-populations from AFC samples was not practicable, we sought to derive iPSCs from bulk AFCs instead assuming that stem cell-like cells within the heterogeneous mixture of cells would facilitate efficient cellular reprogramming in any case. To this end, we employed the original, robust protocol published by Takahashi et al. (2007).

3.2.4.1 Retroviral particle production

Retroviral vectors, like most other plasmids used in the course of this PhD project, were amplified, extracted and identified by restriction digest using adequate enzymes (Table A.2) followed by gel electrophoresis as shown in Figure 3.4 (A). Retroviruses encoding either the reprogramming factors OCT4, SOX2, KLF4, c-MYC (OSKM) or GFP were produced upon transfection of these vectors into packaging Phoenix amphotropic (PA) cells (Figure 3.4 (B)). The viral titer was determined using the GFP retrovirus as a reporter (Figure 3.4 (C)).

3.2.4.2 Retrovirus-mediated iPSC generation

The retroviruses were then utilized to deliver a 1:1:1:1 cocktail of the reprogramming factors OSKM into bulk primary AFCs (line 101) of a proliferative phase (P5). Subsequently, transduced AFCs were maintained under human ESC conditions (Takahashi et al., 2007). Putative AFiPSC aggregates appeared about seven days post-transduction (Figure 3.5 (A)), which was approximately two weeks earlier than what we and others observed for fibroblast-derived iPSCs (Takahashi et al., 2007; Prigione et al., 2010; Wolfrum et al., 2010). Unlike the parental cells, mature AFiPSCs exhibited high nucleus/cytoplasm ratios, grew as sharp edged, densely packed colonies (Figure 3.5 (B, C)) and were indistinguishable from human ESCs (lines H1 or H9) in terms of morphology (Figure 3.5 (D)) and proliferation rate (Wolfrum et al., 2010). Approximately 45 putative AFiPSC colonies resulting from reprogramming of approximately 0.4×10^6 AFCs according to the protocol outlined in the Material and Methods section were initially picked (equivalent to ≈ 0.011 %). Of these, five clonal AFiPSC lines were expanded for a minimum of 25 passages and characterized. Two of the AFiPSC lines underwent the complete set of characterization assays (Wolfrum et al., 2010).

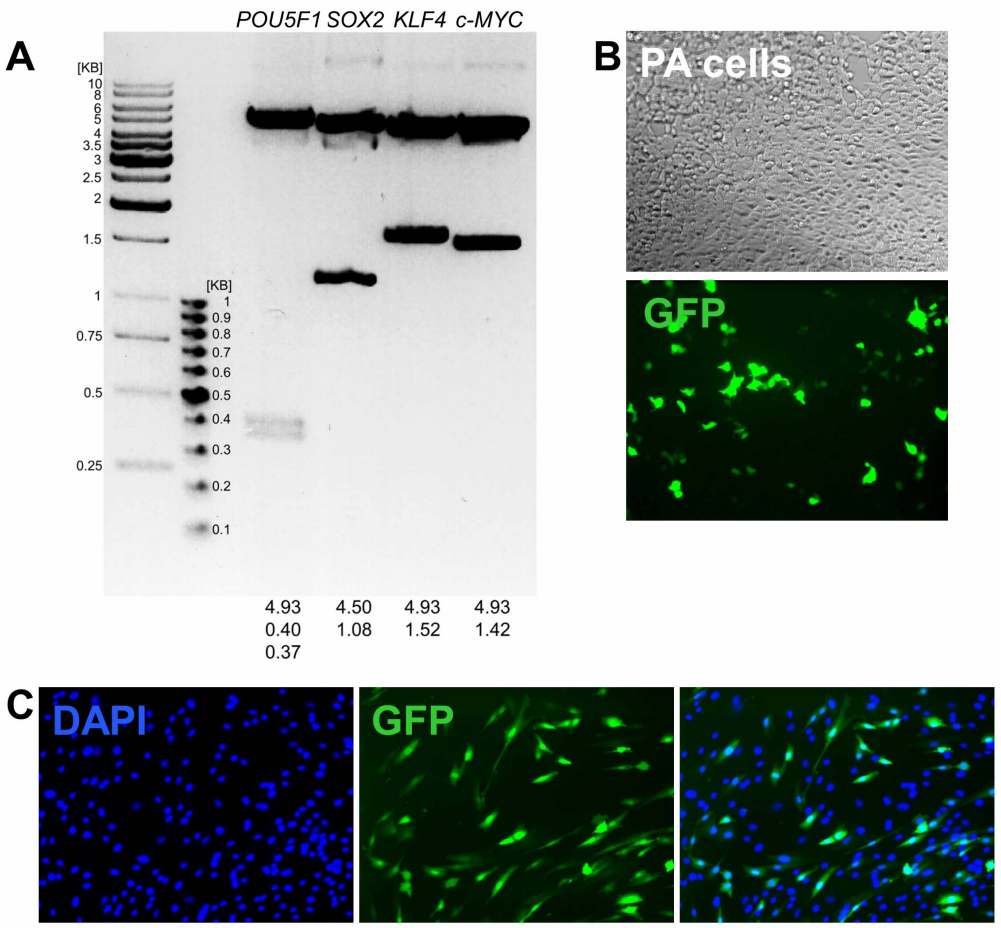

Figure 3.4: Preparation of retroviruses for cellular reprogramming. (A) Gel electrophoresis of reprogramming factor-encoding plasmids after amplification, extraction and restriction digest using suitable restriction enzymes. The numbers at the bottom indicate the size of the expected DNA fragments. (B) Packaging PA cells 18 h after transfection of the GFP-encoding transfer vector. (C) Representative fluorescent images, which were used to determine the number of transducing units per milliliter retroviral supernatant. HFF1 cells were transduced with serial dilutions of the GFP-encoding retrovirus, fixed and cell nuclei counterstained with DAPI to quantify the number of total cells and the number of GFP-positive cells in each sample.

3.2.4.3 Characterization of AFiPSCs

Human iPSCs closely resemble human ESCs, the gold standard of human pluripotent stem cells (PSCs), with respect to morphology and self-renewal. To verify pluripotency, iPSCs have to pass a number of tests (Maherali and Hochedlinger, 2008). Besides the demonstration of their genetic origin from the parental cell line and karyotypic stability post-transduction of integrating retroviruses, these assays are mainly aimed at highlighting the expression of ESC-specific both intracellular and cell surface markers and the pluripotent differentiation potential, i.e. the ability of iPSCs to differentiate into derivatives of all three embryonic germ layers (Maherali and Hochedlinger, 2008). To this end, spontaneous differentiation is initiated, as done for human ESCs, by so-called embryoid body formation *in vitro* (Itskovitz-Eldor et al., 2000)

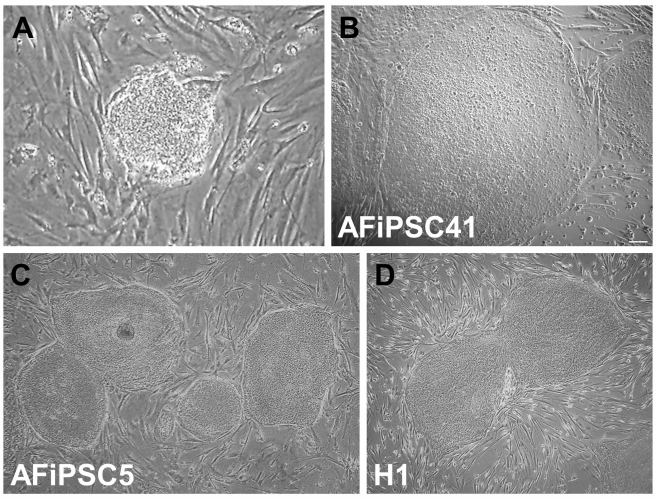

Figure 3.5: Morphology of early and mature AFiPSC and human ESC colonies. (A) Image of one of the first putative AF-derived iPSC aggregates as they appeared approximately seven days post-retroviral transduction of the parental AFC line. (B) Mature, undifferentiated AFiPSC colony. Scale bar = 400 µm. (C) Typical morphology of AFiPSC colonies cultivated on a layer of MEF feeder cells. (D) H1 human ESCs during routine maintenance on a MEF feeder cell layer. Modified from Wolfrum et al. (2010).

and by injection of iPSCs into immune-compromised mice *in vivo* (Thomson et al., 1998). The latter test, the teratoma formation assay, is the most stringent pluripotency test for human iPSCs as chimera contribution, germline transmission and tetraploid complementation—routine assays performed for murine iPSCs—are not feasible in humans (Maherali and Hochedlinger, 2008). We extended this range of standard tests by a trophoblast differentiation assay and genome-wide gene expression profiling to get a more detailed comparison of the retrovirus-derived AFiPSCs with human ESCs, H1 and H9, and iPSCs of other somatic cell origin.

DNA Fingerprinting

To verify the origin of the AFiPSCs, genomic DNA was isolated from various cell lines to amplify genomic regions containing highly variable numbers of tandem tetranucleotide repeats (variable number tandem repeats, VNTRs). By separation on an agarose gel variations of VNTR allele lengths resulted in cell line-specific patterns of amplified genomic DNA and confirmed genetic relatedness of all five AFiPSC lines to the parental AFC line (Figure 3.6) (Wolfrum et al., 2010). Simultaneously, contamination of all AFiPSC lines with the human ESC lines, H1 and H9, could be excluded (Wolfrum et al., 2010).

Karyotypic stability

The retroviruses used to reprogram AFCs are well known to integrate into the host cell genome inducing mutations which cause unpredictable effects such as tumorigenicity of the target cells (Takahashi et al., 2007). Furthermore, iPSCs have been shown to harbor different kinds of mutations and chromosomal aberrations (Mayshar et al., 2010; Pasi et al., 2011; Gore et al., 2011; Prigione et al., 2011b,a). Hence, AFiPSC lines 4, 5, 10 and 41 were karyotyped

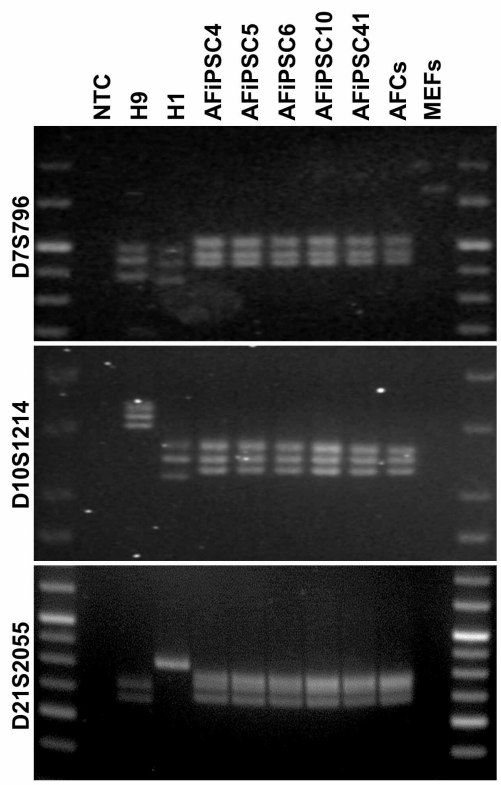

Figure 3.6: Gel electrophoresis of fingerprinting PCR products. Genomic DNA was isolated from all samples (ESC lines H1 and H9, different AFiPSC lines, the parental AFC line 101 and MEFs), amplified using PCR primer sets that flank different genomic regions containing VNTRs (D7S796, D10S1214, D21S2055) and the PCR products resolved on a 3 % agarose gel. NTC, non-template control. Modified from Wolfrum et al. (2010).

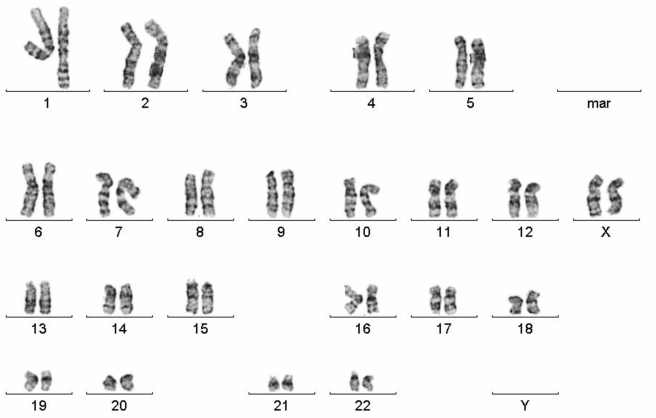

Figure 3.7: AFiPSC karyogram. Different AFiPSC lines were karyotyped but only one representative image of the analyses is depicted. mar, minimal altered region.

to ensure the viral transduction did not induce chromosomal abnormalities. This revealed that all of the tested AFiPSC lines exhibited a normal karyotype several passages after their generation (Figure 3.7). No minimal altered regions were detected in any sample (Wolfrum

et al., 2010).

Expression of human ESC markers

The AFiPSC lines were further characterized and their human pluripotent stem cell (PSC) qualities assessed. Human ESCs, lines H1 and H9, served as a reference throughout the project. AFiPSCs resembled human ESCs not only in terms of morphology but also with respect to activation of the early pluripotency marker alkaline phosphatase (AP, Figure 3.8 (A)) and expression of markers of the undifferentiated ESC state, including OCT4, SOX2, NANOG, SSEA4, TRA-1-60, TRA-1-81 as determined by immunocytochemistry (Figure 3.8 (B)) (Wolfrum et al., 2010). Cadherin-1 (CDH1, E-cadherin) expression within AFiPSC colonies verified the epithelial nature of AFiPSCs, a crucial feature of human ESCs. This was further supported by the absence of vimentin (VIM), a type III intermediate filament expressed in mesenchymal cells (Eastham et al., 2007), within the boundaries of AFiPSC colonies. The presence of vimentin at the periphery of the colonies, however, indicated spontaneous differentiation of AFiPSCs maintained on Matrigel-coated dishes in MEF-CM, a common observation in human ESC cultures (Zwaka and Thomson, 2005; Xu et al., 2005).

Pluripotency and *in vitro* and *in vivo* differentiation

To evaluate the success of cellular reprogramming of human AFCs, pluripotency of AFiPSCs was assessed in greater detail. First, the expression of several self-renewal and pluripotency-associated genes (Adewumi et al., 2007; Babaie et al., 2007; Chavez et al., 2009) was analyzed on the mRNA level employing microarray-based transcriptome-profiling and quantitative real-time polymerase chain reaction (qRT-PCR). NanoDrop measurements at 260 and 280 nm and 260 and 230 nm and agarose gel electrophoresis were routinely performed quality controls to ensure integrity of the isolated total RNA whenever gene expression levels were determined in the course of this PhD project. In a few cases, RNA quality was additionally assessed employing the technology of Agilent RNA 6000 Nano microfluidic chips. Representative results of such RNA quality examinations by agarose gel electrophoresis and microfluidic chip analysis are exemplarily shown in Figure 3.9 (A, B). The presence of sharp 18 S and 28 S ribosomal RNA bands and peaks with a ratio of intensities of approximately 1:2 is indicative of the isolated RNA being intact. Using such quality-checked total RNA, the majority of self-renewal and pluripotency-associated genes determined in AFiPSCs in comparison to primary AFCs was significantly up-regulated as demonstrated by microarray-based transcriptional analysis (Figure 3.9 (C)) (Wolfrum et al., 2010). qRT-PCR validation, performed for a selection of these pluripotency-associated genes, confirmed the array-derived data (Figure 3.9 (D)) (Wolfrum et al., 2010).

Next, embryoid body formation and plating of the resulting aggregates is routinely performed to efficiently differentiate human ESCs into different lineages *in vitro* (Itskovitz-Eldor et al., 2000). Another option to assess spontaneous differentiation of human ESCs *in vivo* entails their sub-cutaneous injection into immuno-deficient mice. As a result pluripotent cells differentiate into derivatives representative of all three embryonic germ layers (Thomson et al.,

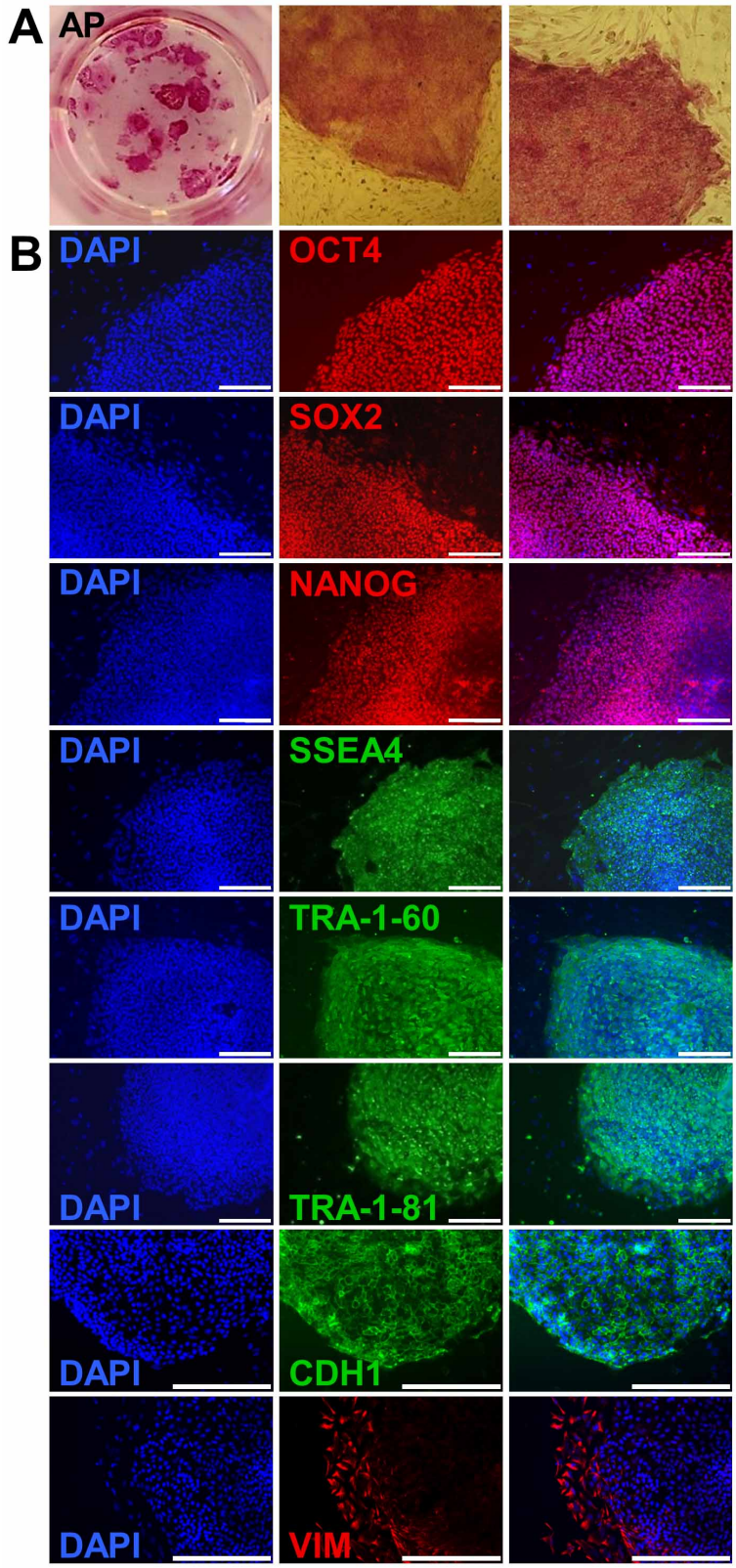

Figure 3.8: Detection of human ESC marker expression in AFiPSCs. (A) AF-derived iPSC lines were stained for AP at P1 and analyzed by light microscopy. (B) The presence of intracellular (OCT4, SOX2, NANOG) and surface ESC markers (SSEA4, TRA-1-60, TRA-1-81, CDH1) as well as expression of the mesenchymal cell-specific intermediate filament (VIM) was assessed in AFiPSCs by immunofluorescent labeling. Scale bars = 200 µm. Modified from Wolfrum et al. (2010).

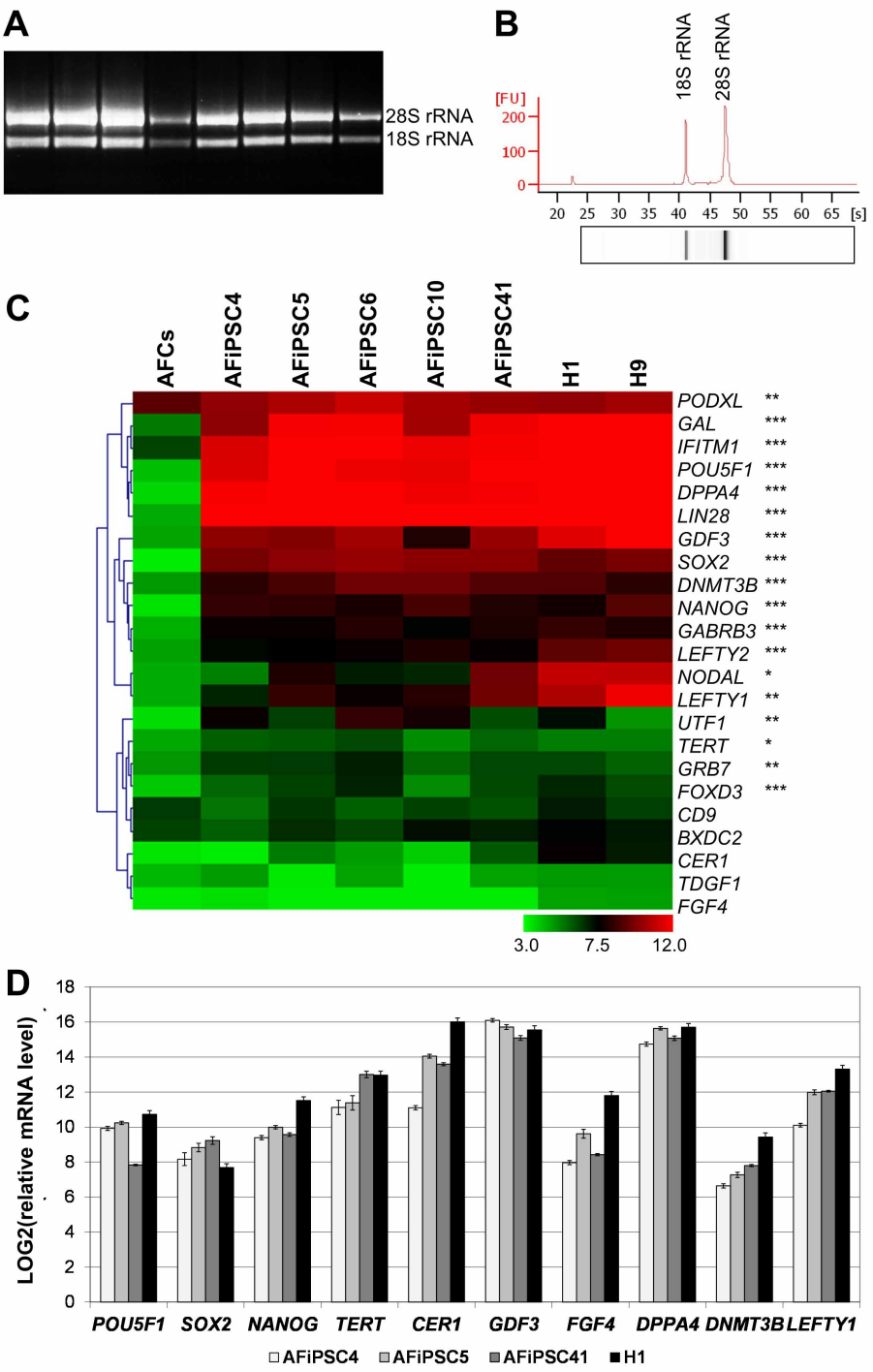

Figure 3.9: Regulation of pluripotency-associated genes in AFiPSCs. (A) Representative images of agarose gel electrophoresis and ethidium bromide staining of isolated total RNA samples. (B) Electropherogram (fluorescence units [FU] over migration time [s]) resulting from the Agilent RNA 6000 Nano Kit-based assessment of RNA integrity. (C) Heatmap depicting microarray-derived expression levels of pluripotency-associated genes in human ESC lines H1 and H9, different AFiPSC lines and the corresponding AFCs. The heatmap is colored by LOG2 average expression values according to the color key below. Genes, which are significantly up-regulated in the group of AFiPSCs compared with the parental AFCs are tagged with asterisks (padj < 0.05 (*), < 0.01 (**), < 0.001 (***)). (D) qRT-PCR confirmation of the microarray data. Bars and error bars represent average LOG2 ratios (AFiPSCs or H1 relative to AFCs, respectively) and SD. n = 3 technical replicates per cell line. Modified from Wolfrum et al. (2010).

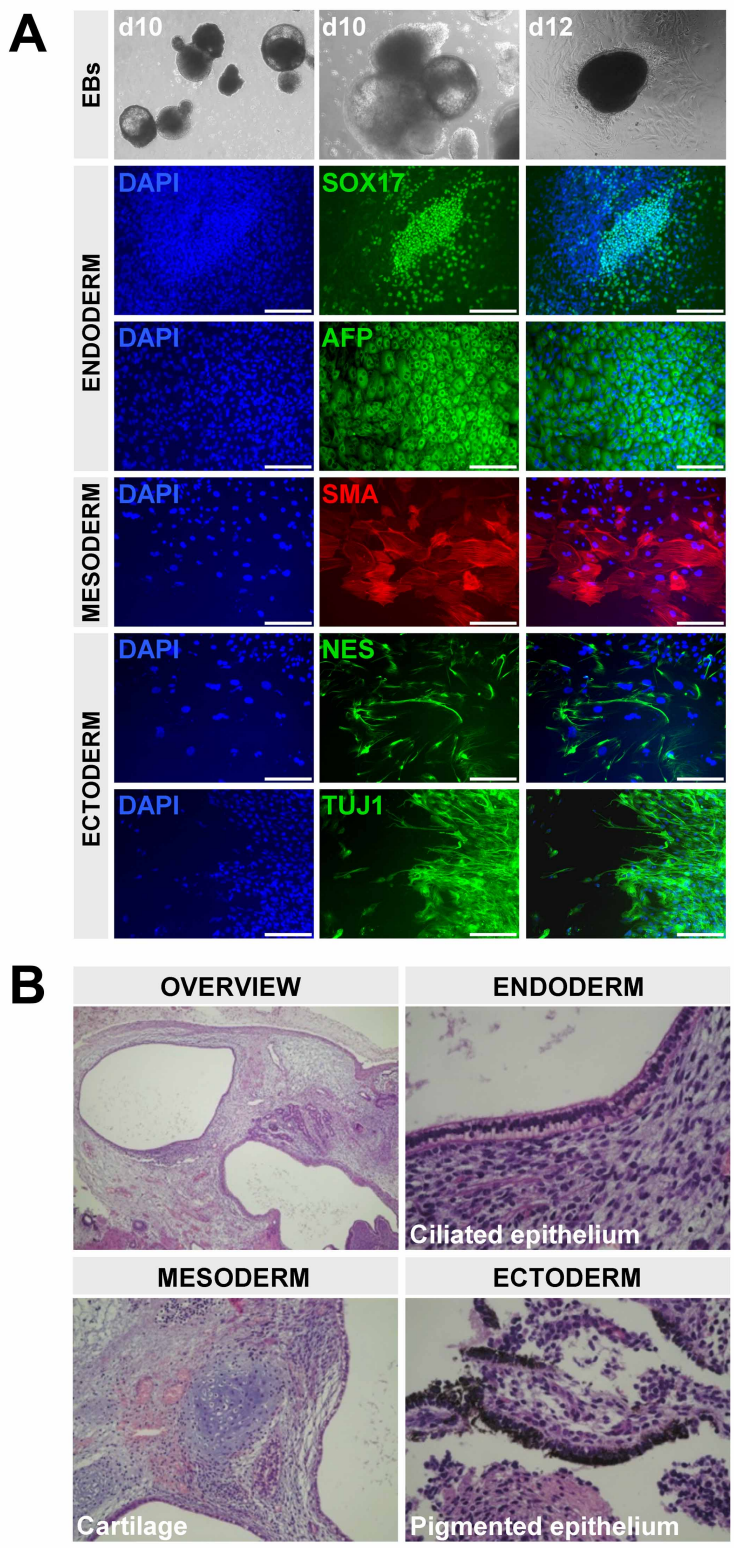

Figure 3.10: Pluripotent capabilities of AFiPSCs. (A) Upper panel: Embryoid body (EB) formation was induced in AFiPSCs *in vitro*. EB morphology is depicted in suspension (d10) and after plating onto gelatinized dishes (d12). Lower panels: The outgrowth of adherent EBs was analyzed by immunofluorescence-based detection of different germ layer marker proteins (AFP, α-fetoprotein; SMA, smooth muscle actin; NES, nestin; TUJ1, class III β-tubulin). Scale bars = 200 µm. (B) *In vivo* teratoma formation of AFiPSCs upon injection into NOD scid gamma mice. Representative images of histological structures corresponding to endo-, ecto- and mesodermal lineages are depicted. Taken from Wolfrum et al. (2010).

1998). When conducted with AFiPSCs both of these assays confirmed pluripotency of the amniotic fluid-derived iPSCs (Figure 3.10) (Wolfrum et al., 2010). Markers or histological structures representing endoderm-, mesoderm- and ectoderm-derived lineages were detected in both assays (Wolfrum et al., 2010).

Trophoblast differentiation

Besides their ability to differentiate into derivatives of the three embryonic germ layers, human ESCs can also develop into the trophoblast lineage *in vitro* (Thomson et al., 1998; Xu, 2006; Greber et al., 2008; Schulz et al., 2008; Vallier et al., 2009b). To test if AFiPSCs share this quality, we stimulated two AFiPSC lines with 100 ng/ml BMP2 or BMP4 for five days. This induced a morphological change from densely packed ESC-like AFiPSC colonies towards clusters of loosely arranged, enlarged cells with typical cobblestone-like appearance (Figure 3.11 (A)), a characteristic feature of trophoblast differentiation of human ESCs (Xu, 2006; Schulz et al., 2008). Accordingly, gene expression profiling and qRT-PCR demonstrated down-regulation of the key pluripotency markers *POU5F1* and *NANOG* and up-regulation of the trophoblast markers *CDX2*, *KRT7*, *HAND1*, *FOXF1*, *GATA3* and *ID2* (Figure 3.11 (B)) (Wolfrum et al., 2010). Treatments with BMP2 and BMP4 induced similar effects, however, BMP4 was more efficient (Wolfrum et al., 2010). The ultimate hallmark of ESCs differentiating into the trophoblast lineage is the secretion of human chorionic gonadotropin, hCG, a hormone secreted by trophoblastic cells of the placenta *in vivo* (Thomson et al., 1998; Xu, 2006). This protein was detectable by immunofluorescent labeling following treatment of AFiPSCs with a combination of 10 ng/ml BMP4 and 10 µM SB431542 over a period of seven days (Figure 3.11 (C)) providing further evidence of the ability of AFiPSCs to derive trophoblast cells (Wolfrum et al., 2010).

Comparative global gene expression analyses of AFCs, AFiPSCs and ESCs

Microarray-based genome-wide gene expression profiling is a high-throughput technology that facilitates the simultaneous measurement of gene expression levels of thousands of genes in one sample. As such it is powerful tool to assess a broad range of gene expression changes associated with distinct treatments of the samples and to demonstrate the correlation of different samples on mRNA level on a global scale. Transcriptomes of primary AFCs (line 101), the corresponding AFiPSCs and the ESC lines H1 and H9 were profiled employing the Illumina BeadStudio platform to further investigate their relatedness with regard to global gene expression. Hierarchical clustering on the basis of Pearson's correlation and linear correlation coefficient analysis of detected gene expression signals revealed distinguishable transcriptomes when AFiPSCs and their parental AFCs at P6 (average linear $R^2 \approx 0.67$) and P17 (average linear $R^2 \approx 0.50$) were analyzed (Figure 3.12 (A, B)) (Wolfrum et al., 2010). In contrast, transcriptomes of AFiPSCs and ESCs were similar, though not identical (average linear $R^2 \approx 0.94$) (Wolfrum et al., 2010). This analysis was also conducted for replicate samples of HFF1-derived FiPSCs generated in our laboratory in comparison to the ESC lines H1 and H9 (Prigione et al., 2010). The resulting average linear correlation coefficient of $R^2 \approx 0.87$, in contrast to $R^2 \approx 0.94$ for AFiP-

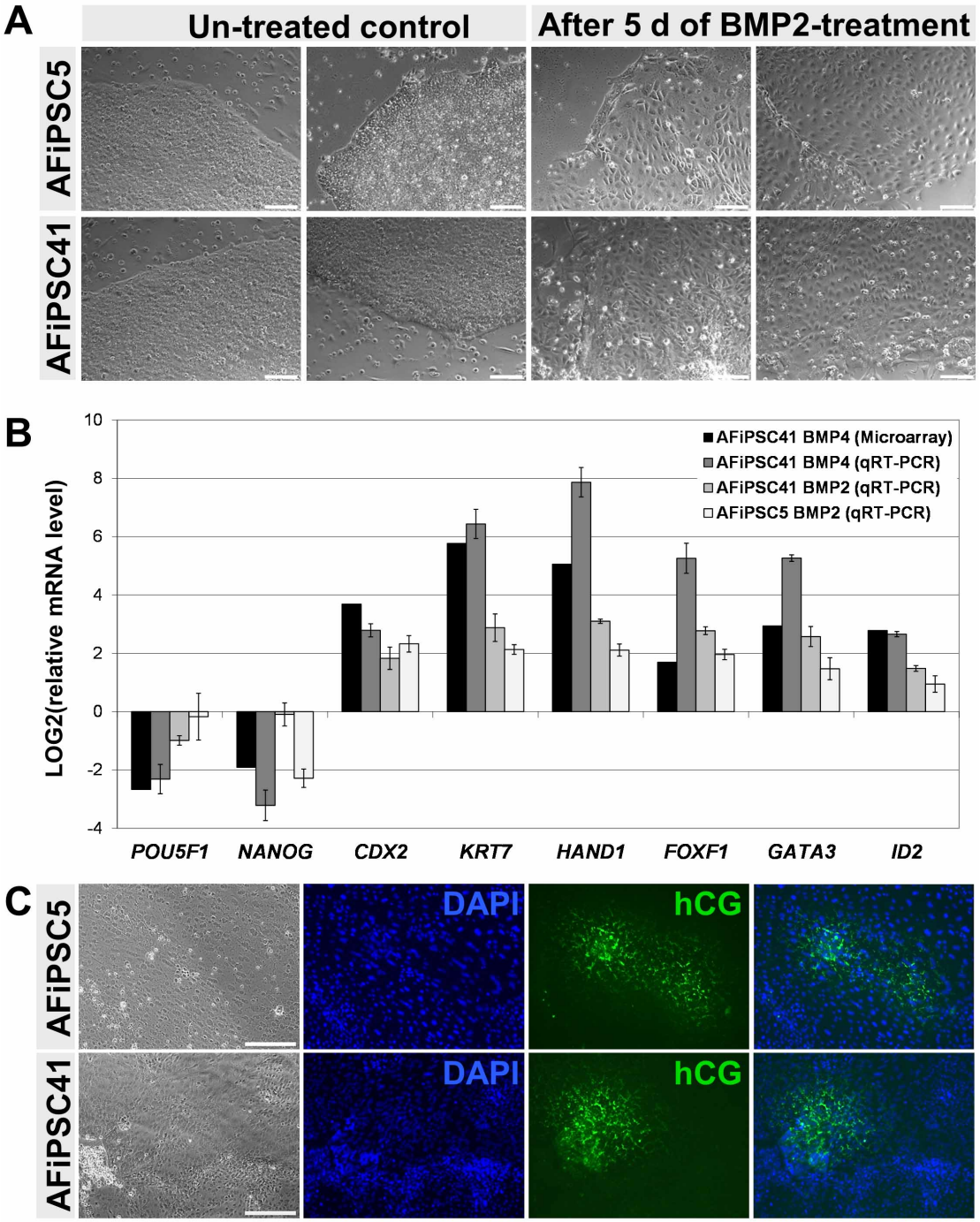

Figure 3.11: Trophoblast differentiation of AFiPSCs. (A) Changes in AFiPSC morphology upon treatment with 100 ng/ml BMP2 over five days. Scale bars = 20 µm. (B) Bar plot depicting qRT-PCR- and microarray-derived expression changes of pluripotency- and trophoblast-associated genes upon treatment of AFiPSCs with 100 ng/ml BMP2 or BMP4 for five days. Bars and error bars represent average LOG2 ratios (BMP-treated AFiPSCs relative to corresponding untreated controls) and SD. Microarray: n = 1, qRT-PCR: n = 3 technical replicates per line and treatment. (C) Phase contrast and images of immunofluorescently labeled human chorion gonadotropin (hCG) in AFiPSCs following seven days of treatment with a combination of 10 ng/ml BMP4 and 10 µM SB431542. Scale bars = 100 µm. Modified from Wolfrum et al. (2010).

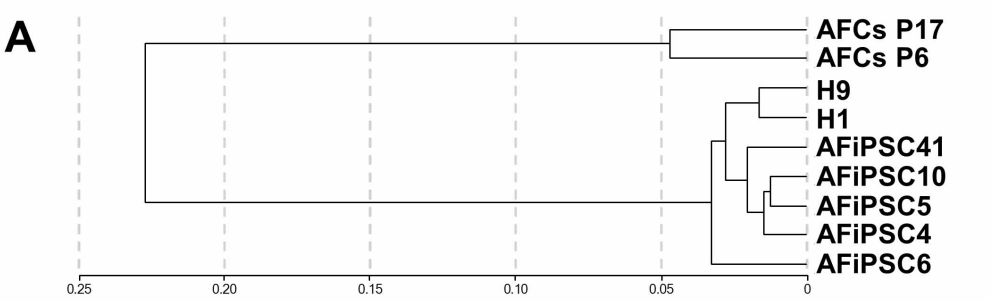

B

	AFCs P6	AFCs P17	AFiPSC4	AFiPSC5	AFiPSC6	AFiPSC10	AFiPSC41	H1	H9
AFCs P6	1.0000								
AFCs P17	0.9012	1.0000							
AFiPSC4	0.6716	0.4988	1.0000						
AFiPSC5	0.6695	0.5007	0.9706	1.0000					
AFiPSC6	0.6364	0.4847	0.9369	0.9496	1.0000				
AFiPSC10	0.6827	0.5115	0.9664	0.9740	0.9531	1.0000			
AFiPSC41	0.6943	0.5191	0.9515	0.9626	0.9246	0.9580	1.0000		
H1	0.6702	0.5191	0.9406	0.9517	0.9130	0.9339	0.9527	1.0000	
H9	0.6613	0.5188	0.9274	0.9480	0.9142	0.9356	0.9408	0.9655	1.0000

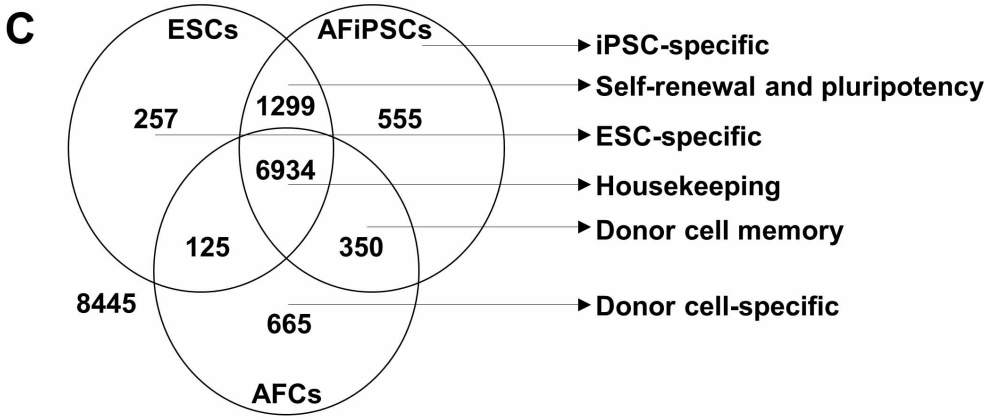

Figure 3.12: Comparative transcriptome analysis of human AFCs, AFiPSCs and ESCs, lines H1 and H9. Total RNA was amplified, labeled and analyzed using the Illumina platform. (A) Hierarchical clustering by means of Pearson's correlation after exclusion of all those genes, which were not expressed in any of the analyzed samples. (B) Table listing linear correlation coefficients (R^2) between indicated samples. (C) Venn diagram summarizing distinct and overlapping gene expression in the different samples. Taken from Wolfrum et al. (2010).

SCs versus human ESCs, emphasizing variable gene expression patterns between iPSCs of different somatic origin (Wolfrum et al., 2010). A Venn diagram highlighted overlapping and distinct gene expression patterns in AFCs versus AFiPSCs and ESCs (Figure 3.12 (C)). In this context we identified gene signatures representative of cellular housekeeping functions (6934 genes, e.g., *GAPDH*, *ACTB*, *PGK1*, *LDHA*), self-renewal and pluripotency (1299 genes, e.g.,

POU5F1, *SOX2*, *NANOG*, *LIN28*), a donor cell memory (350 genes, e.g., *KRT7*, *RGS7*), ESC-specificity (257 genes, e.g., *PRDM14*, *GSC*, *WNT3A*), donor cell (AFCs)-specificity (665 genes, e.g., *OXTR*, *HHAT*, *RGS5*, *NF2*, *CD59*, *TNFSF10*, *NT5E*) and an iPSC (AFiPSC)-specific gene expression signature (555 genes, e.g., *CNTFR*, *SIX6*). The complete gene lists are presented in Wolfrum et al. (2010), Table S3).

Analysis of a common ESC-like core transcriptional regulatory network in AFiPSCs and FiPSCs

To narrow down the self-renewal and pluripotency signature gene list obtained from the Venn diagram comprising the transcriptomes of AFCs, AFiPSCs and ESCs (1299 genes, Figure 3.12 (C)), we compared the same ESC samples with FiPSCs and their respective parental fibroblast line HFF1 (Fibs) (Figure 3.13 (A), the entire gene lists are presented in Wolfrum et al. (2010), Table S5). The HFF1 and FiPSC data sets were independently generated in our laboratory as previously described (Prigione et al., 2010). The resulting, equivalent self-renewal and pluripotency gene signature, in turn, was utilized to detect the overlap between the two separate analyses (AFiPSCs/ESCs: 1299 genes in the self-renewal/pluripotency signature, FiPSCs/ESCs: 922 genes in the self-renewal/pluripotency signature). This overlap comprised 525 genes, which were expressed in all pluripotent cell types (AFiPSCs, FiPSCs and ESCs), highlighting their role in maintaining self-renewal and pluripotency (Figure 3.13 (B), the corresponding gene list is presented in Wolfrum et al. (2010), Table S6). We sought to gain further insight into the TRN that induces and maintains pluripotency in AFiPSCs and FiPSCs and to define distinct functions of the 525 core self-renewal and pluripotency-associated genes of the undifferentiated pluripotent stem cell state. To this end, we next identified the overlap of these 525 genes with genes, the promoters of which are bound by either OCT4 alone or by OCT4, SOX2 and NANOG simultaneously as reported for human ESCs by ChIP-on-chip analyses (Boyer et al., 2005; Jung et al., 2010). This highlighted a subset of pluripotency-associated genes, which are part of an ESC-specific transcriptional regulatory network, comprising, for example, *POU5F1*, *SOX2*, *NANOG*, *DPPA4*, *LEFTY2* and *CDH1* (Figure 3.13 (C)) (Wolfrum et al., 2010). However, this list also contained genes, which are rather known to play essential roles in differentiation processes of human ESCs such as *EOMES* or *HAND1* (Greber et al., 2008). Therefore, we sought to clarify and emphasize the role of these heatmap-listed genes. For this purpose we further combined the heatmap data in Figure 3.13 (C) with gene expression data derived from siRNA-mediated OCT4 (*POU5F1*) knock down experiments in ESCs (Babaie et al., 2007). This resulted in a separation of these genes into three groups: (i) those genes, which follow the expression behaviour of *OCT4* upon loss of pluripotency due to *OCT4* knock down, (ii) those genes, which are inversely regulated and (iii) those genes, which are not significantly affected by the knock down of *OCT4* (Figure 3.13 (C)) (Wolfrum et al., 2010).

The LARGE Principle of Cellular Reprogramming

The reprogramming experiment presented herein and other iPSC studies (Marchetto et al., 2009; Ghosh et al., 2010) demonstrate the conversion of the parental cells' transcriptome to-

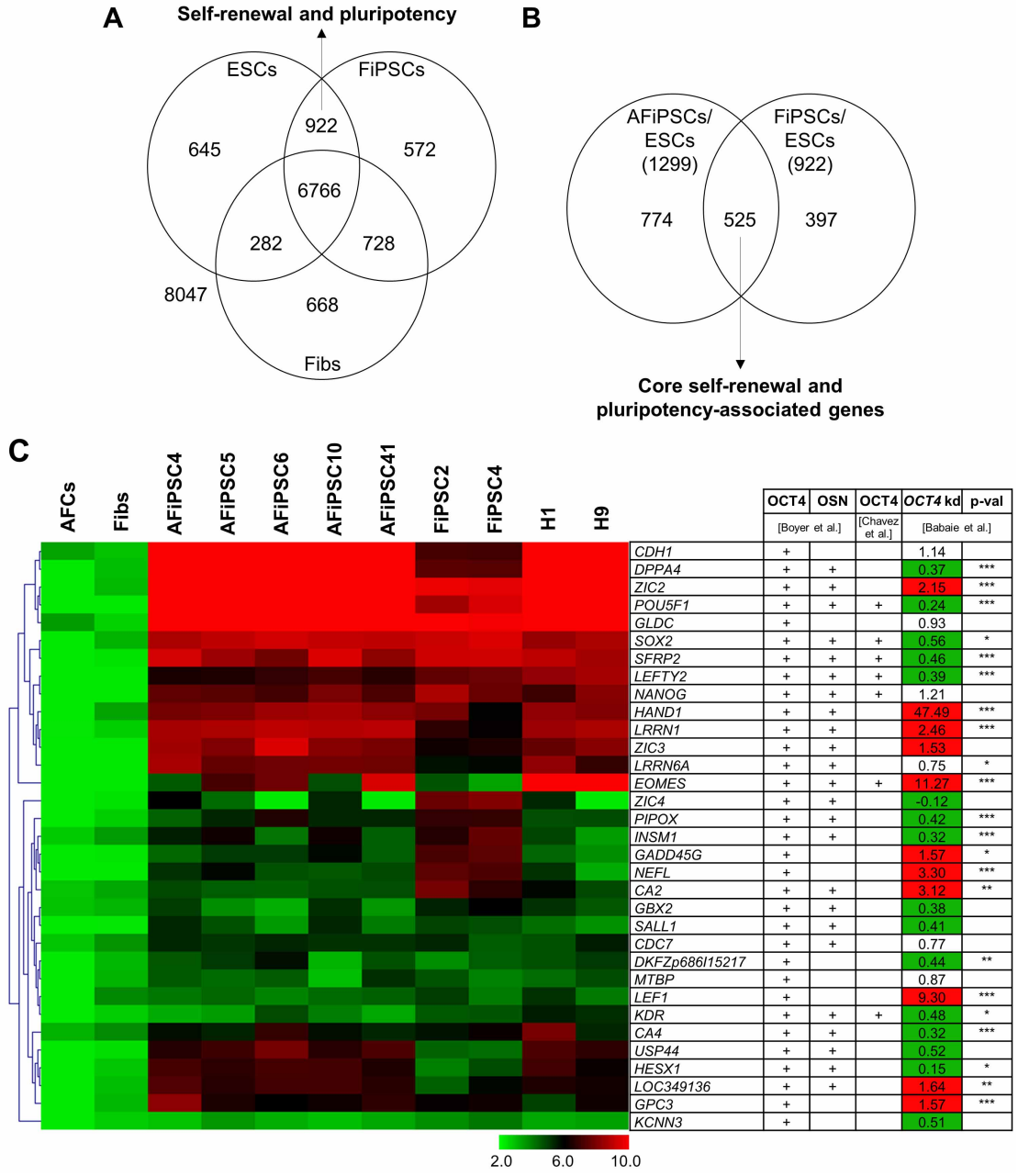

Figure 3.13: Identification of an overlapping ESC-like core TRN in AFiPSCs and FiPSCs. (A) Venn diagram summarizing distinct and overlapping global gene expression in HFF1 fibroblasts (Fibs), HFF1-derived iPSCs (FiPSCs) and ESCs (data obtained from Prigione et al. (2010)). (B) Venn diagram comparing the two self-renewal and pluripotency-associated gene signatures derived from the two previous Venn diagram analyses (AFCs versus AFiPSCs and ESCs (Fig R12C); Fibs versus FiPSCs and ESCs (Figure R13A)) to identify a set of core self-renewal and pluripotency-associated genes. (C) Heatmap depicting microarray-derived LOG2 average gene expression values of a subset of the 525 core self-renewal and pluripotency-associated genes (refer to B), the promoters of which have been shown to be bound by either OCT4 alone or the combination of OCT4, SOX2 and NANOG (OSN, table on the right) as determined by ChIP-chip analyses (Boyer et al., 2005; Jung et al., 2010). The heatmap is colored according to the color key below. Genes were clustered with respect to their expression patterns across the different samples using the Euclidean distance measure. The table on the right also highlights gene expression changes upon siRNA-mediated *OCT4* knock down (*OCT4* kd) in ESCs (H1) including the respective differential expression p-values (p-val) (Babaie et al., 2007). Modified from Wolfrum et al. (2010).

wards a distinct ESC-like state, irrespective of the cell source. Throughout this process, the expression of a subset of genes expressed in the parental cells is Lost (L), whereas the expression of another group of genes is Acquired (A). Yet, the expression of a third subset of genes, detectable in the parental cells, is Retained (R) in the corresponding iPSCs. We refer to this concept as the LARGE (Lost, Acquired, Retained Gene Expression) Principle of Cellular Reprogramming (Figure 3.14 (A)) (Wolfrum et al., 2010). To illustrate the LARGE principle we utilized transcription factor gene expression data as transcription factors usually affect gene expression levels of several downstream targets and, thus, are likely to play an essential role in this concept (Wolfrum et al., 2010). For each of the lost (genes expressed in donor cells, but not in iPSCs), acquired (genes expressed in iPSCs, but not in the donor cells) and retained (genes expressed in donor cells and iPSCs simultaneously, excluding genes of the house keeping gene signature) gene sets derived from the Venn diagram analyses of AFCs/AFiPSCs/ESCs and Fibs/FiPSCs/ESCs (Figure 3.12 (C) and Figure 3.13 (A), Tables S3 and S5 published in Wolfrum et al. (2010)), we arbitrarily picked out genes associated with the Gene Ontology term for transcription factor activity (GO0003700) (Ashburner et al., 2000). Expression data of those 12 transcription factors with the lowest (Lost), highest (Acquired) or least varying (Retained) change, when comparing AFiPSCs or FiPSCs with the corresponding parental cells, were presented in heatmaps (Figure 3.14 (B)) (Wolfrum et al., 2010). This way of illustrating the LARGE principle of cellular reprogramming highlights several key findings: For example, the list of lost genes included, e.g., *HOXB7*, *HOXA9*, *HOXA10*, *PAX8*, *DSCR1* and *MYC*, for AFiPSCs and, e.g., *EMX2*, *FOXF2*, *FOXF1*, *MYC* and *KLF4* for FiPSCs (Wolfrum et al., 2010). The acquired gene expression set can be further divided into two groups on the basis of present or absent overlaps between the two analyses for AFiPSCs and FiPSCs: those, which are universally acquired self-renewal genes present in both, AFiPSCs and FiPSCs, or, more generally, in all pluripotent iPSCs (e.g., *POU5F1*, *SOX2*, *NANOG*), and those acquired gene expressions, which are rather iPSC type-dependent (e.g. *SIX6*, *EGR2* (AFiPSCs) or *PKNOX2*, *HOXD4*, *HOXD10* (FiPSCs); *DLX5* (AFiPSCs and FiPSCs)) (Wolfrum et al., 2010). The retained gene expression sets included genes like *PKNOX2* (AFiPSCs), *HMBOX1* and *MGA* (FiPSCs) or *RAXL1* (AFiPSCs and FiPSCs) (Wolfrum et al., 2010). Moreover, some general aspects were highlighted in Figure 3.14: i. The list of the most (or least) differentially expressed lost, acquired and retained transcription factors overlapped only partly when comparing AFCs turning into AFiPSCs with fibroblasts developing into FiPSCs. ii. The magnitude of gene expression changes or the stability of gene expression retention of lost, acquired or retained gene subsets, respectively, was not equal among all clonal AFiPSC lines (e.g., *DLX1*, *ZNF218*, *PKNOX2*). The same was observed for clonally-derived FiPSC lines (*DLX1*, *NME2*). iii. In many cases, gene expression levels observed for both (the majority of) AFiPSC lines and FiPSC lines were distinct from those detected in human ESCs H1 and H9 (e.g. *LHX2*, *DLX5*, *DLX1*, *ZNF218* etc. (AFiPSCs) and *PRRX1*, *NFE2*, *MLLT1*, *HOXD1*, *DLX5*, *DLX1* etc. (FiPSCs)).

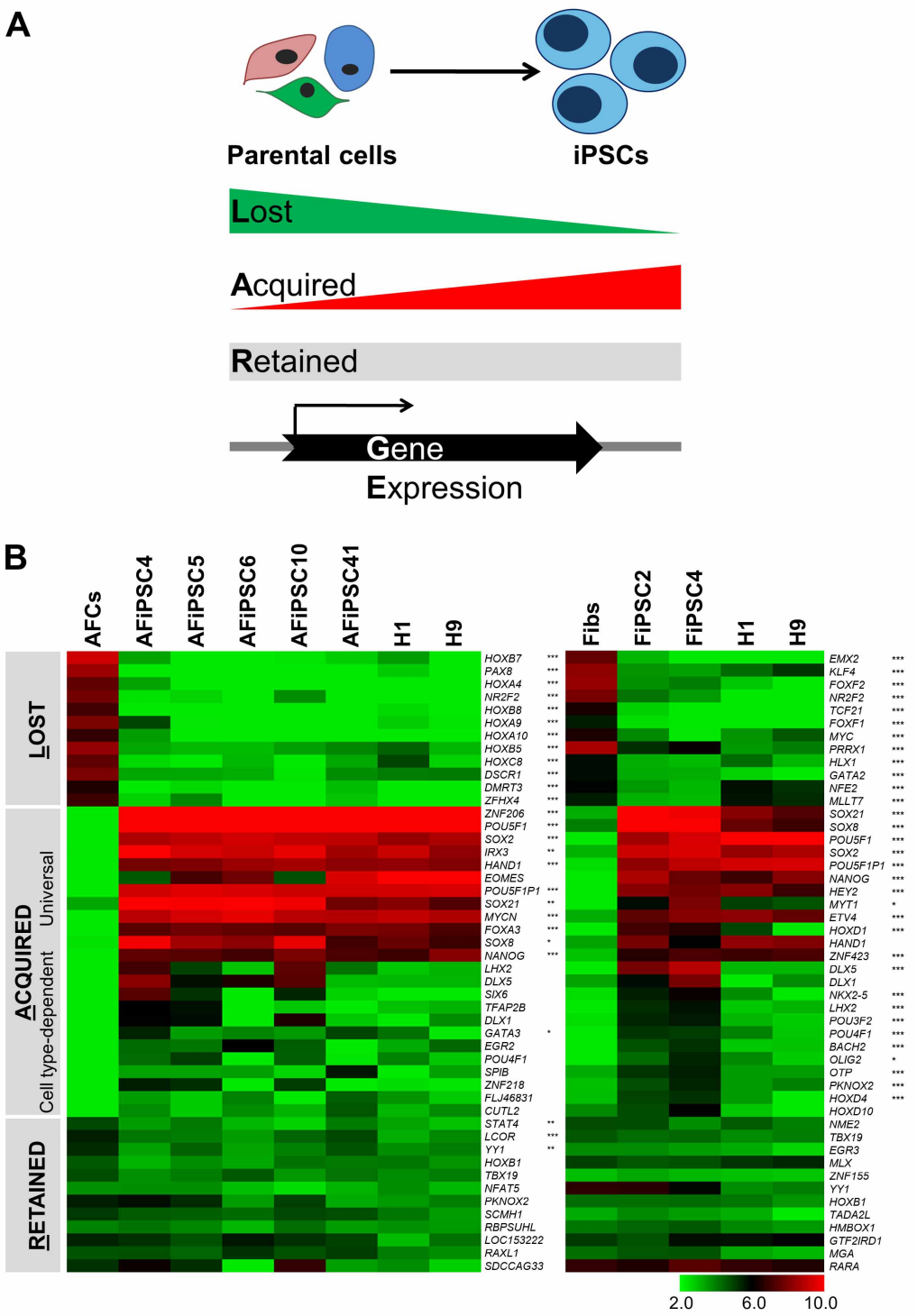

Figure 3.14: The LARGE Principle of Cellular Reprogramming. (A) Schematic representation of the LARGE Principle of Cellular Reprogramming. (B) Transcription factor gene expression data were extracted from the transcriptome data of AFCs, AFiPSCs, ESCs, Fibs and FiPSCs and ranked according to the most effectively down-regulated (the set of lost genes), up-regulated (the set of acquired genes) or the least varying (the set of retained genes) gene expression levels when comparing each donor cell line with the corresponding group of iPSCs. The heatmap depicts LOG2 average expression values of the top 12 or 24 lost, acquired and retained genes for each of the donor cell lines, the respective iPSCs and ESCs as a reference. The heatmap is colored according to the color key below. Significantly up- or down-regulated gene expression in donor versus iPSCs is indicated by asterisks (padj < 0.05 ($*$), < 0.01 ($**$), < 0.001 ($***$)). Taken from Wolfrum et al. (2010).

Expression of senescence-associated genes in primary AFCs and AFiPSCs

Finally, to investigate if reprogramming by-passes the senescence observed in primary AFC cultures (Figure 3.1), we analyzed the expression of senescence and telomere-associated genes in young, proliferating primary AFCs at P6 and senescent AFCs at P17 in comparison to the corresponding, theoretically indefinitely self-renewing AFiPSC lines around P20. H1 and H9 ESCs (P56, P55, respectively) were included for comparison. To this end we derived a list of 116 senescence-associated genes (Table B.1) (Wolfrum et al., 2010) from the Gene Ontology database (Ashburner et al., 2000), including those described by Vaziri et al. (2010). Of those, we identified 64 genes as significantly differentially expressed in AFCs at P17 compared to the union of all AFiPSC lines (Figure 3.15) (Wolfrum et al., 2010). Amongst those, telomere-associated genes and genes involved in cell cycle regulation, e.g., *MAD2L2*, *PARP1*, *RPA3*, *DKC1*, *MSH6*, *CHEK1*, *PLK1*, *POU2F1*, *CDC2*, *BLM*, *WRN*, *DNMT1*, *DNMT3B*, *LMNB1*, and *CDT1*, were down-regulated in primary AFCs compared to AFiPSCs and ESCs (Wolfrum et al., 2010). In contrast, *PIN1*, *LMNA*, *GADD45A*, *CBX6*, *NOX4*, *ENG*, *HIST2H2BE*, *CDKN2A*, *CDKN1A*, *GDF15* and *SERPINE1*, among others, were up-regulated in primary AFCs compared to AFiPSCs and ESCs (Wolfrum et al., 2010).

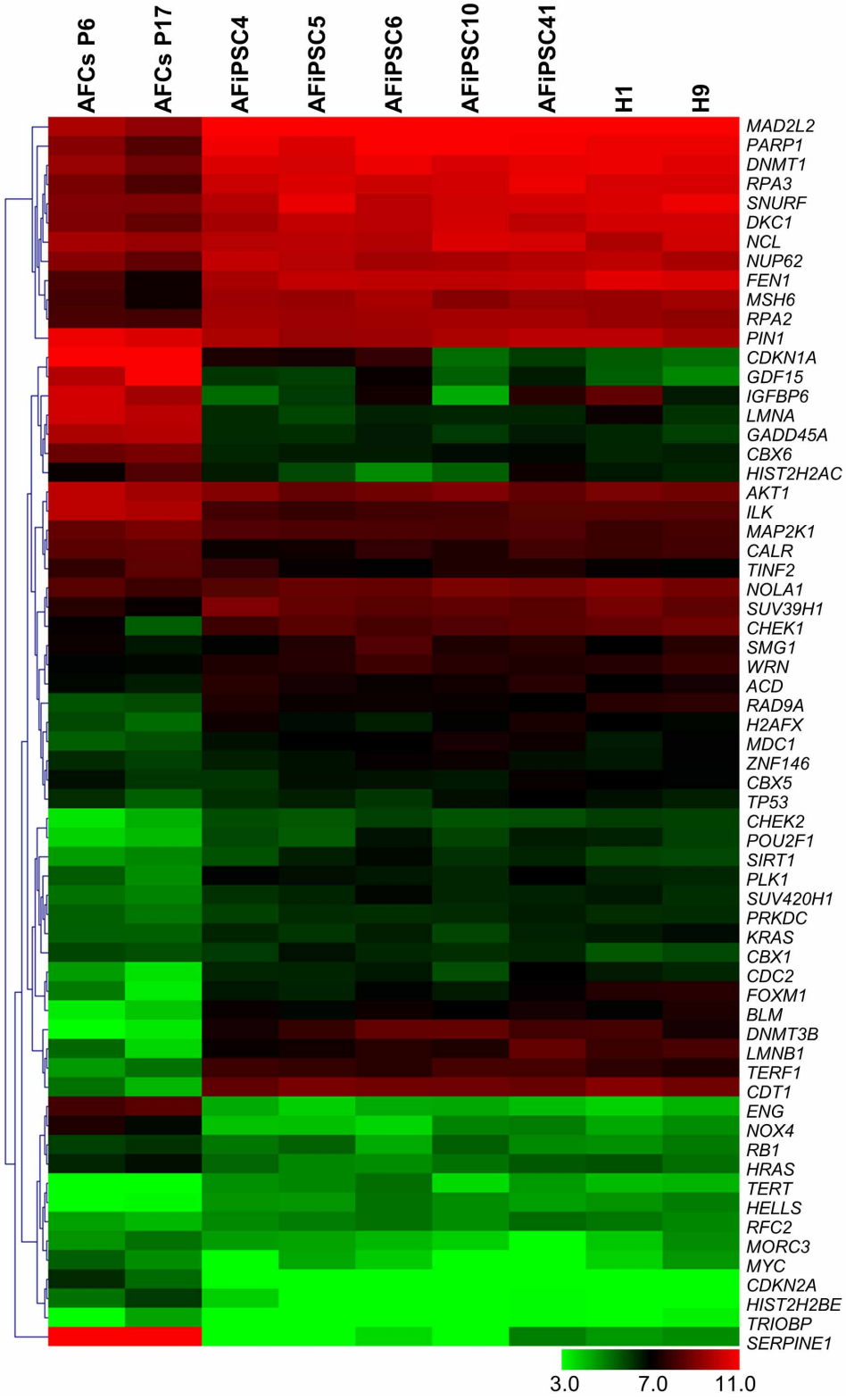

Figure 3.15: Heatmap of senescence-associated gene expression in AFCs, AFiPSCs and ESCs, lines H1 and H9. The heatmap depicts LOG2 average genes expression values of significantly differentially expressed senescence-associated genes resulting from the comparison of the union of AFiPSCs around P20 with the parental AFC line 101 after the onset of senescence at P17 ($\geq$ 1.5 fold up- or down-regulattion, padj $<$ 0.05). The heatmap is colored according to the color key below. Genes were clustered with respect to their expression patterns across the different samples using the Euclidean distance measure. Taken from Wolfrum et al. (2010).

3.2.5 shRNA-mediated *USP44* knock down in AFiPSCs and ESCs

Recently, we have investigated the key transcriptional regulatory network, which governs the human pluripotent stem cell phenotype, by OCT4 ChIP-on-chip analysis (Jung et al., 2010). As one of the key findings of this study, it has been demonstrated that the ubiquitin-specific protease 44 (USP44), a deubiquitinating enzyme, harbors an evolutionary conserved OCT4 binding site and that USP44 is positively regulated by OCT4 in both human ESCs and embryonal carcinoma (EC) cells. To date, USP44 has been reported to play a key role in regulating the cell cycle, i.e. in the control of the spindle checkpoint as it prevents the premature onset of the anaphase (Stegmeier et al., 2007). However, the direct role of USP44 in promoting self-renewal and pluripotency in these cell types is yet unknown. Genetic engineering of human PSCs, i.e. knock-down, knock-out and knock-in of distinct genes to investigate their specific function in the maintenance of self-renewal and differentiation potency, developmental processes or diseases, is an essential part of stem cell biology (Thomson et al., 1998; Menendez et al., 2005; Maury et al., 2011). Referring to previous knock down experiments carried out in our laboratory (Babaie et al., 2007; Greber et al., 2007b), we sought to utilize the retroviral-derived AFiPSC lines along with human ESCs to investigate the functional role of USP44 in maintaining pluripotency and self-renewal in different human PSC types. We aimed to knock down *USP44* by RNA interference in human AF-derived iPSC lines and the ESC line H1. To this end, we aspired to deliver constructs encoding short hairpin RNAs (shRNAs) against *USP44* by lentiviral transduction or by chemical transfection. However, as genetic manipulation of human ESCs is still a major technical challenge (Zwaka and Thomson, 2003; Braam et al., 2008; Giudice and Trounson, 2008; Zafarana et al., 2009; Ma et al., 2010; Maury et al., 2011), the transduction and transfection protocol first required optimization by the use of several GFP-encoding reporter constructs.

3.2.5.1 Lentiviral particle production

Lentiviral particles encoding different shRNAs against *USP44* or TurboGFP (TGFP) were produced in HEK 293 cells and subsequently used to infect HEK and HFF1 cells to verify their ability to transduce human cell lines. For this purpose, the TGFP-encoding lentivirus was used as a positive transduction control as the green fluorescent signal observed in target cells upon lentiviral transduction demonstrated functionality of both freshly prepared and concentrated, frozen lentiviruses (Figure 3.16).

3.2.5.2 Lentiviral transduction of human PSCs

Having verified the ability of the lentiviruses to infect human cell lines, the TGFP-control virus was used to establish human PSC transduction. On the basis of the protocol recently published by Du and Zhang (2010), we first dissociated H1 ESCs and infected single cells in suspension with the TGFP-encoding lentiviral particles. As a result, H1 ESCs massively differentiated and no green fluorescent signal was detectable (Figure 3.17) even up to six days post-transduction.

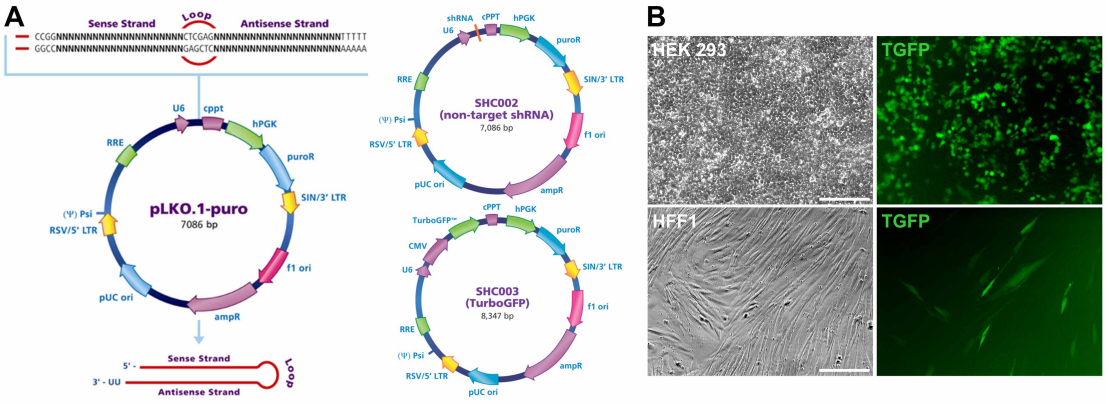

Figure 3.16: GFP expression in HEK 293 and HFF1 fibroblast cells upon transduction with TGFP-encoding lentiviruses. (A) Maps of the lentiviral shRNA, non-target shRNA or TGFP-encoding lentiviral vectors. Obtained from http://www.sigmaaldrich.com/life-science/functional-genomics-and-rnai/shrna/library-information/vector-map.html. (B) Representative images of cells transduced with 50 µl fresh lentiviral particles 72 h post-transduction are shown. Scale bars = 200 µm.

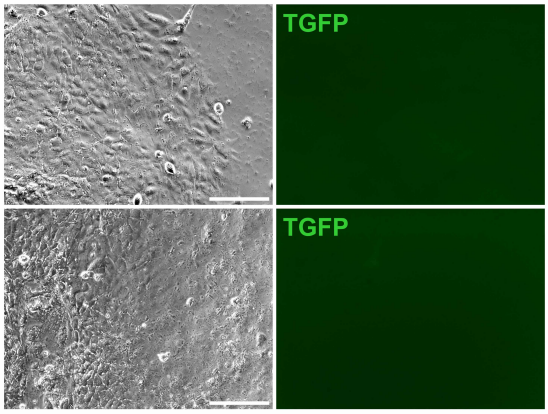

Figure 3.17: GFP expression in H1 ESCs upon TrypLE Select-mediated dissociation and transduction with TGFP-encoding lentiviruses. Images were acquired 72 h post-transduction. Scale bars = 200 µm.

As the ability to maintain human PSCs in the undifferentiated state is crucial for investigating the role of USP44 in supporting self-renewal and pluripotency, we next tested if we were generally able to recover undifferentiated human PSCs upon dissociation of the colonies to single cells without transducing them. Thus, as in the lentiviral transduction protocol, we pre-incubated H1 ESCs with ROCK Inhibitor prior to TrypLE Select-mediated dissociation of the colonies and re-plating of the single cells in growth medium devoid of lentivirus, yet, containing a combination of ROCK Inhibitor and thiazovivin or thiazovivin alone to promote the recovery of undifferentiated human PSC colonies. The absence of tightly packed ESC colonies about one week after dissociation and the presence of spindle- or cobblestone-shaped cells suggested substantial differentiation of H1 ESCs after dissociation and re-plating (Figure 3.18, upper panel). However, after nearly two weeks of cultivation tightly packed

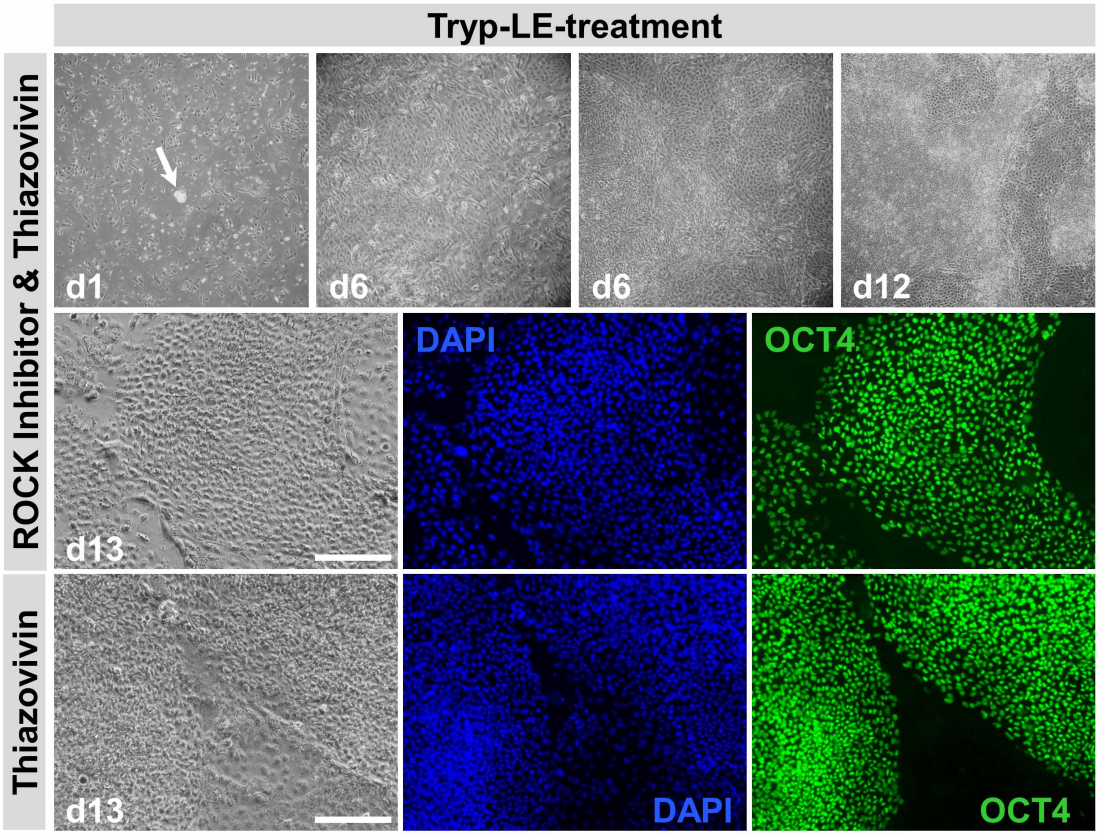

Figure 3.18: Morphology and OCT4 expression in H1 ESCs cultivated with different supplements following TrypLE Select-mediated dissociation. Images of the cellular morphology were acquired at several time-points after dissociation as indicated. Cells were fixed and analyzed for OCT4 expression by immunofluorescent protein labeling 13 days after dissociation. Scale bars = 200 µm.

colonies of putatively undifferentiated ESCs re-emerged in very few cases (Figure 3.18, upper panel, d12). Such colonies expressed the key pluripotency factor OCT4 as determined by immunofluorescent protein labeling.

Nevertheless, the presence of such OCT4-positive colonies was rather exceptional. Presumably, these colonies have grown out of small cell clusters that could not be properly dissociated even after pro-longed TrypLE Select-treatment (indicated by arrow in the upper panel of Figure 3.18).

As the treatment of human PSCs with ROCK inhibitor and thiazovivin did not markedly improve the yield of undifferentiated human PSCs after single cell dissociation even without lentiviral transduction, we tested if it was possible to homogeneously transduce non-dissociated or only partly dissociated colonies of ESCs or AFiPSCs as suggested by the MISSION RNAi human ESC transduction protocol (Sigma). We transduced un-dissociated colonies (with and without centrifugation to enhance the transduction efficiency) and colonies that have been manually dissociated into smaller pieces and Dispase-treated, as during routine passaging of human PSCs. Still, no TGFP expression was detectable in the vast majority of

samples two to five days post-transduction. The few green fluorescent signals observed were the result of TGFP expression in differentiated human PSCs as clearly recognizable from the spindle shaped morphology and the long cell protrusions (Figure 3.19).

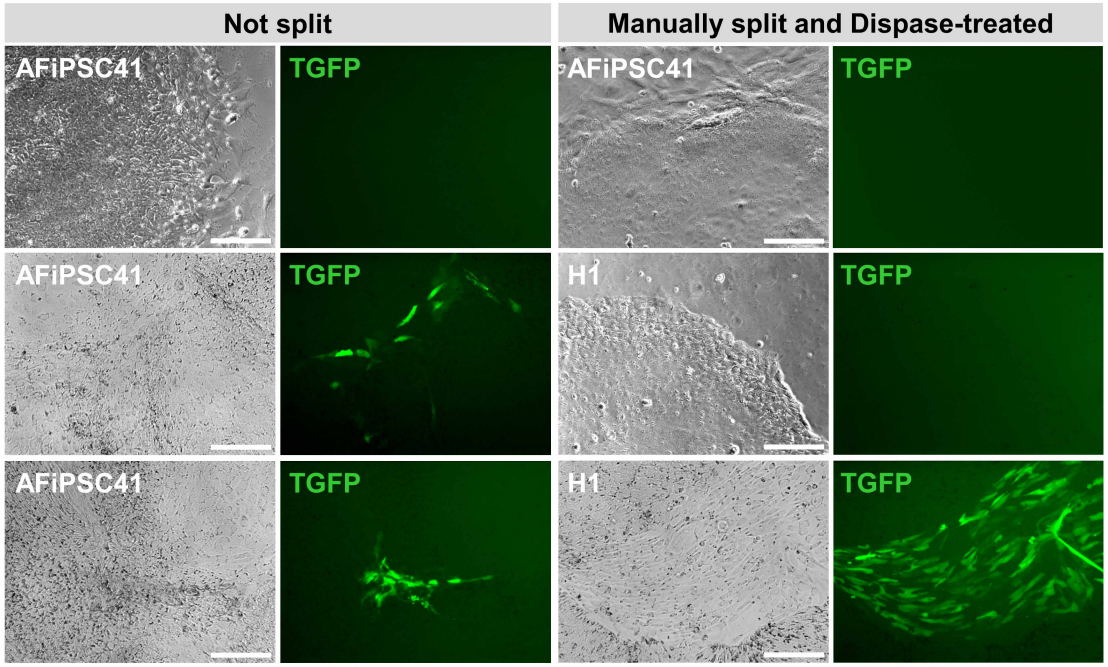

Figure 3.19: GFP expression in un-dissociated or partly dissociated AFiPSCs and ESCs after transduction of TGFP-encoding lentiviruses. Colonies of human PSCs were either not split or manually dissociated and Dispase-treated prior to the incubation with TGFP-encoding lentivirus. Images were acquired 48 h post-transduction (un-dissociated AFiPSC41), 72 h post-transduction (H1 ESCs) or 96 h post-transduction (Dispase-split AFiPSC41). Scale bars = 200 µm.

3.2.5.3 Transfection of human PSCs with lentiviral plasmids

Due to the unaccountable, unsuccessful expression of transgenes in undifferentiated human PSCs following lentiviral transduction, we sought to deliver the *USP44*-targeting shRNAs by plasmid transfection. Hence, the human ESC line H1 and AFiPSC line 41 were transfected with the same *USP44* shRNA-encoding vectors and, for optimization purposes, with the TGFP-encoding control vector or two other positive reporter constructs encoding either *OCT4* promoter-driven EGFP or maxGFP. Various modifications were successively included in the transfection protocol as follows: First, human PSCs were transfected with the *OCT4* promoter-driven EGFP vector to determine if undifferentiated human PSCs can express the desired transgene. These transfections were carried out following dissociation to single cells by TrypLE Select or the putatively more gentle dissociation solution of Accutase (reverse transfection including incubation with thiazovivin to promote the recovery of undifferentiated human PSCs) or following no dissociation. Simultaneously, transfection efficiencies in growth medium and OptiMEM were compared. As already observed for the lentiviral transduction,

the few green fluorescent cells mainly had the morphology of differentiated cells, which, referring to their ability to express this *OCT4* promoter-driven EGFP, however, must still have contained sufficient levels of remnant OCT4. With respect to intact human PSC colonies the only transgene expressing cells were those on the periphery of the colonies, whereas those cells in the center of the tightly packed human PSC colonies were never observed to emit green fluorescence (Figure 3.20). In view of the vimentin expression of putatively differentiated cells

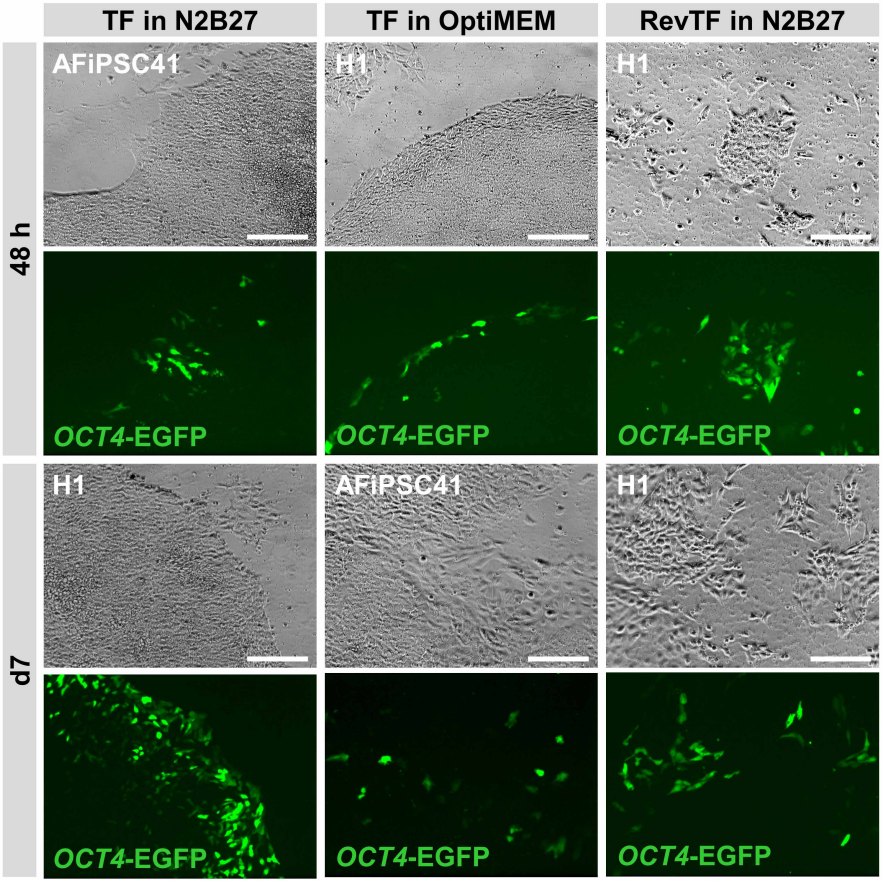

Figure 3.20: GFP expression in un-dissociated or to the single cell level dissociated AFiPSCs and H1 ESCs following transfection of a vector encoding *OCT4* promoter-driven EGFP. Cells were either not dissociated prior to transfection (TF, 100 µl OptiMEM, 2 µg DNA, 6 µl FuGENE HD per 12-well) or TrypLE select-treated and transfected as single cells (reverse transfection, RevTF, 100 µl OptiMEM, 4 µg DNA, 12 µl FuGENE HD in N2B27 defined medium containing thiazovivin). Incubation of complexed DNA was carried out in defined N2B27 medium ON or in OptiMEM for 2 h as indicated. Images were acquired at the indicated time points. Scale bars = 200 µm.

on the periphery of AFiPSC colonies shown earlier (Figure 3.8), this finding is, once more, indicative, that the only transgene expressing cells are presumably not undifferentiated but rather differentiated PSCs.

Irrespective of these findings, we next, attempted to deliver the TGFP-encoding equivalent of the shRNA lentiviral vectors into AFiPSCs and H1 ESCs. In order to also target those cells, which are normally difficult to reach due to the high cell density in the center of human PSC

colonies, transfections were carried out following TrypLE Select-mediated dissociation to single cells, also including thiazovivin-treatment. Again, no TGFP expression could be observed in both cell lines (Figure 3.21).

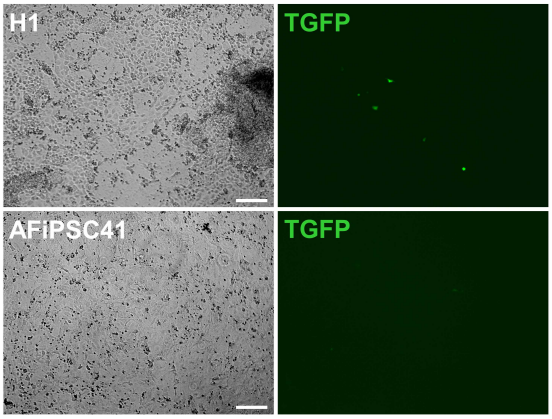

Figure 3.21: GFP expression in TrypLE Select-dissociated AFiPSCs and H1 ESCs following transfection of a lentiviral vector encoding TGFP. The reverse transfections were carried out using 100 µl OptiMEM, 2 µg DNA, 6 µl FuGENE HD in N2B27 defined medium containing thiazovivin. Images were acquired three (AFiPSC41) or five days (H1) post-transfection. Scale bars = 200 µm.

To potentially improve the transfection efficiency, we compared FuGENE HD transfection reagent with Lipofectamine 2000. To this end, after having conducted several preliminary tests, we finally reverse transfected AFiPSCs with different GFP-encoding vectors using both transfection reagents upon pre-incubation with ROCK Inhibitor and dissociation of the colonies to single cells by Accutase-treatment, followed by further incubation with ROCK inhibitor and thiazovivin. In parallel, un-dissociated AFiPSC colonies were transfected with different GFP-encoding plasmids as this had only been done using FuGENE HD before.

Although a transfection efficiency gradient could be observed from Lipofectamine 2000/pmaxGFP over FuGENE HD/pmaxGFP and Lipofectamine 2000/TGFP to FuGENE HD/TGFP, the overall transfection efficiency was repeatedly low (Figure 3.22). Both in case of the dissociated as well as the un-dissociated AFiPSCs the only transgene expressing cells (if any were observable) were those which had already differentiated as evident from the shape of the green fluorescent cells.

In conclusion, the lack of GFP expression in the core of densely packed, undifferentiated human PSC colonies in all of the experiments carried out demonstrated that none of the vector types used and neither the lentiviral nor the transfection-based delivery method facilitated an efficient transgene expression in undifferentiated human PSC colonies. This was observed for both un-dissociated and dissociated colonies of human ESCs as well as for AF-derived iPSCs, irrespective of the use of supplements, i.e. ROCK Inhibitor and thiazovivin, to enhance the viability of single human PSCs. In conclusion, the attempt to investigate the functional role of USP44 in human PSCs requires extensive optimization and could not be pursued further in the course of this PhD project.

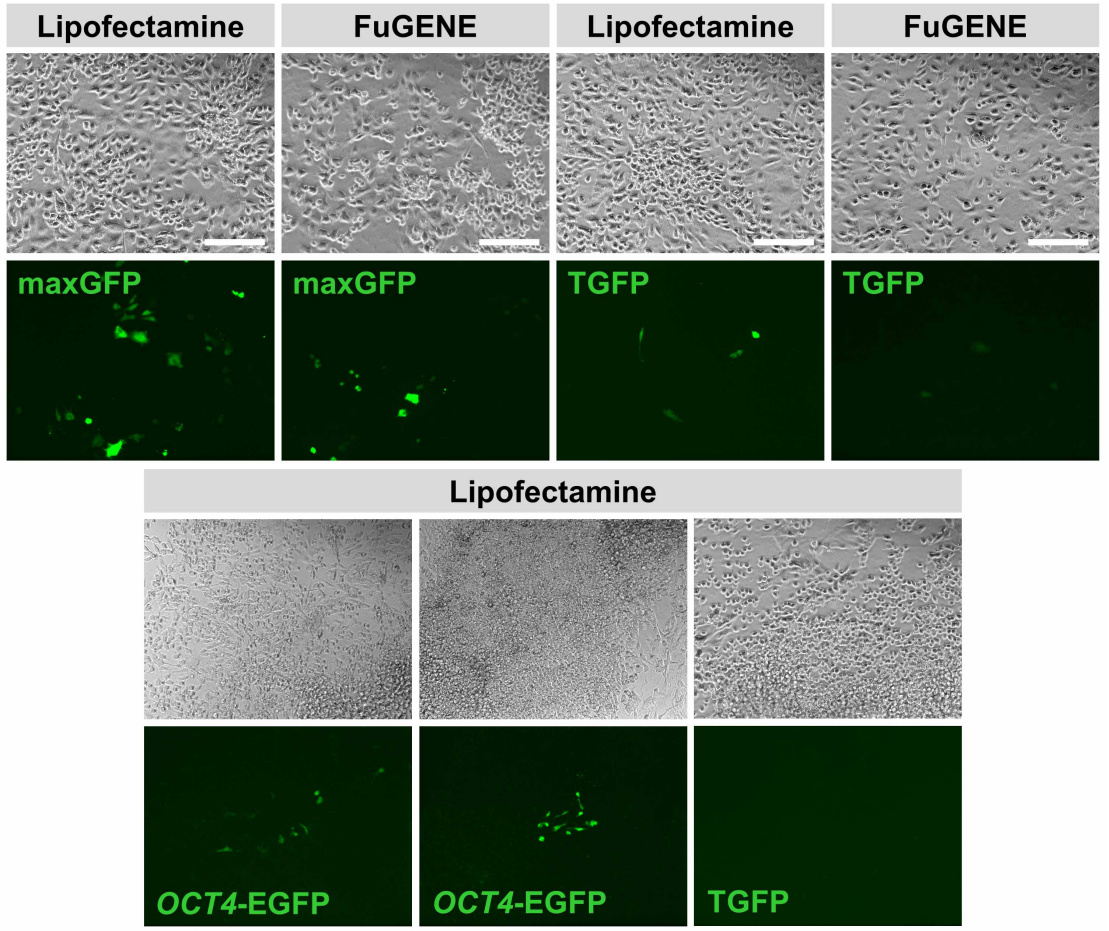

Figure 3.22: GFP expression in AFiPSC line 41 following comparative transfections of different GFP-encoding reporter constructs using Lipofectamine 2000 and FuGENE HD. (A) AFiPSCs were pre-incubated with ROCK Inhibitor, dissociated by incubation with Accutase and reverse transfected using 200 µl OptiMEM, 1 µg DNA and 2 µl Lipofectamine 2000 or 100 µl OptiMEM, 1 µg DNA and 3 µl FuGENE HD in N2B27 defined medium including ROCK inhibitor and thiazovivin. (B) Un-dissociated AFiPSC colonies were transfected with 200 µl OptiMEM, 1 µg DNA and 2 µl Lipofectamine 2000. Images were acquired four days post-transfection. Scale bars = 200 µm.

3.3 Discussion

The very first goal of this project was to sort stem cell-like subpopulations of human AFCs to obtain a suitable source of cells, which could subsequently be reprogrammed more efficiently to iPSCs than other terminally differentiated somatic cells. This was based on the fact that numerous research reports have highlighted the expression of several stem cell markers, mainly neuronal stem or progenitor cell markers, mesenchymal stem cell or pluripotent stem cell markers, which facilitate the selection of cells with stem cell properties by different protocols (In 't Anker et al., 2003; Prusa et al., 2004; Tsai et al., 2004; Karlmark et al., 2005; Bossolasco et al., 2006; Tsai et al., 2006; Chiavegato et al., 2007; De Coppi et al., 2007; Kim et al., 2007; Sessarego et al., 2008; Trovato et al., 2009; You et al., 2009). However, the implementation of

the most noted protocol (De Coppi et al., 2007) was not practicable in our setting. This was due to the change in human AFC morphology, which was observed approximately at P4 to P5. This morphological change involved a major increase in cell size, starting from a heterogeneous population of small ovoid to squamous epithelioid cells that turned into a homogeneous population of large, flat, seemingly fragile fibroblast-like cells. Although the variety of cells present in samples of human amniotic fluid have been investigated intensively (reviewed by Gosden (1983)), the particular morphological change observed here has, to the best of my knowledge, not been described in detail to date. Determination if this shift of morphology was indeed a true morphological change of all cells in the culture or if it was rather due to selection processes during the *in vitro* propagation and whether it was to some extent already associated with the relatively early onset of senescence was beyond the scope of this project. It has been shown, however, that MACS and FACS-based protocols involving human AFCs are successful if performed early after isolation, preferably within the first two passages of culture (Chiavegato et al., 2007; De Coppi et al., 2007; Moschidou et al.). The samples obtained for this project were delivered as frozen aliquots at approximately P2, which required re-expansion before being used in experimental settings. The morphological change occurred during the phase of re-expansion and hampered efficient sorting strategies and, hence, the establishment of stem-cell like subpopulations with verifiable marker expression for down-stream applications.

Provided that sufficient amounts of early passage human AFCs for MACS and FACS-based sorting approaches were available, other surface markers should be considered for the selection of stem cell-like cells for direct reprogramming. In a collaborative project, we have recently shown that proportions of AFCs found in earlier stages of gestation, i.e. the first trimester, express human ESC surface markers such as SSEA4 and AP, SSEA3, TRA-1-60 and TRA-1-81 at single cell level (Moschidou et al.). These stem cell-like cells resemble a subpopulation of AFCs, which are probably closer to PSCs than the CD117-positive fraction (De Coppi et al., 2007; Moschidou et al.). The potential of other human ESC markers such as CD133 (Kaufman et al., 2001) and PODXL (Adewumi et al., 2007), an early marker of pluripotency during iPSCs generation (Mah et al., 2011), for more routinely available second trimester AFCs requires further investigation.

The technical difficulties associated with sorting bulk primary AFCs changed the starting point of this project. However, it did not affect the progress of the project as the use of bulk primary human AFCs, which included putative stem cell-like cells, as starting material for cellular reprogramming was still expected to be highly efficient.

3.3.1 Ground state pluripotency of AFiPSCs

Next, as demonstrated in this first part of this thesis, bulk primary AFCs can be converted into an ESC-like phenotype by retroviral transduction of the Yamanaka cocktail of transcription factors (OSKM). The fact that no enriched stem cell-like AFC samples were available as target cells for cellular reprogramming did not derogate from efficient and especially rapid induction of pluripotency when compared to the generation of iPSCs from skin fibroblast cells (Taka-

hashi et al., 2007; Prigione et al., 2010; Wolfrum et al., 2010). This is in agreement with recent reports, which have been published while this project was on-going: Whereas the experiments described here and elsewhere (Li et al., 2009a; Galende et al., 2010; Anchan et al., 2011) were based on the retroviral transduction of the original cocktail of four reprogramming factors (OCT4 SOX2, KLF2, c-MYC), others have meanwhile accomplished to convert human AFCs into iPSCs by lentiviral or retroviral transduction of just two (OCT4, SOX2) (Ye et al., 2009) or even one reprogramming factor (OCT4), in combination with small chemical compounds (NaB, PS48, A-83-01, PD0325901, CHIR99021 and Parnate) (Zhu et al., 2010), or upon pre-selection of CD34-positive cells (Liu et al., 2012). These findings emphasize that human AFCs acquire the PSC state more easily than fully differentiated somatic cells.

The AFiPSCs generated in the course of this project were positive for all tested human ESC and pluripotency-associated markers. Immunofluorescence-mediated detection of cadherin-1 (E-cadherin), in contrast to vimentin, indicated the uniform epithelial nature of AFiPSCs. These cells passed both the embryoid body formation and teratoma formation assays verifying complete induction of pluripotency in these cells. It has further been demonstrated that AFiPSCs, like ESCs, have the ability to form derivatives of the extraembryonic trophoblast lineage. Generally, the acquisition of key ESC characteristics during cellular reprogramming enhanced the restricted differentiation potential of human AFCs and should, thus, proof beneficial for the application of AFiPSCs in basic and applied research. Although the teratoma formation potential of AFiPSCs, a common feature of iPSCs and ESCs, impedes their potential use in cell replacement therapies, it must be assumed that ways will be found to exploit the full differentiation potential of iPSCs while circumventing tumor formation risks. This could for instance be achieved, by developing highly efficient differentiation protocols, which result in pure terminally differentiated cell types, or accurate sorting strategies to separate fully differentiated cells of interest from potential tumorigenic stem cells. Recent progress has been made in this respect and the realization of the first clinical trials for human ESC-derived therapeutics is leading the way (Drews et al., b; Schwartz et al., 2012b).

3.3.2 Cellular reprogramming by-passes senescence of bulk primary AFCs

Furthermore, cellular reprogramming by-passes senescence of bulk primary AFCs. Acquisition of the ability to propagate indefinitely should also increase the value of AFiPSCs for down-stream applications. The data obtained in the course of this project suggest, that the phenotypically rejuvenated appearance of AFiPSCs is based on a gene expression profile, which averts or at least markedly delays the onset of senescence. Opposing expression of a large number of senescence-associated genes has been highlighted for primary AFCs and AFiPSCs and ESCs. More specifically, high expression levels of various cell cycle and telomere elongation-associated genes such as *MAD2L2*, *PARP1*, *RPA3*, *DKC1*, *MSH6*, *CHEK1*, *PLK1*, *POU2F1*, *CDC2*, *LMNB1* and *CDT1* as well as *TERT* itself were detected in AFiPSCs in contrast to primary AFCs (Wolfrum et al., 2010). The p53/p21 pathway is known to play

an essential role in inducing and maintaining senescence (Brown et al., 1997). In line with this, mRNA levels of several p53 target genes, which are known to be highly expressed in senescent cells (Chang et al., 2000; Young and Smith, 2001; Huang and Vassilev, 2009), e.g., *CDKN1A* (p21), *GDF15*, and *SERPINE1*, were strikingly elevated in primary AFCs compared to AFiPSCs and ESCs (Wolfrum et al., 2010). In contrast, *DNMT1* and *DNMT3B* were expressed at low levels in bulk primary AFCs and significantly up-regulated in AFiPSCs. These DNA-methyltransferases normally establish and maintain CpG methylation patterns during embryonal development. They are also known, however, to repress transcription of *CDKN1A* in opposition to and potentially independent of p53 (Young and Smith, 2001; Zheng et al., 2006; Wolfrum et al., 2010). Hence, it could be speculated that the high expression levels of the DNMTs in AFiPSCs may repress *CDKN1A* and, thus, senescence in these cells (Wolfrum et al., 2010). Although from the results of the microarray-based transcriptome analysis there is strong evidence that senescence of primary human AFCs is indeed by-passed upon the activation of a self-renewal and pluripotency program, further studies are required to assess the actual ability of AFiPSCs to restore telomere restriction fragment length to an ESC level, a subject of controversial discussion in the iPSC field (Suhr et al., 2009; Agarwal et al., 2010; Vaziri et al., 2010; Wolfrum et al., 2010).

3.3.3 The LARGE Principle of Cellular Reprogramming and ESC-specific gene expression signatures

The extensive comparative transcriptome analyses of AFiPSCs, ESCs (H1, H9) and FiPSCs and the corresponding parental cell lines has highlighted mechanistic and functional aspects of cellular reprogramming. The data obtained from the whole genome gene expression analyses was used to devise the LARGE (Lost, Acquired and Retained Gene Expression) Principle of Cellular Reprogramming, i.e. to identify genes, the expression of which was either Lost (L), Acquired (A) or Retained (R) upon the induction of pluripotency in different iPSC types (Wolfrum et al., 2010). In the following paragraphs, some of these gene expression patterns, including several signature genes, will be discussed in greater detail.

The donor cell (AFC)-specific gene signature contains putative immune-suppressive factors such as *CD59*, *TNFSF10*, and *NT5E* (CD73) (Longhi et al., 2006; Hasegawa et al., 2008; Falschlehner et al., 2009), which are thought to contribute to the immune-privileged characteristics of primary AFCs (Walther et al., 2009). Expression of these genes is lost upon the induction of pluripotency. Further investigations will have to elucidate whether this affects potential therapeutic applications of AFiPSCs in comparison to primary AFCs (Wolfrum et al., 2010). Interestingly, active gene expression of *MYC* (AFiPSCs and FiPSCs) and *KLF4* (FiPSCs) was also lost upon reprogramming. This strengthens the idea that the main function of KLF4 and c-MYC is to increase a balanced cellular proliferation, thereby accelerating or enhancing the efficiency of reprogramming processes, while their expression appears to be dispensable in PSCs (Evans and Liu, 2008; Zhao and Daley, 2008; Nandan and Yang, 2009; Wolfrum et al., 2010).

Among the expressed genes, which are universally acquired during reprogramming processes, independent of the original cell source, are key pluripotency-associated factors, namely *POU5F1*, *SOX2* and *NANOG* (Boyer et al., 2005; Jung et al., 2010). These factors interact to establish a core TRN, which is crucial for maintaining self-renewal and pluripotency (Boyer et al., 2005; Jung et al., 2010). At the same time, however, expression of genes which are known to play a role in differentiation and development such as *EOMES* and *HAND1* are acquired (Adjaye et al., 2005; Babaie et al., 2007; Jung et al., 2010; Wolfrum et al., 2010). It has been demonstrated that these genes are direct targets of OCT4, SOX2 and NANOG (Boyer et al., 2005). For instance, these genes are negatively regulated by OCT4 as they are up-regulated upon *OCT4* knock down (Babaie et al., 2007). Yet, the data set presented herein revealed low level expression of some of these developmental-related genes in all our pluripotent cell types, which is in line with ESC and iPSC-related microarray data deposited in repositories such as Amazonia! (Le Carrour et al., 2010; Wolfrum et al., 2010). These observations could be ascribed to spontaneously differentiating cells present in ESC and iPSC cultures as shown earlier and also by others (Zwaka and Thomson, 2005; Xu et al., 2005) or artefacts of distinct cell culture conditions. Investigations to detect distinct epigenetic marks on the promoters of these genes could potentially enable further insight into expression patterns of these genes in pluripotent cells and link it to the concept of bivalent chromatin structures, which mark poised stem cell genes (Bernstein et al., 2006). Further genes implicated in developmental processes, which were found to be acquired in a cell type-dependent manner during cellular reprogramming, included, for example, *SIX6*, *EGR2*, *HOXD4*, *HOXD10*, *PKNOX2* and *DLX5* (Imoto et al., 2001; Panganiban and Rubenstein, 2002; Nunes et al., 2003; Sarnat and Flores-Sarnat, 2005; Schmitt et al., 2009; Wolfrum et al., 2010). The list of Retained genes in both, AFiPSCs and FiPSCs, also included transcription factors such as *RAXL1* which is another gene involved in the regulation of developmental processes (Wang et al., 2004). Persistent gene expression has been described to contribute to differences between iPSCs of different origin and ESCs (Ghosh et al., 2010). It may account for variable differentiation behaviours of iPSCs, irrespective of the reprogramming technique that was applied to generate them (Hu et al., 2010b,a). The impact of such actively expressed, developmental genes on the maintenance of pluripotency and self-renewal and on spontaneous or directed differentiation processes of distinct iPSC types, thus, deserves further investigation.

The expression of some of the distinct signature genes could be attributed to viral integrations into the target cells' genomes. The group-wise analysis of several AFiPSCs or FiPSCs lines versus the parental cell lines and ESCs, however, renders clone-specific viral integrations as a cause for these observations improbable. It could rather be speculated that these gene expression patterns result from an incomplete conversion of chromatin modifications in iPSCs, which could account for a cell type-specific epigenetic memory (Marchetto et al., 2009; Ghosh et al., 2010; Wolfrum et al., 2010) although the existence of such a memory is a subject of debate (reviewed by Drews et al. (b,a)). This is further supported by the identification of ESC-specific genes signatures in the comparison of the different iPSCs with ESCs, including, for example, *PRDM14*, *WNT3A* and *GSC*. While *PRDM14* has been shown to promote the

undifferentiated ESC state (Tsuneyoshi et al., 2008), the role of *WNT3A* in maintaining the self-renewal and pluripotency has long been a matter of debate (Sato et al., 2004; Davidson et al., 2012). At the same time, both *WNT3A* and *GSC*, are primitive streak/mesendoderm markers known to regulate developmental processes (Greber et al., 2008). Regardless of the exact molecular function of these factors in the pluripotent state, the fact that these genes distinguish the transcriptomes of AFiPSCs and FiPSCs from those of ESCs indicates incomplete reprogramming and underscores differences between ESCs and iPSCs on mRNA level that persist upon the acquisition of the ESC phenotype in both iPSC types. Follow-up studies should be designed to identify functional consequences of this observation (Wolfrum et al., 2010). The partially inconsistent gene expression patterns observed in the LARGE heatmap (Figure 3.14), in contrast, have presumably been caused by viral integrations. In order to verify this hypothesis and to identify actual effects of viral integrations on the genome of the iPSCs, it will be inevitable to generate iPSCs without genetic modifications and to perform comparative transcriptome and functional analyses of viral and non-viral-derived iPSCs (Wolfrum et al., 2010).

3.3.4 Genetic modification of human PSCs to knock down *USP44* remains a technical challenge

The attempt to investigate the role of the pluripotency-associated gene *USP44* in maintaining self-renewal and differentiation potential in retrovirus-derived AFiPSCs and ESCs by shRNA-mediated knockdown was not successful. As demonstrated by the use of several reporter constructs, neither lentiviral transduction nor plasmid transfection in combination with different strategies of sample preparations facilitated sufficient transgene expression in undifferentiated PSCs. Instead, most of the genetic manipulation strategies induced severe loss of cell viability and/or massive differentiation. Although difficulties were to be expected, as genetic manipulation of human ESCs remains a technical challenge (Zwaka and Thomson, 2003; Xia et al., 2007; Braam et al., 2008; Giudice and Trounson, 2008; Zafarana et al., 2009; Ma et al., 2010; Maury et al., 2011), this result was yet surprising. After all numerous reports have described successful interference of gene expression in human ESCs employing different approaches such as transient or stable chemical transfection of shRNAs or siRNAs or shRNA or siRNA-encoding constructs (Hay et al., 2004; Matin et al., 2004; Hyslop et al., 2005; Babaie et al., 2007; Vallier et al., 2009a; Adachi et al., 2010; Ma et al., 2010), nucleofection of siRNAs or of shRNA or siRNA-encoding vectors (Fong et al., 2008; Hohenstein et al., 2008), virus-mediated expression of shRNAs or siRNAs (Zaehres et al., 2005; Tulpule et al., 2010; Wang et al., 2012b)electroporation of inducible shRNA-encoding vectors (Zafarana et al., 2009) and homologous recombination upon electroporation [(Zwaka and Thomson, 2003). Cao et al. compared the different gene transfer methods (lipofection, electroporation, nucleofection and lentiviral transduction) in human ESCs and found that lentiviral transduction resulted in the highest efficiency while only barely affecting cell viability [Cao+F 2010 (19551446)]. Likewise, efficient genetic modification by lentiviral transduction has been demonstrated by others

(Gropp et al., 2003; Ma et al., 2003; Gropp and Reubinoff, 2006; Wang et al., 2012b). Lipofection has been shown to be generally less efficient (Cao et al., 2010). However, lipid-based transfection of nucleic acids is known to have a low toxicity on human ESCs (Maury et al., 2011) and of different transfection reagents FuGENE HD, one of the chemicals used in this project, was shown to facilitate efficient and stable transgene expression (Liu et al., 2009). Based on the highly similar phenotypes it seems plausible to convey these findings from human ESCs to iPSCs, for which many corresponding studies remain to be done. In view of these findings it appears unclear at first glance, why our attempts failed. Although the initial experiments were based on a protocol published by an established group in the field (Du and Zhang, 2010), different factors, by themselves or in combination, may have caused the poor outcome.

First of all, as anticipated, transduction or transfection of non-dissociated human PSCs only led to transgene expression in the periphery of the colonies and rendered manipulation of the cells in the center of the colonies impossible. It is not clear, however, if this was due to the limited access of the transduction/transfection reagent to single cells in the densely packed center of the colonies or if this was rather due to differences in the uptake of these reagents between undifferentiated PSCs in the middle of the colony and potential spontaneously differentiating cells at the boundaries. To by-pass this problem and to obtain uniform cultures of transgene-carrying cells by subcloning, the human PSCs were dissociated prior transduction or transfection. This, in turn, brought about another basic problem associated with (genetic) manipulation of human ESCs that certainly contributed to the negative outcome of the experiments described herein—the low cloning efficiency, i.e. the lack of human ESCs, or human PSCs in general, to survive as single cells and to re-grow into mature colonies of undifferentiated cells once dissociated to single cell level (Amit et al., 2000; Thomson et al., 1998). In avoidance of decreased cell viability during the transduction/transfection procedure we dissociated the cells with different putatively gentle reagents such as Accutase (Bajpai et al., 2008) and TrypLE Select (Du and Zhang, 2010) and incubated the cells with Rock inhibitor Y-27632 and thiazovivin, which have been highlighted to diminish dissociation-induced apoptosis of human PSCs (Watanabe et al., 2007; Lin et al., 2009). Unexpectedly, none of these treatments enhanced transduction or transfection. Incubation with neurotrophins is an alternative small molecule approach believed to improve manipulation of human PSCs (Pyle et al., 2006). Further investigations are required, however, to reveal if neurotrophins indeed would have had a positive effect on the transduction and transfection efficiencies. Not even the attempt to manipulate human PSCs as small clumps as a compromise between no dissociation of human PSCs and dissociation to the single cell level, which is routinely applied when human PSCs are genetically modified (Maury et al., 2011), ameliorated gene delivery. As this way of handling PSCs limits the induction of apoptosis this finding supports the hypothesis that undifferentiated PSCs may have means to impede the entrance of transduction or transfection reagents into the cells.

Another critical factor that substantially determines the success of transgene expression in distinct cell lines is the choice of the promoter. The different shRNAs employed in this project were under the control of the human U6 promoter, which was shown to efficiently drive RNA

polymerase III transcription to generate the encoded shRNAs (Zaehres et al., 2005; Tulpule et al., 2010). TurboGFP expression from the corresponding reporter construct, however, was mediated by the ubiquitous cytomegalovirus (CMV) promoter (Figure 3.16). Transgenes under the control of this promoter, in contrast, were reported to be more effectively 'suppressed' upon lentiviral transduction into human ESCs than other ubiquitously active promoters, namely the cytomegalovirus immediate-early enhancer/chicken β-actin hybrid (CAG), phosphoglycerate kinase (PGK) and human elongation factor-1α (EF1α) promoters (Xia et al., 2007). Concerning the transient transfection of CMV-driven genes, published data have been controversial. While one group demonstrated generally weak CMV promoter activity following nucleofection in human ESCs (Chan et al., 2008), another group reported robust transient transcriptional activity of the CMV promoter upon transgene delivery by various chemical methods but inability to select stably transfected cells (Liu et al., 2009). Likewise another study demonstrated highly efficient CMV-driven enhanced GFP expression in human ESCs after chemical transfection followed by a significant decrease (Lebkowski et al., 2001). Yet others have shown that CMV is a suitable promoter for transient transgene expression by nucleofection in human ESCs (Hohenstein et al., 2008). This is also supported by the fact that the pmaxGFP reporter construct, a CMV-driven enhanced GFP-encoding vector by Amaxa (Lonza), is commonly used as a positive nucleofection control in various cell lines, including human ESCs (Fong et al., 2008; Hohenstein et al., 2008). Hence, although the CMV promoter-driven TGFP reporter construct does not appear to be the superior vector for the optimization experiments, the poor outcome of the transduction and transfection experiments cannot solely be attributed to its constrained strength in human PSCs. Especially since the *OCT4* promoter-driven GFP vector was not any more efficient.

In summary, referring to the recent progress with respect to genetic manipulation of human ESCs and considering the various possibilities of incorporating different human PSC handling techniques and applying putatively supportive reagents, a successful knock down of the USP44 gene expression levels appeared achievable. After all, however, it was most likely the combination of the low cloning efficiency of human PSCs together with the generally low transduction and even lower transfection efficiencies in human PSCs that caused the experiments to fail. Hence, implementation of the USP44 knock down strategy still seems to be feasible but requires major optimization efforts.

4

Non-viral generation of amniotic fluid-derived iPSCs

4.1 Introduction

To generate human iPSCs suitable for clinical purposes it is essential to establish cellular reprogramming protocols, which allow for an induction of pluripotency in somatic cells without modification of the target cell genome. In order to pursue the main goal of this PhD project further, the non-viral, integration-free generation of iPSCs from human AFCs to complement the retroviral-derived AFiPSCs, we next aimed at the implementation and optimization of published non-integrating reprogramming methods. As sorting of stem cell-like subpopulations was not feasible due to the reasons described earlier, the same bulk primary human AFCs were used as a starting point for non-viral reprogramming experiments.

4.2 Results

4.2.1 Cellular reprogramming by means of episomal plasmid nucleofection

We attempted to reprogram AFCs by transfection of episomal plasmids as published by (Yu et al., 2009). According to their findings and a recent follow-up publication, the oriP/EBNA1 (Epstein-Barr nuclear antigen-1)-based episomal vectors do not integrate into the host cell genome but rather persist in the cells as stably extra-chromosomally replicating episomes, thus facilitating a sufficient expression of the reprogramming factors to induce pluripotency. Without drug-selection and with pro-longed maintenance of the cells in culture, however, the episomes are lost, which results in fully established iPSC lines free of residual vector or transgene sequences (Yu et al., 2009; Cheng et al., 2012).

Different lines of human AFCs (P5-P10), including the parental cell line from which the retrovirally derived AFiPSCs were obtained, were electroporated with a combination of reprogramming factor-encoding episomal plasmids (Figure 4.1 (A)) and subsequently maintained under human ESC conditions. To potentially achieve a higher reprogramming efficiency, transfected cells were partly treated with BAPN (Tang et al., 1983) or thiazovivin, alone or in combination with SB431542 and PD0325901 (Lin et al., 2009).

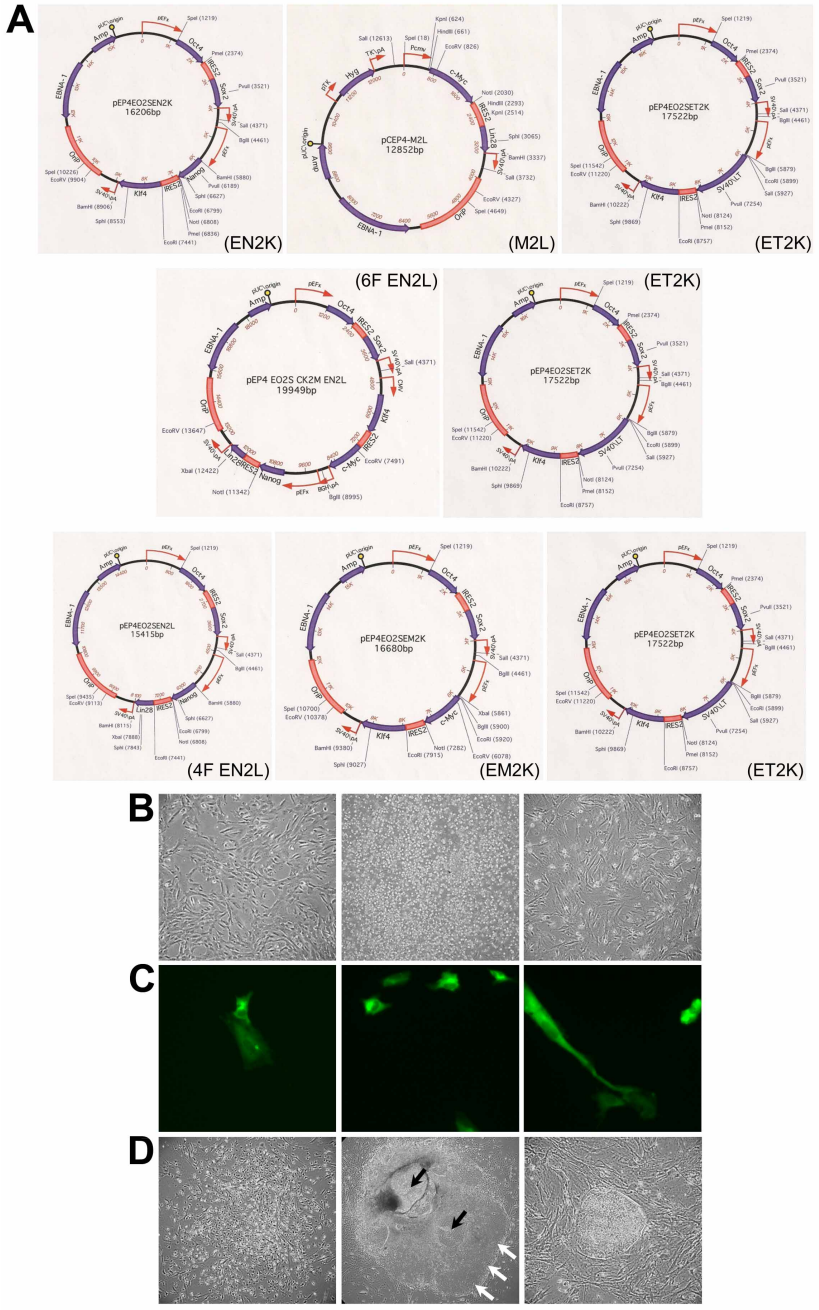

Figure 4.1: Nucleofection of human AFCs with reprogramming factors-encoding episomal plasmids. (A) Maps of the episomal plasmids used to electroporate different lines of human AFCs. The three depicted combinations of vectors and distinct amounts were used according to the protocol by Yu et al. (2009). (B) From left to right: Bulk primary human AFCs (line 102, P5) prior to nucleofection. Floating cells indicate extensive cell death one day post-electroporation. The same nucleofected AFCs on a layer of mitotically inactivated MEF feeder cells one day post-nucleofection after removal of the majority of dead cells; the moderate cell density indicates that only a few electroporated cells attached onto the culture dish. (C) Single positive nucleofection control cells express maxGFP. (D) From left to right: Granulated colony of nucleofected AFCs approximately four weeks post-nucleofection. The only auspicious ESC-like, potential iPSC colony that emerged as a result of all nucleofection experiments one day prior to picking around seven weeks post-nucleofection; the colony contains large parts of differentiated cells (black arrows) next to undifferentiated cells (white arrows). Undifferentiated piece of the same colony one day after picking.

The electroporation procedure induced extensive loss of cell viability, resulting in a low density of nucleofected AFCs among MEF feeder cells as highlighted by the observation of single GFP-expressing cells in the positive control (Figure 4.1 (B, C)). Of the approximately 7.5×10^6 human AFCs that were nucleofected with the reprogramming factor-encoding episomal plasmids in different experiments, three colonies with granulated morphology (one in UM/CM without chemicals, one in UM/CM containing thiazovivin and one in UM/CM containing BAPN) appeared, yet, never developed further into human ESC-like colonies. Overall, only one putative iPSC colonies emerged approximately five weeks post-nucleofection (in UM/CM containing BAPN) (Figure 4.1 (D), approximately 5.5×10^{-5} % efficiency). This colony had the typical ESC morphology, i.e. sharp-edged, dense colonies of cells with high nucleus to cytoplasm ratio, but proliferated markedly slower. Expansion of this potential iPSC colony turned out to be extremely difficult: By the time, the colony appeared ready for picking or splitting, essential parts of it had already spontaneously differentiated (Figure 4.1 (D)). Upon passaging further differentiation re-occurred in substantial proportions of the colony. Hence, no net expansion was achieved overall and this colony was lost after approximately three passages, before any characterization experiments could be performed.

4.2.2 Cellular reprogramming by means of mRNA transfection

After repeated failure of the episomal plasmid based technology to induce pluripotency in somatic cells without introducing genomic modifications in the target cells, we next proceeded to RNA-mediated nuclear reprogramming methods. Among the different non-viral, putatively non-integrating reprogramming techniques available at this time, the focus of this project was on the novel, highly promising mRNA reprogramming approach. Although an mRNA-mediated cellular reprogramming protocol had recently already been published by Warren et al. (2010), the lack of follow-up publications implies there are major hurdles to overcome before this approach becomes reproducible and routinely applicable for successful cellular reprogramming (Wang and Na, 2011). We therefore sought to develop a modified mRNA reprogramming approach building upon the experience and knowledge about *in vitro* mRNA synthesis and transfection of our collaboration partners of the Research Group on Nanomedicines at Ghent University, Ghent, Belgium, and our experience on cellular reprogramming and the culture of human PSCs. As the access to human AFCs was limited, we made use of BJ and HFF1 fibroblasts to optimize the mRNA transfection protocols. However, the actual experiments attempting to reprogram somatic cells were also conducted using bulk human AFCs.

4.2.2.1 *In vitro* mRNA synthesis

First, mRNAs encoding each of the reprogramming factor genes *POU5F1* (transcript variant 1, encoding the OCT4A protein isoform), *SOX2*, *KLF4*, *c-MYC* and *LIN28A* and the green fluorescent reporter protein (GFP) were produced starting from the commercially bought plasmids. Representative images of intermediates generated in the synthesis process are depicted

in Figure 4.2. First, from each reprogramming factor-encoding plasmid an open reading frame

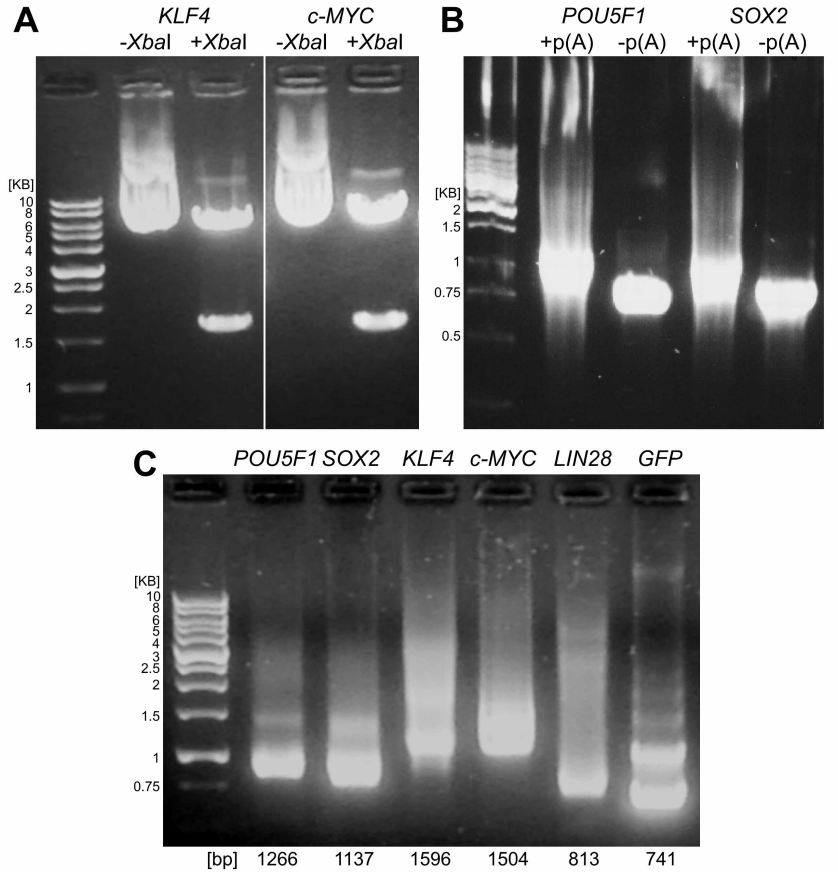

Figure 4.2: *In vitro* synthesis of mRNAs encoding single reprogramming factors—agarose gel electrophoresis of intermediates. (A) Exemplary images of the fragments resulting from the *Xba*I-mediated restriction digest of the *KLF4*- and *c-MYC*-encoding plasmids. (B) Comparison of *in vitro* transcribed *POU5F1*- and *SOX2*-encoding mRNAs prior to and after the poly(A)-tailing reaction (+/−p(A)). (C) Purified *in vitro* transcribed, poly(A)-tailed mRNAs derived from the plasmids encoding either one of the five reprogramming factors or the reporter GFP. Expected gene product sizes (excluding the poly A tail) are indicated at the bottom.

containing fragment was released by restriction enzyme digest and used as template for the *in vitro* transcription reaction (Figure 4.2 (A)). The appearance of a band shift and smear following the poly(A)-tailing reaction indicates successful polyadenylation of the 3'-termini of *in vitro* synthesized, capped mRNAs (Figure 4.2 (B)). Hence, functionality and stability of these mRNAs upon transfection could be assumed. An image of purified *in vitro* transcribed mRNAs including caps and poly(A)-tails of all five reprogramming factors is also shown in Figure 4.2 (C).

4.2.2.2 Quantification of protein expression following mRNA transfection

Next, the *in vitro* synthesized GFP-encoding mRNA was used as a reporter to determine the transfection efficiency of our mRNA transfection protocol. Per 12-well, HFF1 cells were

transfected with 2 µg GFP-encoding mRNA complexed with Lipofectamine RNAiMAX, as described in the 'Materials and Methods' chapter. The resulting GFP expression was assessed by flow cytometry and microscopic analysis. As depicted in Figure 4.3 this revealed that approximately 85% of cells expressed GFP with a very high intensity per cell (Drews et al., 2012).

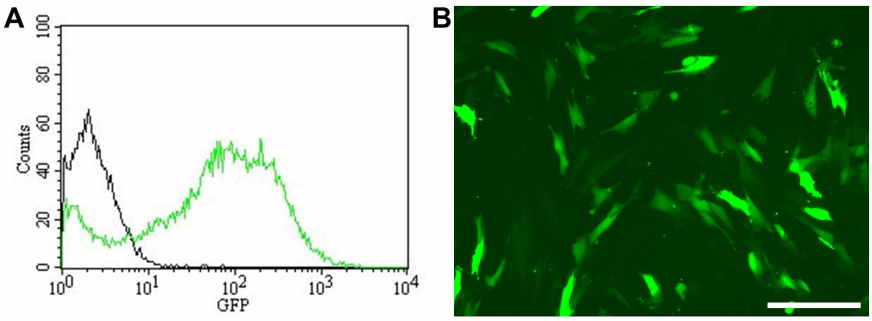

Figure 4.3: GFP expression in mRNA-transfected HFF1 cells. 4 µg GFP-encoding mRNA and 4 µl Lipofectamine, both pre-diluted in 46 µl of OptiMEM, were mixed and incubated for 10 min at RT. Then, 900 µl of OptiMEM were added and this solution was divided over two 12-wells of HFF1 cells and incubated for 2 h, after which the complexes were removed and regular growth medium added. (A) FACS analysis of 10,000 cells for GFP expression 24 h post-transfection (black line: untreated control; green line: GFP-positive cells). (B) Microscopic image of HFF1 cells simultaneously lipofected with GFP-encoding mRNA. Scale bar = 200 µm. Modified from Drews et al. (2012).

4.2.2.3 Immunofluorescence-based detection of the reprogramming factor proteins following mRNA transfection

As proof of principle and to additionally assess the quality and localization of protein expression from the mRNAs delivered by single reprogramming factor transfection (OSKML), HFF1 cells were fixed at different time points post-transfection and protein expression detected using fluorescence dye-labeled antibodies against each of the reprogramming factors. As highlighted in Figure 4.4 (A), protein expression was already detectable (OCT4, SOX2, LIN28) or increased above endogenous background levels (KLF4, c-MYC) 4 h after a single factor mRNA transfection when compared to mock-transfected control cells. The peak of expression was observed 10 to 24 h post-transfection (Drews et al., 2012). In case of SOX2 and LIN28, the fluorescent signal was strong even 48 h after transfection, whereas for OCT4, KLF4 and c-MYC it was nearly decreased to background levels, yet still detectable, at this time point. When HFF1 cells were transfected with the same total amount of mRNA as a 1:1:1:1:1 cocktail of the different reprogramming factors instead of single factors and fixed and stained 24 h post-transfection, the fluorescent signal observed following antibody labeling was markedly reduced when compared to the single factor transfection but still detectable (Figure 4.4 (B)). The expected nuclear localization of the transcription factors OCT4, SOX2, KLF4 and c-MYC

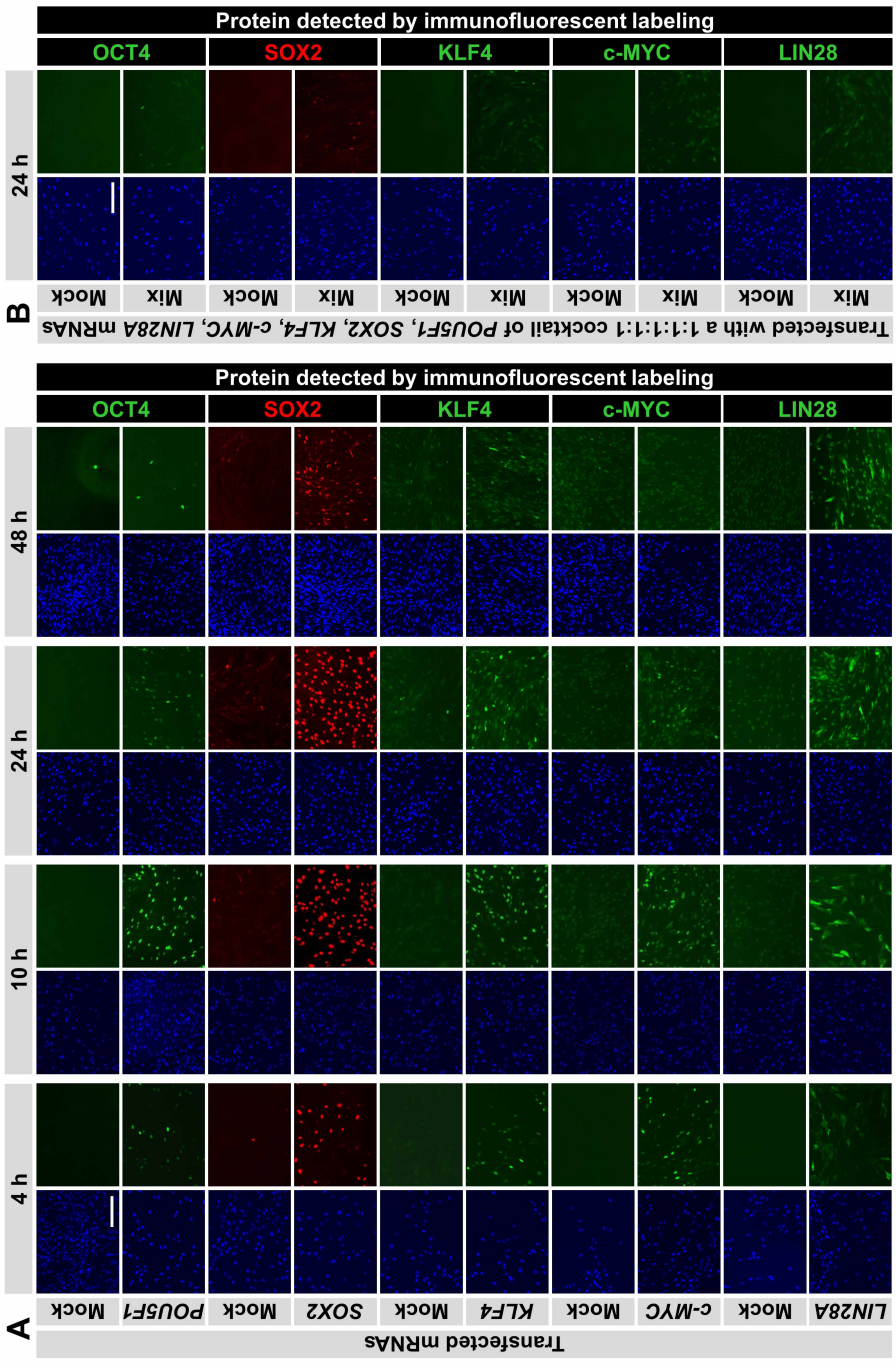

Figure 4.4: Detecting expression of OSKML proteins in mRNA-transfected HFF1 cells. (A) HFF1 cells, grown in 24-wells, were transfected with one of the five reprogramming factors (OSKML) and fixed at indicated time points for the immunofluorescent staining procedure. (B) HFF1 cells were transfected with the same total amount of mRNA per 24-well consisting of a 1:1:1:1:1 cocktail of the five different reprogramming factor-encoding mRNAs and fixed 24 h later for the immunofluorescent staining procedure. Microscope images of the nuclear (DAPI) signal and the corresponding protein-specific signal are shown. Scale bars = 200 µm. Modified from Drews et al. (2012).

as well as the pre-dominantly cytoplasmic localization of the RNA-binding protein LIN28 (Balzer and Moss, 2007) was verified (Drews et al., 2012).

4.2.2.4 mRNA-mediated iPSC generation

Having demonstrated functionality of the *in vitro* synthesized mRNAs upon transfection, next, a total of about 17× 10^6 HFF1, BJ and AFCs (9.6× 10^6 HFF1 cells, P5-P10; 6.4× 10^6 BJ cells, P5-P10; 1.2× 10^6 AFCs, line 101, P10) were employed for reprogramming experiments. To establish our own mRNA-based reprogramming protocol modifications of several parameters were tested including the use of different reprogramming factor-encoding mRNA cocktails (1:1:1:1 of OSKM, 1:1:1:1:1 of OSKML or 3:2:1:1:1 of OSKML), transfections on MEF feeder cells or without MEF feeder cells, with and without Matrigel, different media including and excluding small molecule treatments (thiazovivin, SB431542, PD0325901 (Lin et al., 2009), EDHB (Prigione et al.)) to enhance cellular reprogramming and switching from somatic to human PSC conditions at different time points. Despite the different approaches, no morphological changes and no formation of granulated colonies or colonies with human ESC-like morphology were observed. Instead, with increasing numbers of transfections, which were performed to ensure expression of the reprogramming factors over a sufficient period of time, cells increasingly died and lifted off the plate. To determine the effect of the transfection protocol on cell viability an MTT assay was performed 24 h after daily transfections with Lipofectamine RNAiMAX complexes carrying mRNAs encoding the Yamanaka factors. This demonstrated, the number of transfected cells decreased starting after the second transfection (Figure 4.5 (A)) (Drews et al., 2012). After seven consecutive transfections no viable

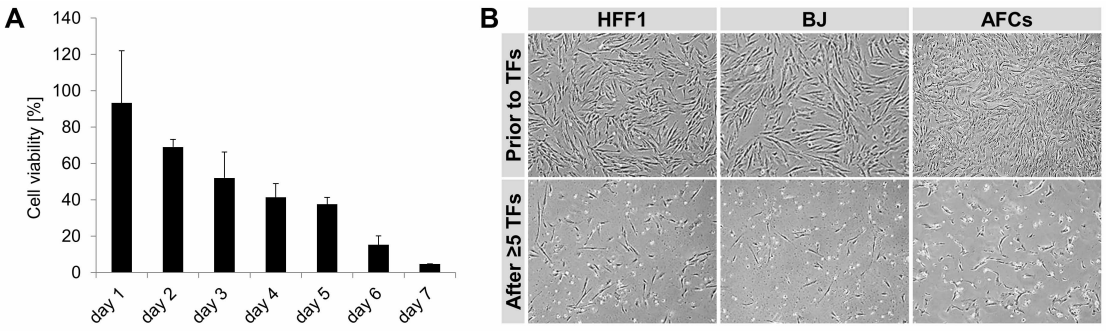

Figure 4.5: Loss of cell viability upon repeated transfection of reprogramming factor-encoding mRNAs into somatic cells. (A) Cytotoxicity of reprogramming factor-encoding mRNA transfections in HFF1 cells. Per 12-well, cells were transfected daily with 2 µg of equal amounts of mRNAs encoding *POU5F1*, *SOX2*, *KLF4* and *c-MYC* by complexing with 2 µl Lipofectamine as described in Materials and methods. Seven consecutive transfections were performed. MTT assay was done 24 h post every transfection. Graphs represent means and SD. n ≥ 2. Taken from Drews et al. (2012). (B) Images of HFF1 and BJ fibroblasts as well as human AFCs (AF101) acquired prior to (upper panel) and after (lower panel) a minimum of five subsequent transfections to deliver four or five reprogramming factors exemplarily illustrate the markedly decreased numbers of viable cells, which were observed for all cell types in either fibroblast, AFC or ESC conditions. TFs, transfections.

cells remained. A severe loss of cell viability during the reprogramming experiments was also observed for all other cell lines (Figure 4.5 (B)). Generally, however, BJs seemed to be more susceptible to cell death than HFF1 cells and AFCs and HFF1 cells were similarly vulnerable.

Maintenance of the target cells in defined human ESC culturing medium NutriStem instead of MEF-CM prior to and after each transfection was the only modification of the reprogramming protocol that slightly increased cell viability upon repeated transfections. This enabled a series of as many as nine consecutive transfections (day 1 and day 2 and every other day henceforth) before low cell viability prohibited any further transfections. However, even this period of 16 days in total, including permanent transfections, were insufficient to trigger any phenotypic changes in the target cells. The addition of small molecules, e.g. EDHB, which promotes reprogramming through indirect stabilization of HIF1α and the resulting influence on the cellular energy metabolism (Prigione et al.), or a combination of EDHB with thiazovivin, SB and PD, which were already shown to enhance the induction of pluripotency (Lin et al., 2009), and maintenance of the target cells on MEF feeder cells under human ESC conditions after the transfection series could not alleviate the loss of cell viability and did not evidently enhance the cellular reprogramming process. In fact, implementation of the mRNA reprogramming protocol by Stemgent using mRNAs and reagents provided in the kit, yet excluding the B18R treatment, lead to the same outcome.

Comparative global gene expression analysis of reprogramming factor mRNA-transfected and mock-transfected human neonatal of fibroblasts

As all the different attempts to induce pluripotency by repeatedly transfecting mRNAs of the reprogramming factors into fibroblasts and AFCs failed due to progressive cell death we sought to investigate this further. It is known that transfection of poly(A) tailed mRNA into human dermal fibroblast cells induces interferon response (Rautsi et al., 2007; Angel and Yanik, 2010). To get a more detailed insight into which pathways are involved, we first analyzed the transcriptome of reprogramming factor (OSKML) mRNAs-transfected HFF1 and BJ neonatal fibroblasts against mock-transfected (Lipofectamine-treated) control cells 24 h post-transfection. To enable profound interpretation of the data, the transcriptome profiles were also compared to gene expression data from untreated, wildtype HFF1 and BJ fibroblast cells, human ESCs (lines H1 and H9) and fibroblast-derived human iPSCs (FiPSCs, retroviral derived from HFF1 and BJ cells) generated and maintained in our laboratory as previously described (Prigione et al., 2010, 2011b).

A global view at the transcriptome data by hierarchical clustering revealed a clear separation of fibroblasts transfected with mRNAs encoding the reprogramming factors from wild-type and mock-transfected fibroblasts as well as from human FiPSCs and ESCs (Figure 4.6 (A)) (Drews et al., 2012). Linear correlation coefficient analysis demonstrated that mRNA-transfected fibroblasts shared decreasing numbers of expressed genes with mock-transfected fibroblasts ($R^2 \approx 0.84$), wild-type fibroblasts ($R^2 \approx 0.73$), FiPSCs ($R^2 \approx 0.60$) and ESCs ($R^2 \approx 0.56$) (Drews et al., 2012). Interestingly, the transcriptomes of mock-transfected and wild-type fibroblasts are more closely related to those of FiPSCs and ESCs ($R^2 \approx 0.71$)

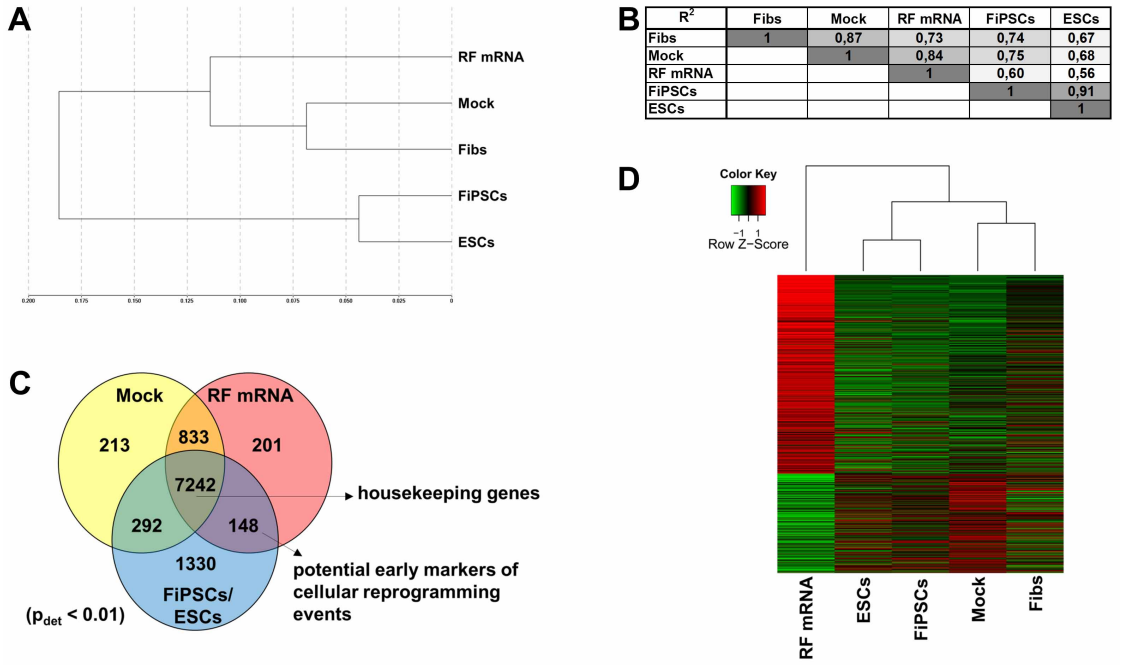

R^2	Fibs	Mock	RF mRNA	FiPSCs	ESCs
Fibs	1	0,87	0,73	0,74	0,67
Mock		1	0,84	0,75	0,68
RF mRNA			1	0,60	0,56
FiPSCs				1	0,91
ESCs					1

Figure 4.6: Microarray-based transcriptome analysis of untreated, mock-transfected and reprogramming factor-transfected human fibroblasts, fibroblast-derived iPSCs and ESCs. (A) Hierarchical clustering (Pearson's correlation) on the basis of the global gene expression data. RF mRNA, reprogramming factor mRNAsâĂŞtransfected human neonatal fibroblasts, HFF1, BJ; Mock, mock-transfected fibroblasts, HFF1, BJ; Fibs, wild-type fibroblasts, HFF1, BJ; FiPSCs, fibroblast-derived iPSCs, two HFF1-, two BJ-derived lines; ESCs, human embryonic stem cells, lines H1 and H9. (B) Linear correlation coefficients (R^2) between the different groups of samples on the basis of the global gene expression data. (C) Venn diagram based on 'detected' genes (pdet $<$ 0.01) in mock-transfected fibroblasts, reprogramming factor-transfected fibroblasts and the union of FiPSCs and ESCs depicting distinct and overlapping transcriptional signatures between the different groups of samples. (D) Heatmap portraying the total of 993 significantly differentially expressed genes in reprogramming factor-transfected fibroblasts compared to mock-transfected fibroblasts (662 genes up-regulated, 331 genes down-regulated, cut off: fold change $\geq$ 1.5 up- or down-regulation and padj $<$ 0.05). For comparison, the corresponding gene expression data for wild-type fibroblasts, FiPSCs and ESCs were included. The heatmap is colored by row-scaled LOG2 average expression signals according to the color key on the top. Samples were clustered by column means. Taken from Drews et al. (2012).

than those of reprogramming factor-transfected fibroblasts from FiPSCs and ESCs ($R^2 \approx 0.58$) (Figure 4.6 (B)) (Drews et al., 2012). This emphasizes that the overall gene expression profile of reprogramming factor mRNA-transfected fibroblasts is indeed different from the original donor cells on one hand and the PSC lines on the other hand. Importantly, a general switch of the global gene expression pattern from the fibroblast-transcriptome towards the transcriptome of a pluripotent cell (down-regulation of fibroblast genes, up-regulation of pluripotency-associated genes) was not apparent as early as 24 h after transfection of the reprogramming factor-encoding mRNAs, despite the high expression levels of the exogenously delivered reprogramming factors themselves (Drews et al., 2012). This is consistent with our previous findings in retrovirus-transduced fibroblasts (Mah et al., 2011).

Nevertheless, we sought to investigate whether potential pluripotency-associated genes are up-regulated as early as 24 h after transfection of the reprogramming factors. To this end we generated a Venn diagram on the basis of 'expressed' genes in mock-transfected control cells, reprogramming factor-transfected fibroblasts and the union of FiPSCs and ESCs, i.e. the overlap of genes present in these two pluripotent cell types, which is presented in (Figure 4.6 (C)) (Drews et al., 2012). The resulting list of 148 putative pluripotency-associated genes, overlapping in reprogramming factor-transfected fibroblasts and the union of FiPSCs and ESCs, is given in Table B.2 (Drews et al., 2012). This list is enriched for genes encoding cellular membrane and transmembrane proteins and genes associated with cell-cell signaling including, for example, *SYT1*, *CXCR7*, *CEACAM1*, *BST2* and *CXCL6* (Table B.3) (Drews et al., 2012).

To get an insight into the gene expression changes directly induced by transfection with reprogramming factor-encoding mRNAs, we conducted a differential gene expression analysis comparing reprogramming factor-transfected fibroblast cells with mock-transfected control cells. As a result, a total of 662 genes were significantly up-regulated in mRNA-transfected fibroblast cells when compared to the mock-transfected, Lipofectamine-treated control fibroblast cells (≥ 1.5 fold increase in expression level, padj < 0.05, the top 100 up-regulated genes are presented in Table B.4, the complete list of 662 genes can be obtained from Drews et al. (2012), Supplementary Table S3). These included *IFNB1*, *CCL5*, *ISG20*, *OAS1*, *MDA5* (*IFIH1*), *RIG-I* (*DDX58*), *IRF7*, *MYD88*, *ADAR* and *TRIF* (*TICAM1*), which were strongly up-regulated, e.g., *IFNB1* = 967, *CCL5*$^{-}$ 441, *OAS1* = 184, *MDA5* = 72, *RIG-I* = 47 fold up-regulation in transfected over mock-transfected cells (Drews et al., 2012). In contrast, 331 genes were observed as significantly down-regulated when comparing mRNA- with mock-transfected fibroblasts (≥ 1.5 fold decrease in expression level, padj < 0.05, the top 100 down-regulated genes are presented in Table B.5, the complete list of 331 genes can be obtained from Drews et al. (2012), Supplementary Table S4). Examples of down-regulated genes included *CCNB1*, *CCNB2 CCNF*, *CDC20* and *BAX* (Drews et al., 2012). The total of 993 significantly differentially expressed genes is depicted in Figure 4.6 (D) including gene expression data of all other groups of samples for comparison (Drews et al., 2012). To better comprehend the role of these differentially expressed genes and to associate these genes with signaling pathways, the two gene lists were functionally annotated using the DAVID database (Dennis et al., 2003; Huang da et al., 2009). As shown in Table 4.1, the three most highly enriched clusters of up-regulated genes, which

altogether comprise 129 of the 662 up-regulated genes, represent the response to bacteria or bacterial structures or drugs (cluster 1, including, e.g., *IFNB1*, *CCL2*, *CCL5*, *IL10*, *IL12*, *MYD88* and *TICAM1* (*TRIF*)), innate immune response/innate immunity (cluster 2, including, e.g., *DDX58* (*RIG-I*), *TRIM25*, *MYD88* and *TICAM1* (*TRIF*)) and regulation of apoptosis (cluster 3, including, e.g. *GADD45A*, *PYCARD*, *CASP7*, *TNFRSF10A*, *TNFSF10* (*TRAIL*) and *NOD1*) (Drews et al., 2012). The corresponding list of significantly enriched KEGG pathways includes the Jak-STAT signaling pathway, the RIG-I-like receptor signaling pathway, the cytosolic DNA-sensing pathway, the Toll-like receptor signaling pathway and apoptosis (Table 4.1, Figure B.2) (Drews et al., 2012). The initiation of apoptosis upon mRNA transfection is further supported by the fact that the list of down-regulated genes is highly enriched for gene clusters associated with cell cycle (cluster 1, including, e.g., *BAX*, *CDKN3*, *CCNB1*, *CCNF*, *CDC20* and *CDKN1B*), cytoskeleton (cluster 2) and chromosome condensation (cluster 3) (Table 4.2, 114 of 331 down-regulated genes in the three most highly enriched clusters) suggesting that proliferation is actively inhibited in mRNA-transfected cells (Drews et al., 2012). Accordingly, the list of down-regulated genes is significantly enriched for cell cycle and p53 signaling pathways as defined by KEGG (Kanehisa and Goto, 2000) (Table 4.2, Figure B.2) (Drews et al., 2012).

Table 4.1: KEGG pathway enrichment analysis and functional annotation clustering of the 662 significantly up-regulated genes in mRNA-transfected fibroblasts versus mock-transfected controls. Modified from Drews et al. (2012).

Category	Term	Count	%	PValue
KEGG_PATHWAY	hsa04630:Jak-STAT signaling pathway	23	3.66	6.06E-07
KEGG_PATHWAY	hsa04622:RIG-I-like receptor signaling pathway	14	2.23	8.16E-06
KEGG_PATHWAY	hsa03050:Proteasome	11	1.75	2.37E-05
KEGG_PATHWAY	hsa04612:Antigen processing and presentation	14	2.23	4.68E-05
KEGG_PATHWAY	hsa04623:Cytosolic DNA-sensing pathway	11	1.75	9.88E-05
KEGG_PATHWAY	hsa05322:Systemic lupus erythematosus	14	2.23	2.96E-04
KEGG_PATHWAY	hsa04620:Toll-like receptor signaling pathway	13	2.07	1.25E-03
KEGG_PATHWAY	hsa04210:Apoptosis	11	1.75	4.03E-03
KEGG_PATHWAY	hsa04060:Cytokine-cytokine receptor interaction	22	3.50	4.25E-03
KEGG_PATHWAY	hsa05120:Epithelial cell signaling in Helicobacter pylori infection	8	1.27	2.66E-02
Annotation Cluster 1	Enrichment Score: 6.1334533046512645			
GOTERM_BP_FAT	GO:0002237~response to molecule of bacterial origin	18	2.86	7.93E-09

Continued on next page

Table 4.1 – *Continued from previous page*

Category	Term	Count	%	PValue
GOTERM_BP_FAT	GO:0032496~response to lipopolysaccharide	16	2.54	7.43E-08
GOTERM_BP_FAT	GO:0009617~response to bacterium	25	3.97	1.03E-07
GOTERM_BP_FAT	GO:0042493~response to drug	17	2.70	4.80E-03
Annotation Cluster 2	Enrichment Score: 5.714405417076349			
SP_PIR_KEYWORDS	immune response	28	4.45	4.98E-09
GOTERM_BP_FAT	GO:0045087~innate immune response	17	2.70	3.38E-05
SP_PIR_KEYWORDS	innate immunity	12	1.91	4.27E-05
Annotation Cluster 3	Enrichment Score: 5.231835180839759			
GOTERM_BP_FAT	GO:0008219~cell death	55	8.74	1.74E-07
GOTERM_BP_FAT	GO:0016265~death	55	8.74	2.14E-07
GOTERM_BP_FAT	GO:0012501~programmed cell death	49	7.79	2.40E-07
GOTERM_BP_FAT	GO:0006915~apoptosis	48	7.63	3.80E-07
GOTERM_BP_FAT	GO:0042981~regulation of apoptosis	58	9.22	5.32E-07
GOTERM_BP_FAT	GO:0043067~regulation of programmed cell death	58	9.22	7.13E-07
GOTERM_BP_FAT	GO:0043065~positive regulation of apoptosis	38	6.04	7.16E-07
GOTERM_BP_FAT	GO:0010941~regulation of cell death	58	9.22	8.23E-07
GOTERM_BP_FAT	GO:0043068~positive regulation of programmed cell death	38	6.04	8.48E-07
GOTERM_BP_FAT	GO:0010942~positive regulation of cell death	38	6.04	9.44E-07
SP_PIR_KEYWORDS	Apoptosis	32	5.09	3.00E-06
GOTERM_BP_FAT	GO:0006916~anti-apoptosis	22	3.50	1.57E-05
GOTERM_BP_FAT	GO:0006917~induction of apoptosis	25	3.97	5.24E-04
GOTERM_BP_FAT	GO:0012502~induction of programmed cell death	25	3.97	5.46E-04
GOTERM_BP_FAT	GO:0043066~negative regulation of apoptosis	26	4.13	9.67E-04
GOTERM_BP_FAT	GO:0043069~negative regulation of programmed cell death	26	4.13	1.17E-03
GOTERM_BP_FAT	GO:0060548~negative regulation of cell death	26	4.13	1.22E-03

Table 4.2: KEGG pathway enrichment analysis and functional annotation clustering of the 331 significantly down-regulated genes in mRNA-transfected fibroblasts versus mock-transfected controls. Modified from Drews et al. (2012).

Category	Term	Count	%	PValue
KEGG_PATHWAY	hsa04110:Cell cycle	11	3.62	4.09E-05
KEGG_PATHWAY	hsa04114:Oocyte meiosis	10	3.29	8.55E-05
KEGG_PATHWAY	hsa00480:Glutathione metabolism	5	1.64	9.72E-03
KEGG_PATHWAY	hsa04914:Progesterone-mediated oocyte maturation	6	1.97	1.47E-02
KEGG_PATHWAY	hsa04115:p53 signaling pathway	5	1.64	2.74E-02
Annotation Cluster 1	Enrichment Score: 23.110790902697754			
GOTERM_BP_FAT	GO:0022402~cell cycle process	58	19.08	2.49E-28
GOTERM_BP_FAT	GO:0007049~cell cycle	65	21.38	6.46E-27
GOTERM_BP_FAT	GO:0022403~cell cycle phase	48	15.79	1.64E-25
SP_PIR_KEYWORDS	cell cycle	48	15.79	6.64E-25
SP_PIR_KEYWORDS	cell division	38	12.50	1.40E-24
GOTERM_BP_FAT	GO:0000279~M phase	42	13.82	7.83E-24
GOTERM_BP_FAT	GO:0000278~mitotic cell cycle	44	14.47	9.38E-24
GOTERM_BP_FAT	GO:0048285~organelle fission	36	11.84	2.06E-23
SP_PIR_KEYWORDS	mitosis	32	10.53	2.86E-23
GOTERM_BP_FAT	GO:0007067~mitosis	35	11.51	6.37E-23
GOTERM_BP_FAT	GO:0000280~nuclear division	35	11.51	6.37E-23
GOTERM_BP_FAT	GO:0000087~M phase of mitotic cell cycle	35	11.51	1.16E-22
GOTERM_BP_FAT	GO:0051301~cell division	39	12.83	1.23E-22
GOTERM_CC_FAT	GO:0005819~spindle	29	9.54	6.83E-22
GOTERM_CC_FAT	GO:0015630~microtubule cytoskeleton	47	15.46	5.17E-20
Annotation Cluster 2	Enrichment Score: 8.063492575694381			
GOTERM_CC_FAT	GO:0005819~spindle	29	9.54	6.83E-22
GOTERM_CC_FAT	GO:0015630~microtubule cytoskeleton	47	15.46	5.17E-20
GOTERM_CC_FAT	GO:0044430~cytoskeletal part	49	16.12	3.99E-12
GOTERM_CC_FAT	GO:0043228~non-membrane-bounded organelle	88	28.95	1.08E-11
GOTERM_CC_FAT	GO:0043232~intracellular non-membrane-bounded organelle	88	28.95	1.08E-11
SP_PIR_KEYWORDS	cytoskeleton	35	11.51	4.41E-10
GOTERM_BP_FAT	GO:0007017~microtubule-based process	23	7.57	4.85E-10
GOTERM_CC_FAT	GO:0005856~cytoskeleton	56	18.42	7.49E-10

Continued on next page

Table 4.2 – *Continued from previous page*

Category	Term	Count	%	PValue
GOTERM_CC_FAT	GO:0005815~microtubule organizing center	21	6.91	1.03E-08
GOTERM_CC_FAT	GO:0005874~microtubule	21	6.91	3.95E-08
GOTERM_CC_FAT	GO:0005813~centrosome	19	6.25	4.54E-08
SP_PIR_KEYWORDS	microtubule	18	5.92	1.49E-07
SP_PIR_KEYWORDS	motor protein	11	3.62	4.40E-05
UP_SEQ_FEATURE	domain:Kinesin-motor	7	2.30	5.42E-05
GOTERM_MF_FAT	GO:0003774~motor activity	11	3.62	9.49E-05
GOTERM_BP_FAT	GO:0007018~microtubule-based movement	10	3.29	1.49E-04
GOTERM_MF_FAT	GO:0003777~microtubule motor activity	8	2.63	2.28E-04
INTERPRO	IPR001752:Kinesin, motor region	6	1.97	4.41E-04
INTERPRO	IPR019821:Kinesin, motor region, conserved site	6	1.97	4.41E-04
SMART	SM00129:KISc	6	1.97	4.97E-04
Annotation Cluster 3	Enrichment Score: 7.969176111621932			
GOTERM_CC_FAT	GO:0000775~chromosome, centromeric region	20	6.58	2.32E-13
SP_PIR_KEYWORDS	centromere	12	3.95	9.49E-12
SP_PIR_KEYWORDS	kinetochore	13	4.28	2.27E-10
GOTERM_CC_FAT	GO:0000793~condensed chromosome	16	5.26	4.40E-09
GOTERM_CC_FAT	GO:0000779~condensed chromosome, centromeric region	12	3.95	1.18E-08
GOTERM_CC_FAT	GO:0005694~chromosome	28	9.21	1.62E-08
GOTERM_CC_FAT	GO:0044427~chromosomal part	25	8.22	3.66E-08
GOTERM_CC_FAT	GO:0000777~condensed chromosome kinetochore	10	3.29	4.94E-07
GOTERM_CC_FAT	GO:0000776~kinetochore	10	3.29	5.67E-06
SP_PIR_KEYWORDS	chromosomal protein	10	3.29	4.72E-04

According to the Interferome database (Samarajiwa et al., 2009), 249 of the 662 up-regulated genes and 40 of the 331 down-regulated genes are so-called interferon-regulated genes (IRGs), i.e. they are transcriptionally regulated by distinct interferons, in this case mainly type I interferons, such as IFNB1, and to a lesser extent type II and III interferons (Table B.6 and Table B.7) (Drews et al., 2012). This emphasizes the key role type I interferons play in the regulation of innate immunity. Thus, the immune response observed upon mRNA transfection of fibroblast cells may be referred to as innate interferon response (Angel and Yanik, 2010; Drews et al., 2012).

Analysis of innate immune response-associated transcript levels in human neonatal fibroblasts following mRNA transfection

Next, the increased expression levels of immune-related genes observed for the microarray-derived transcriptome data were verified by qRT-PCR. On that account we chose to assess the expression of a set of innate immune response-related genes from the microarray-derived data, which were already strongly affected during retroviral reprogramming experiments (Mah et al., 2011). The encoded proteins are known to be relevant at distinct levels of the antiviral innate immune response, as already partly mentioned above. They are either directly involved in the recognition and binding of exogenous, putatively pathogenic, nucleic acids (RIG-I (DDX58) (Pichlmair et al., 2006; Binder et al., 2011), PKR (EIF2AK2) (Baglioni et al., 1981; McAllister and Samuel, 2009), OAS1 (Baglioni et al., 1981; Kristiansen et al., 2010) and IFIT1 (Pichlmair et al., 2011)), key regulators of transcription during the innate immune response (IFNB1 (Yoneyama and Fujita, 2010)), intra- or extracellular transducers of the stimulus (IL12A (CLMF, NKSF1) (Tahara and Lotze, 1995; Katashiba et al., 2011), IRF7 (Kawai et al., 2004; Yoneyama and Fujita, 2010), STAT2 (Uddin et al., 1995), CCL5 (RANTES) (Schall et al., 1990; Genin et al., 2000)) or viral restriction factors (ISG20 (Espert et al., 2003; Zhou et al., 2011), TRIM5 (Rold and Aiken, 2008; Pertel et al., 2011). Interestingly, all of these genes have been shown to be regulated by interferons as determined with the help of the Interferome data base (Table B.6) (Drews et al., 2012). As shown in Figure 4.7, qRT-PCR demonstrated the up-regulation of all 11 genes under investigation in both BJ and HFF1 neonatal fibroblasts 24 h post- transfection of a mix of reprogramming factor-encoding mRNAs when compared to mock-transfected control cells (Drews et al., 2012).

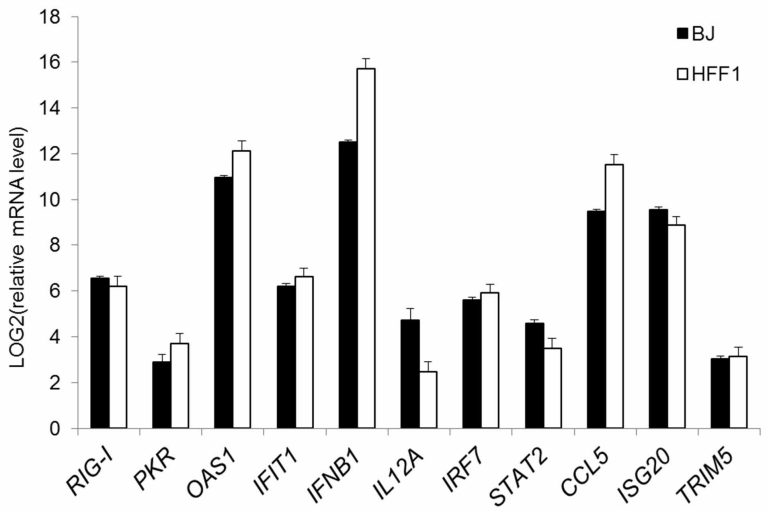

Figure 4.7: qRT-PCR of innate immune response-associated transcripts in mRNA-transfected human fibroblasts. BJ and HFF1 cells were transfected with a 1:1:1:1:1 cocktail of reprogramming factors OSKML-encoding mRNAs (4 µg per 6-well) and harvested 24 h later for RNA isolation. Bars and error bars represent average LOG2 ratios of transfected fibroblasts over mock-transfected controls and SD. n = 3 technical replicates per cell line. Taken from Drews et al. (2012).

Analysis of the innate immune response to different cellular reprogramming approaches in human neonatal fibroblasts

In a next step, we were interested in a comparison of the magnitude of this innate immune response induced by reprogramming experiments based on different delivery protocols. We further intended to determine the immune response triggered by transfection of the commercially available modified mRNAs, which were used for cellular reprogramming by Warren et al. (2010) to ensure that the immunogenic effects observed for the in-house produced, unmodified mRNA was not solely due to the alterations in the *in vitro* synthesis of mRNAs but rather a general mRNA-mediated effect. To this end gene expression levels of the same set of innate immune response-associated genes were assessed after

- retroviral transduction of a 1:1:1:1 cocktail of the reprogramming factors OSKM, one transfection of a 1:1:1:1 cocktail of the reprogramming factors OSKM using the in-house synthesized, unmodified mRNA,
- two subsequent transfections (day1, day2) of a 1:1:1:1 cocktail of the reprogramming factors OSKM using the in-house synthesized, unmodified mRNA,
- one transfection of a 1:1:1:1 cocktail of the reprogramming factors OSKM using commercially bought, modified mRNA or
- one transfection of a mix of pluripotency-promoting miRNAs (miR-302s/367).

(Concerning the series of retroviral and miRNA tests, the experimental setup was based on either our own or published reprogramming experiments (Wolfrum et al., 2010; Anokye-Danso et al., 2011; Miyoshi et al., 2011). The functionality of the modified mRNA from Stemgent was assessed prior to the experiments (Figure B.3).

To verify successful delivery and functionality of the in-house synthesized transfected/transduced factors and, thus, to enable feasibility of comparing the resulting data, protein expression of one of the reprogramming factors (SOX2) was monitored by detection with immunofluorescence dye-labeled antibodies whenever reprogramming factors were directly delivered to the cells as either retroviruses or mRNAs (Figure B.4 (A – C)). For the miRNA approach, expression levels of *PODXL* were assessed by qRT-PCR instead (Figure B.4 (D)). This gene was chosen on the basis of our recent finding that *PODXL*, a surface marker expressed in human ESCs, iPSCs and embryonal carcinoma cells (Tan et al., 2009), is up-regulated as early as 24 h post-transduction of OSKM-encoding retroviruses during cellular reprogramming (Mah et al., 2011).

Despite the fact that only the absolute quantities of gene expression levels resulting from the different mRNA transfection approaches can be directly compared, Figure 4.8 highlights that the magnitude of up-regulation of the innate interferon response genes was notably different in the methods under investigation: Of all the cellular reprogramming techniques applied herein, the transfection of our unmodified reprogramming factor mRNA, although capped and poly(A)-tailed, shows the strongest up-regulation of immune-associated genes

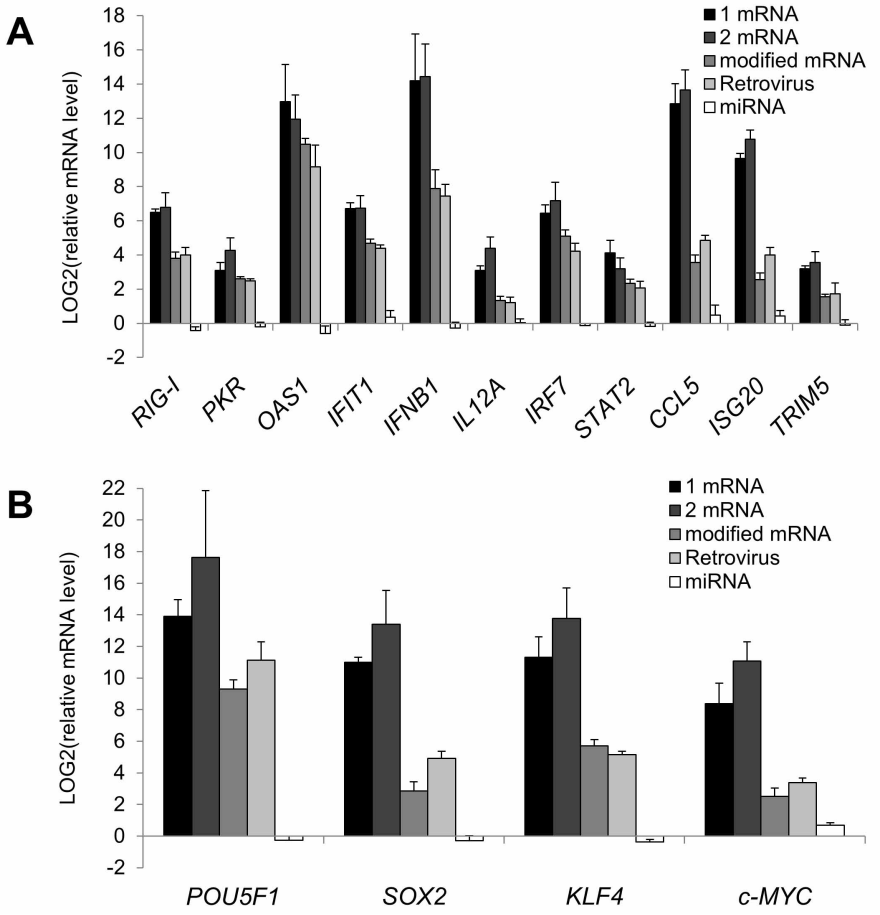

Figure 4.8: Expression levels of innate immune response-associated genes and introduced reprogramming factor genes in HFF1 cells upon delivery of reprogramming factors by diverse methods. HFF1 cells were transfected with a 1:1:1:1 cocktail of mRNAs encoding *POU5F1*, *SOX2*, *KLF4* and *c-MYC*. Transfections were carried out once or twice ('1 mRNA', '2 mRNA', respectively; 4 µg total per 6-well per transfection). The mRNAs were either synthesized in our laboratory ('mRNA') or commercially bought ('modified mRNA'). Alternatively, HFF1 cells were transduced once with a 1:1:1:1 combination of retroviruses encoding *POU5F1*, *SOX2*, *KLF4* and *c-MYC* or transfected once with a 1:1:1:1:1 mix composed of the human miRNA mimics miR-302a, miR-302b, miR-302c, miR-302d and miR-367 (100 pmol total per 6-well). All samples were harvested for RNA isolation 24 h after the last transfection/transduction. (A) Levels of innate immune response-associated transcripts. (B) Expression levels of the reprogramming factor genes. Bars and error bars represent average LOG2 ratios of transfected/transduced fibroblasts over mock-transfected/-transduced controls and SD. n = 6 for '1 mRNA'; n = 4 for '2 mRNA'; n = 3 for 'Retrovirus', 'modified mRNA' and 'miRNA'. Modified from Drews et al. (2012).

(Drews et al., 2012). Interestingly, the second transfection with the same mRNA cocktail 24 h after the first one, slightly increases the expression levels of only a few genes such as *PKR*, *IL12A*, *ISG20*, yet, does not have a strong overall augmenting immunogenic effect. This suggests that the cellular immune response is almost maximally up-regulated already after the first round of transfection (Drews et al., 2012). In contrast, transcript levels of the

reprogramming factors were slightly increased after the second transfection when compared to those levels determined after the first transfection (Drews et al., 2012). Regarding the corresponding immunofluorescent detection of reprogramming factor proteins, which were performed as transfection controls, however, SOX2 expression was negligible after the second round of mRNA transfection (Figure B.4 (C)) (Drews et al., 2012).

Transfection of the commercially available modified mRNAs from Stemgent, which, in contrast to our mRNA, contained pseudouridine and 5-methylcytidine-modified nucleotides and was phosphatase-treated, resulted in markedly reduced expression levels of almost all immune response-associated genes compared to transfection with our unmodified mRNA as expected (Drews et al., 2012). However, transfection of modified mRNAs was unable to prevent the up-regulation of innate interferon response. Transcript levels of most of the immune response-associated genes were still high compared to mock-transfected controls. At the same time, the number of reprogramming factor transcripts in the cell were notably less when compared to the transfections with the same amount of our *in vitro* synthesized, unmodified mRNAs (Figure 4.8) (Drews et al., 2012).

Expression levels of both immune response-associated and reprogramming factor genes of cells transduced with a retroviral reprogramming factor cocktail were similar to those detected upon transfection of commercially available, modified mRNAs (Drews et al., 2012). Finally, an up-regulation of the endogenous reprogramming factor-encoding genes by miRNAs could not be observed as early as 24 h post-transfection as anticipated (Drews et al., 2012). In contrast, *PODXL* transcript levels were elevated when compared to cells transfected with scramble miRNAs 24 h post-transfection although the magnitude of up-regulation was less compared to the single and double transfections of unmodified RNAs and the cocktail of retroviruses (Figure B.4 (D)). Interestingly, transfection of the pluripotency-promoting miRNAs did not trigger any immune response (Figure 4.8) (Drews et al., 2012).

Next, for the in-house synthesized, unmodified mRNA, the retroviruses and the miRNAs we checked whether the immune response is dependent on the specific factors by substituting the reprogramming factors with GFP-encoding mRNAs or retroviruses or a scrambled control, respectively.

Logically, GFP transfection did not induce a marked alteration of reprogramming factor transcript levels despite normal variation (Figure 4.9) (Drews et al., 2012). Yet, the immune response gene expression levels followed the exact same pattern and the absolute transcript quantities were similar when compared to those observed for all respective delivery techniques. This was also observed in the case of retroviral transduction of GFP, in which, for practical reasons, the amount of GFP-encoding particles were equivalent to only one quarter of the total amount of viral transduction units used for the mix of reprogramming factors (Drews et al., 2012).

Effect of immune modulators on the innate immune response in human neonatal fibroblasts upon transfection of reprogramming factor-encoding mRNAs

Knowing that the main roadblock in our mRNA reprogramming experiments is the vigorous

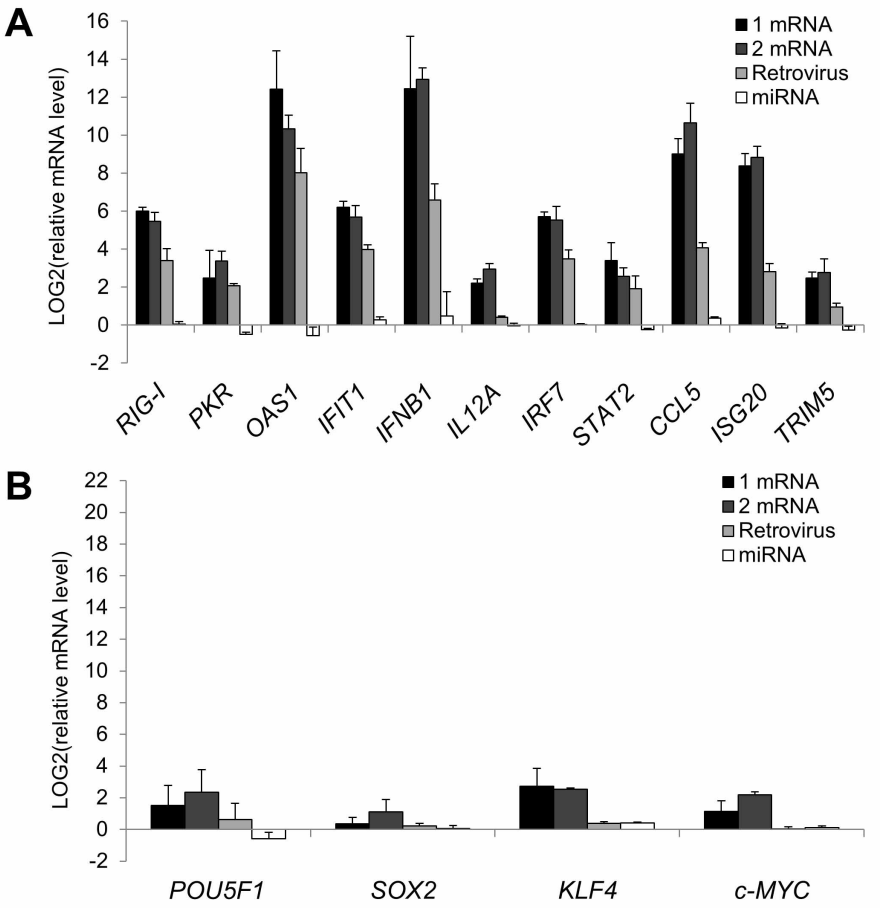

Figure 4.9: Expression levels of immune response-associated genes and reprogramming factor genes in HFF1 cells upon delivery of control genes by diverse methods. Repetition of the HFF1 transfection/transduction experiments as described in Figure 4.8. Yet, this time, the total amount of mRNAs and miRNAs used for reprogramming were substituted with the same amount of GFP-encoding mRNA ('1 mRNA', '2 mRNA'; 4 µg total per 6-well per transfection) or a scrambled miRNA (100 pmol total per 6-well). Similarly, cells were transduced with a GFP-encoding retrovirus equivalent to the amount of retrovirus encoding one of the reprogramming factors in the reprogramming OSKM cocktail. (A) Levels of innate immune response-associated transcripts. (B) Expression levels of the reprogramming factor genes. Bars and error bars represent average LOG2 ratios of transfected/transduced fibroblasts over mock-transfected/-transduced controls and SD. n = 6 for '1 mRNA'; n = 4 for '2 mRNA'; n = 3 for 'Retrovirus' and 'miRNA'. Modified from Drews et al. (2012).

activation of an innate interferon response, we next tried to identify substances that could possibly suppress this immune reaction. Hence, we sought to determine the ability of different immune modulators to prevent up-regulation of the different innate immune response-associated genes by qRT-PCR.

The first molecule of choice to suppress the innate interferon response is B18R, a virus-encoded decoy receptor specific for type I interferons of various species, which neutralizes signaling via type I interferon receptors (INFAR1/2) (Colamonici et al., 1995; Symons et al., 1995; Galligan et al., 2006). B18R was described to prevent transmembrane signaling and

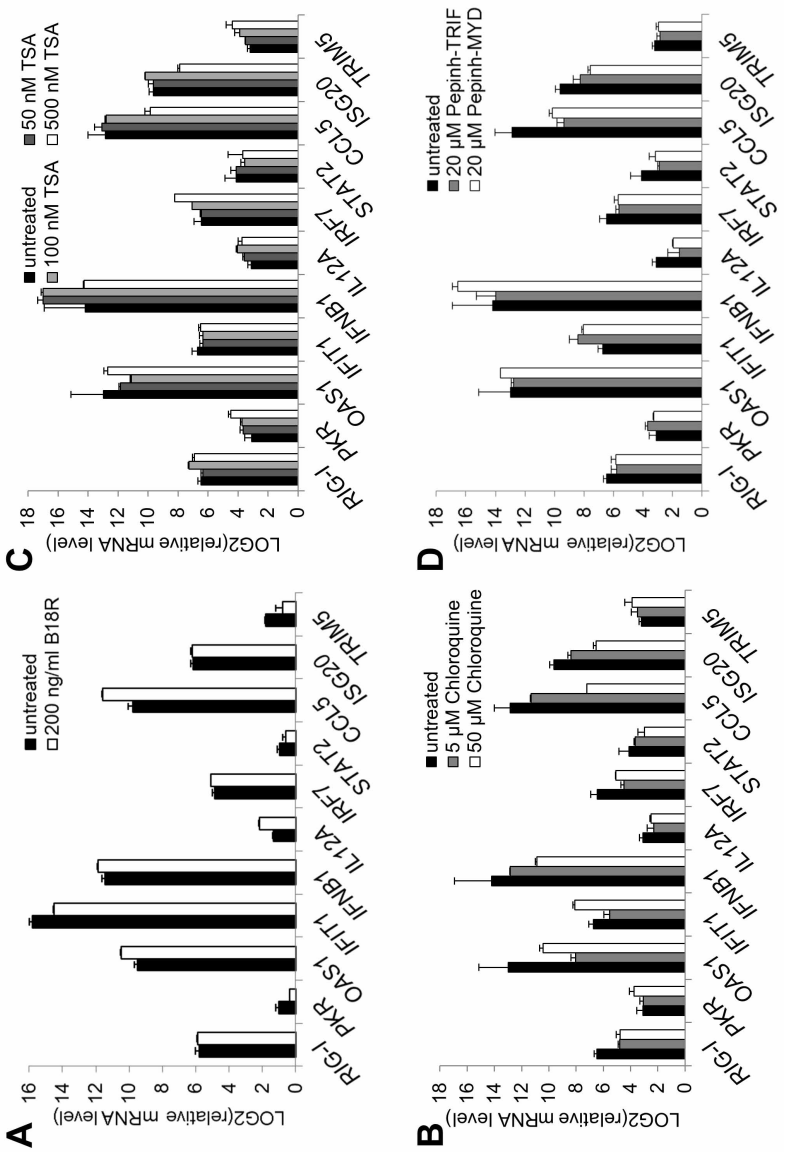

Figure 4.10: Effect of immunomodulators on the expression of innate immune response-associated transcripts in mRNA-transfected human fibroblasts. (A) HFF1 cells were transfected with a 3:2:1:1:1: cocktail of mRNAs encoding *POU5F1*, *SOX2*, *KLF4*, *c-MYC* and *LIN28A* once (4 µg total per 6-well). One hour prior to transfection, during transfection and directly following transfection cells were treated with 200 ng/ml B18R. (B, C, D) HFF1 cells were transfected with a 1:1:1:1: cocktail of mRNAs encoding *POU5F1*, *SOX2*, *KLF4* and *c-MYC* once (4 µg total per 6-well). One hour prior to transfection, during transfection and directly following transfection cells were treated with given concentrations of chloroquine (B), TSA (C) or pepinh-TRIF or pepinh-MYD (D). All samples were harvested for RNA isolation 24 h post-transfection. Bars and error bars represent average LOG2 ratios of (treated) transfected fibroblasts over (treated) mock-transfected controls and SD. n = 1 for B18R; n = 2 for pepinh-TRIF; n = 3 for pepinh-MYD; n = 2 for each concentration of TSA and chloroquine. Taken from Drews et al. (2012).

transcriptional regulation of the interferon regulated genes (Colamonici et al., 1995; Symons et al., 1995). For this reason it was also used in the only mRNA-based reprogramming protocol published so far (Warren et al., 2010). With this in mind, we applied it to our mRNA transfection protocol. As shown in Figure 4.10 (A), in an initial experiment, this treatment did not have any measurable effect on expression levels of the immune response-associated genes after mRNA transfection even though all of these genes are known to be IRGs as determined by the Interferome database (Table B.6) (Drews et al., 2012). However, as this result is in line with our previous finding that B18R did not have any effect on the efficiency of retroviral reprogramming (Mah et al., 2011) we did not pursue investigations using B18R further.

Chloroquine was originally synthesized as an antimalarial drug but pleiotropic functions of this substance have been reported (Cooper and Magwere, 2008). For example, the lysosomotropic substance chloroquine was used in specific transfection setups to increase efficiency either by enhancing endosomal escape of nucleic acids to be delivered through endosomal disruption and/or by delaying the traffic of endocytosed nucleic acids into lysosomes, retarding their degradation (Wattiaux et al., 2000). Several immune-modulatory, anti-inflammatory effects of chloroquine such as the ability to inhibit TNF-α and IL-1β and IL-6 production in lipopolysaccharide-stimulated human monocytes or macrophages (Jang et al., 2006) were discussed by Cooper and Magwere (2008). In the last decade Chloroquine has also been tested as therapeutic against viral infections such as HIV retroviral infections (Savarino et al., 2003). The observation that chloroquine can reduce type I interferon (INFA) production in CpG-DNA-stimulated or viral ssRNA-stimulated plasmacytoid-derived dendritic cells (Diebold et al., 2004; Katashiba et al., 2011) and IL12 production in ssRNA poly(U)-stimulated monocyte-derived dendritic cells (Katashiba et al., 2011) intrigued us to examine the ability of chloroquine to suppress the immune response following mRNA transfection in fibroblast cells. Strong up-regulation of the adapter molecules *MYD88* and *IRF7* (Table B.4), which are mediators of nucleic acid recognition signaling pathways triggered by mRNA transfection (Yoneyama and Fujita, 2010), further encouraged us to test chloroquine. However, when treating cells prior to, during and following mRNA transfections with 5 µM, 50 µM and 100 µM of chloroquine (Diebold et al., 2004; Jang et al., 2006; Katashiba et al., 2011), we primarily noticed strong concentration-dependant cytotoxic effects, which resulted in decreased viability of cells treated with 50 µM chloroquine and death of almost all cells treated with 100 µM chloroquine (Drews et al., 2012). Although a few of the innate interferon response-associated gene expression levels (e.g., *RIG-I*, *OAS1*, *CCL5*, *ISG20*) were slightly reduced upon chloroquine treatment when compared to controls (Figure 4.10 (B)), these reductions were not sufficient to balance the cytotoxic effects of this molecule—especially with the intention to use chloroquine in a protocol including numerous subsequent transfections as required for the induction of pluripotency in somatic cells (Drews et al., 2012).

Trichostatin A (TSA) is a *Streptomyces* metabolite. It was first discovered as an antifungal antibiotic, which was shown to inhibit mammalian histone deacetylases later on (Tsuji et al., 1976; Yoshida et al., 1990). Interestingly, Huangfu et al. (2008) highlighted its potential to enhance cellular reprogramming processes in mouse embryonic fibroblasts. Concerning its

immune-modulatory capacity, it was reported to block un-methylated CpG oligonucleotide-induced up-regulation of INFα, INFβ, IFNλ and INFω and other pro-inflammatory cytokines, namely IL-6, TNF-α, and TRAIL in plasmacytoid dendritic cells, which was associated with blocking nuclear translocation of the transcription factor IRF7 (Salvi et al., 2010). In view of this, we next tested its potential in inhibiting innate interferon response following mRNA transfection of HFF1 fibroblasts, which significantly up-regulated *IRF7*. No remarkable effect on the transcript levels of the innate immune response gene test set was observed (Figure 4.10 (C)) (Drews et al., 2012). Solely the expression levels of *CCL5* and *ISG20* in 500 nM TSA-treated cells were reduced when compared to untreated, mRNA-transfected samples. However, the absolute gene expression values were still much higher than those determined for treated, mock-transfected controls (Drews et al., 2012).

Pepinh-TRIF and pepinh-MYD are two peptide inhibitors designed to contain domains of the signaling adapter molecules TRIF and MYD88, which facilitate interaction with the respective pattern-recognition receptors TLR3 or TLR7/8 (Loiarro et al., 2005; Toshchakov et al., 2005). Competing with endogenous TRIF and MYD88 for association with the PRRs, these two peptide inhibitors were shown to attenuate signaling to the nucleus, thereby suppressing the up-regulation of innate immune response genes, the very first step in pathogen defense. Especially since both *TRIF* and *MYD88* were significantly up-regulated upon mRNA transfection in fibroblast cells (Table B.4 and Table S3 of Drews et al. (2012)), pepinh-TRIF and pepinh-MYD were promising candidates with respect to the modulation of the innate immune response in mRNA-transfected fibroblasts despite the potential lack of TLR7/8 expression in human neonatal foreskin fibroblasts. Treatment of HFF1 cells prior to, during and following mRNA transfections with the suggested concentration of 20 µM, however, did not lead to a marked reduction of any of the immune response-associated transcript levels (Figure 4.10 (D)) (Drews et al., 2012).

4.2.3 Cellular reprogramming by means of miRNA transfection

From the preceding experiments it is known that transfections of miRNAs do not trigger an innate immune response in the target cells. We therefore sought to exploit this circumstance by using this novel approach to induce pluripotency in somatic cells. miRNA-mediated cellular reprogramming is independent of the direct overexpression of the original reprogramming factors OCT4, SOX2 and KLF4, c-MYC or NANOG, LIN28. Instead, it is based on the delivery of miRNAs that are preferentially expressed in ESCs to support the pluripotent phenotype (Anokye-Danso et al., 2011; Miyoshi et al., 2011). On the basis of these findings, we performed a pilot experiment and transfected bulk human AFCs with a cocktail of miRNA mimics of the miR-302/367 cluster and subsequently maintained them under human PSC conditions. Yet, no morphological changes, no formation of colonies with granulated or human ESC-like morphology was observed after treatment of about 1×10^6 cells. The experiments were terminated after approximately one month of culture. In contrast to the techniques employing the original reprogramming factors, the mechanisms underlying miRNA-mediated cellular reprogramming were even more elusive at this point. Thus, further

investigations and optimization were required and are currently on-going in our laboratory to establish the miRNA-mediated induction of pluripotency in somatic cells.

4.3 Discussion

The stem cell field is a competitive area of research that progresses at a breathtaking pace. The groundbreaking development of iPSCs greatly contributed to that. In view of the fact that human iPSCs offer enormous opportunities in regenerative medicine, the field has been striving to generate clinical-grade iPSCs. Most importantly, this comprises the establishment of reprogramming protocols that allow for the induction of pluripotency without genomic alteration of the target cells. Various promising strategies have been reported to achieve this goal including transduction of reprogramming factor-encoding adenoviruses (Zhou and Freed, 2009) or Sendai viruses (Fusaki et al., 2009), nucleofection of episomal plasmids (Yu et al., 2009), treatment with recombinant reprogramming factor proteins (Kim et al., 2009a) and transfection of reprogramming factor-encoding mRNAs (Warren et al., 2010) or human ESC-specific miRNAs (Miyoshi et al., 2011). However, unlike the robust originally published integrating virus-mediated reprogramming method published by Takahashi et al. (2007); Yu et al. (2007), to date none of these methods have successfully been established as a standard reprogramming protocol and the amount of time that has passed since the last reported innovations increases.

4.3.1 Cellular reprogramming by means of episomal plasmids requires further optimization

The first attempt to generate iPSCs from human AFCs by non-viral, non-integrating approaches was based on nucleofection of episomal plasmids as initially published by Thomson and colleagues for human newborn foreskin fibroblast cells (Yu et al., 2009). We employed the most-effective plasmid combination to induce pluripotency in human AFCs. Surprisingly, not a single mature, expandable iPSC colony was obtained during several rounds of nucleofection although several millions of cells had been used as input. There are several possible factors that may have contributed to the poor outcome of these experiments.

Generally, direct reprogramming of somatic cells into iPSCs is thought to depend on the amount, balance and continuity of transgene expression (Yamanaka, 2009b). In the particular case of episomal plasmid-mediated reprogramming meeting all these conditions is especially intricate. First of all, in contrast to the original protocols of virus-mediated reprogramming (Takahashi et al., 2007; Yu et al., 2007), a total of seven reprogramming factors is used (OCT4, SOX2, KLF4, c-MYC, NANOG, LIN28 and SV40 large T antigen) (Yu et al., 2009). These factors are encoded on different vectors, which are combined for nucleofection. Moreover, two genes are regulated by a single promoter sequence and co-expression is mediated by the internal ribosome entry site 2 (IRES2) (Figure 4.1). Taken together, this dramatically reduces the chances of sufficient expression of each of the reprogramming factors and potentially impairs an optimally stoichiometric balanced, well-orchestrated simultaneous expression of

all transgenes particularly in conjunction with the extensive loss of cell viability induced by electroporation. Without active selection it is further unclear, for how long the episomal plasmids remain in the transfected cells to mediate adequate transgene expression (Yu et al., 2009). In addition to that it is a matter of debate, whether all cells in one sample have an equal opportunity to acquire the pluripotent state (stochastic model) or whether only certain cells in one sample are more competent to become iPSCs (elite model) (Yamanaka, 2009b). For human AFCs it is tempting to believe that the few putative stem cell-like subpopulations have greater chances to become fully reprogrammed or that, at least, they require less time. Another major drawback of the episomal plasmid-based approach is the enormous size of the episomal plasmids ranging from 12852 bp to 19949 bp, which is likely to hamper efficient transgene delivery. In summary it should become clearer, why reprogramming by means of episomal plasmids is generally rather inefficient.

However, there might be other more specific factors, which may have additionally contributed to the poor experimental outcome. For example, one might expect the age of the cells, which were used as starting material to be one critical factor. Especially for the one human AFC line, which had already been used for retrovirus-mediated reprogramming, the cells had partly been cultured to P10 prior to nucleofection. As described earlier, human AFCs senesce relatively early (Wolfrum et al., 2010). It could be assumed that a limited proliferation potential of higher passage human AFCs may have impeded this reprogramming approach. Interestingly, however, the episomal plasmid-mediated cellular reprogramming includes the SV40 large T antigen as 'reprogramming factor' as mentioned above (Yu et al., 2009). The oncogene SV40 large T antigen is known to drive cells into the S-phase of cell cycle, thereby inducing proliferation and transformation of cells (Ahuja et al., 2005). Hence, it could be speculated that the SV40 large T antigen expression in the target cells should have balanced potential proliferation deficits. This, together with the observation that the use of early passage human AFCs did not facilitate reprogramming either, leads me to exclude the passage number of the target cells to be a major influencing factor.

Nucleofection is usually performed employing cell line-specific nucleofection solutions and electric impulse parameters (Yu et al., 2009). This is, however, impossible as for heterogeneous samples of human AFCs no particular kit is available. Referring to several reports, which highlight the presence of MSC populations in human AFCs amongst others (In 't Anker et al., 2003; Tsai et al., 2004, 2006; Bossolasco et al., 2006; Kim et al., 2007; De Coppi et al., 2007; Sessarego et al., 2008; You et al., 2009), it was assumed that the use of MSC-specific settings and solutions would promote an efficient transgene delivery, while preventing exceedingly high levels of cell death. It is unclear, however, if the use of a different nucleofection kit and other nucleofection parameters, e.g. for neuronal or epithelial lineage cells, would have been more advantageous.

We included several small molecules to possibly enhance the reprogramming process, namely BAPN (0.25 mM) (Tang et al., 1983) or thiazovivin (2 µM), alone or in combination with ALK4/5/7 inhibitor SB431542 (2 µM) and MEK inhibitor PD0325901 (0.5 µM) (Lin et al., 2009). In the case of heterogeneous human AFCs it cannot be exactly specified,

which particular cell type the reprogramming process starts from (Gosden, 1983). It can be anticipated, however, that at least a certain proportion of the cells is of mesenchymal origin (In 't Anker et al., 2003; Tsai et al., 2004, 2006; Bossolasco et al., 2006; Kim et al., 2007; De Coppi et al., 2007; Sessarego et al., 2008; You et al., 2009). These will have to undergo the process of mesenchymal to epithelial transition (MET) to become iPSCs of epithelial nature (Wang et al., 2010). The combined TGFβ and MEK/ERK pathway inhibition by SB431542 and PD0325901 treatment is believed to enhance the generation of iPSCs from fibroblast cells by promotion of MET (Lin et al., 2009). BAPN has not yet been implicated in direct reprogramming. This chemical is rather known for its ability to inhibit the activity of all lysyl oxidases (Pinnell and Martin, 1968; Lugassy et al., 2012). Activation of lysyl oxidases, in turn, has been shown to be required for hypoxic repression of cadherin-1 (E-cadherin), which induces epithelial to mesenchymal transition (EMT) and thereby mediates cellular transformation and tumor progression (Schietke et al., 2010). In view of these findings, we hypothesized that BAPN may enhance reprogramming of human AFCs by inhibiting lysyl oxidases and, thus, blocking EMT and promoting MET. Interestingly, BAPN treatment was applied in the case where the only potential iPSC colony was obtained, which, however, proliferated markedly slower than other human PSC lines. This observation is especially astonishing in view of the of the SV40 large T antigen transgene expression in those cells. This ESC-like colony also spontaneously differentiated to a high degree so that it could not successfully be established as iPSC line. It is unclear whether this could have been an undesired side effect of the small molecule BAPN. Generally, however, with respect to the use of small molecules in this study it can be concluded that neither BAPN nor any of the other chemicals positively influenced the induction of pluripotency due to the poor overall outcome.

Unfortunately, the majority of episomal-based reprogramming experiments had been conducted prior to two follow-up publications by Chou and co-workers. and Yu and colleagues. While Chou et al. (2011) developed an improved OriP/EBNA episomal plasmid, which encodes five reprogramming factors (OSKML) in a single poly-cistronic unit, to derive iPSCs from human blood mononuclear cells, Yu et al. (2011) described the use of other small molecules to greatly enhance the induction of pluripotency in skin fibroblasts, adipose tissue-derived cells and cord blood cells by nucleofection of the original episomal plasmid vectors. The combinations and amounts of nucleofected episomal plasmids varied only slightly. Yet, besides TGFβ and MEK/ERK pathway inhibition by A-83-01 (0.5 μM) and PD0325901 (0.5 μM), which is similar to our treatment, they found simultaneous treatments with other small molecules to increase the reprogramming efficiency. Hence, it can be anticipated that the combined use of ROCK inhibitor HA-100 (10 μM), PD0325901 (0.5 μM), CHIR99021 (3 μM), A-83-01 (0.5 μM) and hLIF (1000 U/ml) as well as supplementation of MEF-conditioned human ESC medium with 100 ng/ml FGF2, instead of the usual 4 ng/ml in unconditioned medium and 8 ng/ml in MEF-CM (Yu et al., 2011) would have improved the experimental outcome. In fact, it is currently being observed in our laboratory that the implementation of this modified protocol (Yu et al., 2011) instead of the original one (Yu et al., 2009) enables a more efficient induction of pluripotency in human foreskin fibroblasts and MSCs (Matthias

Megges, Kalina Tosheva, Peggy Matz, unpublished data). A modification of the nucleofection protocol to include the above mentioned small molecules and the improved episomal plasmid is thus recommended for future experiments. Considering that episomal-derived iPSCs do not harbor integration events as recently demonstrated by deep whole-genome sequencing (Cheng et al., 2012), an optimization of the episomal plasmid-mediated reprogramming protocol appears worthwhile.

4.3.2 mRNA-mediated induction of pluripotency is hampered by an innate interferon response

The second attempt to generate iPSCs from human AFCs by non-viral, non-integrating approaches was based on transfection of *in vitro* transcribed mRNAs encoding the originally published reprogramming factors (Takahashi et al., 2007; Yu et al., 2007). This approach failed due to severe loss of cell viability following continued transfection of mRNAs into human AFCs and human foreskin fibroblasts. Thus, we examined the effect of the transfections on the cells in greater detail using human foreskin fibroblast cells due to their increased availability.

The genome-wide gene expression analysis revealed that an overall transcriptome shift towards pluripotent cells did not occur as early as 24 h post-transfection of a cocktail of reprogramming factor-encoding mRNAs into human neonatal foreskin fibroblasts. Yet, we could identify an overlap of 148 genes in reprogramming factor mRNA transfected fibroblast cells and the union of pluripotent FiPSCs and ESCs. Their relevance as potential early pluripotency-associated markers of reprogramming warrants further investigations.

As the main result of the microarray-based transcriptome analysis we highlighted the strong innate immune reaction, an interferon-mediated response, to be the key roadblock during reprogramming by means of frequent mRNA transfections, which is in line with other reports (Angel and Yanik, 2010; Mah et al., 2011). According to the recent understanding, purified, *in vitro* synthesized reprogramming factor-encoding mRNA triggers an immune response via its recognition by pattern-recognition receptors (PRRs) upon transfection similarly to microbial or viral infections (Yoneyama and Fujita, 2010; Angel and Yanik, 2010; Drews et al., 2012). In principle, the endocytic uptake route of lipofected nucleic acids (Khalil et al., 2006) suggests a primary role for TLR3 and TLR7/8 in the recognition of the transfected mRNAs due to their endosomal location (Yoneyama and Fujita, 2010). TLR3 preferentially detects double-stranded RNAs, whereas TLR7/8 mainly recognizes single-stranded RNAs (Yoneyama and Fujita, 2010). As mRNAs usually form complex secondary structures (images of predicted minimum free energy secondary structures of the reprogramming factor mRNAs obtained from the *RNAfold* WebServer (Gruber et al., 2008) are depicted in Figure B.1) and parameters such as pH vary along the endocytic pathway, it is generally difficult to precisely predict, exactly which of these PRRs are specifically involved in the detection of the different transfected mRNA molecules (Drews et al., 2012). It is further known that TLR3 and TLR7/8 are preferentially expressed in immune cells (Yoneyama and Fujita, 2010). Accordingly, the microarray data derived in this part of the PhD project point towards an

up-regulated expression of TLR3 in fibroblasts upon mRNA transfection, whereas TLR7/8 receptors are not expressed in any of the samples under investigation. Without confirmation of these data by the more sensitive qRT-PCR, however, this finding, taken by itself, does not exclude latent, low level expression of TLR7/8 in human neonatal foreskin fibroblasts (Drews et al., 2012).

Cytoplasmic receptors should also play an essential role in the recognition of mRNAs as soon as they are accessible in the cytoplasm, e.g., after endosomal escape of the transfected mRNAs (Wattiaux et al., 2000). RIG-I (DDX58) and MDA5 (IFIH1) are such cytoplasmic PRRs and, according to the microarray data, expression of the corresponding genes is highly up-regulated upon mRNA transfection (Table B.4) (Drews et al., 2012). An important role of cytoplasmic receptors is supported by Kato et al, who reported that, indeed, infection of mouse embryonic fibroblasts with several single-stranded RNA viruses was RIG-I- rather than TLR-dependent (Kato et al., 2005). Yet, clarification as to which of the various possible receptors or which combination of receptors is eventually responsible for the detection of so-called pathogen-associated molecular pattern (PAMP) in this particular case of mRNA lipofection requires further detailed investigations.

Regardless of this, our data emphasized that the PRR(s) involved subsequently triggered an increased translation of type I interferons, like *IFNB1*, and pro-inflammatory cytokines such as *CCL2*, *CCL5*, *IL10* and *IL12A* (Drews et al., 2012). Especially the type I interferons, in turn, provoked positive feedback regulation in an autocrine and paracrine fashion, which enhanced different defense mechanisms against the putative pathogen attack in the same and neighboring cells sensitizing them towards foreign nucleic acids (Angel and Yanik, 2010). This may explain why the observed immune response was at its maximum already after the first transfection. As a consequence of the interferon signaling, PRRs like *RIG-I*, *MDA5*, including those which elicit antiviral/antimicrobial activities such as *OAS1*, *PKR* and *ADAR*, were significantly up-regulated in mRNA transfected fibroblast cells along with a number of signaling molecules (*JUN* (as part of the transcription factor AP-1), *IRF7*, *MYD88*, *IRAK4* etc.) (Table B.4 and Table S3 of Drews et al. (2012)). Concomitantly, interferon-responsive cell cycle-associated genes were down-regulated and apoptosis-associated genes up-regulated (Drews et al., 2012). This is in line with Johnston et al. (2005), who demonstrated induction of *IFNB1*, *PKR*, *OAS1* as well as cell death in human dermal fibroblasts stimulated with dsRNA. It must be assumed that, along with the impaired cell viability, protein translation was blocked and the foreign nucleic acids degraded as a result of these gene regulatory processes (Brown et al., 1976; Sen et al., 1976; Clemens and Williams, 1978; Levin et al., 1981; Sadler and Williams, 2008) as further supported by the humble signals detected for immunofluorescence-labeled SOX2 24 h after the second consecutive transfection (Figure B.4). Hence, treatments with the small molecules EDHB, SB431542, PD0325901 and thiazovivin to enhance the process of reprogramming in these cells (Lin et al., 2009; Prigione et al.) were ineffectual, as an efficient expression of the pluripotency-inducing transgenes was suppressed. This probably represents the key difference between retroviral and mRNA-mediated reprogramming. We observed similar transgene and immune response-associated gene expression levels in modified mRNA-transfected and

retrovirally transduced fibroblasts 24 h after the introduction of the reprogramming factor-encoding transgenes (Figure 4.8). Whereas this level of immune response induction still mediates efficient induction of pluripotency in somatic cells when retroviruses are employed (Wolfrum et al., 2010; Mah et al., 2011), it triggers severe loss of cell viability and failure of the reprogramming experiment when the transgenes are delivered as mRNAs. It should be emphasised, at this point, that the observed expression of retrovirally encoded reprogramming factor genes should not have reached the maximum 24 h post-transduction as demonstrated by the increase in immunofluorescent signal intensity of reprogramming factors proteins from 24, to 72 h post-transduction in our recent publication (Mah et al., 2011). In contrast, the exogenous expression levels measured for the modified mRNA-transfected cells were presumably the highest possible. Hence, although the level of the immune response is the similar in both cases, the different outcome of retrovirus versus mRNA-mediated induction of pluripotency are most likely attributable to the consistent reprogramming factor expression from integrated transgene sequences in retrovirally transduced cells (Mah et al., 2011) as opposed to a loss of transgene expression due to a block of processing and active degradation of consecutively delivered mRNAs in non-viral reprogramming (Brown et al., 1976; Sen et al., 1976; Clemens and Williams, 1978; Levin et al., 1981; Sadler and Williams, 2008).

Hence, in order to facilitate efficient reprogramming of somatic cells by means of mRNA transfection it will be inevitable to identify ways to suppress the innate immune response triggered by the transgene delivery. Although B18R, chloroquine, TSA and pepinh-TRIF and pepinh-MYD are known to interfere at distinct levels of innate immune response-associated signaling pathways (Diebold et al., 2004; Loiarro et al., 2005; Toshchakov et al., 2005; Salvi et al., 2010; Warren et al., 2010; Katashiba et al., 2011), we could not demonstrate a measurable immune suppressing effect (Drews et al., 2012). For B18R this was especially surprising as its putative immune suppressing capacity was highlighted for mRNA-mediated reprogramming in human fibroblasts (Warren et al., 2010). With respect to chloroquine, it is likely that its cytotoxic effect superimposed its immune suppressing capacity. Notwithstanding, it remains unknown, why the different substances were ineffective. As most of their above described immune modulatory effects were determined in cells directly involved in the immune system such as macrophages or plasmacytoid-derived dendritic cells there appear to be crucial differences in the signaling pathways, which induce the innate immune response upon recognition of foreign nucleic acids, between immune and fibroblast cells. Functional studies, on the basis of the data set presented herein, should bring further insights and enable the identification of truly effective chemical immune suppressors which mediate efficient induction of pluripotency in somatic cells by mRNAs. Furthermore, reprogramming factor-encoding mRNAs could be co-expressed with siRNAs targeting innate immune response-relevant genes (Angel and Yanik, 2010).

4.3.3 Transfection of miRNAs resembles a promising reprogramming approach

One of the key results of the qRT-PCR analysis comparing immune response-associated transcript levels among different reprogramming approaches was that miRNAs did not markedly induce any of the tested genes. We are convinced that this observation was a result of the length and structural characteristics of the miRNA mimics leading to their recognition as endogenous Dicer products and to evade the immune system (Marques et al., 2006) rather than unsuccessful delivery. In support of this, delivery of the miRNAs into the target cells resulted in an up-regulation of the *PODXL* gene expression (Mah et al., 2011) although the magnitude of up-regulation was less compared to the single and double transfections of unmodified RNAs and the cocktail of retroviruses (Figure B.4). Also referring to recent reports on the generation of iPSCs solely mediated by an overexpression of ESC-specific miRNAs in somatic cells (Anokye-Danso et al., 2011; Miyoshi et al., 2011), we were encouraged to set up a pilot experiment in which bulk human AFCs were transfected with a cocktail of miRNA mimics to enable non-integrative reprogramming (Anokye-Danso et al., 2011; Miyoshi et al., 2011). Unfortunately, this did not facilitate the generation of iPSCs. Yet, in view of the lack of replicating experiments and the fact that these reports have not been reproduced to date this outcome is not surprising. Generally, specific investigations to unveil the roles of miRNAs in stabilizing the pluripotent state of ESCs and iPSCs constitute a rather new area of stem cell research (Mallanna and Rizzino, 2010). The knowledge concerning specific functions and targets of distinct miRNAs is still limited and most of it has resulted from studies in other species including mouse. It has been anticipated that miRNAs contribute to the maintenance of the TRN that governs the PSC state (Jaenisch and Young, 2008), the underlying mechanisms, however, are only currently being unravelled. This was initiated by findings that expression of the distinct miRNAs such as the miR-302/367 cluster is specific for undifferentiated human ESCs (Lakshmipathy et al., 2007; Morin et al., 2008). Although meanwhile, the miR-302/367 cluster has been demonstrated to be directly regulated by the key pluripotency-associated transcription factors OCT4, SOX2 and NANOG (Barroso-delJesus et al., 2008; Card et al., 2008), details of how these and other ESC-specific miRNAs regulate the developmental potential of human PSCs is yet unknown. Regulation of cell cycle progression and potential induction of the TGFβ/Activin A/Nodal signaling pathway by the miR-302/367 cluster may be involved (Card et al., 2008; Barroso-del Jesus et al., 2009). In contrast, miRNAs miR-145 and mature let-7, for example, were identified as highly expressed in differentiated cells instead (Marson et al., 2008; Xu et al., 2009). Research focussing on the interplay of these antagonistic miRNAs and the missing links to the pluripotency-associated TRN in the regulation of 'stemness' and differentiation is currently on-going. It is known, for instance, that introduction of miRNAs of the let-7 family does not induce differentiation in ESCs but that inhibition of let-7 family miRNAs enhances reprogramming (Melton et al., 2010). The fact that somatic cells express miRNAs which putatively balance the transfected pluripotency-associated miRNAs may partly explain why Anokye-Danso et al. (2011) were successful using a lentiviral approach,

whereas we, in our initial experiment, were not. Integration of the miRNA-encoding cassette into the host cell genome mediated a long-term expression at high levels. Although Miyoshi et al. (2011) claimed the generation of iPSCs by transient lipofection of comparable total concentrations of mature miRNAs, it should be tested, if higher concentrations of the miRNA mimics or more than four subsequent transfections would have enabled the induction of pluripotency in human AFCs. In parallel the combination of miRNAs employed by Miyoshi et al. (2011) should be tested, namely miR-200c plus mir-302s and mir-369s family miRNAs. As the field advances targets and down-stream effects of distinct miRNAs will be verified. This will provide several options of improving this miRNA-mediated reprogramming approach, including the establishment of suitable experimental controls, the incorporation of small molecules other than thiazovivin (Li et al., 2009c; Lin et al., 2009; Zhu et al., 2010; Yu et al., 2011; Wang and Adjaye, 2011) and combinations of other pluripotency-associated miRNAs as well as inhibitors of somatic cell-specific miRNAs (Melton et al., 2010; Ebert et al., 2007). Efforts to optimize the miRNA-mediated reprogramming approach are currently on-going in our laboratory.

5

General Discussion

A great deal of biomedical research concentrates on the development of systems to model and, hence, understand and prevent diseases. For cases, where damage has already occurred or the outbreak of a disease is unavoidable, regenerative medicine aims at designing adequate therapeutics combining cell-based approaches, molecular medicines and biomaterials to treat them (Mason and Dunnill, 2008). Different types of stem and progenitor cells in the human body qualify for the development of cellular therapeutics, each accompanied by distinct advantages and disadvantages. Due to their exceptional differentiation potential and capacity to self-renew, human ESCs, for example, are valuable candidates (Thomson et al., 1998). The ethical concerns associated with human ESCs, however, restrict their implementation into regenerative medicine. With the development of iPSCs (Takahashi et al., 2007; Yu et al., 2007), which resemble a true alternative to human ESCs, new perspectives have been opened in the field. Human AFCs are another source of routinely available multipotent and putatively immune-privileged fetal stem cells, which are inherently of great value for application in regenerative medicine (Fauza, 2004; De Coppi et al., 2007; Walther et al., 2009).

We hypothesized the induction of pluripotency in human AFCs to be efficient and to enhance the differentiation potential of human AFCs, while circumventing the early onset of senescence putatively adding even greater value to these cells for regenerative therapies. Hence, the objective of this study was to generate and comparatively characterize iPSCs from human AFCs by viral and non-viral, non-integrative methods.

As demonstrated in the first part of this thesis and by others (Li et al., 2009a; Ye et al., 2009; Galende et al., 2010; Zhu et al., 2010; Anchan et al., 2011; Liu et al., 2012), the induction of pluripotency in human AFCs was, indeed, efficient and faster than reprogramming of human neonatal foreskin fibroblast cells. This finding supports our hypothesis that stem cell-like subpopulations within bulk primary human AFCs promote the de-differentiation process, although the preferential contribution of the stem cell-like cells to the high overall reprogramming efficiency of human AFCs has recently been argued by Anchan et al. (2011). The induction of pluripotency by-passed the naturally occurring arrest of proliferation in AFCs by reversing senescence-associated gene expression patterns. The resulting iPSCs closely resembled human ESCs. Besides the fact that AFCs enable efficient generation of iPSCs, another advantage of using such a 'young' cell type for reprogramming purposes is the reduced risk of genetic lesions in the resulting PSCs (Maherali and Hochedlinger, 2008; Gore et al., 2011; Prigione et al., 2011a). Moreover, the generation of AFiPSCs after amniocentesis would

theoretically facilitate the production of autologous therapeutics, which could be available around the time of birth. Interestingly, it has also been shown that human AFCs can be used as autologous feeder cells at the same time to support the undifferentiated growth of human iPSCs and ESCs (Anchan et al., 2011). The development of xeno-free culturing conditions resembles another important step into developing clinical grade cellular therapeutics (Mallon et al., 2006; Takahashi et al., 2009). One of the key obstacles of generating clinical grade human iPSCs, however, is the lack efficient non-integrative reprogramming techniques (Maherali and Hochedlinger, 2008). Despite the high reprogramming efficiency of human AFCs in robust viral reprogramming approaches, the non-integrative generation of iPSCs from AFCs could not be achieved in the course of this project.

The observed inefficiency of episomal and mRNA-mediated non-integrating reprogramming approaches can be attributed to an insufficient transgene expression with respect to the amount, stoichiometric balance and continuity (Yamanaka, 2009b). With regards to episomal reprogramming, these aspects are most likely not fulfilled but the use of improved vectors (Chou et al., 2011) and the additional support of small molecules to enhance the conversion process (Yu et al., 2011) should be explored. For mRNA-mediated reprogramming prolonged transgene expression is inhibited by a severe induction of an innate immune response (Angel and Yanik, 2010; Drews et al., 2012), which requires adequate suppression. Concerning miRNA-mediated reprogramming the most effective conditions and benchmark data are yet to be determined. The general difficulty of generating human iPSCs without genetic modification is also resembled in the lack reproducing reports following the initial publications (Warren et al., 2010; Anokye-Danso et al., 2011; Miyoshi et al., 2011; Yu et al., 2011). Hence, the outcome of this project corresponds to the current status of the field: Further optimization of non-integrative reprogramming methods remains to be done and will be inevitable to move towards the establishment of clinical grade human iPSCs (Drews et al., 2012).

Based on the observations presented here and elsewhere (Li et al., 2009a; Ye et al., 2009; Galende et al., 2010; Zhu et al., 2010; Anchan et al., 2011; Liu et al., 2012), human AFCs still appear to be a suitable source of cells for the realization of non-viral reprogramming techniques as the fast emergence of ESC-like colonies during reprogramming suggests that AFCs require shorter periods of stoichiometricly balanced transgene expression at sufficient levels. This notion is further supported by the observation that first trimester AFCs, i.e. AFCs obtained during earlier stages of gestation, express human ESCs markers and enable the induction of pluripotency without the use of genetic material (Moschidou et al.) In view of this, the realization of the longed for derivation of iPSCs solely by small molecules (Yamanaka, 2009a; Solanki and Lee, 2010) appears to be feasible even if the more routinely available second trimester AFCs may not exhibit the same human ESC characteristics as their first trimester counterparts.

Alongside with the development of advanced reprogramming approaches, effective screening techniques should be established to verify that despite the use of non-integrating genetic material, indeed, no genetic modifications are induced in the course of the reprogramming process as even small molecule enhancers of the de-differentiation process may be mutagenic

or provoke undefined side-effects (Yamanaka, 2009a). Furthermore, basic guidelines and definitions associated with the generation of clinical grade human iPSCs should be agreed upon (Maherali and Hochedlinger, 2008). This, however, requires sufficient understanding of the molecular biological events underlying cellular reprogramming. Employing human ESCs as the reference for human PSCs will continue to be essential to decipher the molecular differences between human ESCs and iPSCs, an important prerequisite to better understand distinctions between human iPSCs derived from different individuals or different tissues of origin. Such differences, which indicate the existence of an epigenetic memory, have been observed in this and several other studies that have been reviewed and discussed in detail elsewhere (Drews et al., b,a). The functional relevance of such distinct expression patterns, described with the LARGE Principle of Reprogramming, especially in case of AFCs, AFiPSCs and ESCs, will have to be investigated profoundly in order to estimate limitations and to exploit the full potential associated with putative future utilization of amniotic fluid-derived cells. Moreover, this kind of comparative transcriptome analysis should also be extended to include iPSC lines derived by various reprogramming protocols. With respect to the development of 'advanced' regenerative therapies in the context of genetically inherited human disease, e.g. cellular therapeutics generated from genetically corrected patient iPSCs (Raya et al., 2009; Zou et al., 2009; Kazuki et al., 2010; Howden et al., 2011; Sebastiano et al., 2011; Yusa et al., 2011; Wang et al., 2012a), this project highlighted difficulties associated with the genetic manipulation of human PSCs. This is in line with others (Zwaka and Thomson, 2003; Xia et al., 2007; Braam et al., 2008; Giudice and Trounson, 2008; Zafarana et al., 2009; Ma et al., 2010; Maury et al., 2011) and suggests that genetic manipulations should be done in the parental cells prior to reprogramming. This finding further underlines that the excision of transgene sequences upon the acquisition of pluripotency in somatic cells (Kaji et al., 2009; Woltjen et al., 2009) is not the method of choice among the reprogramming approaches proposed to produce footprint-free human iPSCs.

Taken together, amniotic fluid-derived human iPSCs have the potential to be clinically relevant. Their implementation in regenerative medicine in the future, however, warrants further detailed investigation.

6

Conclusion

The high efficiency observed for retrovirus-mediated reprogramming of human AFCs suggests amniotic fluid to be a very suitable source of cells for the realization of less-effective non-integrating reprogramming strategies. The identification of gene expression signatures indicative of an epigenetic memory in these AFiPSCs, however, highlighted the necessity for further functional investigations which should be extended to include AFiPSCs generated by alternative reprogramming protocols in order to estimate limitations and to exploit the full potential of AFiPSCs for future applications in basic and applied research. A need for extensive optimization was further demonstrated by the incapability of genetically modifying AFiPSCs, a prerequisite for potential gene therapy approaches. Concerning attempts to realize non-viral, non-integrating reprogramming protocols with human AFCs, nucleofection of episomal plasmids induced morphological changes but did not facilitate the establishment of fully reprogrammed iPSC lines. This approach is still promising as an improved version of the protocol has very recently enabled the derivation of iPSCs from other somatic cells in our laboratory. In the context of mRNA-mediated reprogramming, the functionality of the mRNA transfection protocol was demonstrated. The acquisition of a pluripotent state in AFCs and human neonatal fibroblasts through mRNAs encoding the reprogramming factors was impeded, however, by activation of an interferon-regulated innate immune response. Subsequently, several anti-inflammatory compounds, namely B18R, chloroquine, TSA, pepinh-TRIF, pepinh-MYD, were analysed for their capability of suppres-sing this immune response but without a positive effect. Hence, although not yet successful, the profound analysis of the innate interferon response associated with the transfection of mRNAs should provide a basis for the development of new strategies to suppress this immune reaction in order to facilitate efficient mRNA-mediated reprogramming in the future. The comparison of different delivery methods with respect to the magnitude of the induced immune response revealed miRNAs to be non-immunogenic, highlighting transfection of miRNAs as an especially promising tool to realize non-integrative induction of pluripotency in human somatic cells despite the failure of pilot experiments in AFCs. In conclusion, this work has emphasized the significance of human AFCs as a starting cell source for direct reprogramming. Yet, concomitantly, obstacles such as the technical difficulties associated with episomal plasmid-mediated reprogramming and the immune response triggered by transfections of mRNAs were revealed. These aspects need to be addressed in order to enable reliable induction of pluripotency in human AFCs with putative relevance for regenerative medicine.

Bibliography

T. Aasen, A. Raya, M. J. Barrero, E. Garreta, A. Consiglio, F. Gonzalez, R. Vassena, J. Bilic, V. Pekarik, G. Tiscornia, M. Edel, S. Boue, and J. C. Izpisua Belmonte. Efficient and rapid generation of induced pluripotent stem cells from human keratinocytes. *Nat Biotechnol*, 26 (11):1276–84, 2008.

K. Adachi, H. Suemori, S. Y. Yasuda, N. Nakatsuji, and E. Kawase. Role of sox2 in maintaining pluripotency of human embryonic stem cells. *Genes Cells*, 15(5):455–70, 2010.

O. Adewumi, B. Aflatoonian, L. Ahrlund-Richter, M. Amit, P. W. Andrews, G. Beighton, P. A. Bello, N. Benvenisty, L. S. Berry, S. Bevan, B. Blum, J. Brooking, K. G. Chen, A. B. Choo, G. A. Churchill, M. Corbel, I. Damjanov, J. S. Draper, P. Dvorak, K. Emanuelsson, R. A. Fleck, A. Ford, K. Gertow, M. Gertsenstein, P. J. Gokhale, R. S. Hamilton, A. Hampl, L. E. Healy, O. Hovatta, J. Hyllner, M. P. Imreh, J. Itskovitz-Eldor, J. Jackson, J. L. Johnson, M. Jones, K. Kee, B. L. King, B. B. Knowles, M. Lako, F. Lebrin, B. S. Mallon, D. Manning, Y. Mayshar, R. D. McKay, A. E. Michalska, M. Mikkola, M. Mileikovsky, S. L. Minger, H. D. Moore, C. L. Mummery, A. Nagy, N. Nakatsuji, C. M. O'Brien, S. K. Oh, C. Olsson, T. Otonkoski, K. Y. Park, R. Passier, H. Patel, M. Patel, R. Pedersen, M. F. Pera, M. S. Piekarczyk, R. A. Pera, B. E. Reubinoff, A. J. Robins, J. Rossant, P. Rugg-Gunn, T. C. Schulz, H. Semb, E. S. Sherrer, H. Siemen, G. N. Stacey, M. Stojkovic, H. Suemori, J. Szatkiewicz, T. Turetsky, T. Tuuri, S. van den Brink, K. Vintersten, S. Vuoristo, D. Ward, T. A. Weaver, L. A. Young, and W. Zhang. Characterization of human embryonic stem cell lines by the international stem cell initiative. *Nat Biotechnol*, 25(7):803–16, 2007.

J. Adjaye, J. Huntriss, R. Herwig, A. BenKahla, T. C. Brink, C. Wierling, C. Hultschig, D. Groth, M. L. Yaspo, H. M. Picton, R. G. Gosden, and H. Lehrach. Primary differentiation in the human blastocyst: comparative molecular portraits of inner cell mass and trophectoderm cells. *Stem Cells*, 23(10):1514–25, 2005.

S. Agarwal, Y. H. Loh, E. M. McLoughlin, J. Huang, I. H. Park, J. D. Miller, H. Huo, M. Okuka, R. M. Dos Reis, S. Loewer, H. H. Ng, D. L. Keefe, F. D. Goldman, A. J. Klingelhutz, L. Liu, and G. Q. Daley. Telomere elongation in induced pluripotent stem cells from dyskeratosis congenita patients. *Nature*, 464(7286):292–6, 2010.

D. Ahuja, M. T. Saenz-Robles, and J. M. Pipas. Sv40 large t antigen targets multiple cellular pathways to elicit cellular transformation. *Oncogene*, 24(52):7729–45, 2005.

R. C. Allsopp, H. Vaziri, C. Patterson, S. Goldstein, E. V. Younglai, A. B. Futcher, C. W. Greider, and C. B. Harley. Telomere length predicts replicative capacity of human fibroblasts. *Proc Natl Acad Sci U S A*, 89(21):10114–8, 1992.

J. Alper. Geron gets green light for human trial of es cell-derived product. *Nat Biotechnol*, 27 (3):213–4, 2009.

M. Amit, M. K. Carpenter, M. S. Inokuma, C. P. Chiu, C. P. Harris, M. A. Waknitz, J. Itskovitz-Eldor, and J. A. Thomson. Clonally derived human embryonic stem cell lines maintain pluripotency and proliferative potential for prolonged periods of culture. *Dev Biol*, 227(2):271–8, 2000.

F. Anokye-Danso, C. M. Trivedi, D. Juhr, M. Gupta, Z. Cui, Y. Tian, Y. Zhang, W. Yang, P. J. Gruber, J. A. Epstein, and E. E. Morrisey. Highly efficient mirna-mediated reprogramming of mouse and human somatic cells to pluripotency. *Cell Stem Cell*, 8(4):376–88, 2011.

R. M. Anchan, P. Quaas, B. Gerami-Naini, H. Bartake, A. Griffin, Y. Zhou, D. Day, J. L. Eaton, L. L. George, C. Naber, A. Turbe-Doan, P. J. Park, M. D. Hornstein, and R. L. Maas. Amniocytes can serve a dual function as a source of ips cells and feeder layers. *Hum Mol Genet*, 20(5):962–74, 2011.

M. Angel and M. F. Yanik. Innate immune suppression enables frequent transfection with rna encoding reprogramming proteins. *PLoS ONE*, 5(7):e11756, 2010.

L. Armstrong, O. Hughes, S. Yung, L. Hyslop, R. Stewart, I. Wappler, H. Peters, T. Walter, P. Stojkovic, J. Evans, M. Stojkovic, and M. Lako. The role of pi3k/akt, mapk/erk and nfkappabeta signalling in the maintenance of human embryonic stem cell pluripotency and viability highlighted by transcriptional profiling and functional analysis. *Hum Mol Genet*, 15(11):1894–913, 2006.

L. Armstrong, K. Tilgner, G. Saretzki, S. P. Atkinson, M. Stojkovic, R. Moreno, S. Przyborski, and M. Lako. Human induced pluripotent stem cell lines show stress defense mechanisms and mitochondrial regulation similar to those of human embryonic stem cells. *Stem Cells*, 28(4):661–73, 2010.

M. Ashburner, C. A. Ball, J. A. Blake, D. Botstein, H. Butler, J. M. Cherry, A. P. Davis, K. Dolinski, S. S. Dwight, J. T. Eppig, M. A. Harris, D. P. Hill, L. Issel-Tarver, A. Kasarskis, S. Lewis, J. C. Matese, J. E. Richardson, M. Ringwald, G. M. Rubin, and G. Sherlock. Gene ontology: tool for the unification of biology. the gene ontology consortium. *Nat Genet*, 25 (1):25–9, 2000.

A. Atala, S. B. Bauer, S. Soker, J. J. Yoo, and A. B. Retik. Tissue-engineered autologous bladders for patients needing cystoplasty. *Lancet*, 367(9518):1241–6, 2006.

A. A. Avilion, S. K. Nicolis, L. H. Pevny, L. Perez, N. Vivian, and R. Lovell-Badge. Multipotent cell lineages in early mouse development depend on sox2 function. *Genes Dev*, 17(1):126–40, 2003.

Y. Babaie, R. Herwig, B. Greber, T. C. Brink, W. Wruck, D. Groth, H. Lehrach, T. Burdon, and J. Adjaye. Analysis of oct4-dependent transcriptional networks regulating self-renewal and pluripotency in human embryonic stem cells. *Stem Cells*, 25(2):500–10, 2007.

C. Baglioni, M. A. Minks, and E. De Clercq. Structural requirements of polynucleotides for the activation of (2' - 5')an polymerase and protein kinase. *Nucleic Acids Res*, 9(19):4939–50, 1981.

R. Bajpai, J. Lesperance, M. Kim, and A. V. Terskikh. Efficient propagation of single cells accutase-dissociated human embryonic stem cells. *Mol Reprod Dev*, 75(5):818–27, 2008.

E. Balzer and E. G. Moss. Localization of the developmental timing regulator lin28 to mrnp complexes, p-bodies and stress granules. *RNA Biol*, 4(1):16–25, 2007.

A. Banfi, A. Muraglia, B. Dozin, M. Mastrogiacomo, R. Cancedda, and R. Quarto. Proliferation kinetics and differentiation potential of ex vivo expanded human bone marrow stromal cells: Implications for their use in cell therapy. *Exp Hematol*, 28(6):707–15, 2000.

O. Bar-Nur, H. A. Russ, S. Efrat, and N. Benvenisty. Epigenetic memory and preferential lineage-specific differentiation in induced pluripotent stem cells derived from human pancreatic islet beta cells. *Cell Stem Cell*, 9(1):17–23, 2011.

B. Barrilleaux and P. S. Knoepfler. Inducing ipscs to escape the dish. *Cell Stem Cell*, 9(2): 103–11, 2011.

A. Barroso-del Jesus, G. Lucena-Aguilar, and P. Menendez. The mir-302-367 cluster as a potential stemness regulator in escs. *Cell Cycle*, 8(3):394–8, 2009.

A. Barroso-delJesus, C. Romero-Lopez, G. Lucena-Aguilar, G. J. Melen, L. Sanchez, G. Ligero, A. Berzal-Herranz, and P. Menendez. Embryonic stem cell-specific mir302-367 cluster: human gene structure and functional characterization of its core promoter. *Mol Cell Biol*, 28(21):6609–19, 2008.

M. A. Baxter, R. F. Wynn, S. N. Jowitt, J. E. Wraith, L. J. Fairbairn, and I. Bellantuono. Study of telomere length reveals rapid aging of human marrow stromal cells following in vitro expansion. *Stem Cells*, 22(5):675–82, 2004.

Y. Benjamini and Y. Hochberg. Controlling the false discovery rate: a practical and powerful approach to multiple testing. *J ROY STAT SOC B*, 57(1):289–300, 1995.

B. E. Bernstein, T. S. Mikkelsen, X. Xie, M. Kamal, D. J. Huebert, J. Cuff, B. Fry, A. Meissner, M. Wernig, K. Plath, R. Jaenisch, A. Wagschal, R. Feil, S. L. Schreiber, and E. S. Lander. A

bivalent chromatin structure marks key developmental genes in embryonic stem cells. *Cell*, 125(2):315–26, 2006.

M. Binder, F. Eberle, S. Seitz, N. Mucke, C. M. Huber, N. Kiani, L. Kaderali, V. Lohmann, A. Dalpke, and R. Bartenschlager. Molecular mechanism of signal perception and integration by the innate immune sensor retinoic acid-inducible gene-i (rig-i). *J Biol Chem*, 286(31):27278–87, 2011.

M. M. Bonab, K. Alimoghaddam, F. Talebian, S. H. Ghaffari, A. Ghavamzadeh, and B. Nikbin. Aging of mesenchymal stem cell in vitro. *BMC Cell Biol*, 7:14, 2006.

P. Bossolasco, T. Montemurro, L. Cova, S. Zangrossi, C. Calzarossa, S. Buiatiotis, D. Soligo, S. Bosari, V. Silani, G. L. Deliliers, P. Rebulla, and L. Lazzari. Molecular and phenotypic characterization of human amniotic fluid cells and their differentiation potential. *Cell Res*, 16(4):329–36, 2006.

L. A. Boyer, T. I. Lee, M. F. Cole, S. E. Johnstone, S. S. Levine, J. P. Zucker, M. G. Guenther, R. M. Kumar, H. L. Murray, R. G. Jenner, D. K. Gifford, D. A. Melton, R. Jaenisch, and R. A. Young. Core transcriptional regulatory circuitry in human embryonic stem cells. *Cell*, 122(6):947–56, 2005.

S. R. Braam, C. Denning, S. van den Brink, P. Kats, R. Hochstenbach, R. Passier, and C. L. Mummery. Improved genetic manipulation of human embryonic stem cells. *Nat Methods*, 5(5):389–92, 2008.

K. J. Brennand, A. Simone, J. Jou, C. Gelboin-Burkhart, N. Tran, S. Sangar, Y. Li, Y. Mu, G. Chen, D. Yu, S. McCarthy, J. Sebat, and F. H. Gage. Modelling schizophrenia using human induced pluripotent stem cells. *Nature*, 473(7346):221–5, 2011.

G. E. Brown, B. Lebleu, M. Kawakita, S. Shaila, G. C. Sen, and P. Lengyel. Increased endonuclease activity in an extract from mouse ehrlich ascites tumor cells which had been treated with a partially purified interferon preparation: dependence of double-stranded rna. *Biochem Biophys Res Commun*, 69(1):114–22, 1976.

J. P. Brown, W. Wei, and J. M. Sedivy. Bypass of senescence after disruption of p21cip1/waf1 gene in normal diploid human fibroblasts. *Science (80-)*, 277(5327):831–4, 1997.

S. Camnasio, A. D. Carri, A. Lombardo, I. Grad, C. Mariotti, A. Castucci, B. Rozell, P. L. Riso, V. Castiglioni, C. Zuccato, C. Rochon, Y. Takashima, G. Diaferia, I. Biunno, C. Gellera, M. Jaconi, A. Smith, O. Hovatta, L. Naldini, S. Di Donato, A. Feki, and E. Cattaneo. The first reported generation of several induced pluripotent stem cell lines from homozygous and heterozygous huntington's disease patients demonstrates mutation related enhanced lysosomal activity. *Neurobiol Dis*, 46(1):41–51, 2012.

F. Cao, X. Xie, T. Gollan, L. Zhao, K. Narsinh, R. J. Lee, and J. C. Wu. Comparison of gene-transfer efficiency in human embryonic stem cells. *Mol Imaging Biol*, 12(1):15–24, 2010.

D. A. Card, P. B. Hebbar, L. Li, K. W. Trotter, Y. Komatsu, Y. Mishina, and T. K. Archer. Oct4/sox2-regulated mir-302 targets cyclin d1 in human embryonic stem cells. *Mol Cell Biol*, 28(20):6426–38, 2008.

B. W. Carey, S. Markoulaki, J. Hanna, K. Saha, Q. Gao, M. Mitalipova, and R. Jaenisch. Reprogramming of murine and human somatic cells using a single polycistronic vector. *Proc Natl Acad Sci U S A*, 106(1):157–62, 2009.

G. Carraro, L. Perin, S. Sedrakyan, S. Giuliani, C. Tiozzo, J. Lee, G. Turcatel, S. P. De Langhe, B. Driscoll, S. Bellusci, P. Minoo, A. Atala, R. E. De Filippo, and D. Warburton. Human amniotic fluid stem cells can integrate and differentiate into epithelial lung lineages. *Stem Cells*, 26(11):2902–11, 2008.

X. Carvajal-Vergara, A. Sevilla, S. L. D'Souza, Y. S. Ang, C. Schaniel, D. F. Lee, L. Yang, A. D. Kaplan, E. D. Adler, R. Rozov, Y. Ge, N. Cohen, L. J. Edelmann, B. Chang, A. Waghray, J. Su, S. Pardo, K. D. Lichtenbelt, M. Tartaglia, B. D. Gelb, and I. R. Lemischka. Patient-specific induced pluripotent stem-cell-derived models of leopard syndrome. *Nature*, 465 (7299):808–12, 2010.

C. Cerdan, S. H. Hong, and M. Bhatia. Formation and hematopoietic differentiation of human embryoid bodies by suspension and hanging drop cultures. *Curr Protoc Stem Cell Biol*, Chapter 1:Unit 1D 2, 2007.

I. Chambers, D. Colby, M. Robertson, J. Nichols, S. Lee, S. Tweedie, and A. Smith. Functional expression cloning of nanog, a pluripotency sustaining factor in embryonic stem cells. *Cell*, 113(5):643–55, 2003.

K. K. Chan, S. M. Wu, P. M. Nissom, S. K. Oh, and A. B. Choo. Generation of high-level stable transgene expressing human embryonic stem cell lines using chinese hamster elongation factor-1 alpha promoter system. *Stem Cells Dev*, 17(4):825–36, 2008.

B. D. Chang, K. Watanabe, E. V. Broude, J. Fang, J. C. Poole, T. V. Kalinichenko, and I. B. Roninson. Effects of p21waf1/cip1/sdi1 on cellular gene expression: implications for carcinogenesis, senescence, and age-related diseases. *Proc Natl Acad Sci U S A*, 97(8):4291–6, 2000.

L. Chavez, A. S. Bais, M. Vingron, H. Lehrach, J. Adjaye, and R. Herwig. In silico identification of a core regulatory network of oct4 in human embryonic stem cells using an integrated approach. *BMC Genomics*, 10:314, 2009.

L. Cheng, N. F. Hansen, L. Zhao, Y. Du, C. Zou, F. X. Donovan, B. K. Chou, G. Zhou, S. Li, S. N. Dowey, Z. Ye, S. C. Chandrasekharappa, H. Yang, J. C. Mullikin, and P. P. Liu. Low incidence of dna sequence variation in human induced pluripotent stem cells generated by nonintegrating plasmid expression. *Cell Stem Cell*, 10(3):337–44, 2012.

A. Chiavegato, S. Bollini, M. Pozzobon, A. Callegari, L. Gasparotto, J. Taiani, M. Piccoli, E. Lenzini, G. Gerosa, I. Vendramin, E. Cozzi, A. Angelini, L. Iop, G. F. Zanon, A. Atala, P. De Coppi, and S. Sartore. Human amniotic fluid-derived stem cells are rejected after transplantation in the myocardium of normal, ischemic, immuno-suppressed or immuno-deficient rat. *J Mol Cell Cardiol*, 42(4):746–59, 2007.

B. K. Chou, P. Mali, X. Huang, Z. Ye, S. N. Dowey, L. M. Resar, C. Zou, Y. A. Zhang, J. Tong, and L. Cheng. Efficient human ips cell derivation by a non-integrating plasmid from blood cells with unique epigenetic and gene expression signatures. *Cell Res*, 21(3):518–29, 2011.

S. Cipriani, D. Bonini, E. Marchina, I. Balgkouranidou, L. Caimi, G. Grassi Zucconi, and S. Barlati. Mesenchymal cells from human amniotic fluid survive and migrate after transplantation into adult rat brain. *Cell Biol Int*, 31(8):845–50, 2007.

M. J. Clemens and B. R. Williams. Inhibition of cell-free protein synthesis by pppa2'p5'a2'p5'a: a novel oligonucleotide synthesized by interferon-treated l cell extracts. *Cell*, 13(3):565–72, 1978.

O. R. Colamonici, P. Domanski, S. M. Sweitzer, A. Larner, and R. M. Buller. Vaccinia virus b18r gene encodes a type i interferon-binding protein that blocks interferon alpha transmembrane signaling. *J Biol Chem*, 270(27):15974–8, 1995.

R. G. Cooper and T. Magwere. Chloroquine: novel uses & manifestations. *Indian J Med Res*, 127(4):305–16, 2008.

C. M. Counter, F. M. Botelho, P. Wang, C. B. Harley, and S. Bacchetti. Stabilization of short telomeres and telomerase activity accompany immortalization of epstein-barr virus-transformed human b lymphocytes. *J Virol*, 68(5):3410–14, 1994.

C. A. Cowan, J. Atienza, D. A. Melton, and K. Eggan. Nuclear reprogramming of somatic cells after fusion with human embryonic stem cells. *Science (80-)*, 309(5739):1369–73, 2005.

K. C. Davidson, A. M. Adams, J. M. Goodson, C. E. McDonald, J. C. Potter, J. D. Berndt, T. L. Biechele, R. J. Taylor, and R. T. Moon. Wnt/beta-catenin signaling promotes differentiation, not self-renewal, of human embryonic stem cells and is repressed by oct4. *Proc Natl Acad Sci U S A*, 2012.

J. C. Davila, G. G. Cezar, M. Thiede, S. Strom, T. Miki, and J. Trosko. Use and application of stem cells in toxicology. *Toxicol Sci*, 79(2):214–23, 2004.

P. De Coppi, J. Bartsch, G., M. M. Siddiqui, T. Xu, C. C. Santos, L. Perin, G. Mostoslavsky, A. C. Serre, E. Y. Snyder, J. J. Yoo, M. E. Furth, S. Soker, and A. Atala. Isolation of amniotic stem cell lines with potential for therapy. *Nat Biotechnol*, 25(1):100–6, 2007.

J. Dennis, G., B. T. Sherman, D. A. Hosack, J. Yang, W. Gao, H. C. Lane, and R. A. Lempicki. David: Database for annotation, visualization, and integrated discovery. *Genome Biol*, 4(5): P3, 2003.

S. S. Diebold, T. Kaisho, H. Hemmi, S. Akira, and C. Reis e Sousa. Innate antiviral responses by means of tlr7-mediated recognition of single-stranded rna. *Science (80-)*, 303(5663):1529–31, 2004.

C. M. Digirolamo, D. Stokes, D. Colter, D. G. Phinney, R. Class, and D. J. Prockop. Propagation and senescence of human marrow stromal cells in culture: a simple colony-forming assay identifies samples with the greatest potential to propagate and differentiate. *Br J Haematol*, 107(2):275–81, 1999.

A. Ditadi, P. de Coppi, O. Picone, L. Gautreau, R. Smati, E. Six, D. Bonhomme, S. Ezine, R. Frydman, M. Cavazzana-Calvo, and I. Andre-Schmutz. Human and murine amniotic fluid c-kit+lin- cells display hematopoietic activity. *Blood*, 113(17):3953–60, 2009.

K. Drews, A. Aldahmash, and J. Adjaye. *Functional genomics of induced pluripotent stem cells.* King Saud University, a. In press.

K. Drews, J. Jozefczuk, A. Prigione, and J. Adjaye. Human induced pluipotent stem cells - from mechanisms to clinical applications. *J Mol Med*, b. In press.

K. Drews, G. Tavernier, J. Demeester, H. Lehrach, S. C. De Smedt, J. Rejman, and J. Adjaye. The cytotoxic and immunogenic hurdles associated with non-viral mrna-mediated reprogramming of human fibroblasts. *Biomaterials*, 33(16):4059–68, 2012.

Z.-W. Du and S.-C. Zhang. Lentiviral vector-mediated transgenesis in human embryonic stem cells. *Methods Mol Biol*, 614:127–134, 2010.

A. M. Eastham, H. Spencer, F. Soncin, S. Ritson, C. L. Merry, P. L. Stern, and C. M. Ward. Epithelial-mesenchymal transition events during human embryonic stem cell differentiation. *Cancer Res*, 67(23):11254–62, 2007.

A. D. Ebert, J. Yu, J. Rose, F. F., V. B. Mattis, C. L. Lorson, J. A. Thomson, and C. N. Svendsen. Induced pluripotent stem cells from a spinal muscular atrophy patient. *Nature*, 457(7227):277–80, 2009.

M. S. Ebert, J. R. Neilson, and P. A. Sharp. Microrna sponges: competitive inhibitors of small rnas in mammalian cells. *Nat Methods*, 4(9):721–6, 2007.

R. Eiges, A. Urbach, M. Malcov, T. Frumkin, T. Schwartz, A. Amit, Y. Yaron, A. Eden, O. Yanuka, N. Benvenisty, and D. Ben-Yosef. Developmental study of fragile x syndrome using human embryonic stem cells derived from preimplantation genetically diagnosed embryos. *Cell Stem Cell*, 1(5):568–77, 2007.

L. Espert, G. Degols, C. Gongora, D. Blondel, B. R. Williams, R. H. Silverman, and N. Mechti. Isg20, a new interferon-induced rnase specific for single-stranded rna, defines an alternative antiviral pathway against rna genomic viruses. *J Biol Chem*, 278(18):16151–8, 2003.

M. A. Esteban, T. Wang, B. Qin, J. Yang, D. Qin, J. Cai, W. Li, Z. Weng, J. Chen, S. Ni, K. Chen, Y. Li, X. Liu, J. Xu, S. Zhang, F. Li, W. He, K. Labuda, Y. Song, A. Peterbauer, S. Wolbank, H. Redl, M. Zhong, D. Cai, L. Zeng, and D. Pei. Vitamin c enhances the generation of mouse and human induced pluripotent stem cells. *Cell Stem Cell*, 6(1):71–9, 2010.

M. Evans. Discovering pluripotency: 30 years of mouse embryonic stem cells. *Nat Rev Mol Cell Biol*, 12(10):680–686, 2011.

P. M. Evans and C. Liu. Roles of krupel-like factor 4 in normal homeostasis, cancer and stem cells. *Acta Biochim Biophys Sin (Shanghai)*, 40(7):554–64, 2008.

C. Falschlehner, U. Schaefer, and H. Walczak. Following trail's path in the immune system. *Immunology*, 127(2):145–54, 2009.

D. Fauza. Amniotic fluid and placental stem cells. *Best Pract Res Clin Obstet Gynaecol*, 18(6): 877–91, 2004.

C. D. Folmes, T. J. Nelson, A. Martinez-Fernandez, D. K. Arrell, J. Z. Lindor, P. P. Dzeja, Y. Ikeda, C. Perez-Terzic, and A. Terzic. Somatic oxidative bioenergetics transitions into pluripotency-dependent glycolysis to facilitate nuclear reprogramming. *Cell Metab*, 14(2): 264–71, 2011.

H. Fong, K. A. Hohenstein, and P. J. Donovan. Regulation of self-renewal and pluripotency by sox2 in human embryonic stem cells. *Stem Cells*, 26(8):1931–8, 2008.

J. L. Fox. Human ipsc and esc translation potential debated. *Nat Biotechnol*, 29(5):375–6, 2011.

S. Frantz. Embryonic stem cell pioneer geron exits field, cuts losses. *Nat Biotechnol*, 30(1): 12–3, 2012.

N. Fusaki, H. Ban, A. Nishiyama, K. Saeki, and M. Hasegawa. Efficient induction of transgene-free human pluripotent stem cells using a vector based on sendai virus, an rna virus that does not integrate into the host genome. *Proc Jpn Acad Ser B Phys Biol Sci*, 85(8):348–62, 2009.

E. Galende, I. Karakikes, L. Edelmann, R. J. Desnick, T. Kerenyi, G. Khoueiry, J. Lafferty, J. T. McGinn, M. Brodman, V. Fuster, R. J. Hajjar, and K. Polgar. Amniotic fluid cells are more efficiently reprogrammed to pluripotency than adult cells. *Cell Reprogram*, 12(2):117–25, 2010.

C. L. Galligan, T. T. Murooka, R. Rahbar, E. Baig, B. Majchrzak-Kita, and E. N. Fish. Interferons and viruses: signaling for supremacy. *Immunol Res*, 35(1-2):27–40, 2006.

J. Gekas, G. Walther, D. Skuk, E. Bujold, I. Harvey, and O. F. Bertrand. In vitro and in vivo study of human amniotic fluid-derived stem cell differentiation into myogenic lineage. *Clin Exp Med*, 10(1):1–6, 2010.

P. Genin, M. Algarte, P. Roof, R. Lin, and J. Hiscott. Regulation of rantes chemokine gene expression requires cooperativity between nf-kappa b and ifn-regulatory factor transcription factors. *J Immunol*, 164(10):5352–61, 2000.

L. Gerrard, D. Zhao, A. J. Clark, and W. Cui. Stably transfected human embryonic stem cell clones express oct4-specific green fluorescent protein and maintain self-renewal and pluripotency. *Stem Cells*, 23(1):124–33, 2005.

A. Ghodsizadeh, A. Taei, M. Totonchi, A. Seifinejad, H. Gourabi, B. Pournasr, N. Aghdami, R. Malekzadeh, N. Almadani, G. H. Salekdeh, and H. Baharvand. Generation of liver disease-specific induced pluripotent stem cells along with efficient differentiation to functional hepatocyte-like cells. *Stem Cell Rev*, 6(4):622–32, 2010.

Z. Ghosh, K. D. Wilson, Y. Wu, S. Hu, T. Quertermous, and J. C. Wu. Persistent donor cell gene expression among human induced pluripotent stem cells contributes to differences with human embryonic stem cells. *PLoS ONE*, 5(2):e8975, 2010.

A. Giudice and A. Trounson. Genetic modification of human embryonic stem cells for derivation of target cells. *Cell Stem Cell*, 2(5):422–33, 2008.

H. Glimm, I. H. Oh, and C. J. Eaves. Human hematopoietic stem cells stimulated to proliferate in vitro lose engraftment potential during their s/g(2)/m transit and do not reenter g(0). *Blood*, 96(13):4185–93, 2000.

A. Gore, Z. Li, H. L. Fung, J. E. Young, S. Agarwal, J. Antosiewicz-Bourget, I. Canto, A. Giorgetti, M. A. Israel, E. Kiskinis, J. H. Lee, Y. H. Loh, P. D. Manos, N. Montserrat, A. D. Panopoulos, S. Ruiz, M. L. Wilbert, J. Yu, E. F. Kirkness, J. C. Izpisua Belmonte, D. J. Rossi, J. A. Thomson, K. Eggan, G. Q. Daley, L. S. Goldstein, and K. Zhang. Somatic coding mutations in human induced pluripotent stem cells. *Nature*, 471(7336):63–7, 2011.

C. M. Gosden. Amniotic fluid cell types and culture. *Br Med Bull*, 39(4):348–54, 1983.

B. Greber, H. Lehrach, and J. Adjaye. Fibroblast growth factor 2 modulates transforming growth factor beta signaling in mouse embryonic fibroblasts and human escs (hescs) to support hesc self-renewal. *Stem Cells*, 25(2):455–64, 2007a.

B. Greber, H. Lehrach, and J. Adjaye. Silencing of core transcription factors in human ec cells highlights the importance of autocrine fgf signaling for self-renewal. *BMC Dev Biol*, 7:46, 2007b.

B. Greber, H. Lehrach, and J. Adjaye. Control of early fate decisions in human es cells by distinct states of tgfbeta pathway activity. *Stem Cells Dev*, 17(6):1065–77, 2008.

M. Gropp and B. Reubinoff. Lentiviral vector-mediated gene delivery into human embryonic stem cells. *Methods Enzymol*, 420:64–81, 2006.

M. Gropp, P. Itsykson, O. Singer, T. Ben-Hur, E. Reinhartz, E. Galun, and B. E. Reubinoff. Stable genetic modification of human embryonic stem cells by lentiviral vectors. *Mol Ther*, 7(2):281–7, 2003.

A. R. Gruber, R. Lorenz, S. H. Bernhart, R. Neubock, and I. L. Hofacker. The vienna rna websuite. *Nucleic Acids Res*, 36(Web Server issue):W70–4, 2008.

A. Haase, R. Olmer, K. Schwanke, S. Wunderlich, S. Merkert, C. Hess, R. Zweigerdt, I. Gruh, J. Meyer, S. Wagner, L. S. Maier, D. W. Han, S. Glage, K. Miller, P. Fischer, H. R. Scholer, and U. Martin. Generation of induced pluripotent stem cells from human cord blood. *Cell Stem Cell*, 5(4):434–41, 2009.

J. Hanna, M. Wernig, S. Markoulaki, C. W. Sun, A. Meissner, J. P. Cassady, C. Beard, T. Brambrink, L. C. Wu, T. M. Townes, and R. Jaenisch. Treatment of sickle cell anemia mouse model with ips cells generated from autologous skin. *Science (80-)*, 318(5858):1920–3, 2007.

G. Hargus, O. Cooper, M. Deleidi, A. Levy, K. Lee, E. Marlow, A. Yow, F. Soldner, D. Hockemeyer, P. J. Hallett, T. Osborn, R. Jaenisch, and O. Isacson. Differentiated parkinson patient-derived induced pluripotent stem cells grow in the adult rodent brain and reduce motor asymmetry in parkinsonian rats. *Proc Natl Acad Sci U S A*, 107(36): 15921–6, 2010.

A. H. Hart, L. Hartley, M. Ibrahim, and L. Robb. Identification, cloning and expression analysis of the pluripotency promoting nanog genes in mouse and human. *Dev Dyn*, 230 (1):187–98, 2004.

T. Hasegawa, D. Bouis, H. Liao, S. H. Visovatti, and D. J. Pinsky. Ecto-5' nucleotidase (cd73)-mediated adenosine generation and signaling in murine cardiac allograft vasculopathy. *Circ Res*, 103(12):1410–21, 2008.

D. C. Hay, L. Sutherland, J. Clark, and T. Burdon. Oct-4 knockdown induces similar patterns of endoderm and trophoblast differentiation markers in human and mouse embryonic stem cells. *Stem Cells*, 22(2):225–35, 2004.

L. Hayflick. The limited in vitro lifetime of human diploid cell strains. *Exp Cell Res*, 37: 614–36, 1965.

L. Hayflick and P. S. Moorhead. The serial cultivation of human diploid cell strains. *Exp Cell Res*, 25:585–621, 1961.

D. Hockemeyer, F. Soldner, E. G. Cook, Q. Gao, M. Mitalipova, and R. Jaenisch. A drug-inducible system for direct reprogramming of human somatic cells to pluripotency. *Cell Stem Cell*, 3(3):346–53, 2008.

H. Hoehn and D. Salk. Morphological and biochemical heterogeneity of amniotic fluid cells in culture. *Methods Cell Biol*, 26:11–34, 1982.

K. A. Hohenstein, A. D. Pyle, J. Y. Chern, L. F. Lock, and P. J. Donovan. Nucleofection mediates high-efficiency stable gene knockdown and transgene expression in human embryonic stem cells. *Stem Cells*, 26(6):1436–43, 2008.

H. Hong, K. Takahashi, T. Ichisaka, T. Aoi, O. Kanagawa, M. Nakagawa, K. Okita, and S. Yamanaka. Suppression of induced pluripotent stem cell generation by the p53-p21 pathway. *Nature*, 460(7259):1132–5, 2009.

A. Hotta, A. Y. Cheung, N. Farra, K. Vijayaragavan, C. A. Seguin, J. S. Draper, P. Pasceri, I. A. Maksakova, D. L. Mager, J. Rossant, M. Bhatia, and J. Ellis. Isolation of human ips cells using eos lentiviral vectors to select for pluripotency. *Nat Methods*, 6(5):370–6, 2009.

S. E. Howden, A. Gore, Z. Li, H. L. Fung, B. S. Nisler, J. Nie, G. Chen, B. E. McIntosh, D. R. Gulbranson, N. R. Diol, S. M. Taapken, D. T. Vereide, K. D. Montgomery, K. Zhang, D. M. Gamm, and J. A. Thomson. Genetic correction and analysis of induced pluripotent stem cells from a patient with gyrate atrophy. *Proc Natl Acad Sci U S A*, 108(16):6537–42, 2011.

P. P. Hsu and D. M. Sabatini. Cancer cell metabolism: Warburg and beyond. *Cell*, 134(5): 703–7, 2008.

B.-Y. Hu, J. P. Weick, J. Yu, L.-X. Ma, X.-Q. Zhang, J. A. Thomson, and S.-C. Zhang. Neural differentiation of human induced pluripotent stem cells follows developmental principles but with variable potency. *Proc Natl Acad Sci U S A*, 107(9):4335–40, 2010a.

Q. Hu, A. M. Friedrich, L. V. Johnson, and D. O. Clegg. Memory in induced pluripotent stem cells: reprogrammed human retinal-pigmented epithelial cells show tendency for spontaneous redifferentiation. *Stem Cells*, 28(11):1981–91, 2010b.

B. Huang and L. T. Vassilev. Reduced transcriptional activity in the p53 pathway of senescent cells revealed by the mdm2 antagonist nutlin-3. *Aging (Albany NY)*, 1(10):845–54, 2009.

W. Huang da, B. T. Sherman, and R. A. Lempicki. Systematic and integrative analysis of large gene lists using david bioinformatics resources. *Nat Protoc*, 4(1):44–57, 2009.

D. Huangfu, R. Maehr, W. Guo, A. Eijkelenboom, M. Snitow, A. E. Chen, and D. A. Melton. Induction of pluripotent stem cells by defined factors is greatly improved by small-molecule compounds. *Nat Biotechnol*, 26(7):795–7, 2008.

L. Hyslop, M. Stojkovic, L. Armstrong, T. Walter, P. Stojkovic, S. Przyborski, M. Herbert, A. Murdoch, T. Strachan, and M. Lako. Downregulation of nanog induces differentiation of human embryonic stem cells to extraembryonic lineages. *Stem Cells*, 23(8):1035–43, 2005.

L. Iacovitti, A. E. Donaldson, and J. Cai. Human amniotic fluid stem cells do not generate dopamine neurons in vitro or after transplantation in vivo. *Stem Cells Dev*, 2008.

I. Imoto, I. Sonoda, Y. Yuki, and J. Inazawa. Identification and characterization of human pknox2, a novel homeobox-containing gene. *Biochem Biophys Res Commun*, 287(1):270–6, 2001.

P. S. In 't Anker, S. A. Scherjon, C. Kleijburg-van der Keur, W. A. Noort, F. H. Claas, R. Willemze, W. E. Fibbe, and H. H. Kanhai. Amniotic fluid as a novel source of mesenchymal stem cells for therapeutic transplantation. *Blood*, 102(4):1548–9, 2003.

M. A. Israel, S. H. Yuan, C. Bardy, S. M. Reyna, Y. Mu, C. Herrera, M. P. Hefferan, S. Van Gorp, K. L. Nazor, F. S. Boscolo, C. T. Carson, L. C. Laurent, M. Marsala, F. H. Gage, A. M. Remes, E. H. Koo, and L. S. Goldstein. Probing sporadic and familial alzheimer's disease using induced pluripotent stem cells. *Nature*, 482(7384):216–20, 2012.

J. Itskovitz-Eldor, M. Schuldiner, D. Karsenti, A. Eden, O. Yanuka, M. Amit, H. Soreq, and N. Benvenisty. Differentiation of human embryonic stem cells into embryoid bodies compromising the three embryonic germ layers. *Mol Med*, 6(2):88–95, 2000.

I. Itzhaki, L. Maizels, I. Huber, L. Zwi-Dantsis, O. Caspi, A. Winterstern, O. Feldman, A. Gepstein, G. Arbel, H. Hammerman, M. Boulos, and L. Gepstein. Modelling the long qt syndrome with induced pluripotent stem cells. *Nature*, 471(7337):225–9, 2011.

R. Jaenisch and R. Young. Stem cells, the molecular circuitry of pluripotency and nuclear reprogramming. *Cell*, 132(4):567–82, 2008.

D. James, A. J. Levine, D. Besser, and A. Hemmati-Brivanlou. Tgfbeta/activin/nodal signaling is necessary for the maintenance of pluripotency in human embryonic stem cells. *Development*, 132(6):1273–82, 2005.

C. H. Jang, J. H. Choi, M. S. Byun, and D. M. Jue. Chloroquine inhibits production of tnf-alpha, il-1beta and il-6 from lipopolysaccharide-stimulated human monocytes/macrophages by different modes. *Rheumatology (Oxford)*, 45(6):703–10, 2006.

J. Jang, H. C. Kang, H. S. Kim, J. Y. Kim, Y. J. Huh, D. S. Kim, J. E. Yoo, J. A. Lee, B. Lim, J. Lee, T. M. Yoon, I. H. Park, D. Y. Hwang, G. Q. Daley, and D. W. Kim. Induced pluripotent stem cell models from x-linked adrenoleukodystrophy patients. *Ann Neurol*, 70(3):402–9, 2011.

J. Jensen, J. Hyllner, and P. Björquist. Human embryonic stem cell technologies and drug discovery. *J Cell Physiol*, 219(3):513–519, 2009.

F. Jia, K. D. Wilson, N. Sun, D. M. Gupta, M. Huang, Z. Li, N. J. Panetta, Z. Y. Chen, R. C. Robbins, M. A. Kay, M. T. Longaker, and J. C. Wu. A nonviral minicircle vector for deriving human ips cells. *Nat Methods*, 7(3):197–9, 2010.

Z. B. Jin, S. Okamoto, F. Osakada, K. Homma, J. Assawachananont, Y. Hirami, T. Iwata, and M. Takahashi. Modeling retinal degeneration using patient-specific induced pluripotent stem cells. *PLoS ONE*, 6(2):e17084, 2011.

J. B. Johnston, S. H. Nazarian, R. Natale, and G. McFadden. Myxoma virus infection of primary human fibroblasts varies with cellular age and is regulated by host interferon responses. *Virology*, 332(1):235–48, 2005.

J. Jozefczuk, K. Drews, and J. Adjaye. Preparation of mouse embryonic fibroblast cells suitable for culturing human embryonic and induced pluripotent stem cells. *J Vis Exp*. In press.

M. Jung, H. Peterson, L. Chavez, P. Kahlem, H. Lehrach, J. Vilo, and J. Adjaye. A data integration approach to mapping oct4 gene regulatory networks operative in embryonic stem cells and embryonal carcinoma cells. *PLoS ONE*, 5(5):e10709, 2010.

L. R. Kaiser. The future of multihospital systems. *Top Health Care Financ*, 18(4):32–45, 1992.

K. Kaji, K. Norrby, A. Paca, M. Mileikovsky, P. Mohseni, and K. Woltjen. Virus-free induction of pluripotency and subsequent excision of reprogramming factors. *Nature*, 458(7239):771–5, 2009.

M. Kanehisa and S. Goto. Kegg: kyoto encyclopedia of genes and genomes. *Nucleic Acids Res*, 28(1):27–30, 2000.

K. R. Karlmark, A. Freilinger, E. Marton, M. Rosner, G. Lubec, and M. Hengstschlager. Activation of ectopic oct-4 and rex-1 promoters in human amniotic fluid cells. *Int J Mol Med*, 16(6):987–92, 2005.

Y. Katashiba, R. Miyamoto, A. Hyo, K. Shimamoto, N. Murakami, M. Ogata, R. Amakawa, M. Inaba, S. Nomura, S. Fukuhara, and T. Ito. Interferon-alpha and interleukin-12 are induced, respectively, by double-stranded dna and single-stranded rna in human myeloid dendritic cells. *Immunology*, 132(2):165–73, 2011.

H. Kato, S. Sato, M. Yoneyama, M. Yamamoto, S. Uematsu, K. Matsui, T. Tsujimura, K. Takeda, T. Fujita, O. Takeuchi, and S. Akira. Cell type-specific involvement of rig-i in antiviral response. *Immunity*, 23(1):19–28, 2005.

D. S. Kaufman, E. T. Hanson, R. L. Lewis, R. Auerbach, and J. A. Thomson. Hematopoietic colony-forming cells derived from human embryonic stem cells. *Proc Natl Acad Sci U S A*, 98(19):10716–21, 2001.

T. Kawai, S. Sato, K. J. Ishii, C. Coban, H. Hemmi, M. Yamamoto, K. Terai, M. Matsuda, J. Inoue, S. Uematsu, O. Takeuchi, and S. Akira. Interferon-alpha induction through toll-like receptors involves a direct interaction of irf7 with myd88 and traf6. *Nat Immunol*, 5 (10):1061–8, 2004.

T. Kawamura, J. Suzuki, Y. V. Wang, S. Menendez, L. B. Morera, A. Raya, G. M. Wahl, and J. C. Izpisua Belmonte. Linking the p53 tumour suppressor pathway to somatic cell reprogramming. *Nature*, 460(7259):1140–4, 2009.

Y. Kazuki, M. Hiratsuka, M. Takiguchi, M. Osaki, N. Kajitani, H. Hoshiya, K. Hiramatsu, T. Yoshino, K. Kazuki, C. Ishihara, S. Takehara, K. Higaki, M. Nakagawa, K. Takahashi, S. Yamanaka, and M. Oshimura. Complete genetic correction of ips cells from duchenne muscular dystrophy. *Mol Ther*, 18(2):386–93, 2010.

R. D. Kelly, H. Sumer, M. McKenzie, J. Facucho-Oliveira, I. A. Trounce, P. J. Verma, and J. C. St John. The effects of nuclear reprogramming on mitochondrial dna replication. *Stem Cell Rev*, 2011.

I. A. Khalil, K. Kogure, H. Akita, and H. Harashima. Uptake pathways and subsequent intracellular trafficking in nonviral gene delivery. *Pharmacol Rev*, 58(1):32–45, 2006.

D. Kim, C. H. Kim, J. I. Moon, Y. G. Chung, M. Y. Chang, B. S. Han, S. Ko, E. Yang, K. Y. Cha, R. Lanza, and K. S. Kim. Generation of human induced pluripotent stem cells by direct delivery of reprogramming proteins. *Cell Stem Cell*, 4(6):472–6, 2009a.

J. Kim, Y. Lee, H. Kim, K. J. Hwang, H. C. Kwon, S. K. Kim, D. J. Cho, S. G. Kang, and J. You. Human amniotic fluid-derived stem cells have characteristics of multipotent stem cells. *Cell Prolif*, 40(1):75–90, 2007.

J. B. Kim, B. Greber, M. J. Arauzo-Bravo, J. Meyer, K. I. Park, H. Zaehres, and H. R. Scholer. Direct reprogramming of human neural stem cells by oct4. *Nature*, 461(7264):649–3, 2009b.

J. B. Kim, V. Sebastiano, G. Wu, M. J. Araúzo-Bravo, P. Sasse, L. Gentile, K. Ko, D. Ruau, M. Ehrich, D. van den Boom, J. Meyer, K. Hübner, C. Bernemann, C. Ortmeier, M. Zenke, B. K. Fleischmann, H. Zaehres, and H. R. Schöler. Oct4-induced pluripotency in adult neural stem cells. *Cell*, 136(3):411–19, 2009c.

K. Kim, A. Doi, B. Wen, K. Ng, R. Zhao, P. Cahan, J. Kim, M. J. Aryee, H. Ji, L. I. Ehrlich, A. Yabuuchi, A. Takeuchi, K. C. Cunniff, H. Hongguang, S. McKinney-Freeman, O. Naveiras, T. J. Yoon, R. A. Irizarry, N. Jung, J. Seita, J. Hanna, P. Murakami, R. Jaenisch, R. Weissleder, S. H. Orkin, I. L. Weissman, A. P. Feinberg, and G. Q. Daley. Epigenetic memory in induced pluripotent stem cells. *Nature*, 467(7313):285–90, 2010.

K. Kim, R. Zhao, A. Doi, K. Ng, J. Unternaehrer, P. Cahan, H. Huo, Y. H. Loh, M. J. Aryee, M. W. Lensch, H. Li, J. J. Collins, A. P. Feinberg, and G. Q. Daley. Donor cell type can influence the epigenome and differentiation potential of human induced pluripotent stem cells. *Nat Biotechnol*, 29(12):1117–9, 2011.

H. Kristiansen, C. A. Scherer, M. McVean, S. P. Iadonato, S. Vends, K. Thavachelvam, T. B. Steffensen, K. A. Horan, T. Kuri, F. Weber, S. R. Paludan, and R. Hartmann. Extracellular 2'-5' oligoadenylate synthetase stimulates rnase l-independent antiviral activity: a novel mechanism of virus-induced innate immunity. *J Virol*, 84(22):11898–904, 2010.

K. Kuhn, S. C. Baker, E. Chudin, M.-H. Lieu, S. Oeser, H. Bennett, P. Rigault, D. Barker, T. K. McDaniel, and M. S. Chee. A novel, high-performance random array platform for quantitative gene expression profiling. *Genome Res*, 14(11):2347–2356, 2004.

A. Kunisato, M. Wakatsuki, H. Shinba, T. Ota, I. Ishida, and K. Nagao. Direct generation of induced pluripotent stem cells from human nonmobilized blood. *Stem Cells Dev*, 20(1): 159–68, 2011.

U. Lakshmipathy, B. Love, L. A. Goff, R. Jornsten, R. Graichen, R. P. Hart, and J. D. Chesnut. Microrna expression pattern of undifferentiated and differentiated human embryonic stem cells. *Stem Cells Dev*, 16(6):1003–16, 2007.

T. Le Carrour, S. Assou, T. S., L. Lhermitte, N. Lamb, T. Rème, V. Pantesco, S. Hamamah, B. Klein, and J. De Vos. Amazonia!: An online resource to google and visualize public human whole genome expression data. *The Open Bioinformatics Journal*, 4:5–10, 2010.

J. S. Lebkowski, J. Gold, C. Xu, W. Funk, C. P. Chiu, and M. K. Carpenter. Human embryonic stem cells: culture, differentiation, and genetic modification for regenerative medicine applications. *Cancer J*, 7 Suppl 2:S83–93, 2001.

G. Lee and L. Studer. Modelling familial dysautonomia in human induced pluripotent stem cells. *Philos Trans R Soc Lond B Biol Sci*, 366(1575):2286–96, 2011.

T. Lemonnier, S. Blanchard, D. Toli, E. Roy, S. Bigou, R. Froissart, I. Rouvet, S. Vitry, J. M. Heard, and D. Bohl. Modeling neuronal defects associated with a lysosomal disorder using patient-derived induced pluripotent stem cells. *Hum Mol Genet*, 20(18):3653–66, 2011.

D. H. Levin, R. Petryshyn, and I. M. London. Characterization of purified double-stranded rna-activated eif-2 alpha kinase from rabbit reticulocytes. *J Biol Chem*, 256(14):7638–41, 1981.

C. Li, J. Zhou, G. Shi, Y. Ma, Y. Yang, J. Gu, H. Yu, S. Jin, Z. Wei, F. Chen, and Y. Jin. Pluripotency can be rapidly and efficiently induced in human amniotic fluid-derived cells. *Hum Mol Genet*, 18(22):4340–9, 2009a.

H. Li, M. Collado, A. Villasante, K. Strati, S. Ortega, M. Canamero, M. A. Blasco, and M. Serrano. The ink4/arf locus is a barrier for ips cell reprogramming. *Nature*, 460(7259): 1136–9, 2009b.

R. Li, J. Liang, S. Ni, T. Zhou, X. Qing, H. Li, W. He, J. Chen, F. Li, Q. Zhuang, B. Qin, J. Xu, W. Li, J. Yang, Y. Gan, D. Qin, S. Feng, H. Song, D. Yang, B. Zhang, L. Zeng, L. Lai, M. A. Esteban, and D. Pei. A mesenchymal-to-epithelial transition initiates and is required for the nuclear reprogramming of mouse fibroblasts. *Cell Stem Cell*, 7(1):51–63, 2010.

W. Li, H. Zhou, R. Abujarour, S. Zhu, J. Young Joo, T. Lin, E. Hao, H. R. Scholer, A. Hayek, and S. Ding. Generation of human-induced pluripotent stem cells in the absence of exogenous sox2. *Stem Cells*, 27(12):2992–3000, 2009c.

B. Liao, X. Bao, L. Liu, S. Feng, A. Zovoilis, W. Liu, Y. Xue, J. Cai, X. Guo, B. Qin, R. Zhang, J. Wu, L. Lai, M. Teng, L. Niu, B. Zhang, M. A. Esteban, and D. Pei. Microrna cluster

302-367 enhances somatic cell reprogramming by accelerating a mesenchymal-to-epithelial transition. *J Biol Chem*, 286(19):17359–64, 2011.

T. Lin, R. Ambasudhan, X. Yuan, W. Li, S. Hilcove, R. Abujarour, X. Lin, H. S. Hahm, E. Hao, A. Hayek, and S. Ding. A chemical platform for improved induction of human ipscs. *Nat Methods*, 6(11):805–8, 2009.

J. Liu, K. L. Jones, H. Sumer, and P. J. Verma. Stable transgene expression in human embryonic stem cells after simple chemical transfection. *Mol Reprod Dev*, 76(6):580–6, 2009.

J. Liu, P. J. Verma, M. V. Evans-Galea, M. B. Delatycki, A. Michalska, J. Leung, D. Crombie, J. P. Sarsero, R. Williamson, M. Dottori, and A. Pebay. Generation of induced pluripotent stem cell lines from friedreich ataxia patients. *Stem Cell Rev*, 7(3):703–13, 2011.

T. Liu, G. Zou, Y. Gao, X. Zhao, H. Wang, Q. Huang, L. Jiang, L. Guo, and W. Cheng. High efficiency of reprogramming cd34(+) cells derived from human amniotic fluid into induced pluripotent stem cells with oct4. *Stem Cells Dev*, 2012.

K. J. Livak and T. D. Schmittgen. Analysis of relative gene expression data using real-time quantitative pcr and the 2(-delta delta c(t)) method. *Methods*, 25(4):402–8, 2001.

Y. H. Loh, S. Agarwal, I. H. Park, A. Urbach, H. Huo, G. C. Heffner, K. Kim, J. D. Miller, K. Ng, and G. Q. Daley. Generation of induced pluripotent stem cells from human blood. *Blood*, 113(22):5476–9, 2009.

M. Loiarro, C. Sette, G. Gallo, A. Ciacci, N. Fanto, D. Mastroianni, P. Carminati, and V. Ruggiero. Peptide-mediated interference of tir domain dimerization in myd88 inhibits interleukin-1-dependent activation of nf-kappab. *J Biol Chem*, 280(16):15809–14, 2005.

M. P. Longhi, C. L. Harris, B. P. Morgan, and A. Gallimore. Holding t cells in check–a new role for complement regulators? *Trends Immunol*, 27(2):102–8, 2006.

J. Lugassy, S. Zaffryar-Eilot, S. Soueid, A. Mordoviz, V. Smith, O. Kessler, and G. Neufeld. The enzymatic activity of lysyl oxidas-like-2 (loxl2) is not required for loxl2-induced inhibition of keratinocyte differentiation. *J Biol Chem*, 287(5):3541–9, 2012.

M. J. Lysaght and J. Crager. Origins. *Tissue Eng Part A*, 15(7):1449–50, 2009.

Y. Ma, A. Ramezani, R. Lewis, R. G. Hawley, and J. A. Thomson. High-level sustained transgene expression in human embryonic stem cells using lentiviral vectors. *Stem Cells*, 21 (1):111–7, 2003.

Y. Ma, J. Jin, C. Dong, E. C. Cheng, H. Lin, Y. Huang, and C. Qiu. High-efficiency sirna-based gene knockdown in human embryonic stem cells. *RNA*, 16(12):2564–9, 2010.

N. Mah, Y. Wang, M. C. Liao, A. Prigione, J. Jozefczuk, B. Lichtner, K. Wolfrum, M. Haltmeier, M. Flottmann, M. Schaefer, A. Hahn, R. Mrowka, E. Klipp, M. A. Andrade-Navarro, and J. Adjaye. Molecular insights into reprogramming-initiation events mediated by the oskm gene regulatory network. *PLoS ONE*, 6(8):e24351, 2011.

N. Maherali and K. Hochedlinger. Guidelines and techniques for the generation of induced pluripotent stem cells. *Cell Stem Cell*, 3(6):595–605, 2008.

N. Maherali, T. Ahfeldt, A. Rigamonti, J. Utikal, C. Cowan, and K. Hochedlinger. A high-efficiency system for the generation and study of human induced pluripotent stem cells. *Cell Stem Cell*, 3(3):340–5, 2008.

S. K. Mallanna and A. Rizzino. Emerging roles of micrornas in the control of embryonic stem cells and the generation of induced pluripotent stem cells. *Dev Biol*, 344(1):16–25, 2010.

B. S. Mallon, K. Y. Park, K. G. Chen, R. S. Hamilton, and R. D. McKay. Toward xeno-free culture of human embryonic stem cells. *Int J Biochem Cell Biol*, 38(7):1063–75, 2006.

M. C. Marchetto, G. W. Yeo, O. Kainohana, M. Marsala, F. H. Gage, and A. R. Muotri. Transcriptional signature and memory retention of human-induced pluripotent stem cells. *PLoS ONE*, 4(9):e7076, 2009.

M. C. Marchetto, C. Carromeu, A. Acab, D. Yu, G. W. Yeo, Y. Mu, G. Chen, F. H. Gage, and A. R. Muotri. A model for neural development and treatment of rett syndrome using human induced pluripotent stem cells. *Cell*, 143(4):527–39, 2010.

R. M. Marion, K. Strati, H. Li, M. Murga, R. Blanco, S. Ortega, O. Fernandez-Capetillo, M. Serrano, and M. A. Blasco. A p53-mediated dna damage response limits reprogramming to ensure ips cell genomic integrity. *Nature*, 460(7259):1149–53, 2009.

J. T. Marques, T. Devosse, D. Wang, M. Zamanian-Daryoush, P. Serbinowski, R. Hartmann, T. Fujita, M. A. Behlke, and B. R. Williams. A structural basis for discriminating between self and nonself double-stranded rnas in mammalian cells. *Nat Biotechnol*, 24(5):559–65, 2006.

A. Marson, S. S. Levine, M. F. Cole, G. M. Frampton, T. Brambrink, S. Johnstone, M. G. Guenther, W. K. Johnston, M. Wernig, J. Newman, J. M. Calabrese, L. M. Dennis, T. L. Volkert, S. Gupta, J. Love, N. Hannett, P. A. Sharp, D. P. Bartel, R. Jaenisch, and R. A. Young. Connecting microrna genes to the core transcriptional regulatory circuitry of embryonic stem cells. *Cell*, 134(3):521–33, 2008.

A. Marteyn, Y. Maury, M. M. Gauthier, C. Lecuyer, R. Vernet, J. A. Denis, G. Pietu, M. Peschanski, and C. Martinat. Mutant human embryonic stem cells reveal neurite and synapse formation defects in type 1 myotonic dystrophy. *Cell Stem Cell*, 8(4):434–44, 2011.

C. Mason and P. Dunnill. A brief definition of regenerative medicine. *Regen Med*, 3(1):1–5, 2008.

I. Mateizel, N. De Temmerman, U. Ullmann, G. Cauffman, K. Sermon, H. Van de Velde, M. De Rycke, E. Degreef, P. Devroey, I. Liebaers, and A. Van Steirteghem. Derivation of human embryonic stem cell lines from embryos obtained after ivf and after pgd for monogenic disorders. *Hum Reprod*, 21(2):503–11, 2006.

I. Mateizel, C. Spits, M. De Rycke, I. Liebaers, and K. Sermon. Derivation, culture, and characterization of vub hesc lines. *In Vitro Cell Dev Biol Anim*, 46(3-4):300–8, 2010.

M. M. Matin, J. R. Walsh, P. J. Gokhale, J. S. Draper, A. R. Bahrami, I. Morton, H. D. Moore, and P. W. Andrews. Specific knockdown of oct4 and beta2-microglobulin expression by rna interference in human embryonic stem cells and embryonic carcinoma cells. *Stem Cells*, 22(5):659–68, 2004.

A. Mattout, A. Biran, and E. Meshorer. Global epigenetic changes during somatic cell reprogramming to ips cells. *J Mol Cell Biol*, 3(6):341–50, 2011.

J. J. Maury, A. B. Choo, and K. K. Chan. Technical advances to genetically engineering human embryonic stem cells. *Integr Biol (Camb)*, 3(7):717–23, 2011.

Y. Mayshar, U. Ben-David, N. Lavon, J. C. Biancotti, B. Yakir, A. T. Clark, K. Plath, W. E. Lowry, and N. Benvenisty. Identification and classification of chromosomal aberrations in human induced pluripotent stem cells. *Cell Stem Cell*, 7(4):521–31, 2010.

C. S. McAllister and C. E. Samuel. The rna-activated protein kinase enhances the induction of interferon-beta and apoptosis mediated by cytoplasmic rna sensors. *J Biol Chem*, 284(3): 1644–51, 2009.

J. McNeish. Embryonic stem cells in drug discovery. *Nat Rev Drug Discov*, 3(1):70–80, 2004.

S. P. Medvedev, E. V. Grigor'eva, A. I. Shevchenko, A. A. Malakhova, E. V. Dementyeva, A. A. Shilov, E. A. Pokushalov, A. M. Zaidman, M. A. Aleksandrova, E. Y. Plotnikov, G. T. Sukhikh, and S. M. Zakian. Human induced pluripotent stem cells derived from fetal neural stem cells successfully undergo directed differentiation into cartilage. *Stem Cells Dev*, 20(6): 1099–1112, 2011.

C. Melton, R. L. Judson, and R. Blelloch. Opposing microrna families regulate self-renewal in mouse embryonic stem cells. *Nature*, 463(7281):621–6, 2010.

P. Menendez, L. Wang, and M. Bhatia. Genetic manipulation of human embryonic stem cells: a system to study early human development and potential therapeutic applications. *Curr Gene Ther*, 5(4):375–85, 2005.

M. Mimeault, R. Hauke, and S. K. Batra. Stem cells: a revolution in therapeutics-recent advances in stem cell biology and their therapeutic applications in regenerative medicine and cancer therapies. *Clin Pharmacol Ther*, 82(3):252–64, 2007.

V. E. Mishiev, V. I. Arshinov, G. I. Klebanov, and I. A. Vladimirov. [heterogeneity of phospholipid membranes detected by the fluorescent probe method]. *Biofizika*, 24(3):546–47, 1979.

N. Miyoshi, H. Ishii, H. Nagano, N. Haraguchi, D. L. Dewi, Y. Kano, S. Nishikawa, M. Tanemura, K. Mimori, F. Tanaka, T. Saito, J. Nishimura, I. Takemasa, T. Mizushima, M. Ikeda, H. Yamamoto, M. Sekimoto, Y. Doki, and M. Mori. Reprogramming of mouse and human cells to pluripotency using mature micrornas. *Cell Stem Cell*, 8(6):633–8, 2011.

A. Moretti, M. Bellin, A. Welling, C. B. Jung, J. T. Lam, L. Bott-Flugel, T. Dorn, A. Goedel, C. Hohnke, F. Hofmann, M. Seyfarth, D. Sinnecker, A. Schomig, and K. L. Laugwitz. Patient-specific induced pluripotent stem-cell models for long-qt syndrome. *N Engl J Med*, 363(15):1397–409, 2010.

R. D. Morin, M. D. O'Connor, M. Griffith, F. Kuchenbauer, A. Delaney, A. L. Prabhu, Y. Zhao, H. McDonald, T. Zeng, M. Hirst, C. J. Eaves, and M. A. Marra. Application of massively parallel sequencing to microrna profiling and discovery in human embryonic stem cells. *Genome Res*, 18(4):610–21, 2008.

D. Moschidou, S. Mukherjee, M. Blundell, K. Drews, G. Jones, H. Abdulrazzak, B. Nowakowska, A. Phoolchund, K. Lay, T. Ramasamy, M. Cananzi, D. Nettersheim, M. Sullivan, J. Frost, G. Moore, J. Vermeesch, N. Fisk, A. Thrasher, A. Atala, J. Adjaye, H. Schorle, P. De Coppi, and P. Guillot. Valproic acid confers functional pluripotency to human amniotic fluid stem cells in a transgene-free approach. *Mol Ther*. Accepted.

A. Mosquera, J. L. Fernandez, A. Campos, V. J. Goyanes, J. Ramiro-Diaz, and J. Gosalvez. Simultaneous decrease of telomere length and telomerase activity with ageing of human amniotic fluid cells. *J Med Genet*, 36(6):494–6, 1999.

A. Nagy. Cre recombinase: the universal reagent for genome tailoring. *Genesis*, 26(2):99–109, 2000.

S. K. Nair, D. Boczkowski, M. Morse, R. I. Cumming, H. K. Lyerly, and E. Gilboa. Induction of primary carcinoembryonic antigen (cea)-specific cytotoxic t lymphocytes in vitro using human dendritic cells transfected with rna. *Nat Biotechnol*, 16(4):364–9, 1998.

M. O. Nandan and V. W. Yang. The role of kruppel-like factors in the reprogramming of somatic cells to induced pluripotent stem cells. *Histol Histopathol*, 24(10):1343–55, 2009.

J. Nichols, B. Zevnik, K. Anastassiadis, H. Niwa, D. Klewe-Nebenius, I. Chambers, H. Schöler, and A. Smith. Formation of pluripotent stem cells in the mammalian embryo depends on the pou transcription factor oct4. *Cell*, 95(3):379–91, 1998.

M. A. Nugent and R. V. Iozzo. Fibroblast growth factor-2. *Int J Biochem Cell Biol*, 32(2): 115–20, 2000.

F. D. Nunes, F. C. de Almeida, R. Tucci, and S. C. de Sousa. Homeobox genes: a molecular link between development and cancer. *Pesqui Odontol Bras*, 17(1):94–8, 2003.

Y. Ohi, H. Qin, C. Hong, L. Blouin, J. M. Polo, T. Guo, Z. Qi, S. L. Downey, P. D. Manos, D. J. Rossi, J. Yu, M. Hebrok, K. Hochedlinger, J. F. Costello, J. S. Song, and M. Ramalho-Santos. Incomplete dna methylation underlies a transcriptional memory of somatic cells in human ips cells. *Nat Cell Biol*, 13(5):541–9, 2011.

K. Okita and S. Yamanaka. Intracellular signaling pathways regulating pluripotency of embryonic stem cells. *Curr Stem Cell Res Ther*, 1(1):103–11, 2006.

G. Panganiban and J. L. Rubenstein. Developmental functions of the distal-less/dlx homeobox genes. *Development*, 129(19):4371–86, 2002.

I. H. Park, N. Arora, H. Huo, N. Maherali, T. Ahfeldt, A. Shimamura, M. W. Lensch, C. Cowan, K. Hochedlinger, and G. Q. Daley. Disease-specific induced pluripotent stem cells. *Cell*, 134(5):877–86, 2008.

C. E. Pasi, A. Dereli-Oz, S. Negrini, M. Friedli, G. Fragola, A. Lombardo, G. Van Houwe, L. Naldini, S. Casola, G. Testa, D. Trono, P. G. Pelicci, and T. D. Halazonetis. Genomic instability in induced stem cells. *Cell Death Differ*, 18(5):745–53, 2011.

M. F. Pera, B. Reubinoff, and A. Trounson. Human embryonic stem cells. *J Cell Sci*, 113 (Pt 1):5–10, 2000.

L. Perin, S. Giuliani, D. Jin, S. Sedrakyan, G. Carraro, R. Habibian, D. Warburton, A. Atala, and R. E. De Filippo. Renal differentiation of amniotic fluid stem cells. *Cell Prolif*, 40(6): 936–48, 2007.

T. Pertel, S. Hausmann, D. Morger, S. Zuger, J. Guerra, J. Lascano, C. Reinhard, F. A. Santoni, P. D. Uchil, L. Chatel, A. Bisiaux, M. L. Albert, C. Strambio-De-Castillia, W. Mothes, M. Pizzato, M. G. Grutter, and J. Luban. Trim5 is an innate immune sensor for the retrovirus capsid lattice. *Nature*, 472(7343):361–5, 2011.

A. Pichlmair, O. Schulz, C. P. Tan, T. I. Naslund, P. Liljestrom, F. Weber, and C. Reis e Sousa. Rig-i-mediated antiviral responses to single-stranded rna bearing 5'-phosphates. *Science (80-)*, 314(5801):997–1001, 2006.

A. Pichlmair, C. Lassnig, C. A. Eberle, M. W. Gorna, C. L. Baumann, T. R. Burkard, T. Burckstummer, A. Stefanovic, S. Krieger, K. L. Bennett, T. Rulicke, F. Weber, J. Colinge, M. Muller, and G. Superti-Furga. Ifit1 is an antiviral protein that recognizes 5'-triphosphate rna. *Nat Immunol*, 12(7):624–30, 2011.

S. R. Pinnell and G. R. Martin. The cross-linking of collagen and elastin: enzymatic conversion of lysine in peptide linkage to alpha-aminoadipic-delta-semialdehyde (allysine) by an extract from bone. *Proc Natl Acad Sci U S A*, 61(2):708–16, 1968.

J. R. Plews, J. Li, M. Jones, H. D. Moore, C. Mason, P. W. Andrews, and J. Na. Activation of pluripotency genes in human fibroblast cells by a novel mrna based approach. *PLoS ONE*, 5(12):e14397, 2010.

A. Prigione, N. Rohwer, K. Drews, K. Blümlein, R. Bukowiecki, H. Lehrach, M. Ralser, T. Cramer, and J. Adjaye. Hif1alpha drives early induction of pluripotency through reprogramming of glycolytic metabolism. *Cell Res*. Submitted.

A. Prigione, B. Fauler, R. Lurz, H. Lehrach, and J. Adjaye. The senescence-related mitochondrial/oxidative stress pathway is repressed in human induced pluripotent stem cells. *Stem Cells*, 28(4):721–33, 2010.

A. Prigione, A. M. Hossini, B. Lichtner, A. Serin, B. Fauler, M. Megges, R. Lurz, H. Lehrach, E. Makrantonaki, C. C. Zouboulis, and J. Adjaye. Mitochondrial-associated cell death mechanisms are reset to an embryonic-like state in aged donor-derived ips cells harboring chromosomal aberrations. *PLoS ONE*, 6(11):e27352, 2011a.

A. Prigione, B. Lichtner, H. Kuhl, E. A. Struys, M. Wamelink, H. Lehrach, M. Ralser, B. Timmermann, and J. Adjaye. Human induced pluripotent stem cells harbor homoplasmic and heteroplasmic mitochondrial dna mutations while maintaining human embryonic stem cell-like metabolic reprogramming. *Stem Cells*, 29(9):1338–48, 2011b.

A.-R. Prusa and M. Hengstschlager. Amniotic fluid cells and human stem cell research: a new connection. *Med Sci Monit*, 8(11):RA253–RA257, 2002.

A. R. Prusa, E. Marton, M. Rosner, G. Bernaschek, and M. Hengstschlager. Oct-4-expressing cells in human amniotic fluid: a new source for stem cell research? *Hum Reprod*, 18(7): 1489–93, 2003.

A. R. Prusa, E. Marton, M. Rosner, D. Bettelheim, G. Lubec, A. Pollack, G. Bernaschek, and M. Hengstschlager. Neurogenic cells in human amniotic fluid. *Am J Obstet Gynecol*, 191(1): 309–14, 2004.

A. D. Pyle, L. F. Lock, and P. J. Donovan. Neurotrophins mediate human embryonic stem cell survival. *Nat Biotechnol*, 24(3):344–50, 2006.

R Development Core Team. *R: A language and environment for statistical computing.*, 2010. URL http://www.R-project.org.

S. T. Rashid, S. Corbineau, N. Hannan, S. J. Marciniak, E. Miranda, G. Alexander, I. Huang-Doran, J. Griffin, L. Ahrlund-Richter, J. Skepper, R. Semple, A. Weber, D. A. Lomas, and L. Vallier. Modeling inherited metabolic disorders of the liver using human induced pluripotent stem cells. *J Clin Invest*, 120(9):3127–36, 2010.

O. Rautsi, S. Lehmusvaara, T. Salonen, K. Hakkinen, M. Sillanpaa, T. Hakkarainen, S. Heikkinen, E. Vahakangas, S. Yla-Herttuala, A. Hinkkanen, I. Julkunen, J. Wahlfors,

and R. Pellinen. Type i interferon response against viral and non-viral gene transfer in human tumor and primary cell lines. *J Gene Med*, 9(2):122–35, 2007.

A. Raya, I. Rodriguez-Piza, G. Guenechea, R. Vassena, S. Navarro, M. J. Barrero, A. Consiglio, M. Castella, P. Rio, E. Sleep, F. Gonzalez, G. Tiscornia, E. Garreta, T. Aasen, A. Veiga, I. M. Verma, J. Surralles, J. Bueren, and J. C. Izpisua Belmonte. Disease-corrected haematopoietic progenitors from fanconi anaemia induced pluripotent stem cells. *Nature*, 460(7251):53–9, 2009.

I. Rodríguez-Pizà, Y. Richaud-Patin, R. Vassena, F. González, M. J. Barrero, A. Veiga, A. Raya, and J. C. Izpisúa Belmonte. Reprogramming of human fibroblasts to induced pluripotent stem cells under xeno-free conditions. *Stem Cells*, 28(1):36–44, 2010.

C. J. Rold and C. Aiken. Proteasomal degradation of trim5alpha during retrovirus restriction. *PLoS Pathog*, 4(5):e1000074, 2008.

P. J. Ross, S. T. Suhr, R. M. Rodriguez, E.-A. Chang, K. Wang, K. Siripattarapravat, T. Ko, and J. B. Cibelli. Human-induced pluripotent stem cells produced under xeno-free conditions. *Stem Cells Dev*, 19(8):1221–9, 2010.

L. Sachs, D. M. Serr, and M. Danon. Prenatal diagnosis of sex using cells from the amniotic fluid. *Science (80-)*, 123(3196):548, 1956.

A. J. Sadler and B. R. Williams. Interferon-inducible antiviral effectors. *Nat Rev Immunol*, 8 (7):559–68, 2008.

A. I. Saeed, V. Sharov, J. White, J. Li, W. Liang, N. Bhagabati, J. Braisted, M. Klapa, T. Currier, M. Thiagarajan, A. Sturn, M. Snuffin, A. Rezantsev, D. Popov, A. Ryltsov, E. Kostukovich, I. Borisovsky, Z. Liu, A. Vinsavich, V. Trush, and J. Quackenbush. Tm4: a free, open-source system for microarray data management and analysis. *BioTechniques*, 34(2):374–8, 2003.

A. I. Saeed, N. K. Bhagabati, J. C. Braisted, W. Liang, V. Sharov, E. A. Howe, J. Li, M. Thiagarajan, J. A. White, and J. Quackenbush. Tm4 microarray software suite. *Methods Enzymol*, 411:134–93, 2006.

V. Salvi, D. Bosisio, S. Mitola, L. Andreoli, A. Tincani, and S. Sozzani. Trichostatin a blocks type i interferon production by activated plasmacytoid dendritic cells. *Immunobiology*, 215 (9-10):756–61, 2010.

S. A. Samarajiwa, S. Forster, K. Auchettl, and P. J. Hertzog. Interferome: the database of interferon regulated genes. *Nucleic Acids Res*, 37(Database issue):D852–7, 2009.

P. Samavarchi-Tehrani, A. Golipour, L. David, H. K. Sung, T. A. Beyer, A. Datti, K. Woltjen, A. Nagy, and J. L. Wrana. Functional genomics reveals a bmp-driven mesenchymal-to-epithelial transition in the initiation of somatic cell reprogramming. *Cell Stem Cell*, 7(1): 64–77, 2010.

A. Sanchez-Danes, Y. Richaud-Patin, I. Carballo-Carbajal, S. Jimenez-Delgado, C. Caig, S. Mora, C. Di Guglielmo, M. Ezquerra, B. Patel, A. Giralt, J. M. Canals, M. Memo, J. Alberch, J. Lopez-Barneo, M. Vila, A. M. Cuervo, E. Tolosa, A. Consiglio, and A. Raya. Disease-specific phenotypes in dopamine neurons from human ips-based models of genetic and sporadic parkinson's disease. *EMBO Mol Med*, 2012.

H. B. Sarnat and L. Flores-Sarnat. Embryology of the neural crest: its inductive role in the neurocutaneous syndromes. *J Child Neurol*, 20(8):637–43, 2005.

N. Sato, L. Meijer, L. Skaltsounis, P. Greengard, and A. H. Brivanlou. Maintenance of pluripotency in human and mouse embryonic stem cells through activation of wnt signaling by a pharmacological gsk-3-specific inhibitor. *Nat Med*, 10(1):55–63, 2004.

A. Savarino, J. R. Boelaert, A. Cassone, G. Majori, and R. Cauda. Effects of chloroquine on viral infections: an old drug against today's diseases? *Lancet Infect Dis*, 3(11):722–727, 2003.

T. J. Schall, K. Bacon, K. J. Toy, and D. V. Goeddel. Selective attraction of monocytes and t lymphocytes of the memory phenotype by cytokine rantes. *Nature*, 347(6294):669–71, 1990.

A. Schellenberg, Q. Lin, H. Schuler, C. M. Koch, S. Joussen, B. Denecke, G. Walenda, N. Pallua, C. V. Suschek, M. Zenke, and W. Wagner. Replicative senescence of mesenchymal stem cells causes dna-methylation changes which correlate with repressive histone marks. *Aging (Albany NY)*, 3(9):873–88, 2011.

R. Schietke, C. Warnecke, I. Wacker, J. Schodel, D. R. Mole, V. Campean, K. Amann, M. Goppelt-Struebe, J. Behrens, K. U. Eckardt, and M. S. Wiesener. The lysyl oxidases lox and loxl2 are necessary and sufficient to repress e-cadherin in hypoxia: insights into cellular transformation processes mediated by hif-1. *J Biol Chem*, 285(9):6658–69, 2010.

S. Schmitt, U. Aftab, C. Jiang, S. Redenti, H. Klassen, E. Miljan, J. Sinden, and M. Young. Molecular characterization of human retinal progenitor cells. *Invest Ophthalmol Vis Sci*, 50 (12):5901–8, 2009.

G. C. Schoenwolf, S. B. Bleyl, P. R. Brauer, and P. H. Francis-West. *Larsen's Human Embryology*. Churchill Livingstone, 4 edition, 2008.

L. C. Schulz, T. Ezashi, P. Das, S. D. Westfall, K. A. Livingston, and R. M. Roberts. Human embryonic stem cells as models for trophoblast differentiation. *Placenta*, 29 Suppl A:S10–6, 2008.

R. E. Schwartz, K. Trehan, L. Andrus, T. P. Sheahan, A. Ploss, S. A. Duncan, C. M. Rice, and S. N. Bhatia. Modeling hepatitis c virus infection using human induced pluripotent stem cells. *Proc Natl Acad Sci U S A*, 109(7):2544–8, 2012a.

S. D. Schwartz, J. P. Hubschman, G. Heilwell, V. Franco-Cardenas, C. K. Pan, R. M. Ostrick, E. Mickunas, R. Gay, I. Klimanskaya, and R. Lanza. Embryonic stem cell trials for macular degeneration: a preliminary report. *Lancet*, 2012b.

V. Sebastiano, M. L. Maeder, J. F. Angstman, B. Haddad, C. Khayter, D. T. Yeo, M. J. Goodwin, J. S. Hawkins, C. L. Ramirez, L. F. Batista, S. E. Artandi, M. Wernig, and J. K. Joung. In situ genetic correction of the sickle cell anemia mutation in human induced pluripotent stem cells using engineered zinc finger nucleases. *Stem Cells*, 29(11):1717–26, 2011.

G. C. Sen, B. Lebleu, G. E. Brown, M. Kawakita, E. Slattery, and P. Lengyel. Interferon, double-stranded rna and mrna degradation. *Nature*, 264(5584):370–3, 1976.

N. Sessarego, A. Parodi, M. Podesta, F. Benvenuto, M. Mogni, V. Raviolo, M. Lituania, A. Kunkl, G. Ferlazzo, F. D. Bricarelli, A. Uccelli, and F. Frassoni. Multipotent mesenchymal stromal cells from amniotic fluid: solid perspectives for clinical application. *Haematologica*, 93(3):339–46, 2008.

K. Si-Tayeb, F. K. Noto, A. Sepac, F. Sedlic, Z. J. Bosnjak, J. W. Lough, and S. A. Duncan. Generation of human induced pluripotent stem cells by simple transient transfection of plasmid dna encoding reprogramming factors. *BMC Dev Biol*, 10:81, 2010.

A. Solanki and K. B. Lee. A step closer to complete chemical reprogramming for generating ips cells. *ChemBioChem*, 11(6):755–7, 2010.

F. Soldner, D. Hockemeyer, C. Beard, Q. Gao, G. W. Bell, E. G. Cook, G. Hargus, A. Blak, O. Cooper, M. Mitalipova, O. Isacson, and R. Jaenisch. Parkinson's disease patient-derived induced pluripotent stem cells free of viral reprogramming factors. *Cell*, 136(5):964–77, 2009.

A. Somers, J. C. Jean, C. A. Sommer, A. Omari, C. C. Ford, J. A. Mills, L. Ying, A. G. Sommer, J. M. Jean, B. W. Smith, R. Lafyatis, M. F. Demierre, D. J. Weiss, D. L. French, P. Gadue, G. J. Murphy, G. Mostoslavsky, and D. N. Kotton. Generation of transgene-free lung disease-specific human induced pluripotent stem cells using a single excisable lentiviral stem cell cassette. *Stem Cells*, 28(10):1728–40, 2010.

F. Stegmeier, M. Rape, V. M. Draviam, G. Nalepa, M. E. Sowa, X. L. Ang, E. R. McDonald, 3rd, M. Z. Li, G. J. Hannon, P. K. Sorger, M. W. Kirschner, J. W. Harper, and S. J. Elledge. Anaphase initiation is regulated by antagonistic ubiquitination and deubiquitination activities. *Nature*, 446(7138):876–881, 2007.

S. Strauss. Geron trial resumes, but standards for stem cell trials remain elusive. *Nat Biotechnol*, 28(10):989–90, 2010.

Y. Strulovici, P. L. Leopold, T. P. O'Connor, R. G. Pergolizzi, and R. G. Crystal. Human embryonic stem cells and gene therapy. *Mol Ther*, 15(5):850–66, 2007.

S. Sugii, Y. Kida, T. Kawamura, J. Suzuki, R. Vassena, Y.-Q. Yin, M. K. Lutz, W. T. Berggren, J. C. Izpisúa Belmonte, and R. M. Evans. Human and mouse adipose-derived cells support feeder-independent induction of pluripotent stem cells. *Proc Natl Acad Sci U S A*, 107(8): 3558–63, 2010.

S. T. Suhr, E. A. Chang, R. M. Rodriguez, K. Wang, P. J. Ross, Z. Beyhan, S. Murthy, and J. B. Cibelli. Telomere dynamics in human cells reprogrammed to pluripotency. *PLoS ONE*, 4 (12):e8124, 2009.

S. T. Suhr, E. A. Chang, J. Tjong, N. Alcasid, G. A. Perkins, M. D. Goissis, M. H. Ellisman, G. I. Perez, and J. B. Cibelli. Mitochondrial rejuvenation after induced pluripotency. *PLoS ONE*, 5(11):e14095, 2010.

N. Sun, N. J. Panetta, D. M. Gupta, K. D. Wilson, A. Lee, F. Jia, S. Hu, A. M. Cherry, R. C. Robbins, M. T. Longaker, and J. C. Wu. Feeder-free derivation of induced pluripotent stem cells from adult human adipose stem cells. *Proc Natl Acad Sci U S A*, 106(37):15720–5, 2009.

N. Sun, M. Yazawa, J. Liu, L. Han, V. Sanchez-Freire, O. J. Abilez, E. G. Navarrete, S. Hu, L. Wang, A. Lee, A. Pavlovic, S. Lin, R. Chen, R. J. Hajjar, M. P. Snyder, R. E. Dolmetsch, M. J. Butte, E. A. Ashley, M. T. Longaker, R. C. Robbins, and J. C. Wu. Patient-specific induced pluripotent stem cells as a model for familial dilated cardiomyopathy. *Sci Transl Med*, 4(130):130ra47, 2012.

A. Swistowski, J. Peng, Q. Liu, P. Mali, M. S. Rao, L. Cheng, and X. Zeng. Efficient generation of functional dopaminergic neurons from human induced pluripotent stem cells under defined conditions. *Stem Cells*, 28(10):1893–904, 2010.

J. A. Symons, A. Alcami, and G. L. Smith. Vaccinia virus encodes a soluble type i interferon receptor of novel structure and broad species specificity. *Cell*, 81(4):551–60, 1995.

H. Tahara and M. T. Lotze. Antitumor effects of interleukin-12 (il-12): applications for the immunotherapy and gene therapy of cancer. *Gene Ther*, 2(2):96–106, 1995.

K. Takahashi and S. Yamanaka. Induction of pluripotent stem cells from mouse embryonic and adult fibroblast cultures by defined factors. *Cell*, 126(4):663–76, 2006.

K. Takahashi, K. Tanabe, M. Ohnuki, M. Narita, T. Ichisaka, K. Tomoda, and S. Yamanaka. Induction of pluripotent stem cells from adult human fibroblasts by defined factors. *Cell*, 131(5):861–72, 2007.

K. Takahashi, M. Narita, M. Yokura, T. Ichisaka, and S. Yamanaka. Human induced pluripotent stem cells on autologous feeders. *PLoS ONE*, 4(12):e8067, 2009.

H. L. Tan, W. J. Fong, E. H. Lee, M. Yap, and A. Choo. mab 84, a cytotoxic antibody that kills undifferentiated human embryonic stem cells via oncosis. *Stem Cells*, 27(8):1792–801, 2009.

S. S. Tang, P. C. Trackman, and H. M. Kagan. Reaction of aortic lysyl oxidase with beta-aminopropionitrile. *J Biol Chem*, 258(7):4331–8, 1983.

J. A. Thomson, J. Itskovitz-Eldor, S. S. Shapiro, M. A. Waknitz, J. J. Swiergiel, V. S. Marshall, and J. M. Jones. Embryonic stem cell lines derived from human blastocysts. *Science (80-)*, 282(5391):1145–7, 1998.

J. Tolar, L. Xia, M. J. Riddle, C. J. Lees, C. R. Eide, R. T. McElmurry, M. Titeux, M. J. Osborn, T. C. Lund, A. Hovnanian, J. E. Wagner, and B. R. Blazar. Induced pluripotent stem cells from individuals with recessive dystrophic epidermolysis bullosa. *J Invest Dermatol*, 131(4): 848–56, 2011.

V. U. Toshchakov, S. Basu, M. J. Fenton, and S. N. Vogel. Differential involvement of bb loops of toll-il-1 resistance (tir) domain-containing adapter proteins in tlr4- versus tlr2-mediated signal transduction. *J Immunol*, 175(1):494–500, 2005.

P. Tropel, J. Tournois, J. Come, C. Varela, C. Moutou, P. Fragner, M. Cailleret, Y. Laabi, M. Peschanski, and S. Viville. High-efficiency derivation of human embryonic stem cell lines following pre-implantation genetic diagnosis. *In Vitro Cell Dev Biol Anim*, 46(3-4): 376–85, 2010.

L. Trovato, R. De Fazio, M. Annunziata, S. Sdei, E. Favaro, R. Ponti, L. Marozio, E. Ghigo, C. Benedetto, and R. Granata. Pluripotent stemcells isolated fromhuman amniotic fluid and differentiation into pancreatic beta-cells. *J Endocrinol Invest*, 32(11):873–6, 2009.

M. S. Tsai, J. L. Lee, Y. J. Chang, and S. M. Hwang. Isolation of human multipotent mesenchymal stem cells from second-trimester amniotic fluid using a novel two-stage culture protocol. *Hum Reprod*, 19(6):1450–6, 2004.

M. S. Tsai, S. M. Hwang, Y. L. Tsai, F. C. Cheng, J. L. Lee, and Y. J. Chang. Clonal amniotic fluid-derived stem cells express characteristics of both mesenchymal and neural stem cells. *Biol Reprod*, 74(3):545–51, 2006.

N. Tsuji, M. Kobayashi, K. Nagashima, Y. Wakisaka, and K. Koizumi. A new antifungal antibiotic, trichostatin. *J Antibiot (Tokyo)*, 29(1):1–6, 1976.

N. Tsuneyoshi, T. Sumi, H. Onda, H. Nojima, N. Nakatsuji, and H. Suemori. Prdm14 suppresses expression of differentiation marker genes in human embryonic stem cells. *Biochem Biophys Res Commun*, 367(4):899–905, 2008.

A. Tulpule, M. W. Lensch, J. D. Miller, K. Austin, A. D'Andrea, T. M. Schlaeger, A. Shimamura, and G. Q. Daley. Knockdown of fanconi anemia genes in human embryonic stem cells reveals early developmental defects in the hematopoietic lineage. *Blood*, 115(17): 3453–62, 2010.

S. Uddin, A. Chamdin, and L. C. Platanias. Interaction of the transcriptional activator stat-2 with the type i interferon receptor. *J Biol Chem*, 270(42):24627–30, 1995.

A. Urbach and N. Benvenisty. Studying early lethality of 45,xo (turner's syndrome) embryos using human embryonic stem cells. *PLoS ONE*, 4(1):e4175, 2009.

A. Urbach, M. Schuldiner, and N. Benvenisty. Modeling for lesch-nyhan disease by gene targeting in human embryonic stem cells. *Stem Cells*, 22(4):635–41, 2004.

J. Utikal, N. Maherali, W. Kulalert, and K. Hochedlinger. Sox2 is dispensable for the reprogramming of melanocytes and melanoma cells into induced pluripotent stem cells. *J Cell Sci*, 122(Pt 19):3502–10, 2009a.

J. Utikal, J. M. Polo, M. Stadtfeld, N. Maherali, W. Kulalert, R. M. Walsh, A. Khalil, J. G. Rheinwald, and K. Hochedlinger. Immortalization eliminates a roadblock during cellular reprogramming into ips cells. *Nature*, 460(7259):1145–8, 2009b.

L. Vallier, M. Alexander, and R. A. Pedersen. Activin/nodal and fgf pathways cooperate to maintain pluripotency of human embryonic stem cells. *J Cell Sci*, 118(Pt 19):4495–509, 2005.

L. Vallier, S. Mendjan, S. Brown, Z. Chng, A. Teo, L. E. Smithers, M. W. Trotter, C. H. Cho, A. Martinez, P. Rugg-Gunn, G. Brons, and R. A. Pedersen. Activin/nodal signalling maintains pluripotency by controlling nanog expression. *Development*, 136(8):1339–49, 2009a.

L. Vallier, T. Touboul, S. Brown, C. Cho, B. Bilican, M. Alexander, J. Cedervall, S. Chandran, L. Ahrlund-Richter, A. Weber, and R. A. Pedersen. Signaling pathways controlling pluripotency and early cell fate decisions of human induced pluripotent stem cells. *Stem Cells*, 27(11):2655–66, 2009b.

D. Van Hoof, S. R. Braam, W. Dormeyer, D. Ward-van Oostwaard, A. J. Heck, J. Krijgsveld, and C. L. Mummery. Feeder-free monolayer cultures of human embryonic stem cells express an epithelial plasma membrane protein profile. *Stem Cells*, 26(11):2777–81, 2008.

M. G. Vander Heiden, L. C. Cantley, and C. B. Thompson. Understanding the warburg effect: the metabolic requirements of cell proliferation. *Science (80-)*, 324(5930):1029–33, 2009.

S. Varum, A. S. Rodrigues, M. B. Moura, O. Momcilovic, C. A. t. Easley, J. Ramalho-Santos, B. Van Houten, and G. Schatten. Energy metabolism in human pluripotent stem cells and their differentiated counterparts. *PLoS ONE*, 6(6):e20914, 2011.

H. Vaziri, K. Chapman, A. Guigova, J. Teichroeb, M. Lacher, H. Sternberg, I. Singec, L. Briggs, J. Wheeler, J. Sampathkumar, R. Gonzalez, D. Larocca, J. Murai, E. Snyder, W. Andrews, W. Funk, and M. West. Spontaneous reversal of the developmental aging of normal human cells following transcriptional reprogramming. *Regen Med*, 5(3):345–363, 2010.

W. Wagner, P. Horn, M. Castoldi, A. Diehlmann, S. Bork, R. Saffrich, V. Benes, J. Blake, S. Pfister, V. Eckstein, and A. D. Ho. Replicative senescence of mesenchymal stem cells: a continuous and organized process. *PLoS ONE*, 3(5):e2213, 2008.

G. Walther, J. Gekas, and O. F. Bertrand. Amniotic stem cells for cellular cardiomyoplasty: promises and premises. *Catheter Cardiovasc Interv*, 73(7):917–24, 2009.

H. Wang, S. Chen, X. Cheng, and Z. Dou. [differentiation of human amniotic fluid stem cells into cardiomyocytes through embryonic body formation]. *Sheng Wu Gong Cheng Xue Bao*, 24(9):1582–7, 2008.

P. Wang and J. Na. Mechanism and methods to induce pluripotency. *Protein Cell*, 2(10):792–9, 2011.

Q. L. Wang, S. Chen, N. Esumi, P. K. Swain, H. S. Haines, G. Peng, B. M. Melia, I. McIntosh, J. R. Heckenlively, S. G. Jacobson, E. M. Stone, A. Swaroop, and D. J. Zack. Qrx, a novel homeobox gene, modulates photoreceptor gene expression. *Hum Mol Genet*, 13(10):1025–40, 2004.

Y. Wang and J. Adjaye. A cyclic amp analog, 8-br-camp, enhances the induction of pluripotency in human fibroblast cells. *Stem Cell Rev*, 7(2):331–41, 2011.

Y. Wang, N. Mah, A. Prigione, K. Wolfrum, M. A. Andrade-Navarro, and J. Adjaye. A transcriptional roadmap to the induction of pluripotency in somatic cells. *Stem Cell Rev*, 6 (2):282–96, 2010.

Y. Wang, C. G. Zheng, Y. Jiang, J. Zhang, J. Chen, C. Yao, Q. Zhao, S. Liu, K. Chen, J. Du, Z. Yang, and S. Gao. Genetic correction of beta-thalassemia patient-specific ips cells and its use in improving hemoglobin production in irradiated scid mice. *Cell Res*, 22(4):637–48, 2012a.

Z. Wang, E. Oron, B. Nelson, S. Razis, and N. Ivanova. Distinct lineage specification roles for nanog, oct4, and sox2 in human embryonic stem cells. *Cell Stem Cell*, 10(4):440–54, 2012b.

O. Warburg. On the origin of cancer cells. *Science (80-)*, 123(3191):309–14, 1956.

G. R. Warnes, B. Bolker, L. Bonebakker, R. Gentleman, W. H. A. Liaw, T. Lumley, M. Maechler, A. Magnusson, S. Moeller, M. Schwartz, and B. Venables. *gplots: Various R programming tools for plotting data. R package version 2.8.0.*, 2010. URL http://CRAN.R-project.org/package=gplots.

L. Warren, P. D. Manos, T. Ahfeldt, Y. H. Loh, H. Li, F. Lau, W. Ebina, P. K. Mandal, Z. D. Smith, A. Meissner, G. Q. Daley, A. S. Brack, J. J. Collins, C. Cowan, T. M. Schlaeger, and D. J. Rossi. Highly efficient reprogramming to pluripotency and directed differentiation of human cells with synthetic modified mrna. *Cell Stem Cell*, 7(5):618–30, 2010.

K. Watanabe, M. Ueno, D. Kamiya, A. Nishiyama, M. Matsumura, T. Wataya, J. B. Takahashi, S. Nishikawa, K. Muguruma, and Y. Sasai. A rock inhibitor permits survival of dissociated human embryonic stem cells. *Nat Biotechnol*, 25(6):681–6, 2007.

R. Wattiaux, N. Laurent, S. Wattiaux-De Coninck, and M. Jadot. Endosomes, lysosomes: their implication in gene transfer. *Adv Drug Deliv Rev*, 41(2):201–8, 2000.

M. Wernig, J. P. Zhao, J. Pruszak, E. Hedlund, D. Fu, F. Soldner, V. Broccoli, M. Constantine-Paton, O. Isacson, and R. Jaenisch. Neurons derived from reprogrammed fibroblasts functionally integrate into the fetal brain and improve symptoms of rats with parkinson's disease. *Proc Natl Acad Sci U S A*, 105(15):5856–61, 2008.

I. Wilmut, A. E. Schnieke, J. McWhir, A. J. Kind, and K. H. Campbell. Viable offspring derived from fetal and adult mammalian cells. *Nature*, 385(6619):810–3, 1997.

K. Wolfrum, Y. Wang, A. Prigione, K. Sperling, H. Lehrach, and J. Adjaye. The large principle of cellular reprogramming: lost, acquired and retained gene expression in foreskin and amniotic fluid-derived human ips cells. *PLoS ONE*, 5(10):e13703, 2010.

K. Woltjen, I. P. Michael, P. Mohseni, R. Desai, M. Mileikovsky, R. Hamalainen, R. Cowling, W. Wang, P. Liu, M. Gertsenstein, K. Kaji, H. K. Sung, and A. Nagy. piggybac transposition reprograms fibroblasts to induced pluripotent stem cells. *Nature*, 458(7239):766–70, 2009.

R. C. Wong, A. Pebay, L. T. Nguyen, K. L. Koh, and M. F. Pera. Presence of functional gap junctions in human embryonic stem cells. *Stem Cells*, 22(6):883–9, 2004.

S. M. Wu and K. Hochedlinger. Harnessing the potential of induced pluripotent stem cells for regenerative medicine. *Nat Cell Biol*, 13(5):497–505, 2011.

X. Xia, Y. Zhang, C. R. Zieth, and S. C. Zhang. Transgenes delivered by lentiviral vector are suppressed in human embryonic stem cells in a promoter-dependent manner. *Stem Cells Dev*, 16(1):167–76, 2007.

C. Xu, M. S. Inokuma, J. Denham, K. Golds, P. Kundu, J. D. Gold, and M. K. Carpenter. Feeder-free growth of undifferentiated human embryonic stem cells. *Nat Biotechnol*, 19(10): 971–4, 2001.

N. Xu, T. Papagiannakopoulos, G. Pan, J. A. Thomson, and K. S. Kosik. Microrna-145 regulates oct4, sox2, and klf4 and represses pluripotency in human embryonic stem cells. *Cell*, 137(4):647–58, 2009.

R. H. Xu. In vitro induction of trophoblast from human embryonic stem cells. *Methods Mol Med*, 121:189–202, 2006.

R. H. Xu, R. M. Peck, D. S. Li, X. Feng, T. Ludwig, and J. A. Thomson. Basic fgf and suppression of bmp signaling sustain undifferentiated proliferation of human es cells. *Nat Methods*, 2(3):185–90, 2005.

R. H. Xu, T. L. Sampsell-Barron, F. Gu, S. Root, R. M. Peck, G. Pan, J. Yu, J. Antosiewicz-Bourget, S. Tian, R. Stewart, and J. A. Thomson. Nanog is a direct target of tgfbeta/activin-mediated smad signaling in human escs. *Cell Stem Cell*, 3(2):196–206, 2008.

E. Yakubov, G. Rechavi, S. Rozenblatt, and D. Givol. Reprogramming of human fibroblasts to pluripotent stem cells using mrna of four transcription factors. *Biochem Biophys Res Commun*, 394(1):189–93, 2010.

S. Yamanaka. A fresh look at ips cells. *Cell*, 137(1):13–7, 2009a.

S. Yamanaka. Elite and stochastic models for induced pluripotent stem cell generation. *Nature*, 460(7251):49–52, 2009b.

L. Ye, J. C. Chang, C. Lin, X. Sun, J. Yu, and Y. W. Kan. Induced pluripotent stem cells offer new approach to therapy in thalassemia and sickle cell anemia and option in prenatal diagnosis in genetic diseases. *Proc Natl Acad Sci U S A*, 106(24):9826–30, 2009.

Y. C. Yeh, H. J. Wei, W. Y. Lee, C. L. Yu, Y. Chang, L. W. Hsu, M. F. Chung, M. S. Tsai, S. M. Hwang, and H. W. Sung. Cellular cardiomyoplasty with human amniotic fluid stem cells: In vitro and in vivo studies. *Tissue Eng Part A*, 16(6):1925–36, 2010.

M. Yoneyama and T. Fujita. Recognition of viral nucleic acids in innate immunity. *Rev Med Virol*, 20(1):4–22, 2010.

M. Yoshida, M. Kijima, M. Akita, and T. Beppu. Potent and specific inhibition of mammalian histone deacetylase both in vivo and in vitro by trichostatin a. *J Biol Chem*, 265(28):17174–9, 1990.

Q. You, X. Tong, Y. Guan, D. Zhang, M. Huang, Y. Zhang, and J. Zheng. The biological characteristics of human third trimester amniotic fluid stem cells. *J Int Med Res*, 37(1):105–12, 2009.

J. I. Young and J. R. Smith. Dna methyltransferase inhibition in normal human fibroblasts induces a p21-dependent cell cycle withdrawal. *J Biol Chem*, 276(22):19610–6, 2001.

J. Yu, M. A. Vodyanik, K. Smuga-Otto, J. Antosiewicz-Bourget, J. L. Frane, S. Tian, J. Nie, G. A. Jonsdottir, V. Ruotti, R. Stewart, I. Slukvin, and J. A. Thomson. Induced pluripotent stem cell lines derived from human somatic cells. *Science (80-)*, 318(5858):1917–20, 2007.

J. Yu, K. Hu, K. Smuga-Otto, S. Tian, R. Stewart, I. Slukvin, and J. A. Thomson. Human induced pluripotent stem cells free of vector and transgene sequences. *Science (80-)*, 324 (5928):797–801, 2009.

J. Yu, K. F. Chau, M. A. Vodyanik, J. Jiang, and Y. Jiang. Efficient feeder-free episomal reprogramming with small molecules. *PLoS ONE*, 6(3):e17557, 2011.

K. Yusa, S. T. Rashid, H. Strick-Marchand, I. Varela, P. Q. Liu, D. E. Paschon, E. Miranda, A. Ordonez, N. R. Hannan, F. J. Rouhani, S. Darche, G. Alexander, S. J. Marciniak, N. Fusaki, M. Hasegawa, M. C. Holmes, J. P. Di Santo, D. A. Lomas, A. Bradley, and L. Vallier. Targeted gene correction of alpha1-antitrypsin deficiency in induced pluripotent stem cells. *Nature*, 478(7369):391–4, 2011.

H. Zaehres, M. W. Lensch, L. Daheron, S. A. Stewart, J. Itskovitz-Eldor, and G. Q. Daley. High-efficiency rna interference in human embryonic stem cells. *Stem Cells*, 23(3):299–305, 2005.

G. Zafarana, S. R. Avery, K. Avery, H. D. Moore, and P. W. Andrews. Specific knockdown of oct4 in human embryonic stem cells by inducible short hairpin rna interference. *Stem Cells*, 27(4):776–82, 2009.

J. Zhang, I. Khvorostov, J. S. Hong, Y. Oktay, L. Vergnes, E. Nuebel, P. N. Wahjudi, K. Setoguchi, G. Wang, A. Do, H. J. Jung, J. M. McCaffery, I. J. Kurland, K. Reue, W. N. Lee, C. M. Koehler, and M. A. Teitell. Ucp2 regulates energy metabolism and differentiation potential of human pluripotent stem cells. *EMBO J*, 30(24):4860–73, 2011a.

S. Zhang, S. Chen, W. Li, X. Guo, P. Zhao, J. Xu, Y. Chen, Q. Pan, X. Liu, D. Zychlinski, H. Lu, M. D. Tortorella, A. Schambach, Y. Wang, D. Pei, and M. A. Esteban. Rescue of atp7b function in hepatocyte-like cells from wilson's disease induced pluripotent stem cells using gene therapy or the chaperone drug curcumin. *Hum Mol Genet*, 20(16):3176–87, 2011b.

R. Zhao and G. Q. Daley. From fibroblasts to ips cells: induced pluripotency by defined factors. *J Cell Biochem*, 105(4):949–55, 2008.

Y. Zhao, X. Yin, H. Qin, F. Zhu, H. Liu, W. Yang, Q. Zhang, C. Xiang, P. Hou, Z. Song, Y. Liu, J. Yong, P. Zhang, J. Cai, M. Liu, H. Li, Y. Li, X. Qu, K. Cui, W. Zhang, T. Xiang, Y. Wu, C. Liu, C. Yu, K. Yuan, J. Lou, M. Ding, and H. Deng. Two supporting factors greatly improve the efficiency of human ipsc generation. *Cell Stem Cell*, 3(5):475–9, 2008.

Q. H. Zheng, L. W. Ma, W. G. Zhu, Z. Y. Zhang, and T. J. Tong. p21waf1/cip1 plays a critical role in modulating senescence through changes of dna methylation. *J Cell Biochem*, 98(5): 1230–48, 2006.

J. Zhou, P. Su, L. Wang, J. Chen, M. Zimmermann, O. Genbacev, O. Afonja, M. C. Horne, T. Tanaka, E. Duan, S. J. Fisher, J. Liao, and F. Wang. mtor supports long-term self-renewal and suppresses mesoderm and endoderm activities of human embryonic stem cells. *Proc Natl Acad Sci U S A*, 106(19):7840–5, 2009.

W. Zhou and C. R. Freed. Adenoviral gene delivery can reprogram human fibroblasts to induced pluripotent stem cells. *Stem Cells*, 27(11):2667–74, 2009.

Z. Zhou, N. Wang, S. E. Woodson, Q. Dong, J. Wang, Y. Liang, R. Rijnbrand, L. Wei, J. E. Nichols, J. T. Guo, M. R. Holbrook, S. M. Lemon, and K. Li. Antiviral activities of isg20 in positive-strand rna virus infections. *Virology*, 409(2):175–88, 2011.

S. Zhu, W. Li, H. Zhou, W. Wei, R. Ambasudhan, T. Lin, J. Kim, K. Zhang, and S. Ding. Reprogramming of human primary somatic cells by oct4 and chemical compounds. *Cell Stem Cell*, 7(6):651–5, 2010.

J. Zou, M. L. Maeder, P. Mali, S. M. Pruett-Miller, S. Thibodeau-Beganny, B. K. Chou, G. Chen, Z. Ye, I. H. Park, G. Q. Daley, M. H. Porteus, J. K. Joung, and L. Cheng. Gene targeting of a disease-related gene in human induced pluripotent stem and embryonic stem cells. *Cell Stem Cell*, 5(1):97–110, 2009.

T. P. Zwaka and J. A. Thomson. Homologous recombination in human embryonic stem cells. *Nat Biotechnol*, 21(3):319–21, 2003.

T. P. Zwaka and J. A. Thomson. Differentiation of human embryonic stem cells occurs through symmetric cell division. *Stem Cells*, 23(2):146–9, 2005.

Curriculum Vitae

For reasons of data protection, the curriculum vitae is not included in the online version.

Publications

Wolfrum K, Wang Y, Prigione A, Sperling K, Lehrach H, Adjaye J (2010): The LARGE Principle of Cellular Reprogramming: Lost, Acquired and Retained Gene Expression in Foreskin and Amniotic Fluid-Derived Human iPS Cells. *PLoS One* 5(10):e13703.

Drews K*, Tavernier G*, Demeester J, Lehrach H, De Smedt SC, Rejman J, Adjaye J (2012): The cytotoxic and immunogenic hurdles associated with non-viral mRNA-mediated reprogramming of human fibroblasts. *Biomaterials*, 33(16):4059-68.
(* shared first authors)

Drews K, Jozefczuk J, Prigione A, Adjaye J: Human induced pluripotent stem—from mechanisms to clinical applications. *Journal of Molecular Medicine*, in press.

Drews K, Aldahmash A, Adjaye J: Functional genomics of induced pluripotent stem cells. In: Embryonic, Induced Pluripotent and Adult Stem Cells: From Basic Research to Clinical Applications, King Saud University, book chapter in press.

Wang Y, Mah N, Prigione A, Wolfrum K, Andrade-Navarro MA, Adjaye J (2010): A transcriptional roadmap to the induction of pluripotency. *Stem Cell Reviews and Reports* 6(2):282-96.

Mah N, Wang Y, Liao MC, Prigione A, Jozefczuk J, Lichtner B, Wolfrum K, Haltmeier M, Schaefer M, Hahn A, Andrade-Navarro MA, Adjaye J (2011): Molecular Insights into Reprogramming-Initiation Events Mediated by the OSKM Gene Regulatory Network. *PLoS ONE* 6(8):e24351.

Tavernier G, Wolfrum K, Demeester J, De Smedt SC, Adjaye J, Rejman J (2012): Activation of pluripotency-associated genes in mouse embryonic fibroblasts by non-viral transfection with in vitro-derived mRNAs encoding Oct4, Sox2, Klf4 and cMyc. *Biomaterials* 33(2):412-7.

Thierbach R, Florian S, Wolfrum K, Voigt A, Drewes G, Blume U, Bannasch P, Ristow M, Steinberg P (2012): Specific alterations of carbohydrate metabolism are associated with hepatocarcinogenesis in mitochondrially impaired mice. *Human Molecular Genetics* 21(3):656-63.

Flöttmann M, Scharp T, Wang Y, Drews K, Cheng X, Wölfl S, Hahn A, Gul S, Mah N, Andrade-Navarro MA, Klipp E, Wolf G, Adjaye J, Mrowka R (2012): Wie aus Hautzellen

Leberzellen werden – Neue Wege zur Reprogrammierung von Körperzellen. *Systembiologie.de* 04:44-48; available from http://www.systembiologie.de/.

Jozefczuk J, Drews K, Adjaye J: Preparation of mouse embryonic fibroblast cells suitable for culturing human embryonic and induced pluripotent stem cells. *Journal of Visualized Experiments*, manuscript in press.

Moschidou D, Mukherjee S, Blundell MP, Drews K, Jones GN, Abdulrazzak H, Nowakowska B, Phoolchund A, Lay K, Ramasamy TS, Cananzi M, Nettersheim D, Sullivan MHF, Frost J, Moore G, Vermeesch JR, Fisk NM, Thrasher AJ, Atala A, Adjaye J, Schorle H, De Coppi P, Guillot PV: Valproic acid confers functional pluripotency to human amniotic fluid stem cells in a transgene-free approach. *Molecular Therapy*, manuscript accepted.

Prigione A, Rohwer N, Drews K, Blümlein K, Bukowiecki R, Lehrach H, Ralser M, Cramer T, Adjaye J: HIF1α drives early induction of pluripotency through reprogramming of glycolytic metabolism. *Cell Research*, manuscript under review.

Qiu W,Andersen TE, Chen L, Abdallah B, Drews K, Adjaye J, Kassem M: High bone mass phenotype is associated with impaired interferon signaling in skeletal (mesenchymal) stem cells: Potential mechanism for enhanced bone formation by Wnt singalling. Manuscript in preparation.

Andersen RK, Zaher W, Larsen KH, Drews K, Kassem M, Abdallah B.: Identification of a predictive molecular signature for *ex vivo* migration of human mesenchymal stromal cells. Manuscript in preparation.

Zusammenfassung (German abstract)

Die Entwicklung humaner induzierter pluripotenter Stammzellen (induced pluripotent stem cells, iPSCs) aus somatischen Zellen eröffnet ungeahnte Möglichkeiten für Forschung und Medizin. Der Verwendung von iPSCs zu therapeutischen Zwecken stehen derzeit jedoch die mit der viralen Reprogrammierung einhergehenden Modifikationen des Genoms im Wege. Das Streben nach alternativen, nicht-mutagenen Reprogrammierungsmethoden ist aufgrund deren geringerer Effizienz eng an die Identifizierung von Zelltypen gekoppelt, die sich einfacher in das Entwicklungsstadium embryonaler Stammzellen (embryonic stem cells, ESCs) zurückversetzen lassen. Humane Fruchtwasserzellen (amniotic fluid cells, AFCs) werden routinemäßig isoliert und weisen Stammzell-ähnliche Eigenschaften auf. Dadurch sind AFCs vermutlich auch durch ineffizientere nicht-mutagenen Methoden zu reprogrammieren. Ziel dieser Arbeit war es, mithilfe viraler und nicht-viraler Techniken aus AFCs iPSCs zu generieren und diese vergleichend zu charakterisieren. Dabei sollten auch humane ESCs, als Standard für pluripotente Stammzellen, sowie iPSCs aus Zellen anderer Gewebe (Fibroblasten-iPSCs, FiPSCs) einbezogen werden. Die retrovirale Reprogrammierung führte schnell und effizient zur Umwandlung humaner AFCs in iPSCs (AFiPSCs). Diese iPSCs glichen human ESCs im Hinblick auf die Morphologie, Proliferation und die Expression von Stammzellmarkern. Ihre Fähigkeit, Zelltypen aller drei embryonalen Keimblätter zu bilden, konnte sowohl *in vitro* als auch *in vivo* bestätigt werden. Als Ergebnis der Behandlung der AFiPSCs mit BMP2 und BMP4 wurde darüber hinaus ihr Potential in Zelllinien des Trophoblasten zu differenzieren demonstriert. Eine detaillierte Microaray-basierte Analyse des Transkriptoms von ESCs, AFiPCs, FiPSCs sowie der jeweiligen parentalen Zellen bestätigte die Aktivität eines transkriptionell regulatorischen Netzwerks in allen pluripotenten Stammzellen. Gleichzeitig wurden beispielsweise aber auch charakteristische Genexpressionsmuster in den verschiedenen identifiziert, die nach der Reprogrammierung erhalten blieben. Diese und ähnliche Befunde wurden im sogenannten “LARGE Principle of Cellular Reprogramming” zusammengefasst. Eine genetische Manipulation der AFiPSCs zur Gen-Funktionsanalyse konnte nicht realisiert werden. Versuche, humane AFCs durch nicht-virale, nicht-mutagene Methoden, wie der Nukleofektion von episomalen Plasmiden oder der Transfektion von Reprogrammierungsfaktoren-kodierenden mRNAs, zu reprogrammieren, scheiterten. Die ausführliche Untersuchung der Ursachen dafür ergab, dass die schwerwiegende Aktivierung einer Interferon-regulierten Immunantwort die Reprogrammierung maßgeblich hemmte. Anschließende

Versuche, diese Immunabwehr durch geeignete immunmodulatorische Substanzen zu unterbinden, blieben jedoch ohne Erfolg. Die im Laufe dieser Arbeit ermittelten Daten stellen dennoch eine wichtige Grundlage für weiterführende Tests dar. Zusammenfassend konnte anhand dieser Arbeit der Stellenwert humaner AFCs für die Generierung von iPSCs hervorgehoben werden. Dabei wurden jedoch auch bestehende Hindernisse aufgezeigt, welche einer potentiellen Anwendung von AFiPSCs zu therapeutischen Zwecken noch im Wege stehen.

A

Supplementary Material and Methods

A.1 Composition and preparation of cell culture media and solutions

A.1.1 'DeCoppi medium' for AFC culture

Components to make 500 ml:

315 ml	α-MEM (Gibco)
75 ml	ESC-qualified fetal bovine serum (ES-FBS, Gibco)
5 ml	L-glutamine (200 mM, Lonza)
5 ml	Penicillin/Streptomycin (PS, 10,000 U/ml each, Lonza)
90 ml	Chang B (Trinova Biochem, Giessen, Germany)

Mix all components and filter (Corning, 0.22µm, PAS).

Supplement with 10 ml Chang C (Trinova Biochem).

A.1.2 BJ, HFF1, HEK293 and PA culture medium

Components to make 500 ml:

450 ml	DMEM (high glucose, Gibco)
50 ml	FBS (Biochrom)

A.1.3 MEF culture medium

Components to make 500 ml:

435 ml	DMEM (high glucose)
50 ml	FBS
5 ml	L-glutamine
5 ml	Non-essential amino acids (NEAA, 100 ×, Gibco)
5 ml	PS

Mix all components and filter.

Preparation of human basic fibroblast growth factor (bFGF, FGF2)

Recombinant human basic fibroblast growth factor (bFGF, FGF2, Peprotech) was dissolved in sterile-filtered PBS containing 0.2 % BSA (Fraction V, 99 % purity, Sigma) at a concentration

of 8 µg/ml. Aliquots were kept at -20 °C.

A.1.4 Unconditioned medium (UM) for human ESC culture

Components to make 500 ml:

385 ml	Knockout DMEM (KO-DMEM, Gibco)
100 ml	Knockout Serum Replacement (KO-SR, Gibco)
5 ml	L-glutamine
5 ml	PS
5 ml	NEAA
35 µl	of 0.14 M β-mercaptoethanol (Sigma), pre-diluted 1:10 in PBS, sterile-filtered

Mix all components and filter. Supplement with 4 ng/ml FGF2 right before use on human PSCs.

A.1.5 Preparation of Matrigel stock solution and Matrigel-coated labware

Growth factor-reduced Matrigel solution (BD) was thawed on ice at 4 °C ON, mixed with KO-DMEM as suggested for the particular batch by the manufacturer, aliquoted and re-frozen. Chilled pipettes and tubes were used whenever Matrigel was diluted. To coat plastic tissue culture labware with Matrigel, aliquots of the stock solution were thawed again (preferably at 4 °C), diluted 1:14 with cold KO-DMEM, dispensed into the required amount of wells or flasks (1.5 ml per well of a six well plate) covering the entire bottom of each well. The plate was sealed with PARAFILM M (Pechiney Plastic Packaging) and kept at 4 °C (10 d maximum).

A.1.6 Defined (N2B27) medium for human PSC culture

Components to make 50 ml:

47 ml	DMEM/F12 (Gibco)
0.5 ml	N2 Supplement (100 ×, Invitrogen)
1 ml	B27 Supplement minus Vitamin A (50 ×, Invitrogen)
340 µl	BSA (Bovine Albumin Fraction V, 7.5 %, Gibco)
0.5 ml	L-glutamine
0.5 ml	PS
0.5 ml	NEAA
3.5 µl	of 0.14 M β-mercaptoethanol, pre-diluted 1:10 in PBS, sterile-filtered

Mix all components and filter.

A.1.7 Freezing media

AFCs:	10 % DMSO (Sigma) in ES-FBS
HFF1, BJ:	10 % DMSO, 50 % FBS in DMEM
HEK293, PA cells:	10 % DMSO, 40 % FBS in DMEM
MEFs:	10 % DMSO, 50 % FBS in DMEM
Human PSCs:	10 % DMSO, 50 % KO-SR in KO-DMEM

A.2 Transformation protocol

Competent *E.coli*, e.g. JM109, cells were thawed on ice. 50 µl bacterial suspension were mixed with 1 µg of plasmid DNA and incubated on ice for 5 min. The cells were heat shocked in a 42 °C water bath for 50 s and put back on ice for 3 min, followed by a 30 min recovering incubation in 1 ml LB medium lacking antibiotics shaking at 175 rpm at 37 °C. *E.coli* were pelleted by centrifugation at 1500 × g for 5 min. The supernatant was poured off and the remaining drop of medium was used to resuspend the cells. Next, 50-100 µl of this suspension was spread onto LB/antibiotic agar plates and the cultures were incubated at 37 °C ON. Single colonies were picked under sterile conditions 12-16 h later and expanded. To prepare glycerol stocks, the cell suspension resulting from the expansion of a single picked colony, was mixed with LB medium containing 30 % glycerol at a ratio of 1:1 and frozen at -80 °C for long-term storage.

A.3 PCR, qRT-PCR and gel electrophoresis

A.3.1 10 × B1 PCR buffer

500 mM	Tris-HCl, pH = 8.8
200 mM	$(NH_4)_2SO_4$
15 mM	$MgCl_2$
0.1 %	Tween 20

in ddH_2O.

A.3.2 Fingerprinting PCR

Reaction master mix, 20 µl per reaction:

ddH_2O	15.75 µl
10 X B1 buffer	2.5 µl
25 mM dNTP mix (1:1:1:1)	0.25 µl
1 µM forward primer	0.5 µl
1 µM reverse primer	0.5 µl
Pfu-Polymerase (10 U/µl)	0.1 µl
Taq-Polymerase (10 U/µl)	0.4 µl
template DNA (15 ng/µl)	5.0 µl
	→ 25 µl/reaction

Fingerprinting PCR cycle protocol:

(35 cycles)	1 min	94 °C
	1 min	55 °C
	1 min	72 °C
	∞	4 °C

If the first PCR reaction did not result in sufficient amplification products, the same PCR was repeated including the following modifications:

ddH_2O	8.25 µl instead of 15.75 µl
5 M Betaine	7.5 µl

0.2 to 1.0 µl of the first reaction mixture were adjusted to a volume of 5 µl with ddH_2O and input as DNA template for re-amplification.

A.3.3 20 × SB electrophoresis buffer

NaOH	8 g
Boric Acid	45 g

ad 1 l with ddH_2O, adjust pH to 8.0.

A.3.4 qRT-PCR cycle protocol

Hold	50 °C	2 min
hold	95 °C	10 min
(40 cycles)	95 °C	15 sec
	60 °C	1 min
	95 °C	15 sec
	60 °C	15 sec
	95 °C	15 sec

A.4 Antibodies, plasmids, primers

Table A.1: List of antibodies used for the immunofluorescent protein labeling procedure.

Human antigen	Species raised in	Company	Catalog no.	Dilution
Primary antibodies				
CD117, APC-conjugated	mouse	Invitrogen	CD11705	1:20
OCT3/4 (C-10)	mouse	Santa Cruz Biotechnology	sc-5279	1:100
SOX2 (Y-17)	goat	SCB	sc-17320	1:100
GKLF (H-180)	rabbit	SCB	sc-20691	1:100

Continued on next page

Table A.1 – *Continued from previous page*

Human antigen	Species raised in	Company	Catalog no.	Dilution
c-MYC (N-262)	rabbit	SCB	sc-764	1:100
LIN28	rabbit	Proteintech	11724-1-AP	1:400
NANOG	goat	R&D Systems	AF1997	1:100
SSEA4	mouse	Millipore	SCR001	1:100
TRA-1-60	mouse	Millipore	SCR001	1:100
TRA-1-81	mouse	Millipore	SCR001	1:100
E-CADHERIN (CDH1)	mouse	BD Biosciences	610181	1:80
VIMENTIN (VIM)	mouse	Sigma-Aldrich	V6630	1:80
SOX17	goat	R&D Systems	AF1924	1:100
ALPHA FETOPROTEIN (AFP)	mouse	Sigma-Aldrich	WH0000174M1	1:300
SMOOTH MUSCLE ACTIN (SMA)	mouse	DakoCytomation	M0851	1:100
NESTIN (NES)	mouse	Millipore	MAB5326	1:200
CLASS III BETA TUBULIN (TUJ1)	mouse	Sigma-Aldrich	T8660	1:400
CHORIONIC GONADOTROPIN BETA (hCGb)	mouse	Abcam	ab763	1:800
Secondary antibodies				
anti-goat IgG, Alexa fluor 488	donkey	Invitrogen	A11055	1:300
anti-goat IgG, Alexa fluor 594	chicken	Invitrogen	A21468	1:300
anti-mouse IgG, Alexa fluor 488	goat	Invitrogen	A11001	1:300
anti-mouse IgG, Alexa fluor 594	goat	Invitrogen	A11005	1:300
anti-rabbit IgG, Alexa fluor 488	donkey	Invitrogen	A21206	1:300
anti-rabbit IgG, Alexa fluor 594	chicken	Invitrogen	A21442	1:300

Table A.2: List of plasmids used for the production of viral particles, nucleofection, lipofection and *in vitro* transcription.

Plasmid	**Company**	**Encoded gene product**	***E.coli* strain**	**Growth medium**	**Antibiotic**	**Restriction enzyme for diagnostic digest**
Retroviral reprogramming:						
pMXs-hOCT3/4	17217, Addgene	OCT4	JM109	LB medium	Ampicillin (100 µg/ml)	*Xho*I
pMXs-hSOX2	17218, Addgene	SOX2	JM109	LB medium	Ampicillin (100 µg/ml)	*Not*I
pMXs-hKLF4	17219, Addgene	KLF4	JM109	LB medium	Ampicillin (100 µg/ml)	*Not*I
pMXs-hc-MYC	17220, Addgene	c-MYC	JM109	LB medium	Ampicillin (100 µg/ml)	*Not*I
pLIB GFP	(PT3189-5, Clontech)	GFP	JM109	LB medium	Ampicillin (100 µg/ml)	—
USP44 knock down:						
pLKO.1-puro_non-target shRNA	SHC002, Sigma	Non-target shRNA	JM109	TB medium	Carbenicillin (100 µg/ml)	—
pLKO.1-puro_TRCN0000038814	Sigma	shRNA against *USP44* (clone: NM_032147.1-2653s1c1)	n/a	TB medium	Carbenicillin (100 µg/ml)	—
pLKO.1-puro_TRCN0000038815	Sigma	shRNA against *USP44* (clone: NM_032147.1-830s1c1)	n/a	TB medium	Carbenicillin (100 µg/ml)	—
pLKO.1-puro_TRCN0000038816	Sigma	shRNA against *USP44* (clone: NM_032147.1-2364s1c1)	n/a	TB medium	Carbenicillin (100 µg/ml)	—

Continued on next page

Table A.2 – *Continued from previous page*

Plasmid	**Company**	**Encoded gene product**	***E.coli* strain**	**Growth medium**	**Antibiotic**	**Restriction enzyme for diagnostic digest**
pLKO.1-puro_TRCN0000038817	Sigma	shRNA against *USP44* (clone: NM_032147.1-449s1c1)	n/a	TB medium	Carbenicillin (100 µg/ml)	—
pLKO.1-puro_TGFP	SHC003, Sigma	TurboGFP	JM109	TB medium	Carbenicillin (100 µg/ml)	—
phOCT4-EGFP	Dr. W. Cui	EGFP	TOP10	LB medium	Kanamycin (50 µg/ml),	—
Episomal plasmid-mediated reprogramming:						
pEP4 E02S EN2L ('4F EN2L')	20922 Addgene	OCT4, SOX2, NANOG, LIN28	n/a	LB medium	Ampicillin (100 µg/ml)	*Bam*HI, *Eco*RI
pEP4 E02S EM2K ('EM2K')	20923 Addgene	OCT4, SOX2, c-MYC, KLF4	n/a	LB medium	Ampicillin (100 µg/ml)	*Bam*HI, *Eco*RI, *Nsi*I
pEP4 E02S CK2M EN2L ('6F EN2L')	20924 Addgene	OCT4, SOX2, KLF4, c-MYC, NANOG, LIN28,	n/a	LB medium	Ampicillin (100 µg/ml)	*Bam*HI, *Nsi*I
pEP4 E02S EN2K ('EN2K')	20925 Addgene	OCT4, SOX2, NANOG, KLF4	n/a	LB medium	Ampicillin (100 µg/ml)	*Bam*HI, *Eco*RI
pCEP4-M2L ('M2L')	20926 Addgene	c-MYC, LIN28	n/a	LB medium	Ampicillin (100 µg/ml)	*Spe*I, *Hind*III
pEP4 E02S ET2K ('ET2K')	20927 Addgene	OCT4, SOX2, SV40LT, KLF4	n/a	LB medium	Ampicillin (100 µg/ml)	*Bam*HI, *Eco*RI, *Nsi*I
IVT, mRNA-mediated reprogramming:						
pcDNA3.3_OCT4	26816, Addgene	OCT4	DH5a	LB medium	Ampicillin (100 µg/ml)	—
pcDNA3.3_SOX2	26817, Addgene	SOX2	DH5a	LB medium	Ampicillin (100 µg/ml)	—

Continued on next page

Table A.2 – *Continued from previous page*

Plasmid	**Company**	**Encoded gene product**	***E.coli* strain**	**Growth medium**	**Antibiotic**	**Restriction enzyme for diagnostic digest**
pcDNA3.3_KLF4	26815, Addgene	KLF4	DH5a	LB medium	Ampicillin (100 µg/ml)	—
pcDNA3.3_c-MYC	26818, Addgene	c-MYC	DH5a	LB medium	Ampicillin (100 µg/ml)	—
pcDNA3.3_LIN28A	26819, Addgene	LIN28A	DH5a	LB medium	Ampicillin (100 µg/ml)	—
pGEM4Z-EGFP-A64	Prof. Dr. E. Gilboa	GFP	KRX	LB medium	Ampicillin (100 µg/ml)	—

LB medium: 10 g NaCl, 10 g Peptone (Roth), 5 g yeast extract (Sigma) in 1 l ddH_2O; TB medium: complete TB medium (basal TB medium + TB Phosphates, AppliChem, Darmstadt, Germany).

Table A.3: List of primers used for qRT-PCR and DNA fingerprinting analyses.

Gene	Sequence forward primer (5‘-3’)	Sequence reverse primer (5‘-3’)	Amplicon length [bp]
qRT-PCR, housekeeping genes:			
ACTB	TCAAGATCATTGCTCCTCCTGAG	ACATCTGCTGGAAGGTGGACA	87
GAPDH	CTGGTAAAGTGGATATTGTTGCCAT	TGGAATCATATTGGAACATGTAAACC	81
qRT-PCR, retrovirus-mediated reprogramming:			
CDX2	TCACTACAGTCGCTACATCACCATC	TTAACCTGCCTCTCAGAGAGCC	78
CER1	ACCACGATGCACTTGCCACT	CCGTCTTCACCTTGCACTGG	94
DNMT3B	GCTCACAGGGCCCGATACTT	GCAGTCCTGCAGCTCGAGTTTA	93
DPPA4	TGGTGTCAGGTGGTGTGTGG	CCAGGCTTGACCAGCATGAA	91
FGF4	CCCTTCTTCACCGATGAGTGC	CATTCTTGCTCAGGGCGATG	109
FOXF1	AAAGGAGCCACGAAGCAAGC	AGGCTGAAGCGAAGGAAGAGG	81
GATA3	ACTCCAGCCACATGCTGACC	AGCATCGAGCAGGGCTCTAAC	117
GDF3	TTGGCACAAGTGGATCATTGC	TTGGCACAAGTGGATCATTGC	96
HAND1	TCCCTTTTCCGCTTGCTCTC	CATCGCCTACCTGATGGACG	114
ID2	AATCCTGCAGCACGTCATCG	CTGGTGATGCAGGCTGACAA	85
KRT7	AGATCGCCACCTACCGCAAG	ATTCACGGCTCCCACTCCAT	74
LEFTY1	AATGTGTCATTGTTTACTTGTCCTGTC	CAGGTCTTAGGTCCAGAGTGGTG	76
NANOG	CCTGTGATTTGTGGGCCTG	GACAGTCTCCGTGTGAGGCAT	78
POU5F1	GTGGAGGAAGCTGACAACAA	ATTCTCCAGGTTGCCTCTCA	120
SOX2	GTATCAGGAGTTGTCAAGGCAGAG	TCCTAGTCTTAAAGAGGCAGCAAAC	78
TERT	ACGGCGACATGGAGAACAAG	GAGGTGTCACCAACAAGAAATCATC	90
qRT-PCR, non-viral reprogramming:			
CCL5	CATATTCCTCGGACACCACA	GAGCACTTGCCACTGGTGTA	100
c-MYC	ACTCTGAGGAGGAACAAGAA	TGGAGACGTGGCACCTCTT	159
IFIT1	AAAAGCCCACATTTGAGGTG	GAAATTCCTGAAACCGACCA	168

Continued on next page

Table A.3 – *Continued from previous page*

Gene	Sequence forward primer (5‘-3’)	Sequence reverse primer (5‘-3’)	Amplicon length [bp]
IFNB	CATTACCTGAAGGCCAAGGA	CAGCATCTGCTGGTTGAAGA	178
IL12A	TGGCCCTGTGCCTTAGTAGT	CAGAAGCTTTGCATTCATGG	80
IRF7	GGGTGTGTCTTCCCTGGATA	GCTCCATAAGGAAGCACTCG	92
ISG20	CAGAACAGCCTGCTTGGAC	CGGATTCTCTGGGAGATTTG	80
KLF4	GGGCCCAATTACCCATCCTT	CTTTGGCTTGGGCTCCTCTG	114
LIN28A	GTCTGGAATCCATCCGTGTC	TCCTTTTGATCTGCGCTTCT	101
OAS1	CGATCCCAGGAGGTATCAGA	TCCAGTCCTCTTCTGCCTGT	116
PKR	TCGCTGGTATCACTCGTCTG	GATTCTGAAGACCGCCAGAG	183
PODXL	CAGCATCAACTACCCACCGATAC	GATCCTCACACTTTGCCCAGTTAC	81
POU5F1	GTGGAGGAAGCTGACAACAA	ATTCTCCAGGTTGCCTCTCA	120
RIG-I	GTTGTCCCCATGCTGTTCTT	GCAAGTCTTACATGGCAGCA	124
SOX2	AACCAGAAAAACAGCCCGGACCG	GGTTCTCCTGGGCCATCTTGCG	94
STAT2	GACTGAAATCATCCGCCATT	GGATTCGGGGATAGAGGAAG	83
TRIM5	GAGAAGCTCAGGGAGGTCAA	CTCACAAAGCCAGCAAATGA	123
PCR, DNA fingerprinting:			
D7S796	TTTTGGTATTGGCCATCCTA	GAAAGGAACAGAGAGACAGGG	—
D10S1214	ATTGCCCCAAAACTTTTTTG	TTGAAGACCAGTCTGGGAAG	—
D21S2055	AACAGAACCAATAGGCTATCTATC	TACAGTAAATCACTTGGTAGGAGA	—

B

Supporting Data

Table B.1: List of 116 senescence-associated genes derived from the Gene Ontology database (Ashburner et al., 2000), including those described by Vaziri et al. (2010). These genes served as input for the differential gene expression analysis between AFCs (P17) and the group of all AFiPSC lines. Modified from (Wolfrum et al., 2010).

Symbol	Definition
ACD	Homo sapiens adrenocortical dysplasia homolog (mouse) (ACD), mRNA.
AKT1	Homo sapiens v-akt murine thymoma viral oncogene homolog 1 (AKT1), transcript variant 3, mRNA.
ATM	Homo sapiens ataxia telangiectasia mutated (includes complementation groups A, C and D) (ATM), transcript variant 1, mRNA.
ATR	Homo sapiens ataxia telangiectasia and Rad3 related (ATR), mRNA.
BCL2	Homo sapiens B-cell CLL/lymphoma 2 (BCL2), nuclear gene encoding mitochondrial protein, transcript variant beta, mRNA.
BLM	Homo sapiens Bloom syndrome (BLM), mRNA.
BRCA1	Homo sapiens breast cancer 1, early onset (BRCA1), transcript variant BRCA1-delta11b, mRNA.
BRCA2	Homo sapiens breast cancer 2, early onset (BRCA2), mRNA.
C20ORF52	Homo sapiens chromosome 20 open reading frame 52 (C20orf52), mRNA.
CALR	Homo sapiens calreticulin (CALR), mRNA.
CBX1	Homo sapiens chromobox homolog 1 (HP1 beta homolog Drosophila) (CBX1), mRNA.
CBX5	Homo sapiens chromobox homolog 5 (HP1 alpha homolog, Drosophila) (CBX5), mRNA.
CBX6	Homo sapiens chromobox homolog 6 (CBX6), mRNA.
CDC2	Homo sapiens cell division cycle 2, G1 to S and G2 to M (CDC2), transcript variant 2, mRNA.
CDKN1A	Homo sapiens cyclin-dependent kinase inhibitor 1A (p21, Cip1) (CDKN1A), transcript variant 2, mRNA.
CDKN2A	Homo sapiens cyclin-dependent kinase inhibitor 2A (melanoma, p16, inhibits CDK4) (CDKN2A), transcript variant 4, mRNA.
CDT1	Homo sapiens chromatin licensing and DNA replication factor 1 (CDT1), mRNA.
CHEK1	Homo sapiens CHK1 checkpoint homolog (S. pombe) (CHEK1), mRNA.

Continued on next page

Table B.1 – *Continued from previous page*

Symbol	Definition
CHEK2	Homo sapiens CHK2 checkpoint homolog (S. pombe) (CHEK2), transcript variant 1, mRNA.
DCLRE1C	Homo sapiens DNA cross-link repair 1C (PSO2 homolog, S. cerevisiae) (DCLRE1C), transcript variant c, mRNA.
DDIT3	Homo sapiens DNA-damage-inducible transcript 3 (DDIT3), mRNA.
DKC1	Homo sapiens dyskeratosis congenita 1, dyskerin (DKC1), mRNA.
DNAJA3	Homo sapiens DnaJ (Hsp40) homolog, subfamily A, member 3 (DNAJA3), mRNA.
DNMT1	Homo sapiens DNA (cytosine-5-)-methyltransferase 1 (DNMT1), mRNA.
DNMT3B	Homo sapiens DNA (cytosine-5-)-methyltransferase 3 beta (DNMT3B), transcript variant 6, mRNA.
DOT1L	Homo sapiens DOT1-like, histone H3 methyltransferase (S. cerevisiae) (DOT1L), mRNA.
EMD	Homo sapiens emerin (Emery-Dreifuss muscular dystrophy) (EMD), mRNA.
ENG	Homo sapiens endoglin (Osler-Rendu-Weber syndrome 1) (ENG), mRNA.
EXO1	Homo sapiens exonuclease 1 (EXO1), transcript variant 3, mRNA.
FANCF	Homo sapiens Fanconi anemia, complementation group F (FANCF), mRNA.
FEN1	Homo sapiens flap structure-specific endonuclease 1 (FEN1), mRNA.
FOXM1	Homo sapiens forkhead box M1 (FOXM1), transcript variant 1, mRNA.
GADD45A	Homo sapiens growth arrest and DNA-damage-inducible, alpha (GADD45A), mRNA.
GDF15	Homo sapiens growth differentiation factor 15 (GDF15), mRNA.
GMCL1	Homo sapiens germ cell-less homolog 1 (Drosophila) (GMCL1), mRNA.
H2AFX	Homo sapiens H2A histone family, member X (H2AFX), mRNA.
HADH2	Homo sapiens hydroxyacyl-Coenzyme A dehydrogenase, type II (HADH2), transcript variant 1, mRNA.
HELLS	Homo sapiens helicase, lymphoid-specific (HELLS), mRNA.
HIST2H2AC	Homo sapiens histone cluster 2, H2ac (HIST2H2AC), mRNA.
HIST2H2BE	Homo sapiens histone cluster 2, H2be (HIST2H2BE), mRNA.
HRAS	Homo sapiens v-Ha-ras Harvey rat sarcoma viral oncogene homolog (HRAS), transcript variant 2, mRNA.
IGFBP6	Homo sapiens insulin-like growth factor binding protein 6 (IGFBP6), mRNA.
ILK	Homo sapiens integrin-linked kinase (ILK), transcript variant 1, mRNA.
KRAS	Homo sapiens v-Ki-ras2 Kirsten rat sarcoma viral oncogene homolog (KRAS), transcript variant b, mRNA.
LBR	Homo sapiens lamin B receptor (LBR), transcript variant 1, mRNA.
LIMS1	Homo sapiens LIM and senescent cell antigen-like domains 1 (LIMS1), mRNA.
LMNA	Homo sapiens lamin A/C (LMNA), transcript variant 2, mRNA.
LMNB1	Homo sapiens lamin B1 (LMNB1), mRNA.
MAD2L2	Homo sapiens MAD2 mitotic arrest deficient-like 2 (yeast) (MAD2L2), mRNA.
MAP2K1	Homo sapiens mitogen-activated protein kinase kinase 1 (MAP2K1), mRNA.
MDC1	Homo sapiens mediator of DNA damage checkpoint 1 (MDC1), mRNA.
MDM2	Homo sapiens Mdm2, transformed 3T3 cell double minute 2, p53 binding protein (mouse) (MDM2), transcript variant MDM2, mRNA.

Continued on next page

Table B.1 – *Continued from previous page*

Symbol	Definition
MNT	Homo sapiens MAX binding protein (MNT), mRNA.
MORC3	Homo sapiens MORC family CW-type zinc finger 3 (MORC3), mRNA.
MORF4	Homo sapiens mortality factor 4 (MORF4), mRNA.
MRE11A	Homo sapiens MRE11 meiotic recombination 11 homolog A (S. cerevisiae) (MRE11A), transcript variant 1, mRNA.
MSH2	Homo sapiens mutS homolog 2, colon cancer, nonpolyposis type 1 (E. coli) (MSH2), mRNA.
MSH6	Homo sapiens mutS homolog 6 (E. coli) (MSH6), mRNA.
MYC	Homo sapiens v-myc myelocytomatosis viral oncogene homolog (avian) (MYC), mRNA.
NCL	Homo sapiens nucleolin (NCL), mRNA.
NHP2L1	Homo sapiens NHP2 non-histone chromosome protein 2-like 1 (S. cerevisiae) (NHP2L1), transcript variant 1, mRNA.
NOLA1	Homo sapiens nucleolar protein family A, member 1 (H/ACA small nucleolar RNPs) (NOLA1), transcript variant 2, mRNA.
NOX4	Homo sapiens NADPH oxidase 4 (NOX4), mRNA.
NPM1	Homo sapiens nucleophosmin (nucleolar phosphoprotein B23, numatrin) (NPM1), transcript variant 2, mRNA.
NRAS	Homo sapiens neuroblastoma RAS viral (v-ras) oncogene homolog (NRAS), mRNA.
NUP62	Homo sapiens nucleoporin 62kDa (NUP62), transcript variant 1, mRNA.
PARP1	Homo sapiens poly (ADP-ribose) polymerase family, member 1 (PARP1), mRNA.
PCNA	Homo sapiens proliferating cell nuclear antigen (PCNA), transcript variant 1, mRNA.
PDCD4	Homo sapiens programmed cell death 4 (neoplastic transformation inhibitor) (PDCD4), transcript variant 2, mRNA.
PIN1	Homo sapiens protein (peptidylprolyl cis/trans isomerase) NIMA-interacting 1 (PIN1), mRNA.
PLK1	Homo sapiens polo-like kinase 1 (Drosophila) (PLK1), mRNA.
PML	Homo sapiens promyelocytic leukemia (PML), transcript variant 2, mRNA.
POT1	Homo sapiens POT1 protection of telomeres 1 homolog (S. pombe) (POT1), transcript variant 2, transcribed RNA.
POU2F1	Homo sapiens POU class 2 homeobox 1 (POU2F1), mRNA.
PRELP	Homo sapiens proline/arginine-rich end leucine-rich repeat protein (PRELP), transcript variant 2, mRNA.
PRKCD	Homo sapiens protein kinase C, delta (PRKCD), transcript variant 2, mRNA.
PRKDC	Homo sapiens protein kinase, DNA-activated, catalytic polypeptide (PRKDC), transcript variant 1, mRNA.
RAD9A	Homo sapiens RAD9 homolog A (S. pombe) (RAD9A), mRNA.
RAI17	Homo sapiens zinc finger, MIZ-type containing 1 (ZMIZ1), mRNA.
RB1	Homo sapiens retinoblastoma 1 (including osteosarcoma) (RB1), mRNA.
RBL1	Homo sapiens retinoblastoma-like 1 (p107) (RBL1), transcript variant 1, mRNA.

Continued on next page

Table B.1 – *Continued from previous page*

Symbol	Definition
RBL2	Homo sapiens retinoblastoma-like 2 (p130) (RBL2), mRNA.
RFC2	Homo sapiens replication factor C (activator 1) 2, 40kDa (RFC2), transcript variant 1, mRNA.
RGN	PREDICTED: Homo sapiens regucalcin (senescence marker protein-30), transcript variant 1 (RGN), mRNA.
RIF1	Homo sapiens RAP1 interacting factor homolog (yeast) (RIF1), mRNA.
RPA1	Homo sapiens replication protein A1, 70kDa (RPA1), mRNA.
RPA2	Homo sapiens replication protein A2, 32kDa (RPA2), mRNA.
RPA3	Homo sapiens replication protein A3, 14kDa (RPA3), mRNA.
SERPINE1	Homo sapiens serpin peptidase inhibitor, clade E (nexin, plasminogen activator inhibitor type 1), member 1 (SERPINE1), mRNA.
SIRT1	Homo sapiens sirtuin (silent mating type information regulation 2 homolog) 1 (S. cerevisiae) (SIRT1), mRNA.
SIRT6	Homo sapiens sirtuin (silent mating type information regulation 2 homolog) 6 (S. cerevisiae) (SIRT6), mRNA.
SMG1	Homo sapiens PI-3-kinase-related kinase SMG-1 (SMG1), mRNA.
SMG6	Homo sapiens Smg-6 homolog, nonsense mediated mRNA decay factor (C. elegans) (SMG6), mRNA.
SNURF	Homo sapiens SNRPN upstream reading frame (SNURF), transcript variant 1, mRNA.
SOD1	Homo sapiens superoxide dismutase 1, soluble (amyotrophic lateral sclerosis 1 (adult)) (SOD1), mRNA.
SRF	Homo sapiens serum response factor (c-fos serum response element-binding transcription factor) (SRF), mRNA.
SUV39H1	Homo sapiens suppressor of variegation 3-9 homolog 1 (Drosophila) (SUV39H1), mRNA.
SUV39H2	Homo sapiens suppressor of variegation 3-9 homolog 2 (Drosophila) (SUV39H2), mRNA.
SUV420H1	Homo sapiens suppressor of variegation 4-20 homolog 1 (Drosophila) (SUV420H1), transcript variant 1, mRNA.
SUV420H2	Homo sapiens suppressor of variegation 4-20 homolog 2 (Drosophila) (SUV420H2), mRNA.
SYNE1	Homo sapiens spectrin repeat containing, nuclear envelope 1 (SYNE1), transcript variant alpha, mRNA.
TBX2	Homo sapiens T-box 2 (TBX2), mRNA.
TBX3	Homo sapiens T-box 3 (ulnar mammary syndrome) (TBX3), transcript variant 2, mRNA.
TERF1	Homo sapiens telomeric repeat binding factor (NIMA-interacting) 1 (TERF1), transcript variant 1, mRNA.
TERF2	Homo sapiens telomeric repeat binding factor 2 (TERF2), mRNA.
TERT	Homo sapiens telomerase reverse transcriptase (TERT), transcript variant 1, mRNA.
TINF2	Homo sapiens TERF1 (TRF1)-interacting nuclear factor 2 (TINF2), mRNA.
TNKS1BP1	Homo sapiens tankyrase 1 binding protein 1, 182kDa (TNKS1BP1), mRNA.

Continued on next page

Table B.1 – *Continued from previous page*

Symbol	Definition
TNKS2	Homo sapiens tankyrase, TRF1-interacting ankyrin-related ADP-ribose polymerase 2 (TNKS2), mRNA.
TP53	Homo sapiens tumor protein p53 (Li-Fraumeni syndrome) (TP53), mRNA.
TP73L	Homo sapiens tumor protein p73-like (TP73L), mRNA.
TPP1	Homo sapiens tripeptidyl peptidase I (TPP1), mRNA.
TRIOBP	Homo sapiens TRIO and F-actin binding protein (TRIOBP), transcript variant 1, mRNA.
WRN	Homo sapiens Werner syndrome (WRN), mRNA.
XPA	Homo sapiens xeroderma pigmentosum, complementation group A (XPA), mRNA.
ZNF146	Homo sapiens zinc finger protein 146 (ZNF146), mRNA.

Table B.2: List of 148 genes overlapping in reprogramming factor-transfected fibroblasts and the union of FiPSCs and ESCs (reported in Figure 4.6 C). Modified from Drews et al. (2012).

Symbol	Definition
ADRA1B	Homo sapiens adrenergic, alpha-1B-, receptor (ADRA1B), mRNA.
ANKRD1	Homo sapiens ankyrin repeat domain 1 (cardiac muscle) (ANKRD1), mRNA.
ARHGAP17	Homo sapiens Rho GTPase activating protein 17 (ARHGAP17), transcript variant 1, mRNA.
ARHGEF10L	Homo sapiens Rho guanine nucleotide exchange factor (GEF) 10-like (ARHGEF10L), transcript variant 1, mRNA.
ARL6IP4	Homo sapiens ADP-ribosylation-like factor 6 interacting protein 4 (ARL6IP4), transcript variant 4, mRNA.
ARL9	Homo sapiens ADP-ribosylation factor-like 9 (ARL9), mRNA.
ASPHD2	Homo sapiens aspartate beta-hydroxylase domain containing 2 (ASPHD2), mRNA.
ATP8B4	Homo sapiens ATPase, class I, type 8B, member 4 (ATP8B4), mRNA.
BBS7	Homo sapiens Bardet-Biedl syndrome 7 (BBS7), transcript variant 1, mRNA.
BCAP29	Homo sapiens B-cell receptor-associated protein 29 (BCAP29), transcript variant 4, mRNA.
BCKDHB	Homo sapiens branched chain keto acid dehydrogenase E1, beta polypeptide (maple syrup urine disease) (BCKDHB), nuclear gene encoding mitochondrial protein, transcript variant 1, mRNA.
BEST1	Homo sapiens bestrophin 1 (BEST1), mRNA.
BST2	Homo sapiens bone marrow stromal cell antigen 2 (BST2), mRNA.
BTN2A2	Homo sapiens butyrophilin, subfamily 2, member A2 (BTN2A2), transcript variant 1, mRNA.
C10orf35	Homo sapiens chromosome 10 open reading frame 35 (C10orf35), mRNA.
C12orf66	Homo sapiens chromosome 12 open reading frame 66 (C12orf66), mRNA.
C21orf91	Homo sapiens chromosome 21 open reading frame 91 (C21orf91), mRNA.
C5orf39	Homo sapiens chromosome 5 open reading frame 39 (C5orf39), mRNA.
CALML4	Homo sapiens calmodulin-like 4 (CALML4), transcript variant 1, mRNA.

Continued on next page

Table B.2 – *Continued from previous page*

Symbol	Definition
CCNT1	Homo sapiens cyclin T1 (CCNT1), mRNA.
CDC6	Homo sapiens cell division cycle 6 homolog (S. cerevisiae) (CDC6), mRNA.
CEACAM1	Homo sapiens carcinoembryonic antigen-related cell adhesion molecule 1 (biliary glycoprotein) (CEACAM1), transcript variant 2, mRNA.
CH25H	Homo sapiens cholesterol 25-hydroxylase (CH25H), mRNA.
CHRNB1	Homo sapiens cholinergic receptor, nicotinic, beta 1 (muscle) (CHRNB1), mRNA.
CORO7	Homo sapiens coronin 7 (CORO7), mRNA.
COX15	Homo sapiens COX15 homolog, cytochrome c oxidase assembly protein (yeast) (COX15), nuclear gene encoding mitochondrial protein, transcript variant 1, mRNA.
CPT1B	Homo sapiens carnitine palmitoyltransferase 1B (muscle) (CPT1B), nuclear gene encoding mitochondrial protein, transcript variant 4, mRNA.
CTH	Homo sapiens cystathionase (cystathionine gamma-lyase) (CTH), transcript variant 1, mRNA.
CXCL6	Homo sapiens chemokine (C-X-C motif) ligand 6 (granulocyte chemotactic protein 2) (CXCL6), mRNA.
CXCR7	Homo sapiens chemokine (C-X-C motif) receptor 7 (CXCR7), mRNA.
CYP11A1	Homo sapiens cytochrome P450, family 11, subfamily A, polypeptide 1 (CYP11A1), nuclear gene encoding mitochondrial protein, transcript variant 1, mRNA.
CYP2J2	Homo sapiens cytochrome P450, family 2, subfamily J, polypeptide 2 (CYP2J2), mRNA.
DHRS12	Homo sapiens dehydrogenase/reductase (SDR family) member 12 (DHRS12), transcript variant 2, mRNA.
DHRS2	Homo sapiens dehydrogenase/reductase (SDR family) member 2 (DHRS2), transcript variant 1, mRNA.
DLL1	Homo sapiens delta-like 1 (Drosophila) (DLL1), mRNA.
DMKN	Homo sapiens dermokine (DMKN), transcript variant 1, mRNA.
DNASE1L1	Homo sapiens deoxyribonuclease I-like 1 (DNASE1L1), transcript variant 1, mRNA.
DTNA	Homo sapiens dystrobrevin, alpha (DTNA), transcript variant 6, mRNA.
DUSP16	Homo sapiens dual specificity phosphatase 16 (DUSP16), mRNA.
E2F6	Homo sapiens E2F transcription factor 6 (E2F6), mRNA.
EGR2	Homo sapiens early growth response 2 (Krox-20 homolog, Drosophila) (EGR2), mRNA.
EPHB1	Homo sapiens EPH receptor B1 (EPHB1), mRNA.
FANCD2	Homo sapiens Fanconi anemia, complementation group D2 (FANCD2), transcript variant 2, mRNA.
FKBP1B	Homo sapiens FK506 binding protein 1B, 12.6 kDa (FKBP1B), transcript variant 2, mRNA.
FLJ10357	Homo sapiens hypothetical protein FLJ10357 (FLJ10357), mRNA.
FNDC3A	Homo sapiens fibronectin type III domain containing 3A (FNDC3A), transcript variant 1, mRNA.

Continued on next page

Table B.2 – *Continued from previous page*

Symbol	Definition
FOS	Homo sapiens v-fos FBJ murine osteosarcoma viral oncogene homolog (FOS), mRNA.
FOSB	Homo sapiens FBJ murine osteosarcoma viral oncogene homolog B (FOSB), mRNA.
FOXA1	Homo sapiens forkhead box A1 (FOXA1), mRNA.
FUZ	Homo sapiens fuzzy homolog (Drosophila) (FUZ), mRNA.
FZD8	Homo sapiens frizzled homolog 8 (Drosophila) (FZD8), mRNA.
GALNT10	Homo sapiens UDP-N-acetyl-alpha-D-galactosamine:polypeptide N-acetylgalactosaminyltransferase 10 (GalNAc-T10) (GALNT10), transcript variant 2, mRNA.
GALNT12	Homo sapiens UDP-N-acetyl-alpha-D-galactosamine:polypeptide N-acetylgalactosaminyltransferase 12 (GalNAc-T12) (GALNT12), mRNA.
GRB10	Homo sapiens growth factor receptor-bound protein 10 (GRB10), transcript variant 1, mRNA.
GSG1L	Homo sapiens GSG1-like (GSG1L), mRNA.
GZF1	Homo sapiens GDNF-inducible zinc finger protein 1 (GZF1), mRNA.
HDHD3	Homo sapiens haloacid dehalogenase-like hydrolase domain containing 3 (HDHD3), mRNA.
HIST1H4H	Homo sapiens histone cluster 1, H4h (HIST1H4H), mRNA.
IFI27	Homo sapiens interferon, alpha-inducible protein 27 (IFI27), transcript variant 2, mRNA.
IL1A	Homo sapiens interleukin 1, alpha (IL1A), mRNA.
IL20RB	Homo sapiens interleukin 20 receptor beta (IL20RB), mRNA.
IMAA	Homo sapiens SLC7A5 pseudogene (IMAA), non-coding RNA.
INHBE	Homo sapiens inhibin, beta E (INHBE), mRNA.
ISG20	Homo sapiens interferon stimulated exonuclease gene 20kDa (ISG20), mRNA.
ITGB2	Homo sapiens integrin, beta 2 (complement component 3 receptor 3 and 4 subunit) (ITGB2), mRNA.
JAG1	Homo sapiens jagged 1 (Alagille syndrome) (JAG1), mRNA.
KCNK1	Homo sapiens potassium channel, subfamily K, member 1 (KCNK1), mRNA.
KCNS1	Homo sapiens potassium voltage-gated channel, delayed-rectifier, subfamily S, member 1 (KCNS1), mRNA.
KIF5C	Homo sapiens kinesin family member 5C (KIF5C), mRNA.
KLHL26	Homo sapiens kelch-like 26 (Drosophila) (KLHL26), mRNA.
KLHL3	Homo sapiens kelch-like 3 (Drosophila) (KLHL3), mRNA.
LAMA1	Homo sapiens laminin, alpha 1 (LAMA1), mRNA.
LAMC2	Homo sapiens laminin, gamma 2 (LAMC2), transcript variant 2, mRNA.
LAMP3	Homo sapiens lysosomal-associated membrane protein 3 (LAMP3), mRNA.
LMO2	Homo sapiens LIM domain only 2 (rhombotin-like 1) (LMO2), mRNA.
LOC201175	Homo sapiens hypothetical protein LOC201175 (LOC201175), mRNA.
LPHN2	Homo sapiens latrophilin 2 (LPHN2), mRNA.
LRRC3	Homo sapiens leucine rich repeat containing 3 (LRRC3), mRNA.
MAD2L1BP	Homo sapiens MAD2L1 binding protein (MAD2L1BP), transcript variant 2, mRNA.

Continued on next page

Table B.2 – *Continued from previous page*

Symbol	Definition
MAGED1	Homo sapiens melanoma antigen family D, 1 (MAGED1), transcript variant 2, mRNA.
MESDC1	Homo sapiens mesoderm development candidate 1 (MESDC1), mRNA.
MID2	Homo sapiens midline 2 (MID2), transcript variant 1, mRNA.
MIER2	Homo sapiens mesoderm induction early response 1, family member 2 (MIER2), mRNA.
MMP10	Homo sapiens matrix metallopeptidase 10 (stromelysin 2) (MMP10), mRNA.
MTO1	Homo sapiens mitochondrial translation optimization 1 homolog (S. cerevisiae) (MTO1), nuclear gene encoding mitochondrial protein, transcript variant 1, mRNA.
NCOR2	Homo sapiens nuclear receptor co-repressor 2 (NCOR2), transcript variant 2, mRNA.
NDUFV3	Homo sapiens NADH dehydrogenase (ubiquinone) flavoprotein 3, 10kDa (NDUFV3), nuclear gene encoding mitochondrial protein, transcript variant 2, mRNA.
NELL1	Homo sapiens NEL-like 1 (chicken) (NELL1), mRNA.
NFKBIE	Homo sapiens nuclear factor of kappa light polypeptide gene enhancer in B-cells inhibitor, epsilon (NFKBIE), mRNA.
NSUN5C	Homo sapiens NOL1/NOP2/Sun domain family, member 5C (NSUN5C), transcript variant 1, mRNA.
NUDCD1	Homo sapiens NudC domain containing 1 (NUDCD1), mRNA.
PHF2	Homo sapiens PHD finger protein 2 (PHF2), mRNA.
PHF20L1	Homo sapiens PHD finger protein 20-like 1 (PHF20L1), transcript variant 2, mRNA.
PPIE	Homo sapiens peptidylprolyl isomerase E (cyclophilin E) (PPIE), transcript variant 1, mRNA.
PPIF	Homo sapiens peptidylprolyl isomerase F (cyclophilin F) (PPIF), nuclear gene encoding mitochondrial protein, mRNA.
PRKD2	Homo sapiens protein kinase D2 (PRKD2), mRNA.
PRKX	Homo sapiens protein kinase, X-linked (PRKX), mRNA.
PTGER4	Homo sapiens prostaglandin E receptor 4 (subtype EP4) (PTGER4), mRNA.
PTHLH	Homo sapiens parathyroid hormone-like hormone (PTHLH), transcript variant 3, mRNA.
PTPRR	Homo sapiens protein tyrosine phosphatase, receptor type, R (PTPRR), transcript variant 1, mRNA.
PUS3	Homo sapiens pseudouridylate synthase 3 (PUS3), mRNA.
RARRES3	Homo sapiens retinoic acid receptor responder (tazarotene induced) 3 (RARRES3), mRNA.
RASGRP3	Homo sapiens RAS guanyl releasing protein 3 (calcium and DAG-regulated) (RASGRP3), mRNA.
RBM38	Homo sapiens RNA binding motif protein 38 (RBM38), transcript variant 2, mRNA.
REC8	Homo sapiens REC8 homolog (yeast) (REC8), transcript variant 1, mRNA.

Continued on next page

Table B.2 – *Continued from previous page*

Symbol	Definition
RELB	Homo sapiens v-rel reticuloendotheliosis viral oncogene homolog B (RELB), mRNA.
RFTN2	Homo sapiens raftlin family member 2 (RFTN2), mRNA.
RG9MTD3	Homo sapiens RNA (guanine-9-) methyltransferase domain containing 3 (RG9MTD3), mRNA.
RNF144B	Homo sapiens ring finger 144B (RNF144B), mRNA.
RNF19B	Homo sapiens ring finger protein 19B (RNF19B), mRNA.
ROR2	Homo sapiens receptor tyrosine kinase-like orphan receptor 2 (ROR2), mRNA.
RPSA	Homo sapiens ribosomal protein SA (RPSA), transcript variant 1, mRNA.
RSPO2	Homo sapiens R-spondin 2 homolog (Xenopus laevis) (RSPO2), mRNA.
RSPO3	Homo sapiens R-spondin 3 homolog (Xenopus laevis) (RSPO3), mRNA.
RTKN	Homo sapiens rhotekin (RTKN), transcript variant 1, mRNA.
SEMA4D	Homo sapiens sema domain, immunoglobulin domain (Ig), transmembrane domain (TM) and short cytoplasmic domain, (semaphorin) 4D (SEMA4D), mRNA.
SH3BP1	Homo sapiens SH3-domain binding protein 1 (SH3BP1), mRNA.
SLC44A3	Homo sapiens solute carrier family 44, member 3 (SLC44A3), mRNA.
SLC46A1	Homo sapiens solute carrier family 46 (folate transporter), member 1 (SLC46A1), mRNA.
SLC6A9	Homo sapiens solute carrier family 6 (neurotransmitter transporter, glycine), member 9 (SLC6A9), transcript variant 3, mRNA.
SLCO4A1	Homo sapiens solute carrier organic anion transporter family, member 4A1 (SLCO4A1), mRNA.
SMG6	Homo sapiens Smg-6 homolog, nonsense mediated mRNA decay factor (C. elegans) (SMG6), mRNA.
SMOX	Homo sapiens spermine oxidase (SMOX), transcript variant 2, mRNA.
SOX8	Homo sapiens SRY (sex determining region Y)-box 8 (SOX8), mRNA.
STRA6	Homo sapiens stimulated by retinoic acid gene 6 homolog (mouse) (STRA6), mRNA.
SYT1	Homo sapiens synaptotagmin I (SYT1), mRNA.
SYT7	Homo sapiens synaptotagmin VII (SYT7), mRNA.
TAC3	Homo sapiens tachykinin 3 (neuromedin K, neurokinin beta) (TAC3), transcript variant 1, mRNA.
TACSTD2	Homo sapiens tumor-associated calcium signal transducer 2 (TACSTD2), mRNA.
TAGLN3	Homo sapiens transgelin 3 (TAGLN3), transcript variant 3, mRNA.
TCN2	Homo sapiens transcobalamin II; macrocytic anemia (TCN2), mRNA.
TESK2	Homo sapiens testis-specific kinase 2 (TESK2), mRNA.
TNFRSF10A	Homo sapiens tumor necrosis factor receptor superfamily, member 10a (TNFRSF10A), mRNA.
TNK2	Homo sapiens tyrosine kinase, non-receptor, 2 (TNK2), transcript variant 1, mRNA.
TSPAN33	Homo sapiens tetraspanin 33 (TSPAN33), mRNA.
TTC7A	Homo sapiens tetratricopeptide repeat domain 7A (TTC7A), mRNA.

Continued on next page

Table B.2 – *Continued from previous page*

Symbol	Definition
TXNL4B	Homo sapiens thioredoxin-like 4B (TXNL4B), mRNA.
UBE2L6	Homo sapiens ubiquitin-conjugating enzyme E2L 6 (UBE2L6), transcript variant 2, mRNA.
ULBP1	Homo sapiens UL16 binding protein 1 (ULBP1), mRNA.
VGF	Homo sapiens VGF nerve growth factor inducible (VGF), mRNA.
WWC1	Homo sapiens WW and C2 domain containing 1 (WWC1), mRNA.
ZFYVE16	Homo sapiens zinc finger, FYVE domain containing 16 (ZFYVE16), mRNA.
ZNF225	Homo sapiens zinc finger protein 225 (ZNF225), mRNA.
ZNF408	Homo sapiens zinc finger protein 408 (ZNF408), mRNA.
ZNF442	Homo sapiens zinc finger protein 442 (ZNF442), mRNA.
ZNF509	Homo sapiens zinc finger protein 509 (ZNF509), mRNA.
ZNF670	Homo sapiens zinc finger protein 670 (ZNF670), mRNA.
ZSCAN12	Homo sapiens zinc finger and SCAN domain containing 12 (ZSCAN12), mRNA.

Table B.3: Functional annotation and KEGG pathway enrichment analysis corresponding to the list of 148 genes overlapping in reprogramming factor-transfected fibroblasts and the union of FiPSCs and ESCs (reported in Figure 4.6 C). Modified from Drews et al. (2012).

Category	Term	Count	%	PValue
GOTERM_MF_FAT	GO:0005112~Notch binding	3	2.08	2.12E-03
GOTERM_BP_FAT	GO:0051591~response to cAMP	4	2.78	5.27E-03
SP_PIR_KEYWORDS	transmembrane protein	12	8.33	8.13E-03
INTERPRO	IPR013032:EGF-like region, conserved site	8	5.56	8.84E-03
GOTERM_BP_FAT	GO:0010817~regulation of hormone levels	6	4.17	8.99E-03
GOTERM_BP_FAT	GO:0007267~cell-cell signaling	12	8.33	1.23E-02
SP_PIR_KEYWORDS	heparin-binding	4	2.78	1.23E-02
GOTERM_BP_FAT	GO:0051180~vitamin transport	3	2.08	1.72E-02
KEGG_PATHWAY	hsa04010:MAPK signaling pathway	7	4.86	2.11E-02
SP_PIR_KEYWORDS	membrane	59	40.97	2.24E-02
OMIM_DISEASE	Systematic association mapping identifies NELL1 as a novel IBD disease gene	2	1.39	2.27E-02
SP_PIR_KEYWORDS	manganese	5	3.47	2.63E-02
SP_PIR_KEYWORDS	Rotamase	3	2.08	3.05E-02
INTERPRO	IPR001774:Delta/Serrate/lag-2 (DSL) protein	2	1.39	3.13E-02
SP_PIR_KEYWORDS	tumor antigen	3	2.08	3.20E-02
GOTERM_BP_FAT	GO:0008285~negative regulation of cell proliferation	8	5.56	3.30E-02
GOTERM_MF_FAT	GO:0030145~manganese ion binding	5	3.47	3.31E-02
GOTERM_MF_FAT	GO:0003755~peptidyl-prolyl cis-trans isomerase activity	3	2.08	3.41E-02

Continued on next page

Table B.3 – *Continued from previous page*

Category	Term	Count	%	PValue
SMART	SM00051:DSL	2	1.39	3.56E-02
UP_SEQ_FEATURE	domain:DSL	2	1.39	3.66E-02
GOTERM_MF_FAT	GO:0016859~cis-trans isomerase activity	3	2.08	3.75E-02
INTERPRO	IPR011651:Notch ligand, N-terminal	2	1.39	3.90E-02
GOTERM_BP_FAT	GO:0006865~amino acid transport	4	2.78	4.04E-02
INTERPRO	IPR008266:Tyrosine protein kinase, active site	4	2.78	4.19E-02
GOTERM_BP_FAT	GO:0055114~oxidation reduction	11	7.64	4.32E-02
SP_PIR_KEYWORDS	glycoprotein	42	29.17	4.37E-02
PIR_SUPERFAMILY	PIRSF001719:fos transforming protein	2	1.39	4.38E-02
SP_PIR_KEYWORDS	phosphoprotein	65	45.14	4.40E-02
GOTERM_MF_FAT	GO:0008201~heparin binding	4	2.78	4.74E-02
UP_SEQ_FEATURE	domain:Leucine-zipper	4	2.78	4.88E-02
SP_PIR_KEYWORDS	tyrosine-protein kinase	4	2.78	4.91E-02
GOTERM_BP_FAT	GO:0030097~hemopoiesis	6	4.17	4.93E-02
KEGG_PATHWAY	hsa04010:MAPK signaling pathway	7	4.86	2.11E-02

Table B.4: List of the top 100 up-regulated genes extracted from the 662 genes significantly up-regulated in fibroblasts upon transfection with mRNAs encoding reprogramming factors. The complete list is available from Drews et al. (2012).

Symbol	Definition	Ratio	p_{adj}
IFNB1	Homo sapiens interferon, beta 1, fibroblast (IFNB1), mRNA.	967.26	1.49E-03
CCL5	Homo sapiens chemokine (C-C motif) ligand 5 (CCL5), mRNA.	441.42	2.26E-02
RSAD2	Homo sapiens radical S-adenosyl methionine domain containing 2 (RSAD2), mRNA.	402.81	4.38E-36
IFI27	Homo sapiens interferon, alpha-inducible protein 27 (IFI27), transcript variant 2, mRNA.	397.68	4.38E-36
POU5F1	Homo sapiens POU class 5 homeobox 1 (POU5F1), transcript variant 1, mRNA.	309.93	4.38E-36
IFI44L	Homo sapiens interferon-induced protein 44-like (IFI44L), mRNA.	300.15	4.38E-36
OASL	Homo sapiens 2'-5'-oligoadenylate synthetase-like (OASL), transcript variant 1, mRNA.	244.22	2.73E-07
ISG20	Homo sapiens interferon stimulated exonuclease gene 20kDa (ISG20), mRNA.	241.68	4.38E-36
MX2	Homo sapiens myxovirus (influenza virus) resistance 2 (mouse) (MX2), mRNA.	241.26	4.38E-36
IL29	Homo sapiens interleukin 29 (interferon, lambda 1) (IL29), mRNA.	208.74	3.13E-02

Continued on next page

Table B.4 – *Continued from previous page*

Symbol	Definition	Ratio	p_{adj}
OAS2	Homo sapiens 2'-5'-oligoadenylate synthetase 2, 69/71kDa (OAS2), transcript variant 2, mRNA.	191.33	9.28E-23
OAS1	Homo sapiens 2',5'-oligoadenylate synthetase 1, 40/46kDa (OAS1), transcript variant 3, mRNA.	184.42	1.52E-19
HERC5	Homo sapiens hect domain and RLD 5 (HERC5), mRNA.	183.16	4.38E-36
CMPK2	Homo sapiens cytidine monophosphate (UMP-CMP) kinase 2, mitochondrial (CMPK2), nuclear gene encoding mitochondrial protein, mRNA.	154.10	4.38E-36
POU5F1P1	Homo sapiens POU class 5 homeobox 1 pseudogene 1 (POU5F1P1), non-coding RNA.	151.12	4.38E-36
IL28A	Homo sapiens interleukin 28A (interferon, lambda 2) (IL28A), mRNA.	135.51	4.33E-08
TNFSF10	Homo sapiens tumor necrosis factor (ligand) superfamily, member 10 (TNFSF10), mRNA.	115.84	4.38E-36
TNFSF13B	Homo sapiens tumor necrosis factor (ligand) superfamily, member 13b (TNFSF13B), mRNA.	115.74	9.89E-05
IFIT2	Homo sapiens interferon-induced protein with tetratricopeptide repeats 2 (IFIT2), mRNA.	95.23	4.38E-36
BST2	Homo sapiens bone marrow stromal cell antigen 2 (BST2), mRNA.	92.81	4.38E-36
IFIH1	Homo sapiens interferon induced with helicase C domain 1 (IFIH1), mRNA.	72.29	4.38E-36
HERC6	Homo sapiens hect domain and RLD 6 (HERC6), mRNA.	71.71	4.89E-11
MX1	Homo sapiens myxovirus (influenza virus) resistance 1, interferon-inducible protein p78 (mouse) (MX1), mRNA.	59.49	4.38E-36
BATF2	Homo sapiens basic leucine zipper transcription factor, ATF-like 2 (BATF2), mRNA.	59.03	4.38E-36
LGALS9	Homo sapiens lectin, galactoside-binding, soluble, 9 (LGALS9), transcript variant 1, mRNA.	58.45	3.42E-04
DDX58	Homo sapiens DEAD (Asp-Glu-Ala-Asp) box polypeptide 58 (DDX58), mRNA.	47.10	4.38E-36
EPSTI1	Homo sapiens epithelial stromal interaction 1 (breast) (EPSTI1), transcript variant 2, mRNA.	45.13	4.38E-36
RARRES3	Homo sapiens retinoic acid receptor responder (tazarotene induced) 3 (RARRES3), mRNA.	44.18	8.73E-04
CYP2J2	Homo sapiens cytochrome P450, family 2, subfamily J, polypeptide 2 (CYP2J2), mRNA.	41.39	4.41E-09
ISG15	Homo sapiens ISG15 ubiquitin-like modifier (ISG15), mRNA.	40.07	4.38E-36
IFIT3	Homo sapiens interferon-induced protein with tetratricopeptide repeats 3 (IFIT3), mRNA.	39.92	4.38E-36
IRF7	Homo sapiens interferon regulatory factor 7 (IRF7), transcript variant b, mRNA.	35.81	2.55E-25
GBP4	Homo sapiens guanylate binding protein 4 (GBP4), mRNA.	35.75	4.11E-02

Continued on next page

Table B.4 – *Continued from previous page*

Symbol	Definition	Ratio	p_{adj}
PSMB9	Homo sapiens proteasome (prosome, macropain) subunit, beta type, 9 (large multifunctional peptidase 2) (PSMB9), transcript variant 1, mRNA.	35.42	5.24E-19
IL28B	Homo sapiens interleukin 28B (interferon, lambda 3) (IL28B), mRNA.	33.83	2.03E-02
CFB	Homo sapiens complement factor B (CFB), mRNA.	32.60	5.19E-06
IFI35	Homo sapiens interferon-induced protein 35 (IFI35), mRNA.	32.54	4.38E-36
IFIT1	Homo sapiens interferon-induced protein with tetratricopeptide repeats 1 (IFIT1), transcript variant 2, mRNA.	31.23	4.38E-36
SLC15A3	Homo sapiens solute carrier family 15, member 3 (SLC15A3), mRNA.	30.54	4.38E-36
XAF1	Homo sapiens XIAP associated factor 1 (XAF1), transcript variant 2, mRNA.	29.57	6.87E-24
C15orf48	Homo sapiens chromosome 15 open reading frame 48 (C15orf48), transcript variant 2, mRNA.	26.12	9.36E-14
RTP4	Homo sapiens receptor (chemosensory) transporter protein 4 (RTP4), mRNA.	25.65	1.81E-03
DHX58	Homo sapiens DEXH (Asp-Glu-X-His) box polypeptide 58 (DHX58), mRNA.	24.58	4.38E-36
GMPR	Homo sapiens guanosine monophosphate reductase (GMPR), mRNA.	23.90	4.38E-36
PRIC285	Homo sapiens peroxisomal proliferator-activated receptor A interacting complex 285 (PRIC285), transcript variant 2, mRNA.	23.89	4.38E-36
IFI44	Homo sapiens interferon-induced protein 44 (IFI44), mRNA.	23.75	4.38E-36
APOBEC3G	Homo sapiens apolipoprotein B mRNA editing enzyme, catalytic polypeptide-like 3G (APOBEC3G), mRNA.	23.45	4.38E-36
PARP10	PREDICTED: Homo sapiens poly (ADP-ribose) polymerase family, member 10 (PARP10), mRNA.	23.18	4.38E-36
TMEM140	Homo sapiens transmembrane protein 140 (TMEM140), mRNA.	23.18	4.38E-36
DTX3L	Homo sapiens deltex 3-like (Drosophila) (DTX3L), mRNA.	21.84	2.31E-07
IFITM1	Homo sapiens interferon induced transmembrane protein 1 (9-27) (IFITM1), mRNA.	21.36	4.38E-36
PARP14	Homo sapiens poly (ADP-ribose) polymerase family, member 14 (PARP14), mRNA.	20.29	4.38E-36
PARP12	Homo sapiens poly (ADP-ribose) polymerase family, member 12 (PARP12), mRNA.	19.92	4.38E-36
CXCL16	Homo sapiens chemokine (C-X-C motif) ligand 16 (CXCL16), mRNA.	19.00	2.07E-18

Continued on next page

Table B.4 – *Continued from previous page*

Symbol	Definition	Ratio	p_{adj}
ECGF1	Homo sapiens endothelial cell growth factor 1 (platelet-derived) (ECGF1), mRNA.	18.93	5.89E-09
IL18BP	Homo sapiens interleukin 18 binding protein (IL18BP), transcript variant A, mRNA.	18.12	2.97E-03
UBA7	Homo sapiens ubiquitin-like modifier activating enzyme 7 (UBA7), mRNA.	18.01	4.38E-36
LAMP3	Homo sapiens lysosomal-associated membrane protein 3 (LAMP3), mRNA.	17.15	6.02E-03
TRIM22	Homo sapiens tripartite motif-containing 22 (TRIM22), mRNA.	17.12	4.38E-36
DDX60	Homo sapiens DEAD (Asp-Glu-Ala-Asp) box polypeptide 60 (DDX60), mRNA.	17.11	4.38E-36
SAMD9L	Homo sapiens sterile alpha motif domain containing 9-like (SAMD9L), mRNA.	17.02	4.38E-36
INDO	Homo sapiens indoleamine-pyrrole 2,3 dioxygenase (INDO), mRNA.	15.77	5.63E-06
PLSCR1	Homo sapiens phospholipid scramblase 1 (PLSCR1), mRNA.	15.72	4.38E-36
SP110	Homo sapiens SP110 nuclear body protein (SP110), transcript variant b, mRNA.	15.42	2.97E-27
SAMHD1	Homo sapiens SAM domain and HD domain 1 (SAMHD1), mRNA.	15.36	4.38E-36
ZMYND15	Homo sapiens zinc finger, MYND-type containing 15 (ZMYND15), mRNA.	15.26	7.60E-05
IFI6	Homo sapiens interferon, alpha-inducible protein 6 (IFI6), transcript variant 2, mRNA.	14.88	1.12E-23
KIAA1618	Homo sapiens KIAA1618 (KIAA1618), mRNA.	14.55	4.38E-36
UBE2L6	Homo sapiens ubiquitin-conjugating enzyme E2L 6 (UBE2L6), transcript variant 2, mRNA.	14.16	1.99E-07
PLEKHA4	Homo sapiens pleckstrin homology domain containing, family A (phosphoinositide binding specific) member 4 (PLEKHA4), mRNA.	13.25	4.38E-36
C19orf66	Homo sapiens chromosome 19 open reading frame 66 (C19orf66), mRNA.	13.14	4.38E-36
TAP1	Homo sapiens transporter 1, ATP-binding cassette, sub-family B (MDR/TAP) (TAP1), mRNA.	13.07	4.38E-36
MT1M	Homo sapiens metallothionein 1M (MT1M), mRNA.	12.41	4.38E-36
GBP5	Homo sapiens guanylate binding protein 5 (GBP5), mRNA.	12.00	4.22E-14
FBXO6	Homo sapiens F-box protein 6 (FBXO6), mRNA.	11.78	4.38E-36
RASGRP3	Homo sapiens RAS guanyl releasing protein 3 (calcium and DAG-regulated) (RASGRP3), mRNA.	11.26	8.33E-05
IFI30	Homo sapiens interferon, gamma-inducible protein 30 (IFI30), mRNA.	10.95	4.38E-36

Continued on next page

Table B.4 – *Continued from previous page*

Symbol	Definition	Ratio	p_{adj}
TRIM21	Homo sapiens tripartite motif-containing 21 (TRIM21), mRNA.	10.82	4.38E-36
LGALS3BP	Homo sapiens lectin, galactoside-binding, soluble, 3 binding protein (LGALS3BP), mRNA.	10.72	4.38E-36
SAMD9	Homo sapiens sterile alpha motif domain containing 9 (SAMD9), mRNA.	10.56	4.38E-36
MAFA	Homo sapiens v-maf musculoaponeurotic fibrosarcoma oncogene homolog A (avian) (MAFA), mRNA.	10.45	8.62E-05
MYD88	Homo sapiens myeloid differentiation primary response gene (88) (MYD88), mRNA.	10.25	4.38E-36
HIST1H4H	Homo sapiens histone cluster 1, H4h (HIST1H4H), mRNA.	10.12	3.59E-06
NCOA7	Homo sapiens nuclear receptor coactivator 7 (NCOA7), mRNA.	10.02	4.38E-36
HSH2D	Homo sapiens hematopoietic SH2 domain containing (HSH2D), mRNA.	9.97	1.48E-07
PARP9	Homo sapiens poly (ADP-ribose) polymerase family, member 9 (PARP9), mRNA.	9.84	7.06E-09
NELL1	Homo sapiens NEL-like 1 (chicken) (NELL1), mRNA.	9.56	4.38E-36
CD274	Homo sapiens CD274 molecule (CD274), mRNA.	9.56	4.38E-36
TAP2	Homo sapiens transporter 2, ATP-binding cassette, sub-family B (MDR/TAP) (TAP2), transcript variant 1, mRNA.	9.03	1.82E-19
NMI	Homo sapiens N-myc (and STAT) interactor (NMI), mRNA.	8.80	4.38E-36
MLKL	Homo sapiens mixed lineage kinase domain-like (MLKL), mRNA.	8.74	6.17E-04
CEACAM1	Homo sapiens carcinoembryonic antigen-related cell adhesion molecule 1 (biliary glycoprotein) (CEACAM1), transcript variant 2, mRNA.	8.69	9.79E-17
UNC93B1	Homo sapiens unc-93 homolog B1 (C. elegans) (UNC93B1), mRNA.	8.67	1.89E-12
GBP1	Homo sapiens guanylate binding protein 1, interferon-inducible, 67kDa (GBP1), mRNA.	8.66	4.38E-36
STAT1	Homo sapiens signal transducer and activator of transcription 1, 91kDa (STAT1), transcript variant alpha, mRNA.	8.32	4.38E-36
HES4	Homo sapiens hairy and enhancer of split 4 (Drosophila) (HES4), mRNA.	8.31	4.38E-36
WARS	Homo sapiens tryptophanyl-tRNA synthetase (WARS), transcript variant 2, mRNA.	8.30	4.38E-36
ZNFX1	Homo sapiens zinc finger, NFX1-type containing 1 (ZNFX1), mRNA.	8.02	4.38E-36
APOL6	Homo sapiens apolipoprotein L, 6 (APOL6), mRNA.	7.90	4.38E-36

Continued on next page

Table B.4 – *Continued from previous page*

Symbol	Definition	Ratio	p_{adj}
CXCL2	Homo sapiens chemokine (C-X-C motif) ligand 2 (CXCL2), mRNA.	7.78	4.61E-02

Table B.5: List of the top 100 down-regulated genes extracted from the 331 genes significantly down-regulated in fibroblasts upon transfection with mRNAs encoding reprogramming factors. The complete list is available from Drews et al. (2012).

Symbol	Definition	Ratio	p_{adj}
TNFRSF10D	Homo sapiens tumor necrosis factor receptor superfamily, member 10d, decoy with truncated death domain (TNFRSF10D), mRNA.	0.09	1.13E-03
ACO1	Homo sapiens aconitase 1, soluble (ACO1), mRNA.	0.15	2.16E-33
PIF1	Homo sapiens PIF1 5'-to-3' DNA helicase homolog (S. cerevisiae) (PIF1), mRNA.	0.18	1.19E-02
TNFAIP8L1	Homo sapiens tumor necrosis factor, alpha-induced protein 8-like 1 (TNFAIP8L1), mRNA.	0.19	2.73E-04
GSTM3	Homo sapiens glutathione S-transferase M3 (brain) (GSTM3), mRNA.	0.20	9.37E-04
FAM3C	Homo sapiens family with sequence similarity 3, member C (FAM3C), transcript variant 2, mRNA.	0.20	2.41E-13
NFIA	Homo sapiens nuclear factor I/A (NFIA), mRNA.	0.23	7.05E-03
MIB1	Homo sapiens mindbomb homolog 1 (Drosophila) (MIB1), mRNA.	0.24	8.14E-03
CEP70	Homo sapiens centrosomal protein 70kDa (CEP70), mRNA.	0.25	1.29E-11
NT5DC2	Homo sapiens 5'-nucleotidase domain containing 2 (NT5DC2), mRNA.	0.25	8.67E-36
C7orf41	Homo sapiens chromosome 7 open reading frame 41 (C7orf41), mRNA.	0.25	8.93E-07
PELI2	Homo sapiens pellino homolog 2 (Drosophila) (PELI2), mRNA.	0.25	4.45E-02
STK11	Homo sapiens serine/threonine kinase 11 (STK11), mRNA.	0.26	1.35E-02
NR2F6	Homo sapiens nuclear receptor subfamily 2, group F, member 6 (NR2F6), mRNA.	0.28	3.36E-21
HSPA12A	Homo sapiens heat shock 70kDa protein 12A (HSPA12A), mRNA.	0.29	2.07E-12
C9orf140	Homo sapiens chromosome 9 open reading frame 140 (C9orf140), mRNA.	0.29	4.09E-04
PRKCA	Homo sapiens protein kinase C, alpha (PRKCA), mRNA.	0.29	8.67E-36
FAM102B	Homo sapiens family with sequence similarity 102, member B (FAM102B), mRNA.	0.30	3.93E-05
BAX	Homo sapiens BCL2-associated X protein (BAX), transcript variant sigma, mRNA.	0.30	7.79E-06

Continued on next page

Table B.5 – *Continued from previous page*

Symbol	Definition	Ratio	p_{adj}
CERK	Homo sapiens ceramide kinase (CERK), transcript variant 2, mRNA.	0.30	3.83E-18
GREM2	Homo sapiens gremlin 2, cysteine knot superfamily, homolog (Xenopuslaevis) (GREM2), mRNA.	0.31	6.01E-04
HMGB3	Homo sapiens high-mobility group box 3 (HMGB3), mRNA.	0.31	5.01E-15
MEX3B	Homo sapiens mex-3 homolog B (C. elegans) (MEX3B), mRNA.	0.32	9.47E-04
VGLL3	Homo sapiens vestigial like 3 (Drosophila) (VGLL3), mRNA.	0.32	7.32E-09
USP47	Homo sapiens ubiquitin specific peptidase 47 (USP47), mRNA.	0.32	1.76E-02
HSD17B6	Homo sapiens hydroxysteroid (17-beta) dehydrogenase 6 homolog (mouse) (HSD17B6), mRNA.	0.32	1.85E-02
PCBD2	Homo sapiens pterin-4 alpha-carbinolaminedehydratase/dimerization cofactor of hepatocyte nuclear factor 1 alpha (TCF1) 2 (PCBD2), mRNA.	0.33	4.00E-02
SOX11	Homo sapiens SRY (sex determining region Y)-box 11 (SOX11), mRNA.	0.33	2.95E-16
TMEM168	Homo sapiens transmembrane protein 168 (TMEM168), mRNA.	0.34	5.88E-10
CDCA3	Homo sapiens cell division cycle associated 3 (CDCA3), mRNA.	0.34	2.96E-14
DLG7	Homo sapiens discs, large homolog 7 (Drosophila) (DLG7), mRNA.	0.34	2.25E-22
H2AFV	Homo sapiens H2A histone family, member V (H2AFV), transcript variant 2, mRNA.	0.34	1.47E-03
C19orf54	Homo sapiens chromosome 19 open reading frame 54 (C19orf54), mRNA.	0.35	9.44E-03
MAP4K2	Homo sapiens mitogen-activated protein kinase kinase kinase kinase 2 (MAP4K2), mRNA.	0.35	1.83E-33
OLFML2B	Homo sapiens olfactomedin-like 2B (OLFML2B), mRNA.	0.35	8.72E-07
FAM101B	Homo sapiens family with sequence similarity 101, member B (FAM101B), mRNA.	0.36	7.49E-19
NEK2	Homo sapiens NIMA (never in mitosis gene a)-related kinase 2 (NEK2), mRNA.	0.36	5.75E-05
RAB40B	Homo sapiens RAB40B, member RAS oncogene family (RAB40B), mRNA.	0.37	1.37E-07
GPSM2	Homo sapiens G-protein signalling modulator 2 (AGS3-like, C. elegans) (GPSM2), mRNA.	0.37	3.06E-11
GSTA4	Homo sapiens glutathione S-transferase A4 (GSTA4), mRNA.	0.38	1.79E-08

Continued on next page

Table B.5 – *Continued from previous page*

Symbol	Definition	Ratio	p_{adj}
ABHD8	Homo sapiens abhydrolase domain containing 8 (ABHD8), mRNA.	0.38	3.62E-11
CCNB1	Homo sapiens cyclin B1 (CCNB1), mRNA.	0.38	9.58E-06
PIM1	Homo sapiens pim-1 oncogene (PIM1), mRNA.	0.38	2.60E-05
HNRPA1L-2	Homo sapiens heterogeneous nuclear ribonucleoprotein A1 pseudogene (HNRPA1L-2), non-coding RNA.	0.39	3.01E-17
ARHGAP10	Homo sapiens Rho GTPase activating protein 10 (ARHGAP10), mRNA.	0.39	2.92E-16
ATXN1	Homo sapiens ataxin 1 (ATXN1), mRNA.	0.39	4.22E-02
KIF20A	Homo sapiens kinesin family member 20A (KIF20A), mRNA.	0.39	1.41E-16
TBC1D4	Homo sapiens TBC1 domain family, member 4 (TBC1D4), mRNA.	0.39	1.93E-03
TSHZ1	Homo sapiens teashirt zinc finger homeobox 1 (TSHZ1), mRNA.	0.40	1.34E-03
CNN1	Homo sapiens calponin 1, basic, smooth muscle (CNN1), mRNA.	0.40	4.31E-02
FHL1	Homo sapiens four and a half LIM domains 1 (FHL1), mRNA.	0.40	2.82E-04
SNAP23	Homo sapiens synaptosomal-associated protein, 23kDa (SNAP23), transcript variant 1, mRNA.	0.40	8.95E-05
DIXDC1	Homo sapiens DIX domain containing 1 (DIXDC1), transcript variant 1, mRNA.	0.40	3.30E-02
TBL1XR1	Homo sapiens transducin (beta)-like 1X-linked receptor 1 (TBL1XR1), mRNA.	0.40	7.46E-05
SDC2	Homo sapiens syndecan 2 (SDC2), mRNA.	0.41	8.02E-03
TXNDC12	Homo sapiens thioredoxin domain containing 12 (endoplasmic reticulum) (TXNDC12), mRNA.	0.41	1.80E-13
FAM171A1	Homo sapiens family with sequence similarity 171, member A1 (FAM171A1), mRNA.	0.41	1.65E-26
GAS2L3	Homo sapiens growth arrest-specific 2 like 3 (GAS2L3), mRNA.	0.41	1.10E-04
CENPF	Homo sapiens centromere protein F, 350/400ka (mitosin) (CENPF), mRNA.	0.41	2.07E-12
FAM64A	Homo sapiens family with sequence similarity 64, member A (FAM64A), mRNA.	0.41	1.25E-17
ASPM	Homo sapiens asp (abnormal spindle) homolog, microcephaly associated (Drosophila) (ASPM), mRNA.	0.41	5.33E-06
C5orf21	Homo sapiens chromosome 5 open reading frame 21 (C5orf21), mRNA.	0.41	1.09E-22
ITGAE	Homo sapiens integrin, alpha E (antigen CD103, human mucosal lymphocyte antigen 1; alpha polypeptide) (ITGAE), mRNA.	0.41	3.49E-20

Continued on next page

Table B.5 – *Continued from previous page*

Symbol	Definition	Ratio	p_{adj}
RAB22A	Homo sapiens RAB22A, member RAS oncogene family (RAB22A), mRNA.	0.41	6.76E-21
WNT5A	Homo sapiens wingless-type MMTV integration site family, member 5A (WNT5A), mRNA.	0.41	9.39E-20
MACF1	Homo sapiens microtubule-actin crosslinking factor 1 (MACF1), transcript variant 2, mRNA.	0.42	4.95E-03
PLK1	Homo sapiens polo-like kinase 1 (Drosophila) (PLK1), mRNA.	0.42	5.02E-12
FAM83D	Homo sapiens family with sequence similarity 83, member D (FAM83D), mRNA.	0.42	3.95E-21
C15orf23	Homo sapiens chromosome 15 open reading frame 23 (C15orf23), mRNA.	0.42	5.00E-09
APOLD1	Homo sapiens apolipoprotein L domain containing 1 (APOLD1), mRNA.	0.42	1.58E-07
EPHB4	Homo sapiens EPH receptor B4 (EPHB4), mRNA.	0.42	3.94E-06
PRRT2	Homo sapiens proline-rich transmembrane protein 2 (PRRT2), mRNA.	0.43	4.02E-06
WRB	Homo sapiens tryptophan rich basic protein (WRB), mRNA.	0.43	1.43E-11
AURKA	Homo sapiens aurora kinase A (AURKA), transcript variant 5, mRNA.	0.43	1.61E-13
CDC2L6	Homo sapiens cell division cycle 2-like 6 (CDK8-like) (CDC2L6), mRNA.	0.43	2.38E-22
HNRNPA0	Homo sapiens heterogeneous nuclear ribonucleoprotein A0 (HNRNPA0), mRNA.	0.43	4.13E-10
MKI67	Homo sapiens antigen identified by monoclonal antibody Ki-67 (MKI67), mRNA.	0.43	1.91E-03
CENPA	Homo sapiens centromere protein A (CENPA), transcript variant 2, mRNA.	0.43	1.45E-10
SLC35B4	Homo sapiens solute carrier family 35, member B4 (SLC35B4), mRNA.	0.43	8.27E-03
PREPL	Homo sapiens prolylendopeptidase-like (PREPL), transcript variant C, mRNA.	0.44	2.17E-08
CNTROB	Homo sapiens centrobin, centrosomal BRCA2 interacting protein (CNTROB), transcript variant 1, mRNA.	0.44	4.57E-03
PSRC1	Homo sapiens proline/serine-rich coiled-coil 1 (PSRC1), transcript variant 4, mRNA.	0.45	6.64E-05
TACC3	Homo sapiens transforming, acidic coiled-coil containing protein 3 (TACC3), mRNA.	0.45	1.65E-18
CCNB2	Homo sapiens cyclin B2 (CCNB2), mRNA.	0.45	7.04E-15
NEDD4L	Homo sapiens neural precursor cell expressed, developmentally down-regulated 4-like (NEDD4L), mRNA.	0.45	1.21E-05
YIF1A	Homo sapiens Yip1 interacting factor homolog A (S. cerevisiae) (YIF1A), mRNA.	0.45	1.50E-02

Continued on next page

Table B.5 – *Continued from previous page*

Symbol	Definition	Ratio	p_{adj}
DLEU1	Homo sapiens deleted in lymphocytic leukemia 1 (non-protein coding) (DLEU1), non-coding RNA.	0.45	1.05E-07
CENPE	Homo sapiens centromere protein E, 312kDa (CENPE), mRNA.	0.45	9.26E-05
SNRPD3	Homo sapiens small nuclear ribonucleoprotein D3 polypeptide 18kDa (SNRPD3), mRNA.	0.45	9.67E-04
CXXC5	Homo sapiens CXXC finger 5 (CXXC5), mRNA.	0.46	1.19E-02
CDCA8	Homo sapiens cell division cycle associated 8 (CDCA8), mRNA.	0.46	2.19E-08
ODF2	Homo sapiens outer dense fiber of sperm tails 2 (ODF2), transcript variant 2, mRNA.	0.46	9.48E-04
MXD3	Homo sapiens MAX dimerization protein 3 (MXD3), mRNA.	0.46	7.00E-03
SEPHS1	Homo sapiens selenophosphate synthetase 1 (SEPHS1), mRNA.	0.46	5.08E-19
PKNOX1	Homo sapiens PBX/knotted 1 homeobox 1 (PKNOX1), mRNA.	0.47	3.56E-04
GALNT11	Homo sapiens UDP-N-acetyl-alpha-D-galactosamine:polypeptide N-acetylgalactosaminyltransferase 11 (GalNAc-T11) (GALNT11), mRNA.	0.47	2.71E-04
TMEM119	Homo sapiens transmembrane protein 119 (TMEM119), mRNA.	0.47	9.75E-13
CYB5B	Homo sapiens cytochrome b5 type B (outer mitochondrial membrane) (CYB5B), nuclear gene encoding mitochondrial protein, mRNA.	0.47	5.77E-22
PPP2R5D	Homo sapiens protein phosphatase 2, regulatory subunit B', delta isoform (PPP2R5D), transcript variant 2, mRNA.	0.47	4.78E-07
KLHDC8B	Homo sapiens kelch domain containing 8B (KLHDC8B), mRNA.	0.47	3.53E-09

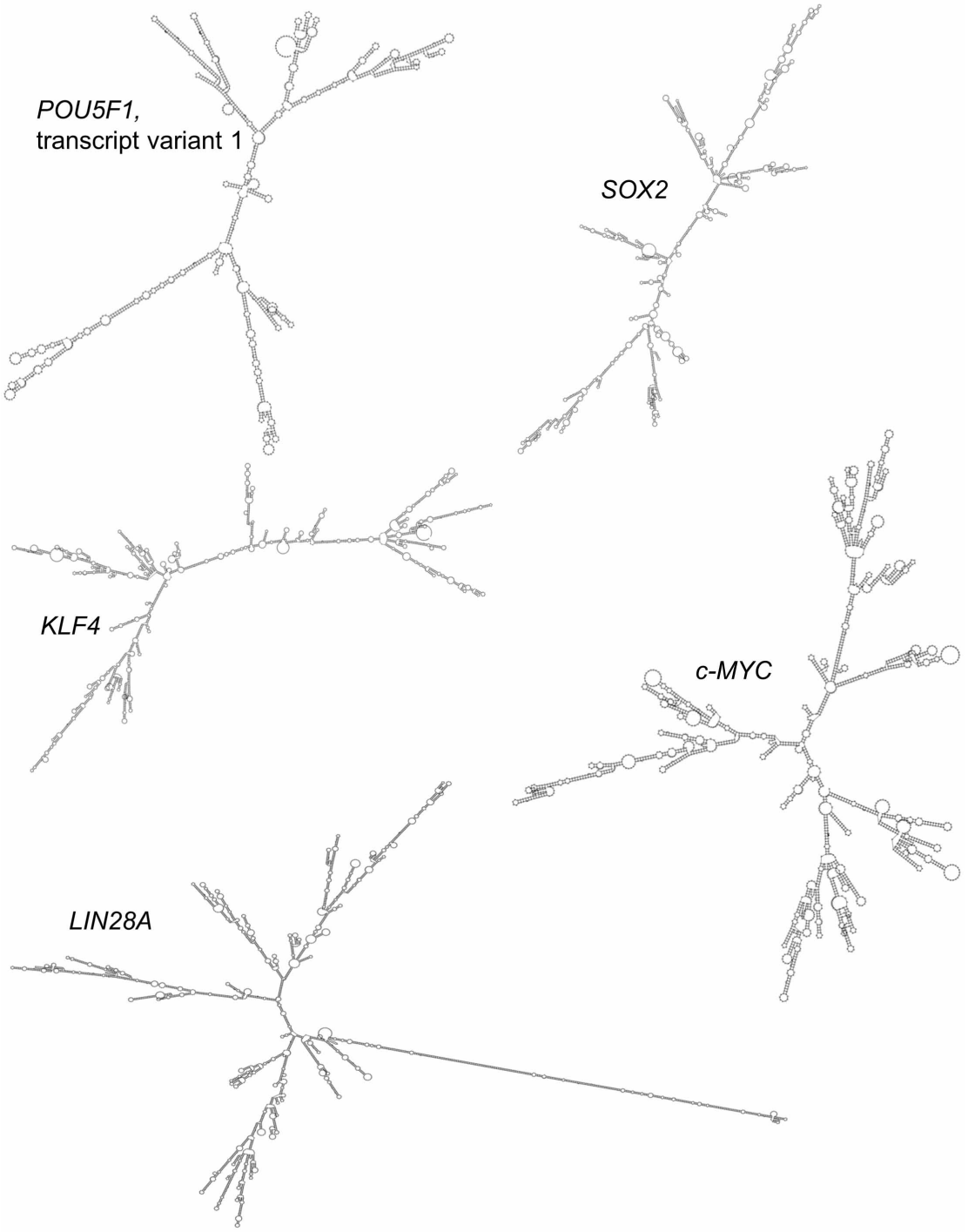

Figure B.1: Complex secondary structures of the reprogramming factor-encoding mRNAs. The depicted minimum free energy structures were predicted by the *RNAfold* WebServer (Gruber et al., 2008) on the basis of the mRNA sequence of each of the reprogramming factor genes.

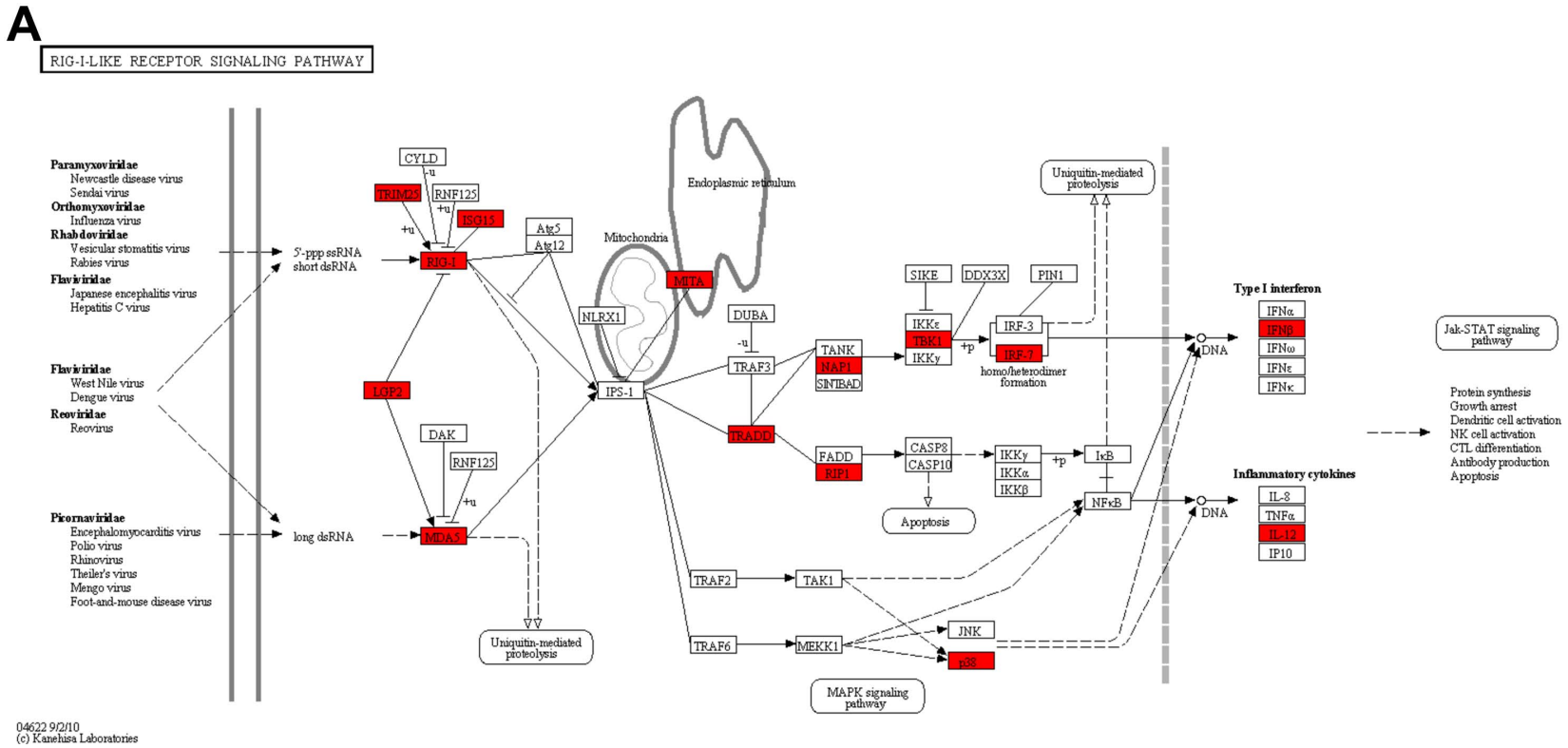

Figure B.2: KEGG pathway enrichment analysis of significantly differentially expressed genes in reprogramming factor-transfected fibroblasts with respect to mock-transfected control cells. The lists of 662 significantly up-regulated and 331 significantly down-regulated genes, obtained from the microarray-based transcriptome analysis of reprogramming factor mRNA vs. mock-transfected fibroblasts, were assessed for enrichment of genes involved in distinct cellular pathways using the DAVID database. (A, B, C) Selection of three KEGG pathways, which the list of 662 up-regulated genes was enriched for (Table 4.1). (D, E) Selection of two KEGG pathways the list of 331 down-regulated genes was significantly enriched for (Table 4.2. Genes, which are up-regulated in reprogramming factor mRNA-transfected fibroblasts in comparison to mock-transfected fibroblasts are highlighted in red, down-regulated genes are highlighted in green. Taken from Drews et al. (2012). – *Continued on next page*

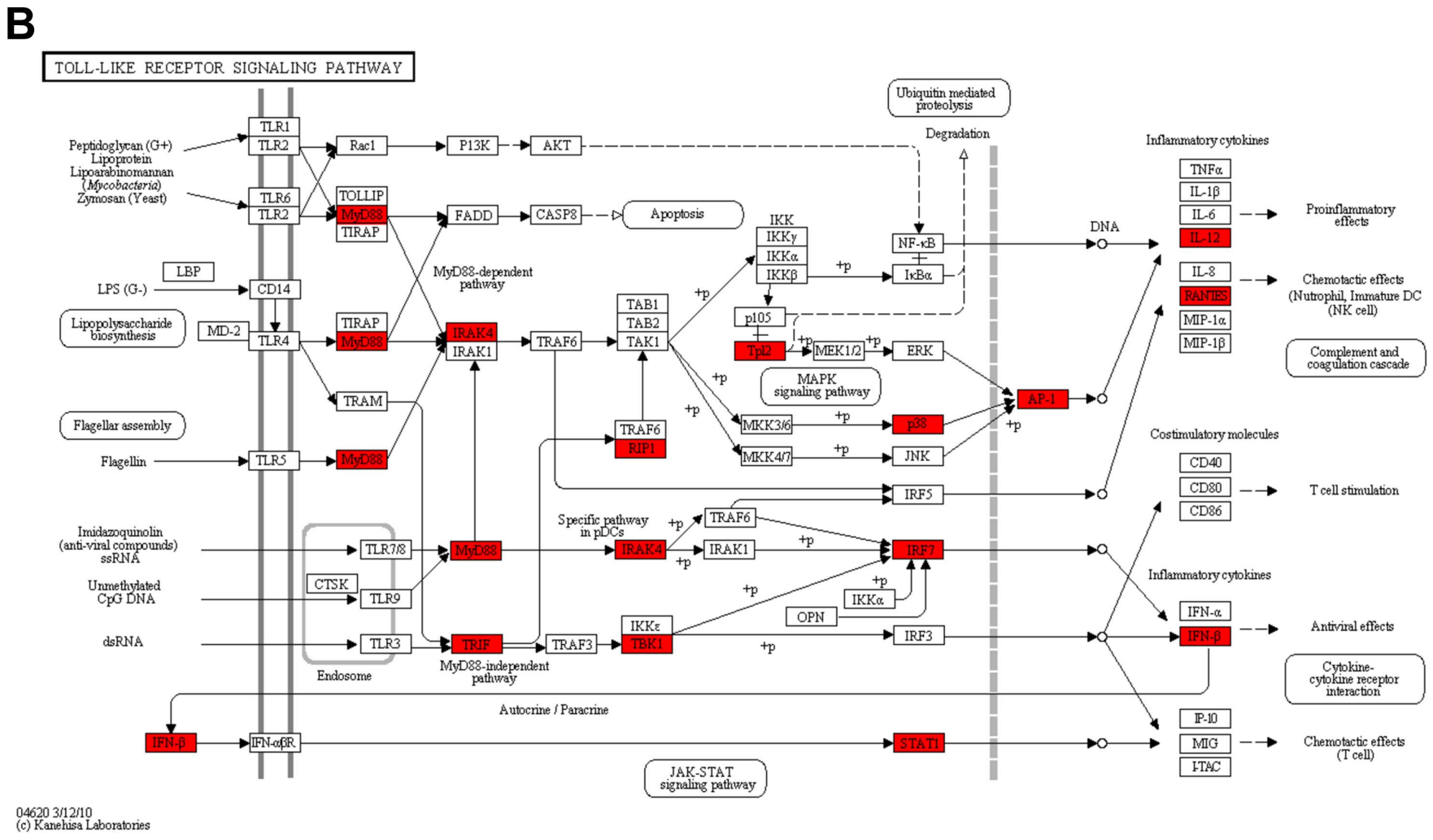

Figure B.2 – *Continued from previous page*

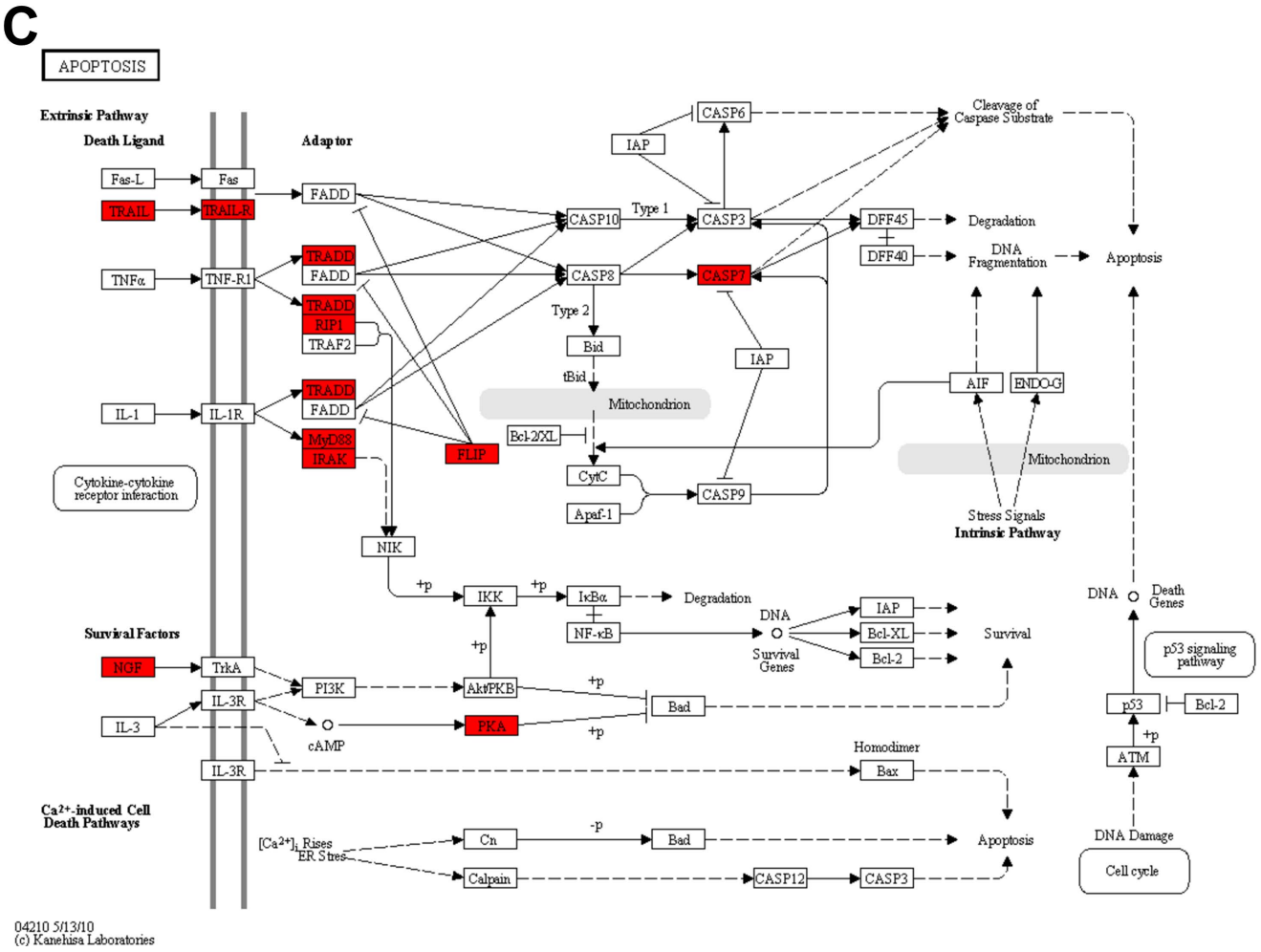

Figure B.2 – *Continued from previous page*

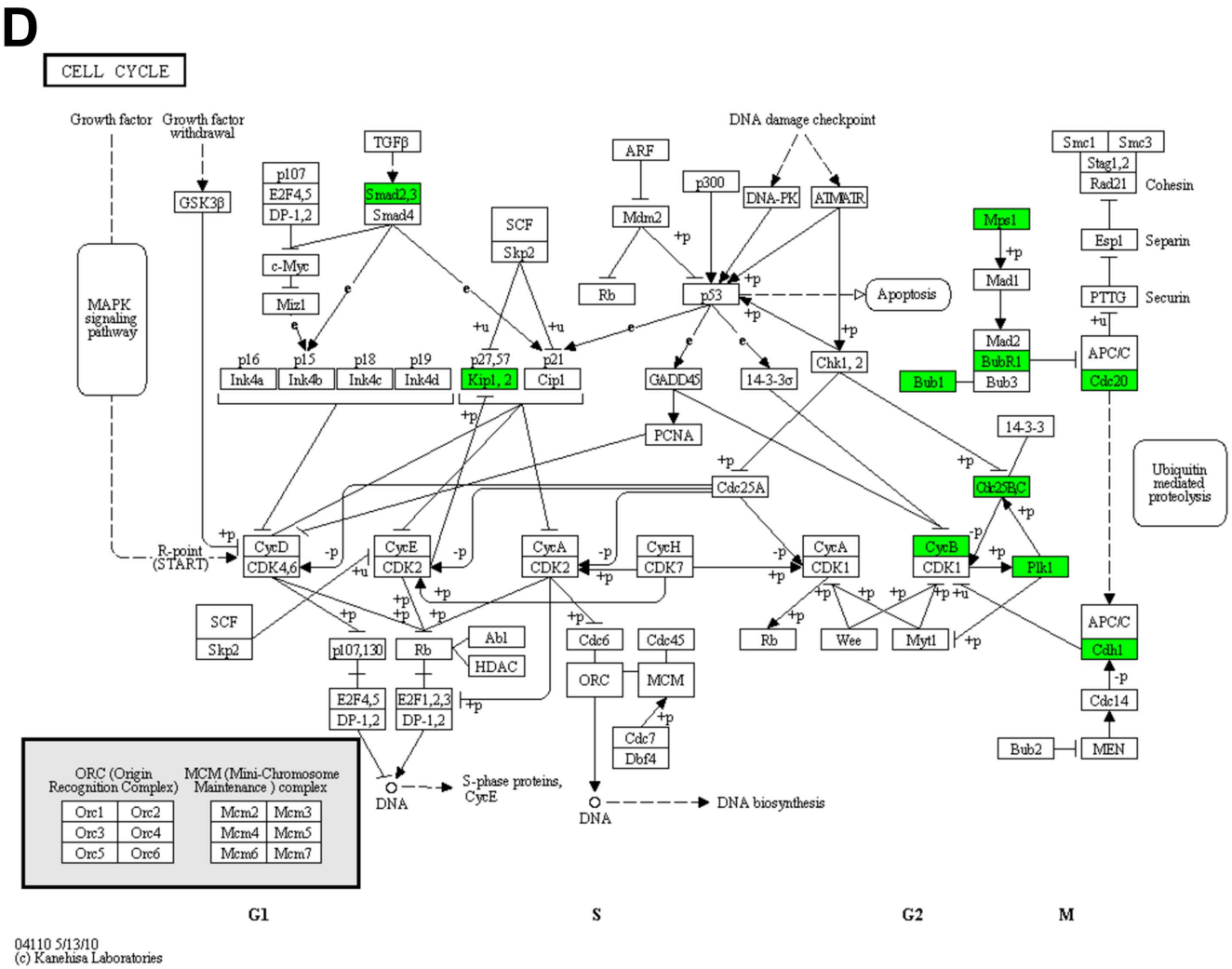

Figure B.2 – *Continued from previous page*

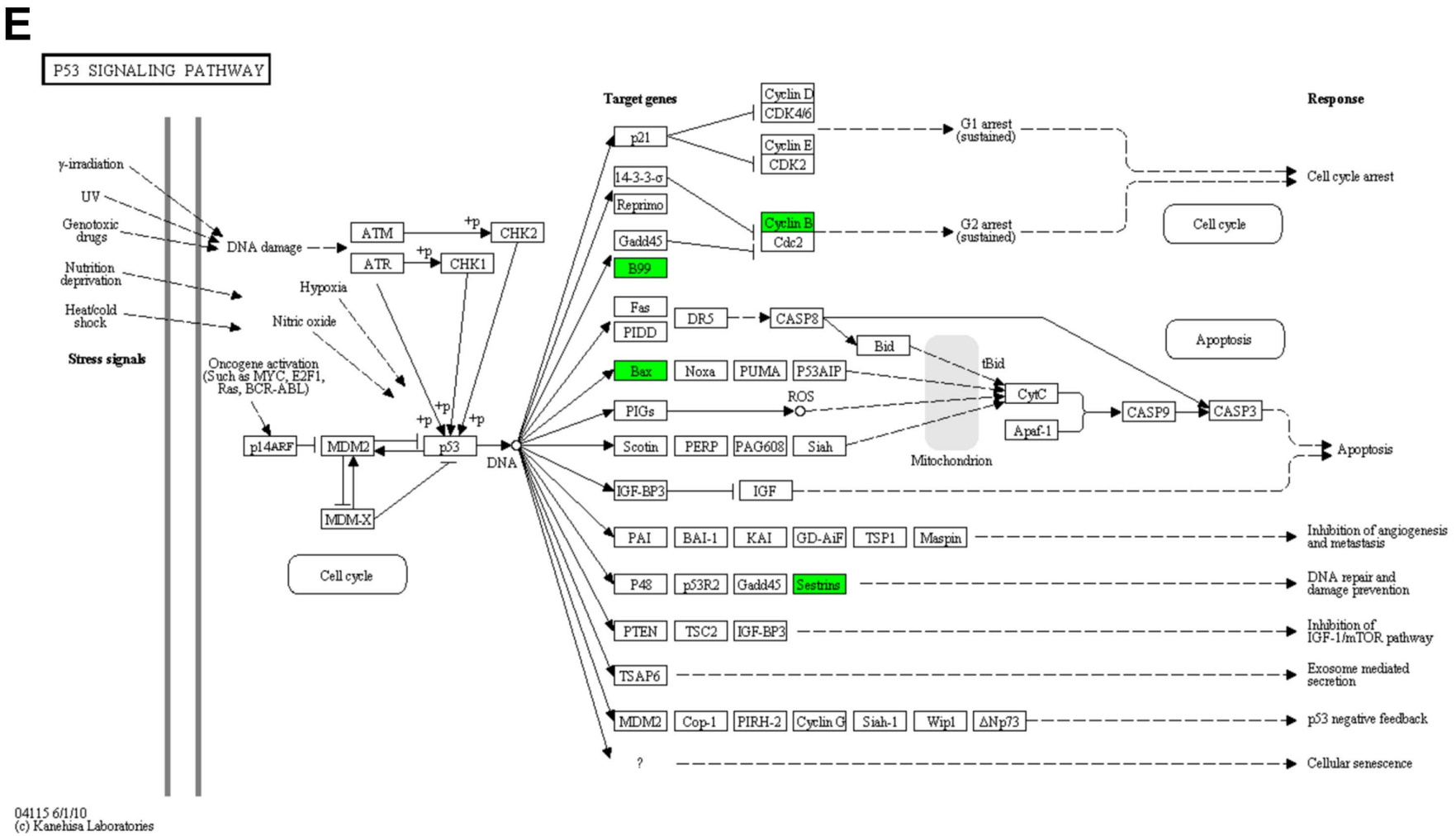

Figure B.2 – *Continued from previous page*

Table B.6: List of 249 interferon-regulated genes derived from the list of 662 genes up-regulated in reprogramming factor mRNA-transfected fibroblasts with respect to mock-transfected control cells. The numbers on the right refer to the number of datasets that have shown the different types of interferons to regulate the listed genes. Taken from Drews et al. (2012).

Symbol	Chromosome	Definition	Type 1	Type 2	Type 3
ADAM17	2	ADAM 17 precursor (EC 3.4.24.86)	1	0	0
ADAR	1	Double-stranded RNA-specific adenosine deaminase (EC 3.5.4.-)	6	3	1
ANKFY1	17	Ankyrin repeat and FYVE domain-containing protein 1	1	0	1
APOBEC3G	22	DNA dC→dU-editing enzyme APOBEC-3G (EC 3.5.4.-)	3	2	1
APOL2	22	Apolipoprotein-L2	2	1	1
APOL6	22	Apolipoprotein-L6	4	1	3
AZI2	3	5-azacytidine-induced protein 2	2	0	1
B2M	15	Beta-2-microglobulin precursor	4	1	1
BCL2L13	22	Bcl-2-like 13 protein	2	2	0
BRD2	c6_COX	Bromodomain-containing protein 2	1	0	0
BST2	19	Bonemarrowstromalantigen 2 precursor	13	4	3
BTN3A2	6	Butyrophilin subfamily 3 member A2 precursor	2	1	0
BTN3A3	6	Butyrophilin subfamily 3 member A3 precursor	1	1	0
C19orf28	19	Putative transporter C19orf28	1	0	0
C1S	12	Complement C1s subcomponent precursor (EC 3.4.21.42)	4	2	0
CALCOCO2	17	calcium binding and coiled-coil domain 2	0	1	0
CASP7	10	Caspase-7 precursor	5	4	1
CCL2	17	Small inducible cytokine A2 precursor	6	3	0
CCL5	17	Small inducible cytokine A5 precursor	3	2	0
CCND3	6	G1/S-specific cyclin-D3	1	1	0
CCNL1	3	Cyclin-L1	1	0	0
CD274	9	Programmed cell death 1 ligand 1 precursor	0	1	0
CD58	1	Lymphocyte function-associated antigen 3 precursor	1	1	0

Continued on next page

Table B.6 – *Continued from previous page*

Symbol	Chromosome	Definition	Type 1	Type 2	Type 3
CDC5L	6	Cell division cycle 5-like protein	1	0	0
CEACAM1	19	Carcinoembryonic antigen-related cell adhesion molecule 1 precursor	1	0	0
CEBPZ	2	CCAAT/enhancer-binding protein zeta	1	1	0
CFB	c6_COX	Complement factor B precursor (EC 3.4.21.47)	5	3	0
CFLAR	2	CASP8 and FADD-like apoptosis regulator precursor	1	0	1
CHMP5	9	Charged multivesicular body protein 5	1	0	0
CLDN1	3	Claudin-1	1	0	0
COMT	22	Catechol O-methyltransferase (EC 2.1.1.6)	2	1	0
CTGF	6	Connective tissue growth factor precursor	3	2	0
CTSL1	9	Cathepsin L precursor (EC 3.4.22.15)	1	0	0
CXCL16	17	Small inducible cytokine B16 precursor	1	0	0
CXCL2	4	Macrophage inflammatory protein 2-alpha precursor	2	2	0
CYP2J2	1	Cytochrome P450 2J2 (EC 1.14.14.1)	1	1	0
DDX58	9	Probable ATP-dependent RNA helicase DDX58 (EC 3.6.1.-)	10	4	3
DEDD	1	Death effector domain-containing protein	1	0	0
DHX58	17	Probable ATP-dependent helicase LGP2 (EC 3.6.1.-)	0	1	0
DNAJA1	9	DnaJ homolog subfamily A member 1	1	1	0
DTX3L	3	Protein deltex 3-like protein	1	0	0
DUSP1	5	Dual specificity protein phosphatase 1 (EC 3.1.3.48) (EC 3.1.3.16)	3	3	0
DUSP5	10	Dual specificity protein phosphatase 5 (EC 3.1.3.48) (EC 3.1.3.16)	1	0	1
DYNLT1	6	Dynein light chain Tctex-type 1	1	1	0

Continued on next page

Table B.6 – *Continued from previous page*

Symbol	Chromosome	Definition	Type 1	Type 2	Type 3
ECE1	1	Endothelin-convertingenzyme 1 (EC 3.4.24.71)	1	0	1
EDN1	6	Endothelin-1 precursor	0	1	0
EFR3_HUMAN	8	Protein EFR3-like	0	1	0
EHD4	15	EH domain-containing protein 4	1	0	1
EIF2AK2	2	Interferon-induced, double-stranded RNA-activated protein kinase (EC 2.7.11.1)	15	3	3
ELF1	13	ETS-related transcription factor Elf-1	1	1	0
EPHA2	1	Ephrin type-A receptor 2 precursor (EC 2.7.10.1)	1	0	0
EPSTI1	13	epithelial stromal interaction 1 isoform 2	1	0	1
EXOSC9	4	Exosome complex exonuclease RRP45 (EC 3.1.13.-)	1	1	0
F3	1	Tissue factor precursor	2	3	0
FAM125A	19	Protein FAM125A	1	0	1
FAM46A	6	Protein FAM46A	0	1	0
FOSL1	11	Fos-related antigen 1	2	1	0
FST	5	Follistatin precursor	1	0	0
GADD45A	1	Growth arrest and DNA-damage-inducible protein GADD45 alpha	2	1	0
GADD45B	19	Growth arrest and DNA-damage-inducible protein GADD45 beta	1	0	0
GBP1	1	Interferon-induced guanylate-binding protein 1	15	6	2
GBP2	1	Interferon-induced guanylate-binding protein 2	8	2	0
GBP3	1	Guanylate-binding protein 3	4	3	0
GBP4	1	Guanylate-binding protein 4	3	1	0
GBP5	1	Guanylate-binding protein 5	4	0	1
GCA	2	Grancalcin	2	0	1
GLIPR1	12	Glioma pathogenesis-related protein 1 precursor	1	1	0
GMPR	6	GMP reductase 1 (EC 1.7.1.7)	4	3	0
GRINA	8	glutamate receptor, ionotropic, N-methyl D-asparate-associated protein 1	1	0	0

Continued on next page

Table B.6 – *Continued from previous page*

Symbol	Chromosome	Definition	Type 1	Type 2	Type 3
GSDMDC1	8	Gasdermin domain-containing protein 1	1	0	0
H1F0	22	Histone H1.0	2	1	0
H4_HUMAN	6	Histone H4	0	1	0
HAX1	1	HS1-associating protein X-1	1	1	0
HBEGF	5	Heparin-binding EGF-like growth factor precursor	0	1	0
HERC5	4	Probable E3 ubiquitin-protein ligase HERC5 (EC 6.3.2.-)	6	1	2
HERC6	4	Probable E3 ubiquitin-protein ligase HERC6 (EC 6.3.2.-)	2	0	1
HES4	1	Transcription factor HES-4	1	0	0
HIST1H2AC	6	Histone H2A type 1-C	2	1	0
HIST3H2A	1	Histone H2A type 3	1	0	0
HSH2D	19	Hematopoietic SH2 domain-containing protein	1	0	1
HSPA1B	6	Heatshock 70 kDa protein 1	2	2	0
ICAM2	17	Intercellular adhesion molecule 2 precursor	1	0	0
ID3	1	DNA-binding protein inhibitor ID-3	1	1	0
IFI16	1	Gamma-interferon-inducibleprotein Ifi-16	9	4	1
IFI27	14	Interferon-alpha-induced 11.5 kDa protein	13	3	3
IFI35	17	Interferon-induced 35 kDa protein	14	3	2
IFI44	1	Interferon-induced protein 44	11	5	2
IFI44L	1	histocompatibility 28	8	3	2
IFI6	1	Interferon-induced protein 6-16 precursor	19	5	2
IFIH1	2	Interferon-induced helicase C domain-containing protein 1 (EC 3.6.1.-)	8	2	3
IFIT1	10	Interferon-induced protein with tetratricopeptide repeats 1	17	3	2
IFIT2	10	Interferon-induced protein with tetratricopeptide repeats 2	15	6	2
IFIT3	10	Interferon-induced protein with tetratricopeptide repeats 3	15	4	3
IFIT5	10	Interferon-induced protein with tetratricopeptide repeats 5	11	3	3
IFITM1	11	Interferon-induced transmembrane protein 1	14	2	3

Continued on next page

Table B.6 – *Continued from previous page*

Symbol	Chromosome	Definition	Type 1	Type 2	Type 3
IFITM2	11	Interferon-induced transmembrane protein 2	3	1	0
IFITM3	11	Interferon-induced transmembrane protein 3	4	0	2
IFNB1	9	Interferon beta precursor	0	1	0
IL10	1	Interleukin-10 precursor	0	1	0
IL11	19	Interleukin-11 precursor	0	1	0
IL12A	3	Interleukin-12 subunit alpha precursor	0	1	0
IL15	4	Interleukin-15 precursor	4	2	0
IL15RA	10	Interleukin-15 receptor alpha chain precursor	6	3	1
IRF1	5	Interferon regulatory factor 1	12	6	1
IRF7	11	Interferon regulatory factor 7	15	4	1
IRF9	14	Transcriptional regulator ISGF3 subunit gamma	11	3	3
ISG15	1	Interferon-induced 17 kDa protein precursor	20	5	3
ISG20	15	Interferon-stimulated gene 20 kDa protein (EC 3.1.13.1)	15	5	3
ITGA2	5	Integrin alpha-2 precursor	1	1	0
ITGA3	17	Integrin alpha-3 precursor	1	0	0
JAK2	9	Tyrosine-protein kinase JAK2	3	1	0
JUN	1	Transcription factor AP-1	2	2	1
JUNB	19	Transcription factorjun-B	1	1	0
KCTD14	11	BTB/POZ domain-containing protein KCTD14	1	1	0
KLF11	2	Krueppel-likefactor 11	2	0	0
LAMB1	7	Laminin subunit beta-1 precursor	1	0	0
LAMP3	3	Lysosome-associated membrane glycoprotein 3 precursor	5	3	1
LAP3	4	Cytosol aminopeptidase (EC 3.4.11.1)	2	0	1
LARS2	3	Probable leucyl-tRNA synthetase, mitochondrial precursor (EC 6.1.1.4)	1	1	0
LGALS3BP	17	Galectin-3-binding protein precursor	9	4	2
LGALS9	17	Galectin-9	6	4	0
LGMN	14	Legumain precursor (EC 3.4.22.34)	1	0	0
LMO2	11	Rhombotin-2	2	1	0

Continued on next page

Table B.6 – *Continued from previous page*

Symbol	Chromosome	Definition	Type 1	Type 2	Type 3
LY6E	8	Lymphocyte antigen 6E precursor	6	2	1
MAD2L1BP	6	MAD2L1-binding protein	1	1	0
MAP3K8	10	Mitogen-activated protein kinase kinase kinase 8 (EC 2.7.11.25)	1	2	0
MCL1	1	Induced myeloid leukemia cell differentiation protein Mcl-1	3	2	1
MOV10	1	Putative helicase MOV-10 (EC 3.6.1.-)	0	1	0
MTMR11	1	myotubularin related protein 11	1	1	0
MVP	16	Major vault protein	1	1	0
MX1	21	Interferon-induced GTP-binding protein Mx1	15	4	2
MX2	21	Interferon-induced GTP-binding protein Mx2	12	3	2
MYC	8	Myc proto-oncogene protein	3	2	0
MYD88	3	Myeloid differentiation primary response protein MyD88	6	1	1
N4BP1_-HUMAN	16	NEDD4-binding protein 1	2	0	1
NFE2L3	7	Nuclear factor erythroid 2-related factor 3	2	0	1
NLRC5	16	nucleotide-binding oligomerization domains 27	0	1	0
NMI	2	N-myc-interactor	8	1	1
NP_-001091948.1	c6_COX	major histocompatibility complex, class I, F isoform 3 precursor	0	1	0
NP_005507.3	6	major histocompatibility complex, class I, E precursor	0	1	0
NP_057563.3	3	scotin	0	1	0
NP_060101.2	4	CDNA FLJ10787 fis	0	1	0
NP_060851.2	19	CDNA FLJ38823 fis	0	1	0
NP_954590.1	17	XIAP associated factor-1 isoform 2	0	1	0
NP_997198.2	2	thymidylate kinase family LPS-inducible member	0	1	0
NRBP1	2	Nuclear receptor-binding protein	0	1	0
NT5C3	7	Cytosolic 5-nucleotidase III (EC 3.1.3.5)	2	0	1

Continued on next page

Table B.6 – *Continued from previous page*

Symbol	Chromosome	Definition	Type 1	Type 2	Type 3
OAS1	12	2-5-oligoadenylate synthetase 1 (EC 2.7.7.-)	16	5	3
OAS2	12	2-5-oligoadenylate synthetase 2 (EC 2.7.7.-)	13	4	3
OASL	12	59 kDa 2-5-oligoadenylate synthetase-like protein	11	5	2
OGFR	20	Opioid growth factor receptor	2	1	1
OPTN	10	Optineurin	1	0	0
PAPD4	5	PAP associated domain-containing 4	1	0	0
PARP10	8	Poly [ADP-ribose] polymerase 10 (EC 2.4.2.30)	0	1	0
PARP12	7	Poly [ADP-ribose] polymerase 12 (EC 2.4.2.30)	0	1	0
PARP4	13	Poly [ADP-ribose] polymerase 4 (EC 2.4.2.30)	2	1	0
PBEF1	7	Nicotinamide phosphoribosyl transferase (EC 2.4.2.12)	2	0	0
PDGFRL	8	Platelet-derived growth factor receptor-like protein precursor	4	1	0
PHF11	13	PHD fingerprotein 11	2	0	2
PLAUR	19	Urokinase plasminogen activator surface receptor precursor	1	1	0
PLEKHA4	19	Pleckstrin homology domain-containing family A member 4	2	1	0
PLSCR1	3	Phospholipid scramblase 1	15	3	3
PMAIP1	18	Phorbol-12-myristate-13-acetate-induced protein 1	5	2	1
PML	15	Probable transcription factor PML	9	4	2
PR285_-HUMAN	20	Peroxisomal proliferator-activated receptor A-interacting complex 285 kDa protein (EC 3.6.1.-)	0	1	0
PRKD2	19	Serine/threonine-protein kinase D2 (EC 2.7.11.13)	2	1	1
PRNP	20	Major prion protein precursor	2	1	0
PROCR	20	Endothelial protein C receptor precursor	1	1	0
PSCD1	17	Cytohesin-1	1	0	0
PSMA2	7	Proteasome subunit alpha type 2 (EC 3.4.25.1)	2	1	0

Continued on next page

Table B.6 – *Continued from previous page*

Symbol	Chromosome	Definition	Type 1	Type 2	Type 3
PSMA3	14	Proteasome subunit alpha type 3 (EC 3.4.25.1)	2	1	0
PSMA4	15	Proteasome subunit alpha type 4 (EC 3.4.25.1)	1	1	0
PSMB10	16	Proteasome subunit beta type 10 precursor (EC 3.4.25.1)	0	1	0
PSMB2	1	Proteasome subunit beta type 2 (EC 3.4.25.1)	1	1	0
PSMB8	6	Proteasome subunit beta type 8 precursor (EC 3.4.25.1)	7	2	0
PSMB9	6	Proteasome subunit beta type 9 precursor (EC 3.4.25.1)	12	3	3
PSME1	14	Proteasome activator complex subunit 1	2	1	0
PSME2	14	Proteasome activator complex subunit 2	2	1	0
PTGER4	5	Prostaglandin E2 receptor EP4 subtype	1	0	0
PTGS2	1	Prostaglandin G/H synthase 2 precursor (EC 1.14.99.1)	0	1	0
RAB24	5	Ras-related protein Rab-24	0	1	0
RAB9A	X	Ras-related protein Rab-9	0	1	0
RARRES3	11	Retinoic acid receptor responder protein 3	4	2	1
RBCK1	20	RanBP-type and C3HC4-type zinc finger-containing protein 1	5	1	1
RIPK1	6	Receptor-interacting serine/threonine-protein kinase 1 (EC 2.7.11.1)	1	0	1
RNF19B	1	IBR domain-containingprotein 3	1	0	0
RNF213	17	RING fingerprotein 213	0	1	0
RNF31	14	RING fingerprotein 31	0	1	0
RSAD2	2	radical S-adenosyl methionine domain containing 2	10	4	2
RTP4	3	Receptor-transporting protein 4	4	2	1
SAMD9	7	Sterile alpha motif domain-containing protein 9	3	1	2
SAMD9L	7	Sterile alpha motif domain-containing protein 9-like	1	0	1
SAMHD1	20	SAM domain and HD domain-containing protein 1	4	2	1

Continued on next page

Table B.6 – *Continued from previous page*

Symbol	Chromosome	Definition	Type 1	Type 2	Type 3
SAT1	X	Diamine acetyltransferase 1 (EC 2.3.1.57)	1	1	0
SC4MOL	4	C-4 methylsteroloxidase (EC 1.14.13.72)	1	1	0
SECTM1	17	Secreted and transmembrane protein 1 precursor	2	2	0
SERPINE1	7	Plasminogen activator inhibitor 1 precursor	2	2	0
SERPING1	11	Plasma protease C1 inhibitor precursor	5	2	0
SERTAD1	19	SERTA domain-containing protein 1	1	0	0
SH3GLB1	1	SH3 domain GRB2-like protein B1	1	0	0
SLC15A3	11	solute carrier family 15, member 3	1	1	0
SLC30A1	1	Zinc transporter 1	1	1	0
SLFN12	17	Schlafen family member 12	1	0	0
SOCS1	16	Suppressor of cytokine signaling 1	5	3	1
SP100	2	Nuclear autoantigen Sp-100	0	1	0
SP110	2	Sp110 nuclearbodyprotein	0	1	0
SPHK1	17	Sphingosine kinase 1 (EC 2.7.1.-)	1	0	0
SPSB1	1	SPRY domain-containing SOCS box protein 1	1	0	0
STAT1	2	Signal transducer and activator of transcription 1-alpha/beta	18	2	3
STAT2	12	Signal transducer and activator of transcription 2	9	3	1
STAT6	12	Signal transducer and activator of transcription 6	1	1	0
STOML1	15	Stomatin-likeprotein 1	1	0	0
TAP1	6	Antigen peptidetransporter 1	9	2	2
TAP2	6	Antigen peptidetransporter 2	4	1	1
TAPBP	6	tapasinisoform 1 precursor	1	0	0
TCN2	22	Transcobalamin-2 precursor	1	0	0
TDRD7	9	Tudor domain-containing protein 7	7	2	2
TFPI2	7	Tissue factor pathway inhibitor 2 precursor	1	0	0
TLK2	17	Serine/threonine-protein kinase tousled-like 2 (EC 2.7.11.1)	2	1	0

Continued on next page

Table B.6 – *Continued from previous page*

Symbol	Chromosome	Definition	Type 1	Type 2	Type 3
TM4SF1	3	Transmembrane 4 L6 family member 1	2	0	0
TMEM110	3	Transmembrane protein 110	0	1	0
TMEM140	7	Transmembrane protein 140	2	0	2
TNFRSF10A	8	Tumor necrosis factor receptor superfamily member 10A precursor	0	1	0
TNFSF10	3	Tumor necrosis factor ligand superfamily member 10	0	1	0
TNFSF13B	13	Tumor necrosis factor ligand superfamily member 13B	3	1	0
TRADD	16	Tumor necrosis factor receptor type 1-associated DEATH domain protein	1	0	0
TRAFD1	12	TRAF-type zinc finger domain-containing protein 1	1	0	0
TRIM14	9	Tripartitemotif-containingprotein 14	5	2	1
TRIM21	11	52 kDa Ro protein	8	3	1
TRIM22	11	Tripartite motif-containing protein 22	12	4	2
TRIM25	17	Tripartite motif-containing protein 25	5	2	1
TRIM26	6	Tripartite motif-containing protein 26	2	1	0
TRIM38	6	Tripartite motif-containing protein 38	4	2	1
TRIM5	11	Tripartite motif-containing protein 5 (EC 6.3.2.-)	3	1	1
TRIM56	7	Tripartite motif-containing protein 56	2	1	1
TXNIP	1	Thioredoxin-interacting protein	1	1	0
UBE1L	3	Ubiquitin-activating enzyme E1 homolog	5	1	0
UBE2E1	3	Ubiquitin-conjugating enzyme E2 E1 (EC 6.3.2.19)	0	1	0
UBE2L6	11	Ubiquitin/ISG15-conjugating enzyme E2 L6 (EC 6.3.2.19)	10	2	3
UGCG	9	Ceramide glucosyl transferase (EC 2.4.1.80)	2	1	0
UNC93B1	11	UNC93 homolog B1	1	0	1
USP42	7	Ubiquitin carboxyl-terminal hydrolase 42 (EC 3.1.2.15)	1	0	0

Continued on next page

Table B.6 – *Continued from previous page*

Symbol	Chromosome	Definition	Type 1	Type 2	Type 3
VAMP5	2	Vesicle-associated membrane protein 5	1	1	0
VEGFC	4	Vascular endothelial growth factor C precursor	3	1	0
WARS	14	Tryptophanyl-tRNAsynthetase, cytoplasmic (EC 6.1.1.2)	8	1	0
XRN1	3	5-3 exoribonuclease 1 (EC 3.1.11.-)	1	0	1
ZC3HAV1	7	Zincfinger CCCH type antiviral protein 1	4	0	2
ZFP36	19	Tristetraproline	1	1	0
ZNFX1	20	NFX1-type zinc finger-containing protein 1	0	1	0

Table B.7: List of 40 interferon-regulated genes derived from the list of 331 genes down-regulated in reprogramming factor mRNA-transfected fibroblasts with respect to mock-transfected control cells. The numbers on the right refer to the number of datasets that have shown the different types of interferons to regulate the listed genes. Taken from Drews et al. (2012).

Symbol	Chromosome	Definition	Type 1	Type 2	Type 3
ACO1	9	Iron-responsive element-binding protein 1	1	1	0
ALS2CR2	2	Pseudokinase ALS2CR2	1	0	0
ANLN	7	Actin-binding protein anillin	1	0	0
ANP32A	15	Acidic leucine-rich nuclear phosphoprotein 32 family member A	1	1	0
CCNB1	5	G2/mitotic-specific cyclin-B1	1	1	0
CCNF	16	G2/mitotic-specific cyclin-F	1	1	0
CDC20	1	Cell division cycle protein 20 homolog (p55CDC)	1	0	0
CKAP5	11	Cytoskeleton-associated protein 5	1	0	0
CXXC5	5	CXXC finger 5	1	0	0
DR1	1	TATA-binding protein-associated phosphoprotein	1	1	0
FAM3C	7	Protein FAM3C precursor (Protein GS3786)	1	1	0
FBN2	5	Fibrillin-2 precursor	1	1	0
FEZ1	11	Fasciculation and elongation protein zeta 1 (Zygin-1) (Zygin I)	1	1	0

Continued on next page

Table B.7 – *Continued from previous page*

Symbol	Chromosome	Definition	Type 1	Type 2	Type 3
FHL1	X	Four and a half LIM domains protein 1	2	2	0
GPER	7	Chemokine receptor-like 2	0	1	0
HNRNPA1	12	Heterogeneous nuclear ribonucleoprotein A1	1	1	0
HSPA2	14	Heat shock-related 70 kDa protein 2	1	0	0
ICAM3	19	Intercellular adhesion molecule 3 precursor	1	0	0
ITGAE	17	Integrin alpha-E precursor	1	1	0
ITGAV	2	Integrin alpha-V precursor	1	0	0
KRT10	17	Keratin, type I cytoskeletal 10	0	1	0
LPP	3	Lipoma-preferred partner	1	0	0
MLTK_HUMAN	2	Mitogen-activated protein kinase kinase kinase MLT (EC 2.7.11.25)	0	1	0
MYH10	17	Myosin-10	0	1	0
NEK2	1	Serine/threonine-protein kinase Nek2 (EC 2.7.11.1)	1	1	0
PIM1	6	Proto-oncogene serine/threonine-protein kinase Pim-1 (EC 2.7.11.1)	3	3	0
PKP4	2	Plakophilin-4	1	1	0
PTPN11	12	Tyrosine-protein phosphatase non-receptor type 11 (EC 3.1.3.48)	1	1	0
PTPN13	4	Tyrosine-protein phosphatase non-receptor type 13 (EC 3.1.3.48)	1	0	0
RAB40B	17	Ras-related protein Rab-40B	0	1	0
RHOBTB3	5	Rho-related BTB domain-containing protein 3	1	1	0
SFPQ	1	Splicing factor, proline- and glutamine-rich	1	1	0
SMAD3	15	Mothers against decapentaplegic homolog 3	2	2	0
SPA17	11	Sperm surface protein Sp17	1	1	0
STAU2	8	Double-stranded RNA-binding protein Staufen homolog 2	1	0	0
TCFL5	20	Transcription factor-like 5 protein	1	0	0
TNFRSF10D	8	Tumor necrosis factor receptor superfamily member 10D precursor	0	1	0

Continued on next page

Table B.7 – *Continued from previous page*

Symbol	Chromosome	Definition	Type 1	Type 2	Type 3
TOP2B	3	DNA topoisomerase 2-beta (EC 5.99.1.3)	1	1	0
TTK	6	Dual specificity protein kinase TTK (EC 2.7.12.1)	1	1	0
UBE4B	1	Ubiquitin conjugation factor E4 B	1	1	0

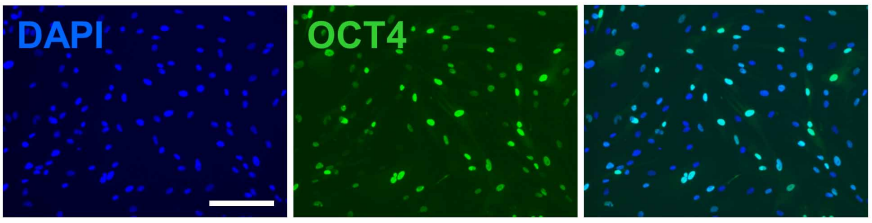

Figure B.3: Detection of OCT4 protein expression in HFF1 cells upon transfection of the commercially bought, modified mRNA. HFF1 cells, grown in 24-wells, were transfected with commercially bought, modified mRNA-encoding *POU5F1* and fixed 24 h post-transfection for the immunofluorescent labeling procedure. Microscope images of the nuclear (DAPI) signals, the OCT4-specific signals and merged images are shown. Scale bar = 200 µm.

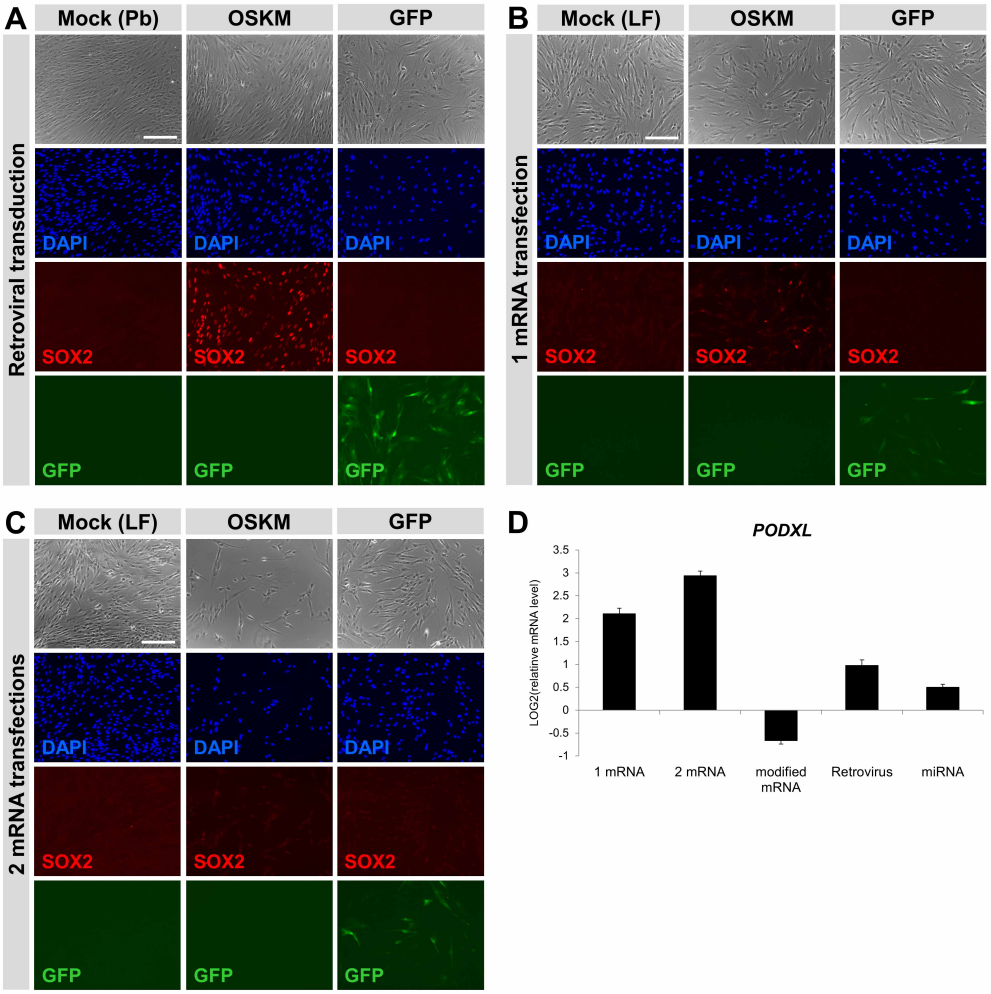

Figure B.4: Detection of SOX2 protein expression and quantification of *PODXL* transcript levels in HFF1 cells as quality controls of the different reprogramming protocols. These quality control assays accompany the results presented in Figures 4.8 and 4.9. HFF1 cells were transfected with a 1:1:1:1 cocktail of mRNAs encoding *POU5F1*, *SOX2*, *KLF4* and *c-MYC*. Transfections were carried out once or twice with in-house synthesized mRNA (4 µg total per 6-well per transfection; '1 mRNA', '2 mRNA') or once with commercially bought mRNA (4 µg total per 6-well per transfection; 'modified mRNA'). Alternatively, HFF1 cells were transduced once with a 1:1:1:1 combination of retroviruses encoding *POU5F1*, *SOX2*, *KLF4* and *c-MYC* or transfected once with a 1:1:1:1:1 mix composed of the miRNAs miR-302a, miR-302b, miR-302c, miR-302d and miR-367 (100 pmol total per 6-well). Additionally, the total amount of mRNAs and miRNAs used for reprogramming were substituted with the same amount of GFP-encoding mRNA or a scrambled, non-target miRNA. Similarly, cells were transduced with a GFP-encoding retrovirus equivalent to the amount of retrovirus encoding one of the reprogramming factors in the reprogramming cocktail. All samples were fixed for immunofluorescence-mediated detection of protein expression or harvested for RNA isolation at indicated time points. (A) Microscopic images of GFP expression and SOX2 protein expression detected by fluorescence-dye labeled antibodies 96 h post-transduction. (B) Microscopic images of GFP expression and SOX2 protein expression detected by fluorescence-dye labeled antibodies 24 h after the first transfection and (C) 24 h after the second transfection with in-house *in vitro* synthesized mRNAs. Scale bars = 200 µm. (D) *PODXL* transcript levels. Bars and error bars represent average LOG2 ratios of transfected/transduced fibroblasts over mock-transfected/-transduced controls and SD. n = 6 for '1 mRNA'; n = 4 for '2 mRNA'; n = 3 for 'Retrovirus', 'modified mRNA' and 'miRNA'. Modified from Drews et al. (2012).

Selbständigkeitserklärung

Hiermit erkläre ich, dass ich die vorliegende Arbeit selbständig und unter Verwendung keiner anderen als der von mir angegebenen Quellen und Hilfsmittel verfasst habe. Ferner erkläre ich, dass ich bisher weder an der Freien Universität Berlin noch anderweitig versucht habe, eine Dissertation einzureichen oder mich einer Doktorprüfung zu unterziehen.

Katharina Drews May 24, 2012